LEABHARLANN CHOLÁISTE NA TRÍONÓIDE, BAILE ÁTHA CLIATH | TRINITY COLLEGE LIBRARY DUBLIN
Ollscoil Átha Cliath | The University of Dublin

Terms and Conditions of Use of Digitised Theses from Trinity College Library Dublin

Copyright statement

All material supplied by Trinity College Library is protected by copyright (under the Copyright and Related Rights Act, 2000 as amended) and other relevant Intellectual Property Rights. By accessing and using a Digitised Thesis from Trinity College Library you acknowledge that all Intellectual Property Rights in any Works supplied are the sole and exclusive property of the copyright and/or other IPR holder. Specific copyright holders may not be explicitly identified. Use of materials from other sources within a thesis should not be construed as a claim over them.

A non-exclusive, non-transferable licence is hereby granted to those using or reproducing, in whole or in part, the material for valid purposes, providing the copyright owners are acknowledged using the normal conventions. Where specific permission to use material is required, this is identified and such permission must be sought from the copyright holder or agency cited.

Liability statement

By using a Digitised Thesis, I accept that Trinity College Dublin bears no legal responsibility for the accuracy, legality or comprehensiveness of materials contained within the thesis, and that Trinity College Dublin accepts no liability for indirect, consequential, or incidental, damages or losses arising from use of the thesis for whatever reason. Information located in a thesis may be subject to specific use constraints, details of which may not be explicitly described. It is the responsibility of potential and actual users to be aware of such constraints and to abide by them. By making use of material from a digitised thesis, you accept these copyright and disclaimer provisions. Where it is brought to the attention of Trinity College Library that there may be a breach of copyright or other restraint, it is the policy to withdraw or take down access to a thesis while the issue is being resolved.

Access Agreement

By using a Digitised Thesis from Trinity College Library you are bound by the following Terms & Conditions. Please read them carefully.

I have read and I understand the following statement: All material supplied via a Digitised Thesis from Trinity College Library is protected by copyright and other intellectual property rights, and duplication or sale of all or part of any of a thesis is not permitted, except that material may be duplicated by you for your research use or for educational purposes in electronic or print form providing the copyright owners are acknowledged using the normal conventions. You must obtain permission for any other use. Electronic or print copies may not be offered, whether for sale or otherwise to anyone. This copy has been supplied on the understanding that it is copyright material and that no quotation from the thesis may be published without proper acknowledgement.

Nitrogen and Carbon Isotopes in Fossil Aquatic Ecosystems

Joanne Hellawell

Submitted in accordance with the requirements for the degree of
Doctor of Philosophy

The University of Dublin
Trinity College
School of Natural Sciences

June, 2009

TRINITY COLLEGE
10 APR 2012
LIBRARY DUBLIN
9422

Declaration

I declare that:

a) No part of this thesis has been submitted as an exercise for a degree at this or any other University;

b) This thesis is entirely my own work;

c) I agree that the Library may lend or copy this thesis on request.

Signed

Joanne Hellawell

Summary

In a modern ecosystem, the trophic level of organisms can be distinguished on the basis of their nitrogen and organic carbon isotopic signature (DeNiro & Epstein 1978 and 1981). Due to fractionation during the assimilation of food and the creation of new body tissues, these stable isotopes reflect the diet of each consumer, thus their relative position in a food web can be inferred based on their biochemistry. $\delta^{15}N$ is considered to be a direct indicator of trophic level, whereas $\delta^{13}C_{org}$ is thought to reflect the influence of different potential food sources (e.g. Minagawa & Wada 1984; Hecky & Hesslein 1995). These stable isotopes have also been used to infer the feeding habits of prehistoric animals, in particular in the interpretation of diet of early humans from archaeological sites (e.g. Drucker & Bocherens 2004; Hedges & Reynard 2007). The purpose of this study was to investigate whether the isotopes of $\delta^{15}N$ and $\delta^{13}C_{org}$ could be applied to a much older fossil ecosystem to distinguish the community structure and palaeoecology. The Eocene fish from the Green River Formation lagerstätte in SW Wyoming, USA, were chosen as the experimental fauna. Although exceptional preservation does not necessarily imply preservation of the original isotopic values, these fish are thought to have been subject to little diagenetic change (Norris *et al.* 2000). Regular mass mortality horizons occur throughout the stratigraphy, representing census assemblages of co-existing taxa in a tightly constrained temporal framework, thus presenting an ideal testing ground for this study. The feeding preferences of each species collected for analysis are already well defined by previous authors from observations of trophic adaptation and gut content as well as direct field evidence (see Grande 1984). Proving that bulk $\delta^{15}N$ and $\delta^{13}C_{org}$ data can reveal trophic interactions in a well-documented ancient ecosystem will expand the use of this technique to reveal trophic interactions of more poorly known fossil ecosystems where there are perhaps no extant equivalent species. As well as the stable isotope analyses central to this study, a combination of other geochemical techniques were used to assess the authenticity of the data set and to infer the palaeoenvironment setting, thereby placing the results in context. Whole rock $\delta^{13}C$ and $\delta^{18}O$ values are reported from Fossil Lake for the first time and confirm that it was a closed-lake system with little inference of disruption to either hydrological balance or environment.

Careful consideration was given to the preparation of Green River fossil specimens prior to analysis. The removal of all carbonate sediment from the fossils was essential, and the best method found by experimentation. The results have wide implications for future geochemical analysis of fossil material. Due to the low N content of the fossils, standard mass spectrometry techniques were modified to ensure that robust isotopic data would be produced. The results of $\delta^{15}N$ isotopic analyses of Green River fish did not appear to reflect their trophic level. This outcome suggests that the $\delta^{15}N$ data obtained is largely an artefact of either post-mortem contamination or a result of diagenetic fractionation of the original signature. Intraorganism fractionation did appear to be preserved, however. $\delta^{13}C_{org}$ was not analysed in the majority specimens due to analytical difficulties and assumed unreliability based on laboratory experimentation. Given that nitrogen and organic carbon were present in the fossils, further research was required to assess the origin of their isotopic signatures. Comprehensive laboratory experiments were devised using extant fish to identify changes in their stable isotopic composition over a six-month period. Scales were found to be the most reliable tissues for retaining the original isotopic signature over the course of the experiments, and variation in vertebrae and muscle tissues did not appear to be a direct result of any particular set of simulated conditions. In an attempt to characterize the organic content of the fossils further, organic geochemical techniques were employed to extract the lipid content and identify whether original fish organic matter was likely to be retaining the $\delta^{15}N$ isotopic values. This strand of research proved inconclusive; however palaeoenvironmental information was gained regarding the original assemblage of micro-organisms present in Fossil Lake. The absence of cyanobacteria and Archaea at time of deposition is inferred and the presence of dinoflagellates confirmed. Annual blooms of toxic dinoflagellates are proposed as a mechanism for the fish mass mortalities recurrent in Fossil Lake. As a further test of using the $\delta^{15}N$ and $\delta^{13}C_{org}$ isotopic technique to gather information from fossilized hard tissues, a fossil ecosystem with ecologically distinct taxa from the Cretaceous of Argentina was targeted and analysed. The data produced appears to be robust based on expected isotopic differences given their extant equivalents. The retrieval of this isotopic data from biomineralized tissues opens up new possibilities for further ecological assessments using isotopes in ancient communities, albeit with the caveats identified within this thesis.

Acknowledgements

I am deeply indebted to many people for offering their time and expertise towards the successful production of this thesis. Firstly, I would like to thank my supervisor, Dr Chris Nicholas, for the inception of the project and his faith in my ability to carry out this research. This research would not have been possible however, without the technical expertise of Dr Robbie Goodhue to whom I am very grateful. I would also like to thank Mr Neil Kearney, Mr Declan Burke, Ms Maura Morgan, Mr Frances Hendron and Mr Noel McGinley at TCD, as well as Mr Brian Hellawell, for their technical aid and assistance. Other practical support was given in the laboratory by Mrs Hannah Urquhart who generously gave up her time. For scientific discussion and advice, I would like to thank my friends Mrs Margrét Steinþórsdóttir, Dr Susannah Maidment, Dr Ian Burke, Dr Rebecca Bartlett, Dr Lucy Wilson, Dr Adam Stuart Smith and Miss Aoife O'Halloran. I am also indebted to colleagues Dr Mags Duncan and Dr Patrick Wyse Jackson for their kindnesses, teachings and counsel. This thesis would not have come to fruition without the help and assistance of Mrs Clodagh Nolan, TCD Unilink Service, and Dr Niamh Murphy, TCD Health Centre, and I thank them both wholeheartedly for their continued support and encouragement.

Fieldwork in Wyoming, discussed in Chapter 2, would not have been possible without the boundless generosity of many people, in particular Mr Rick Hebdon and Ms Tanya Hester of Warfield Fossils. Mr Arvid Aase, Fossil Butte National Monument, and Prof. Paul Buchheim, Loma Linda University, assisted with planning the field campaign by generously sharing their extensive knowledge of the area. Assistance in the field and access to quarries was given by experts Mr Robert DeJonghe, Mr Glen Frasier, Ms Wendi Bell, Mr Jerome Montgomery and Mr Charlie Nunn. I also owe a tremendous debt of gratitude to my field assistants in Wyoming, Dr Susannah Maidment and Ms Emma Hellawell, for their hard work, support and dedication. For initial pilot analyses of fossil fish I would like to thank Dr Peter Ditchfield, University of Oxford. For insightful discussion of algal mats I would like to thank Dr Patrick Orr, UCD, for generously sharing his time and knowledge. For useful discussions during the planning of experiments detailed in Chapter 4, I am grateful to Prof. Robert Beynon, University of Liverpool and

Mr Peter Kenny, TCD. Mr Colin Reid and Ms Clodagh Dooley, Centre for Microscopy and Analysis, TCD, provided assistance with all SEM work, while Mr Alistair Haddow helped with photomicrographs. The research of biomarkers discussed in Chapter 7 was enabled by Dr Fiona Gill, OGU, University of Bristol and I am very much obliged to her for her enduring help and guidance. I am grateful to Prof. Richard Evershed and Dr Rich Pancost for allowing me to complete the research and being generous with their time and expertise. Miss Amy Styring, Dr Tim Knowles and Mr Desmond Davis also collaborated and assisted. For the conception and realisation of the field campaign in Patagonia detailed in Chapter 8, I am beholden to Dr Daniel Poiré, Universidad Nacional de La Plata. I would like to thank co-collaborators Mr Augusto Valera, UNLP, and Dr Francisco Goin and Dr Alberto Cione, Museo de La Plata for help with sedimentological and taxonomic descriptions and affinities. I must also thank Ms Sidzel Koefoed and Mr Juan Pablo Perez Panera for their generosity, openness and friendship both during and after the campaign.

Generous funding and sponsorship was granted for this project by Science Foundation Ireland. Financial assistance for fieldwork and conference travel was also given by the Trinity Trust Travel Grant Award Scheme. The AAPS Charles Sternberg Scholarship 2007 facilitated the purchase and transportation of the large ash plate discussed in Chapter 5, while a Palaeontological Association Sylvester-Bradley Award 2007 made possible the field campaign in Patagonia. I am also the grateful recipient of the TCD Julian Boldy Bursary 2007 and a One-Year Postgraduate Award for Continuing Students, which both generously contributed to my living expenses.

Finally, I would like to thank my family, friends and flatmates for their unfailing support throughout this PhD project.

Contents

General headings **Page**

Chapter 1: Introduction

1.1 Overview 1

1.2 Background 1

1.2.1 Trophic enrichment of N and C isotopes 1

1.2.2 Current uses of N and C isotopes in modern ecology 3

1.2.3 Current uses of N and C isotopes in material of archaeological age and older 4

1.3 Thesis outline 6

1.3.1 Primary aim 6

1.3.2 Considerations 7

1.3.3 Wider implications 8

Chapter 2: Green River field area, Wyoming, USA

2.1 Overview 9

2.2 Introduction 9

2.2.1 Background 9

2.2.2 Previous work 11

2.3 Location and geological setting 12

2.3.1 Regional geology 12

2.3.2 Fossil Basin Tertiary strata 14

2.3.3 Geological age 14

2.3.4 Localities 15

2.3.5 Stratigraphy 18

2.4 Micro-scale sedimentary structures 29

2.4.1 Composition of laminae 29

2.4.2 Laminae thickness as a proxy for climatic cycles 29

2.4.3 Evidence of a microbial origin of laminae 30

2.5 Palaeontology 33

2.5.1 Fossil Lake taxa 33

2.5.2 Causes of fish mass mortality events 37

2.5.3 Conditions leading to preservation of mass mortalities 38

2.6 Sampling procedure 42

Chapter 3: Methods
3.1 N and C_{org} stable isotope analysis of fossil samples 43
3.1.1 Sampling and sample treatment 43
3.1.2 Delta notation and reference material 46
3.1.3 Instrumentation and apparatus 47
3.1.4 Analysis of samples with low N concentrations 48
3.1.5 Ascarite modification of EA 51
3.1.6 Experimental amplification of N values 52
3.1.7 Data quality 53
3.2 C and O stable isotope analysis of carbonate samples 54
3.3 X-ray powder diffraction (XRD) analysis of samples 54
3.4 Analysis of whole rock suite and refractory elements 55
3.5 CHN analysis of fossil and carbonate samples 55
3.6 Analysis of lipid biomarkers in fossil and carbonate samples 56
3.6.1 Soxhlet extraction 56
3.6.2 Removal of sulphur 58
3.6.3 Bond Elut® column chromatography 59
3.6.4 Neutral fraction protocol 59
3.6.4.1 Alumina column chromatography 59
3.6.5 Acid fraction protocol 60
3.6.5.1 Saponification 60
3.6.5.2 Acidification 60
3.6.5.3 Methylation 61
3.6.6 Trimethylsilyl (TMS) derivatisation 61
3.6.7 Gas chromatography 62
3.6.8 Gas chromatography-mass spectrometry 63
3.7 Analysis of amino acids in fossil and carbonate samples 63
3.7.1 Hydrolysis 64
3.7.2 Ion exchange chromatography 64
3.7.2.1 Preparation of DOWEX™ ion exchange resin 64
3.7.2.2 Elution using ion exchange columns 65
3.7.3 Esterification 65
3.7.4 Acetylation 65
3.7.5 Gas chromatography 66

3.8 GC-IRMS stable isotope analysis of fossil and carbonate samples 66
3.9 SEM analysis of fossil and carbonate samples 67

Chapter 4: Acid treatment effects on fossil fish skeletal $\delta^{15}N$ and $\delta^{13}C$
4.1 Overview 69
4.2 Introduction 69
4.2.1 Introduction to fossil extraction treatments 69
4.2.2 The nature of this study 70
4.2.3 Common chemical techniques used in microfossil extraction 71
4.2.4 Common chemical techniques used with fossil and modern vertebrates 72
4.2.5 Objectives of this study 73
4.3 Methods 76
4.4 Results 78
4.4.1 Variations in pH 78
4.4.2 Variations in $\delta^{15}N$ 80
4.4.3 Variations in $\delta^{13}C$ 81
4.4.4 Variations in weight 82
4.5 Discussion 83
4.5.1 Variations in pH 83
4.5.2 Variations in isotopic signature and weight 86
4.6 Conclusion 88

Chapter 5: Fossil fish analyses and chemostratigraphy of Fossil Lake
5.1 Overview 91
5.2 Introduction 91
5.2.1 Rationale 91
5.2.2 Trophic system in Fossil Lake 93
5.2.3 Initial stable isotope analyses 95
5.2.4 The nature of preservation in collected specimens 97
5.2.5 Isotopic fractionation between tissues and possible $\delta^{13}C_{carbonate}$ contamination 98
5.2.6 Palaeoproductivity and palaeoenvironmental change 100
5.3 Method 101
5.3.1 Outline of analyses and initial preparation 101

5.3.2 Preservation of differential isotopic fractionation among fossil fish tissues 103
5.3.3 N and C_{org} isotopic analysis of fossil fish plus $\delta^{13}C$ and $\delta^{18}O$ analysis of micrite 104
5.4 Results 105
5.4.1 SEM imaging and EDS microanalysis 105
5.4.2 Preservation of original fractionation of $\delta^{15}N$ and $\delta^{13}C_{org}$ between fish tissues 108
5.4.3 Fossil fish $\delta^{15}N$ and matrix $\delta^{13}C$ and $\delta^{18}O$ from ash plate 110
5.4.4 Fossil fish $\delta^{15}N$ and micrite $\delta^{13}C$ and $\delta^{18}O$ from the RH F-2 stratigraphy 112
5.4.5 Major, trace and rare earth elements from the RH F-2 stratigraphy 114
5.5 Discussion 116
5.5.1 SEM observations and EDS data 116
5.5.2 Fractionation of $\delta^{15}N$ and $\delta^{13}C_{org}$ among fish tissues 117
5.5.3 N and C_{org} content of fossil fish 118
5.5.4 $\delta^{15}N$ isotopic signatures of fish from an ancient ecosystem 119
5.5.5 Interpretation of palaeoenvironment 121
5.5.6 Interpretation of chemostratigraphy 124
5.6 Conclusion 125

Chapter 6: Experimental modelling of post-mortem isotopic variation
6.1 Overview 127
6.2 Introduction 127
6.2.1 Previous work 127
6.2.2 Outline 129
6.3 Experiment design and rationale 131
6.3.1 Independent variables 131
6.3.2 Time scale and sampling intervals 134
6.3.3 Method of euthanasia 135
6.3.4 Storage of extra samples 136
6.4 Method 137
6.4.1 Preparation 137
6.4.2 Sampling and analysis 140
6.5 Results 142

6.5.1 N and C_{org} isotope data from fish samples 142
6.5.2 C:N ratio data from fish samples 148
6.5.3 C and O isotope data from sediment samples 150
6.5.4 Temperature, pH, nitrate and ammonia data from water samples 151
6.5.5 Visual assessment of decay experiments 153
6.6 Discussion 155
6.6.1 Assessment of data from fish 155
6.6.2 Assessment of sediment and water data 158
6.6.3 Limitations of the data set 160
6.7 Conclusion 163

Chapter 7: Biomarkers in Green River fossil fish and sediment samples
7.1 Overview 165
7.2 Introduction to biomarkers and their preservation potential 165
7.2.1 Preservation of biomarkers 165
7.2.2 Lipid preservation 166
7.2.3 Protein preservation 167
7.3 Previous investigations of biomarkers preserved in macrofossils 168
7.4 Biomarker study of Fossil Lake sediments and fish bones 171
7.5 Results and interpretation 172
7.5.1 CHN analyses 172
7.5.2 Fatty acid methyl esters (FAMEs) 173
7.5.3 Apolar fraction 175
7.5.4 Polar fraction 177
7.5.5 GC-IRMS data 177
7.5.6 Amino acid data 177
7.6 Discussion 178
7.6.1 Robustness of results 178
7.6.2 A mechanism for mass mortality in Fossil Lake 179
7.7 Conclusion 181

Chapter 8: N and C isotopes in the Cretaceous Mata Amarilla fossils
8.1 Overview 183
8.2 Introduction 183

8.3 Location and geological setting 185
8.4 Palaeontology and palaeoenvironment 188
8.4.1 Macrofauna 188
8.4.2 Macroflora 190
8.4.3 Suggested palaeoenvironment 190
8.5 Samples for isotopic analyses 191
8.5.1 Sample locations 191
8.5.2 Sample preparation 192
8.5.3 Sample identification 194
8.6 Results of N and C isotope analyses 196
8.6.1 Freshwater samples from the bone bed locality 196
8.6.2 Marine samples from unit 6 197
8.6.3 Dinosaur bone samples from south of Lake Viedma 198
8.6.4 Comparison of N and C isotope results from all samples 199
8.6.5 C:N ratios of all samples 201
8.7 Discussion 202
8.7.1 Possible diagenetic alteration 202
8.7.2 Assessing robustness of data 202
8.7.3 A possible insight from C:N ratios 204
8.7.4 Expected isotopic differences in the data set 205
8.7.5 Possible causes of variation in the data set 207
8.8 Conclusion 208

Chapter 9: Summary of main findings and implications for future work
9.1 Research outcomes 211
9.1.1 Main findings 211
9.1.2 Analytical problems and caveats 212
9.1.3 Implications for future studies 213
9.1.4 Thesis results in context 214
9.2 Suggestions for further work 217
9.2.1 Constraining isotopic shift using compound specific isotope analyses 217
9.2.2 Selection of a fossil ecosystem for future study 218
9.2.3 Proxies for diagenetic alteration of fossil fluorapatite 219
9.2.4 Further work regarding the palaeoenvironment of Fossil Lake 220

9.2.5 Suggestions for future biomarker analyses of Fossil Lake fish 222

References 223

Appendices

Appendix 1

Photographs of Green River fish

Appendix 2

Chapter 4 results tables

Chapter 5 results tables

Chapter 6 ethical approval documentation

Chapter 6 results tables

Chapter 7 additional diagrams

Chapter 7 results tables

List of figures

1.1: Schematic illustration of the stepwise enrichment of $\delta^{15}N$ and $\delta^{13}C$ between species in a simplified food chain. (After DeNiro & Epstein 1978 and 1981). 2

1.2: Stepwise enrichment of $\delta^{15}N$ between species feeding at different trophic levels in an intertidal community in Usujuri, Japan (from Minagawa & Wada 1984). 3

2.1: Map of the Green River Lake Complex during the late Early Eocene (redrawn after Grande and Buchheim 1994), showing present-day state boundaries, capital cities and smaller cities in the vicinity. 10

2.2: Simplified geological map showing the locations of Tertiary basins including Fossil Basin (redrawn after Smith *et al.* 2008), showing present-day state boundaries. 13

2.3: Fossil Lake, enlarged from map in Figure 2.1, showing general locations of F-1 and F-2 quarries in relation to the local topographic high of Fossil Butte (after Grande & Buchheim 1994). 16

2.4: Topographic map with orange circles denoting the locations of quarries where samples were collected from for this study. 17

2.5: A) Stratigraphic section of the exposed split-fish-layer units in quarry RH F-2. 20

B) Stratigraphic section of the exposed split-fish-layer units in quarry RD F-2. 21

C) Stratigraphic section of the exposed split-fish-layer units in quarry CN F-2. 22

D) Stratigraphic section of the exposed strata in quarry SH F-1. 23

E) Stratigraphic section of the exposed 18-inch-layer units in quarry SH F-1. 24

F) Stratigraphic section of the exposed 18-inch-layer units in quarry RH F-1. 25

G) Stratigraphic sections of all units logged in vertical and lateral relation to one another. 27

2.6: Examples of main lithological units. **A)** A typical section of the outcrop at quarry RH F-2 with prominent ash beds labelled. Scale bar 20cm. **B)** A typical section of the 18-inch-layer at quarry SH F-1 with main fossil-bearing beds labelled. 28

2.7: Photomicrographs of laminated strata. 32

2.8: A montage of photographs showing some common and rare finds from the field campaign. 34

2.9: Examples of fish from centre lake and nearshore localities. 36

2.10: Suggested environment of deposition in Fossil Lake leading to fish mass mortalities and their preservation (redrawn after Martill 1988 and Buchheim & Eugster 1998). 41

3.1: Sample preparation using acid. **A)** F-1 specimen RH290713 prior to preparation; **B)** F-1 specimen RH290713 after immersion in acetic acid for a 48 h period. 43

3.2: Precautions were taken to ensure minimal sample contamination. **A)** Over-pressured glove box used in laboratory preparation of fossil samples. **B)** A specially designed fan using a standard 80mm PC fan with filter attachments was sufficient to exclude airborne particulates and eliminate them from the system. 45

3.3: A typical profile for an L-alanine reference sample showing N_2 and CO_2 reference peaks and the measured N_2 and CO_2 peaks at 247.87 seconds and 372.49 seconds, respectively. 48

3.4: A typical graph showing the linearity of L-alanine reference samples of various weights, showing a slight deterioration in linearity below 1000mV. 50

3.5: A graph showing the linearity of samples of internal standard RH260705 of various weights, showing deterioration in linearity below 300mV. 51

3.6: Experimental amplification of N values. 52

3.7: Schematic representation of Soxhlet extraction equipment. 57

4.1: Carbonate contamination of isotope values. **A)** Typical Green River fossil N and C isotope values when all carbonate has been removed from the samples; **B)** Samples where not all carbonate residue was removed, leading to more positive C values due to inorganic carbon contamination. 74

4.2: Fossil specimen used for experimentation. **A)** *Phareodus testis* RH260705 *in situ*, scale bar 5cm; **B)** Some sections of vertebrae from sample RH260705 prior to preparation. 76

4.3: pH values at t_1 for all acids at nine intervals from 1.5 to 768 hours. 79

4.4: $\delta^{15}N$ mean isotope ratios for samples left in acid for a total of 1.5 to 768 hours. 80

4.5: $\delta^{13}C_{org}$ mean isotope ratios for samples left in acid for a total of 1.5 to 768 hours. 81

4.6: Weight at t_1 for samples at nine intervals from 1.5 to 768 hours. 83

4.7: XRD traces of RH260705 aliquots **A)** before and **B)** after being treated with various acids for 84

768 hours.

5.1: Photographs representative of fish species used for these experiments: **A)** *Knightia eocaena*; **B)** *Knightia alta*; **C)** *Diplomystus dentatus*; **D)** *Priscacara liops*; **E)** *Mioplosus labracoides*; **F)** *Phareodus encaustus*. 93

5.2: A large *D. dentatus* preserved with a small *M. labracoides* in its mouth, attesting to the voracity of *Diplomystus*. Such fossils are known locally as 'aspirations'. Specimen from the collection of R. Hebdon. 94

5.3: $\delta^{15}N$ and $\delta^{13}C_{org}$ results from three Eocene fossil fish species used in the pilot study. 96

5.4: The nature of preservation in collected specimens: **A)** *Phareodus encaustus* skull showing premaxilla and dentary; **B)** Close up of *Phareodus encaustus* skull during preparation showing imprint of gill filaments discovered beneath the operculum. 98

5.5: The large ash plate procured for this project with 27 fish from a mass mortality event. 102

5.6: Various SEM images of samples of AP7 and SH270701. 105

5.7: EDS spectra of **A)** fossil fish and **B)** micrite. The fossil fish are all composed of fluorapatite and the micritic matrix is calcium carbonate with few impurities. 106

5.8: Mean $\delta^{15}N$ and $\delta^{13}C_{org}$ values for replicate samples of different tissue types from *P. liops*, *P. encaustus* and *O. mykiss*. 108

5.9: A visual representation of C:N values, showing standard deviation from the mean plus maximum and minimum C:N ratios found in all *O. mykiss*, *P. liops*, and *P. encaustus* tissues. 109

5.10: $\delta^{15}N$ values for 26 fossil fish of 6 separate species from the large ash plate, plotted against the standard length of each fish. 111

5.11: $\delta^{15}N$ values from small clupeomorph fossils collected throughout the RH F-2 stratigraphy, plotted against height above arbitrary quarry base. $\delta^{13}C$ and $\delta^{18}O$ data from whole rock carbonate samples are also shown. 113

5.12: Correlation between: **A)** $\delta^{13}C$ and $\delta^{18}O$ data from carbonate samples, $R^2 = 0.82$; **B)** fossil clupeomorph $\delta^{15}N$ data and $\delta^{18}O$ data from whole rock carbonate samples, $R^2 = 0.07$. 113

5.13: Major element data from ICP-OES analysis of whole rock carbonate samples from throughout the RH F-2 stratigraphy. 114

6.1: To recreate the possible conditions experienced in Eocene Fossil Lake to investigate post-mortem changes in N & $C_{organic}$ isotope signatures in fish, a series of microcosm experiments involving extant fish were devised. 131

6.2: Twelve possible combinations of the three independent variables chosen for these experiments. 134

6.3: Some of the preparation procedures used. 139

6.4: On sampling days each of twelve fish, plus replicates, were dissected and scales, muscle and caudal vertebrae were sampled. These were further sub-sampled and analysed using CF-IRMS. 141

6.5: Graphs showing the $\delta^{15}N$ and $\delta^{13}C_{org}$ mean isotopic ratios for the vertebrae, muscle and scales analysed on each of 10 sampling days, 1 to 192. 145

6.6: Three graphs showing the spread of vertebrae and scales isotopic data for day 192, with the data range at day 1 indicated using grey ellipses. 148

6.7: C:N ratios were determined from the percent element data produced simultaneously with the isotopic measurements. 149

6.8: Sediment **A)** $\delta^{13}C$ and **B)** $\delta^{18}O$ data from samples collected from underneath the decaying fish throughout the experiments. 150

6.9: Samples of water from within each jar were measured at the end of each time period: **A)** Nitrate (NO_3^-) data plotted against time; **B)** Ammonia (NH_3) data plotted against time. 152

6.10: Visual assessment of fish specimens during experiments. 154

7.1: Samples from slab RH270701 prior to treatment. **A)** Fish A and **B)** Fish B. 172

7.2: CHN results for all three samples showing organic carbon and nitrogen values. Nitrogen is not present in the sediment but is present in small amounts in both fish samples. 173

7.3: FAMEs profiles for. **A)** sediment, **B)** Fish A and **C)** Fish B samples. Filled circles indicate straight chain fatty acids, even-over-odd predominance. 174

7.4: Dinosterane is shown to have eluted from the apolar lipid fraction for the sediment sample at 37.86 minutes. Dinosterane structure redrawn from Moldowan *et al.* (2001). 176

8.1: Map showing location of the field area of interest in the Santa Cruz Province, Argentina (redrawn after Iglesias *et al.* 2007). The extent of the Austral Basin is shown in pale blue. 185

8.2: Map showing location of the study area near the town of Tres Lagos and Estancia Mata Amarilla (redrawn after Iglesias *et al.* 2007 and Cione *et al.* 2007). 186

8.3: An outcrop of the Mata Amarilla Formation seen from a distance. The formation consists of repetitively interbedded units of dark and light grey mudstones and massive whitish sandstones. 187

8.4: Schematic stratigraphic section of the Mata Amarilla Formation in the Tres Lagos area showing the location of the bone bed (redrawn after Poiré *et al.* 2004a, Iglesias *et al.* 2007 and Cione *et al.* 2007). 188

8.5: N and C bulk isotope results for samples from the bone bed. 197

8.6: N and C bulk isotope results for samples from unit 6. 198

8.7: N and C bulk isotope results for dinosaur bone fragments DB1 and DB2 found south of Lake Viedma. 199

8.8: Average N and C isotope data for all samples analysed from the Mata Amarilla Formation. 200

8.9: C:N ratios for all samples analysed from the Mata Amarilla Formation. 201

List of abbreviations used

Al_2O_3 – alumina

BF_3 - boron trifluoride

BHPs – bacteriohopanepolyols

BSTFA - N,O-bis(trimethylsilyl)trifluoro-acetamide

CF-IRMS - continuous flow isotope ratio mass spectrometry

CMA - Centre for Microscopy and Analysis

C_{org} - organic carbon

CP – certified pure

DCM – dichloromethane

DDW - Bi-distilled DCM-extracted water

DIW – deionised water

EA – elemental analyser

EDS - Energy dispersive spectroscopy

ENSO - El Niño-Southern Oscillation

FAMEs – fatty acid methyl esters

FTIR - Fourier transform infrared spectroscopy

GC – gas chromatograph

GC-IRMS – gas chromatography isotope ratio mass spectrometry

GC-MS – gas chromatography-mass spectrometry

HCl – hydrochloric acid

IC – inorganic carbon

ICP-MS - inductively coupled plasma mass spectrometry

ICP-OES - inductively coupled plasma optical emission spectrometry

i.d. – internal diameter

iPA – isopropyl alcohol

LOI – loss on ignition

MALDI–MS - matrix-assisted laser desorption/ionization–mass spectrometry

MeOH – methanol

MISS - microbially induced sedimentary structures

MS - mass spectrometry

NaOCl - sodium hypochlorite

Na_2SO_4 - sodium sulphate anhydrous

NCPs - non-collagenous proteins

NH_4OH - ammonium hydroxide solution

OM – organic matter

pK_a – acid dissociation constant

py-GC-MS - Pyrolysis-gas chromatography-mass spectrometry

RBF – round bottomed flask

RSD – relative standard deviation

SEM – scanning electron microscopy

TCD – Trinity College Dublin

TEF - trophic enrichment factor

TEM - transmission electron microscopy

TLE - total lipid extract

TMAH - tetramethylammonium hydroxide

TMS - trimethylsilyl

TOC – total organic carbon

XRD - X-ray powder diffraction

Chapter 1: Introduction

1.1 Overview

The trophic level of organisms feeding within the same ecosystem can be distinguished on the basis of their nitrogen and organic carbon isotopic signature. Various authors have successfully applied this technique to modelling trophic structure in present day and Neogene ecosystems. However, the purpose of this study is to investigate whether the $\delta^{15}N$ and $\delta^{13}C_{org}$ isotope technique could be applied to a much older fossil ecosystem and used to reconstruct the community structure and palaeoecology. The Early Eocene fish of the Green River Formation of SW Wyoming are part of an exceptionally preserved diverse aquatic community and preliminary analyses yielded isotopic signatures comparable to those of modern fish. Specimens were therefore collected from a succession of mass mortality layers to enable further isotopic study of various fish assemblages, coupled with an investigation of the background chemostratigraphy. These results could then be used to infer relationships between organisms and changes in their habitat through time. Several considerations arising in the collection and interpretation of these data were investigated in detail. The wider application of this technique was also explored, particularly in relation to a second, older, fossil assemblage with a very different style of preservation.

1.2 Background

1.2.1 Trophic enrichment of N an C isotopes

The stable isotopes of nitrogen (^{14}N and ^{15}N) and organic carbon (^{12}C and ^{13}C) are fractionated by all animals during the assimilation of food and the creation of new body tissues (DeNiro & Epstein 1978 and 1981). ^{15}N and ^{13}C content increase with trophic level in consumers and the resulting ratio of heavy to light isotopes ($\delta^{15}N$ and $\delta^{13}C$) in tissues define the trophic level occupied by an organism. This increase results from preferential excretion of the lighter ^{14}N and ^{12}C as a by-product of protein synthesis, leaving the animal enriched in ^{15}N and ^{13}C when compared with its diet (Kling *et al.* 1992). Consumers become enriched in $\delta^{15}N$ relative to their food source by approximately 3-4‰ (DeNiro & Epstein 1981; Minagawa & Wada 1984; Peterson & Fry 1987) and enriched in

$\delta^{13}C$ by just 1‰ (DeNiro & Epstein 1978; Peterson & Fry 1987), shown schematically in Figure 1.1. In top predators the concentration of ^{15}N and ^{13}C are therefore at a maximum (Cabana & Rasmussen 1994). As a consequence of this stepwise trophic level enrichment in $\delta^{15}N$, stable nitrogen isotope ratios of consumer tissues represent a time-integrated indicator of relative trophic position, based on the pathways of energy flow (Fry 1988; Kling *et al.* 1992). In general the overall enrichment is a function of body mass, with larger animals at the top of the food chain having much more positive $\delta^{15}N$ signatures than the smaller organisms at the base (Jennings & Mackinson 2003). Using $\delta^{15}N$ data, trophic level can be calculated directly for an entire ecosystem by using one species of a known trophic level as a reference (see Pinnegar *et al.* 2002). An example of the stepwise relationship between $\delta^{15}N$ and trophic level in an ecosystem is shown in Figure 1.2. Because consumers generally have carbon isotope compositions similar to their foods, $\delta^{13}C$ measurements place constraints on the influence of different potential food sources (Kling *et al.* 1992; Hecky & Hesslein 1995; Vander Zanden & Rasmussen 1999).

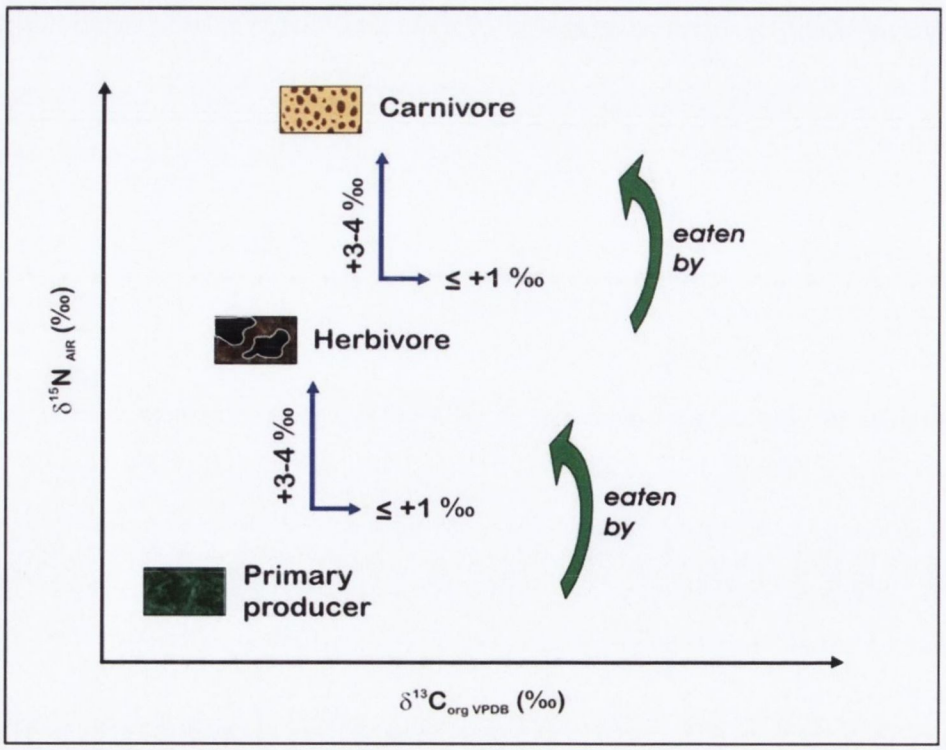

Figure 1.1: Schematic illustration of the stepwise enrichment of $\delta^{15}N$ and $\delta^{13}C$ between species in a simplified food chain. (After DeNiro & Epstein 1978 and 1981).

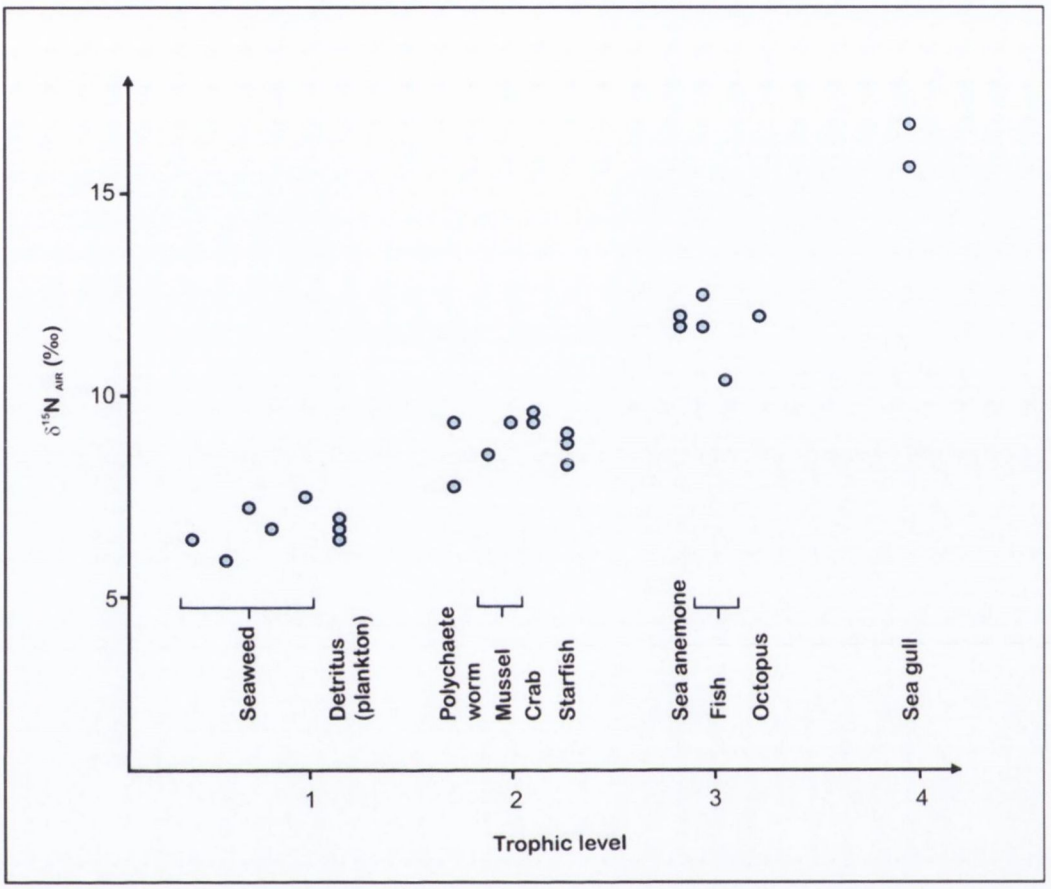

Figure 1.2: Stepwise enrichment of $\delta^{15}N$ between species feeding at different trophic levels in an intertidal community in Usujuri, Japan (from Minagawa & Wada 1984).

1.2.2 Current uses of N and C isotopes in modern ecology

Increasingly, ecologists are utilising stable isotopes from tissues of animals to resolve trophic structure and feeding relationships at the whole-community level. Using these chemical techniques coupled with classical food web studies has proven to be a powerful tool in understanding the interactions of organisms within an ecosystem. Food webs depict the complex trophic interactions inherent among organisms within ecosystems and have traditionally been coupled with analyses of gut content data to decipher predator-prey relationships and food chain length (Post 2005). However, many trophic interactions cannot be visually observed and gut analysis is misleading if the gut contents are not assimilated (Kling *et al.* 1992). Stable nitrogen and organic carbon isotope ratios are increasingly being used to provide time-integrated information about feeding relationships

and energy flow through food webs (see Vander Zanden & Rasmussen 1999 and references therein), negating the use of gut content analyses and circumventing the difficulties in collecting the requisite quantitative dietary data for the many species that interact in a typical food web. Stable isotopes and therefore information regarding trophic level are assimilated into all tissues over the life span of an animal; the isotopic composition of soft tissue reflects the average diet integrated over a length of time usually of the order of weeks to months (Trueman *et al.* 2005; Sakano *et al.* 2005). Tissues can be sampled from live creatures and their isotopic composition can provide detailed information regarding dietary habits and niches previously unknown. The strategy has been particularly useful for gaining information regarding animals whose behaviour is not easily observed, such as sperm whales and giant squid in the deep ocean (e.g. Ruiz-Cooley *et al.* 2004; Cherel & Hobson 2005). Stable isotopes of N and C have also been used to investigate spatial and temporal changes in feeding habits of animals, such as the migratory patterns of fish and birds (e.g. Kline *et al.*1998; Guelinckx *et al.* 2006; Inger *et al.*. 2006), particularly those avian species to which exogenous markers such as satellite tags cannot be applied (see Hobson 2008). This technique does have some limitations however. In aquatic ecosystems, scavenging and benthic organisms that feed on detritus complicate the simplistic model of $\delta^{15}N$ trophic enrichment as the detritus can be derived from different trophic levels, but stable isotopes are still extremely useful in determining diet source of most other organisms (Pinnegar & Polunin 2000).

1.2.3 Current uses of N and C isotopes in material of archaeological age and older

In many isotopic studies of prehistoric animals collagen has been extracted from bone and tooth dentine for nitrogen and organic carbon isotopic analysis in order to interpret human diet source (e.g. Wright & Schwarcz 1999; Drucker & Bocherens 2004; Fischer *et al.* 2007; Hedges & Reynard 2007). In studies of prehistoric organisms the $\delta^{15}N$ and $\delta^{13}C_{org}$ of collagen can then be compared with that of coeval animals in order to determine the percentage contribution of different protein sources to the human diet. The majority of these studies have focussed on terrestrial organisms with relatively few involving fish bones, and even then as a means to interpret human diet (e.g. Schoeninger *et al.* 1983; Bocherens *et al.* 1991; Bonsall *et al.* 1997). Bone and dentine collagen is generally

considered to be a reliable source of both $\delta^{15}N$ and $\delta^{13}C$ when reconstructing diet and palaeoenvironment in archaeological settings (Iacumin *et al.* 2000). The general increase in $\delta^{15}N$ and $\delta^{13}C_{org}$ of animals at successive trophic levels is seen in all tissues produced during the lifetime of the animal and is due to the specific and roughly constant enrichment of the consumer's slow turnover body proteins over their diet (Hedges & Reynard 2007). Any preserved original organic matter should therefore reflect the trophic level within a given ecosystem of all fossil animals due to the biochemical assimilation of dietary components into consumers' tissues during life. N and C isotope values in modern bone apatite and tooth dentine reflect the whole diet including protein, fats, and carbohydrates (Ambrose & Norr 1993). Bone tissues turn over slowly, thus providing the dietary N and C isotope average of at least the last several years of an individual's life, while in mammals tooth dentine does not turn over and thus represents diet composition at the age of tooth formation (Kosiba *et al.* 2007). However, in much older fossils the collagen is presumed to have been degraded within the first 10-30 k.y. post-mortem (Briggs *et al.* 2000), although remnants of organic matter can persist. The majority of studies involving pre-Quaternary fossilised vertebrate organisms have focussed on the analysis of oxygen isotopes from biogenic phosphates for palaeoclimate and physiological reconstruction (e.g. Kolodny *et al.* 1983; Barrick & Showers 1994; Fricke *et al.* 1998; Showers *et al.* 2002). Whether $\delta^{18}O$ values from fossils of geological age are original or the product of diagenetic alteration has been the source of much controversy. In particular, bone and dentine values may not be reliable (see McArthur *et al.* 1987; Longinelli 1996; Blake *et al.* 1997; Trueman *et al.* 2003), although tooth enamel is thought to be more resistant to diagenetic change (Sharp *et al.* 2000). The $\delta^{15}N$ and $\delta^{13}C$ isotopic compositions of bone and dentine from deep time appears to have been overlooked, perhaps due to assumptions that sample fidelity will have been degraded by decay and diagenetic change, although it has long been known that remnant organic matter within crystalline aggregates of hydroxyapatite can survive (DeNiro & Weiner 1988). Subsequent to the inception of this PhD project, two studies utilising $\delta^{15}N$ and $\delta^{13}C_{org}$ values to interpret ancient food webs that include vertebrate organisms have been reported (Schweizer *et al.* 2006 and 2007). Both focus on German Tertiary fossil lagerstätten from

lacustrine ecosystems and conclude that the $\delta^{15}N$ and $\delta^{13}C$ values are valid and can be used to reconstruct trophic structure.

1.3 Thesis outline

1.3.1 Primary aim

The primary aim of this PhD project was to investigate the potential of using nitrogen and organic carbon isotopes to reconstruct feeding habit and trophic structure of an extinct aquatic community. The Eocene Green River Formation of southwest Wyoming, USA, provided an excellent opportunity to sample a fossil ecosystem within a tightly constrained temporal framework. This fossil lagerstätte consists of hundreds of mass mortality events from an ancient lake over a short period of time, preserving mainly fish but also many other fossil animals including insects, amphibians, reptiles, birds and small mammals. A pilot study prior to the field campaign confirmed that $\delta^{15}N$ and $\delta^{13}C_{org}$ data could be retrieved from the Eocene fossil fish, albeit with extremely low N concentrations. In a previous study $\delta^{18}O$ values from lake sediments in the Green River Formation were assumed to be pristine and unaffected by diagenesis or modern meteoric waters (Norris *et al.* 2000), thereby implying that any $\delta^{15}N$ and $\delta^{13}C_{org}$ values obtained are also likely to be unaffected post-deposition. Extensive fieldwork was carried out in order to collect specimens for stable isotopic analysis, with the primary objective of collecting as many fossil species from assumed different trophic levels from one bedding surface, thereby representing a census assemblage of co-existing taxa. By collecting more than one such bedding plane at different stratigraphic levels comparisons could then be made on aspects such as the preservation of isotopic signatures and possible ecosystem and environmental changes over time. Specimens of the same species but at different ontogenetic stages were also targeted to assess whether change of diet with age or 'switching' (*sensu* Richter & Baszio 2006) could be identified from their isotopic composition. Modern day analogues from the literature could then be used to interpret $\delta^{15}N$ and $\delta^{13}C_{org}$ isotope data derived from the fossil material. Previous studies detailing observations of trophic adaptation and gut content from palaeontological specimens could then also be used as an independent test of the veracity of the isotopic data.

1.3.2 Considerations

A thorough investigation of the Green River field area was carried out and is presented in Chapter 2, placing the fossils collected for the main section of this study in context. Several strands of research were then necessary in order to facilitate the primary aim of this project. Firstly, and most importantly, standard mass spectrometry techniques were modified to render them sensitive to the low N concentrations of the fossil material, as discussed in Chapter 3. Secondly, it was imperative that the carbonate matrix in which the fossil samples were interred was removed completely prior to analysis of $\delta^{13}C_{org}$ isotopic signatures. Any inorganic carbonate that remained after preparation would readily mask the $\delta^{13}C_{org}$ signatures retrieved and thus confound interpretations. Via experimentation the best method for removing all traces of carbonate was obtained, while also ensuring that any etching or isotopic alteration of the fossil samples was precluded; these results are presented in Chapter 4. Having successfully obtained $\delta^{15}N$ and $\delta^{13}C_{org}$ values from Eocene fossil fish, the background chemostratigraphy of the ancient lake sediments was also explored to infer context and palaeoenvironment, both discussed in Chapter 5. It was also necessary to investigate potential post-mortem change in extant fish to ensure accurate evaluation of the isotopic data. Little is known regarding the potential isotopic fractionation of N and C in modern organisms after death and during early diagenesis and so a comprehensive suite of laboratory-based taphonomy experiments were undertaken, presented in Chapter 6. All $\delta^{15}N$ and $\delta^{13}C_{org}$ values obtained herein were from bulk sample analyses and consideration was given to the nature of the organic matter in which they were preserved. In an attempt to reconcile the fact that N and C_{org} isotopes could be retrieved from fossil fish of such antiquity, the organic matter was characterised and results are presented in Chapter 7. Finally, as a further test of whether N and C isotopes from fossils could provide useful trophodynamic information, material from a different setting with a different style of preservation was investigated. A fossil aquatic ecosystem from the Cretaceous of Argentina was targeted and the results of isotopic analyses are presented and discussed in Chapter 8. Overall this is a varied study with many component parts which compliment each other and contribute to answering the main research questions.

1.3.3 Wider implications

Detailed food web data and analyses are lacking for many ancient ecosystems, largely because of low taxonomic resolution coupled with uncertain and incomplete information about feeding interactions (Dunne *et al.* 2008). Recent analyses of gut content and bite mark data in Phanerozoic food webs where soft body preservation is extensive have yielded information suggesting that many ancient communities demonstrate a topology remarkably similar to modern food webs (Dunne *et al.* 2008). In ancient communities where morphological detail is lacking and no extant analogues are available, these impediments to resolving trophic interactions are essentially insurmountable at present. However, the indigenous organic fraction of fossils can contain exciting information on the evolutionary biology, palaeoecology, and taxonomy of organisms which can be deciphered using geochemical techniques (Ostrom *et al.* 1994). Nitrogen and organic carbon isotopes measured from this preserved organic matter in fossil organisms could potentially resolve many palaeoecological questions. This is a novel, developing, technique for studying fossils and many facets of its applicability need to be explored and constrained before it can become a mainstream practice. This thesis concentrates on applying the analysis of $\delta^{15}N$ and $\delta^{13}C_{org}$ values to a well-studied ancient ecosystem; the isotopic results obtained could then be confirmed by direct comparison to trophic adaptations of the fish inferred by observation. Proving this technique in a well-documented ancient ecosystem could therefore expand the use of bulk $\delta^{15}N$ and $\delta^{13}C_{org}$ data to reveal trophic interactions within other more poorly known fossil ecosystems, especially those that lack living equivalent species (e.g. Burgess Shale fauna or conodont animals). The bulk techniques used herein can be applied readily without the requirement of complicated chemical extraction and preparation procedures. The successful development of the procedures described herein will lead to an economic and viable method for rapid palaeoecological analysis pertinent to numerous fossil locations worldwide, providing palaeobiologists with a new tool to study ancient ecosystems.

Chapter 2: Green River field area, Wyoming, USA

2.1 Overview

The Green River Formation of southwest Wyoming, USA, contains abundant well-preserved fossil organisms that thrived during the Eocene. The formation represents a system of three lakes that existed in intermontane basins during the Early and Middle Eocene (Bradley 1963); Fossil Lake was the smallest and the deepest of the three (Grande 1984) with a maximum area of deposition of 60km by 30km (Buchheim 1994a). This extinct lacustrine community thrived for several million years (Grande and Buchheim 1994), deposited within finely laminated carbonate beds that now yield many thousands of fossil fish every year, often preserved in mass mortality layers. Fossil Lake provides an excellent locality for this study by virtue of its accessibility, the diversity of preserved species it contains and the geologic context provided by a long history of previous studies. This research aims to complement these previous investigations and to provide a more complete picture of the palaeoecology and depositional environment of Fossil Lake. A variety of specimens were collected from different stratigraphic levels in the lake and from the different fossil communities found there.

2.2 Introduction

2.2.1 Background

To investigate whether the stable isotopes of nitrogen and organic carbon can be used to identify trophic level in an extinct fossil ecosystem, the fish of the Eocene Green River Formation in Wyoming, USA, were targeted for sampling. In order to understand more about their palaeoenvironment, whole rock samples were also collected for geochemical analysis and detailed sedimentary logging was carried out in the field. Fossil fish from the Green River Formation are known internationally for their abundance and outstanding preservation. The three main lakes, Lake Uinta, Lake Gosiute and Fossil Lake, are shown in Figure 2.1 with their approximate areal extent as they would have appeared in the late Early Eocene. The three freshwater lakes formed in a series of intermontane basins in the central Rocky Mountains, USA, and supported a varied and abundant flora and fauna (Grande 1984). This study focuses on Fossil Lake, the smallest and deepest of the three,

with laminated freshwater carbonate beds that are now quarried commercially every year, yielding many thousands of fossil fish. The area that was once occupied by Fossil Lake is situated in south western Wyoming, to the west of the city of Kemmerer (population ~3000). Approximately 24km west of Kemmerer towards the centre of the Fossil Lake deposits stands the topographic high of Fossil Butte National Monument, home to a unit of the National Park Service with public information regarding the palaeontology of the area and a small display of fossils. In this sparsely populated area with rugged terrain there are extensive outcrops of the Fossil Lake strata although most are on federal land, with private or state-leased commercial quarries that yield large numbers of fossil fish. The scientific quarry at Fossil Butte National Monument is available to palaeontologists from outside the National Park Service, however better exposures are available on private land,

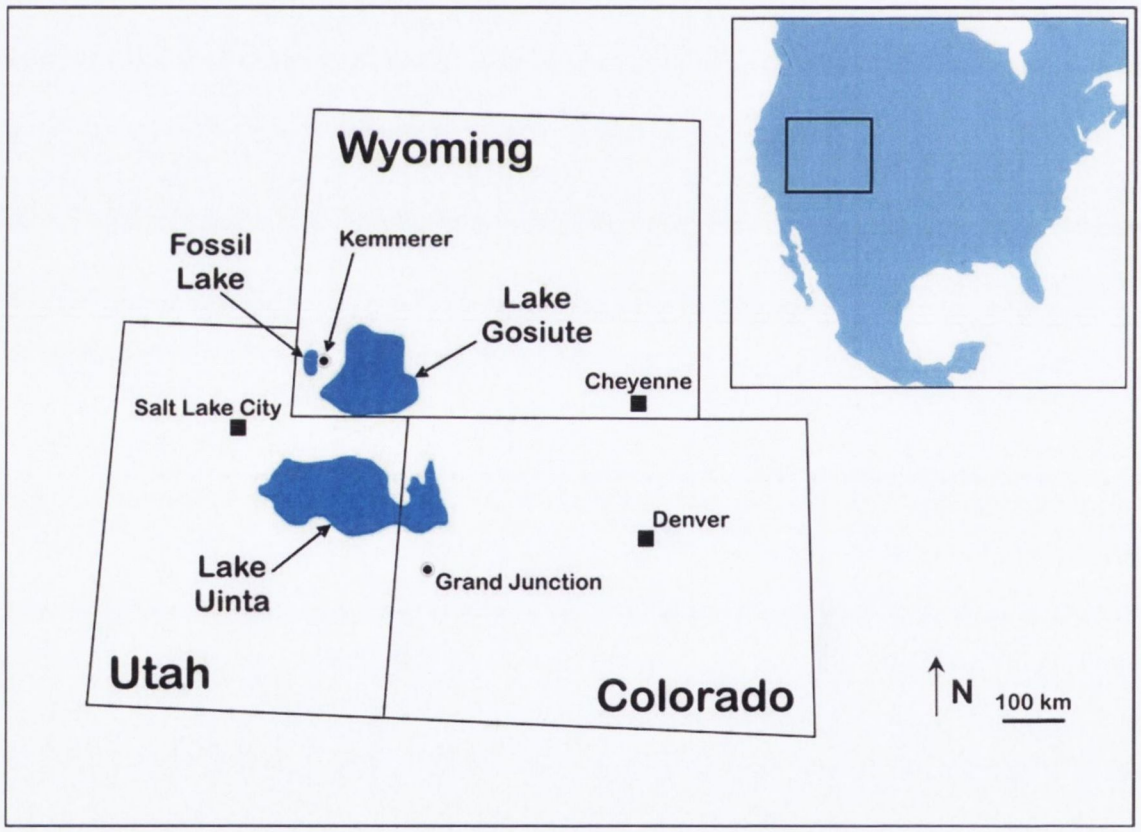

Figure 2.1: Map of the Green River Lake Complex during the late Early Eocene (redrawn after Grande and Buchheim 1994), showing present-day state boundaries, capital cities and smaller cities in the vicinity.

therefore commercial quarry owners and managers were contacted regarding access and specific sections then targeted for specimen collection. Commercial quarries have been operating in the area since the late 19th century and many thousands of the common fossil fish as well as other rare fossils from the area are now held in both public and private collections around the world.

2.2.2 Previous work

The greater Green River Basin was explored as early as 1807 with the first map showing the major geographic features produced in 1837 (Roehler 1992). Hayden (1869) named the Green River and Wasatch formations and mentioned the vast quantities of fossil fish that could be found within the Green River Formation, many of which were found during construction of the Union Pacific Railroad through the area. Pioneering descriptions of the palaeontology were underway at this time with several small papers on the fossil fish being published by Leidy (1856) and Cope (1877; 1878). Two large volumes published by Cope in 1884 regarding Tertiary vertebrates of the western USA contain references to three localities of Green River fish, including the 'Twin Creek' locality which is now known as Fossil Butte. Most of the early geological investigations were concentrated on the wider Green River Basin area, with the smaller Fossil Lake to the west not studied in detail until the early 1900s, although the geology of Fossil Butte itself had been reported as early as 1879 (McGrew and Casilliano 1975). Veatch (1907) and Schultz (1914) carried out the main pioneering geological investigations of the Fossil Lake area, with Bradley first investigating the palaeoenvironment and fossil fish preservation there in 1948. However, it was not until 1970 that formal descriptions of the geological units making up Fossil Lake were published by Oriel & Tracey in their seminal report, subdividing the Green River Formation in the basin into the Fossil Butte and Angelo Members (Oriel & Tracey 1970). Since that time major contributions to our understanding of the geology and palaeoecology of the basin have been made by Buchheim (e.g. 1994a; 1994b; 1998), with extensive studies of the fish fauna being made by Grande (1984; 2001; 2008). This study complements these earlier investigations and provides a more detailed picture of the depositional environments and the palaeoecology of two specific geological sections within Fossil Lake. Both sections contain abundant well-preserved fauna and some flora

and, according to the informal divisions proposed by Buchheim (1994a), are located in the middle unit of the Fossil Butte Member of the Green River Formation.

2.3 Location and geological setting

2.3.1 Regional geology

The Eocene Green River Formation was deposited in a series of continental basins in Utah, Colorado and Wyoming, USA (Figure 2.2), and formed in an area of regional compressional tectonics related to the Sevier and Laramide orogenies (see DeCelles 2004 for an exhaustive review of the Cordilleran thrust belt and foreland basin evolution). The freshwater lake system that formed within the continental basins covered more than 110,000km^2 at its maximum extent (Bohacs *et al.* 2002). The fault bounded basins in which Lake Uinta and Lake Gosiute formed occupy the segmented foreland province to the east of the Cordilleran fold and thrust belt (Smith *et al.* 2008) which comprises Palaeozoic to Mesozoic lithologies (Buchheim & Eugster 1998). Fossil Lake occupied a small, elongate intermontane basin known as Fossil Basin within the eastern margin of the fold and thrust belt, with the long axis trending approximately north-south (Smith *et al.* 2008). Fossil Basin is located between latitude 41°25' and 42°20' N and longitude 110°53' to 110°35' W and occupies approximately 1800km^2 of counties Lincoln and Uinta in southwest Wyoming (Oriel & Tracey 1970). The basin is bounded by faults of the Tunp Range to the west, in the north unnamed en echelon ridges east of the Crawford Mountains and in the south is bound by the Uinta Mountain range (McGrew & Casilliano 1975). The eastern margin of the basin is bound by the topographic high of Oyster Ridge which formed a barrier between Fossil Basin and the Green River Basin to the east during deposition of many of the Tertiary units (Oriel & Tracey 1970). Strike-elongate extensional basins in the area such as Fossil Basin are generally thought to contain 2-5km thick packages of alluvial and lacustrine strata (Constenius 1996). The Eocene lake system is thought to have developed primarily due to exposure of erosion-resistant lithologies within cores of Laramide uplifts, allowing widespread and prolonged deposition of organic-rich lacustrine mudstone (Carroll *et al.* 2006). Calc-alkaline volcaniclastic materials from the Absaroka and Challis volcanic fields, to the north and northwest respectively, regularly contributed to the basin infill forming thin tuff partings in the

lakefloor sedimentation (Chandler 2006). The Green River Formation within Fossil Basin gently dips by a few degrees forming an asymmetrical syncline trending northeast that is most evident in the southeast corner of the basin (Buchheim & Eugster 1998).

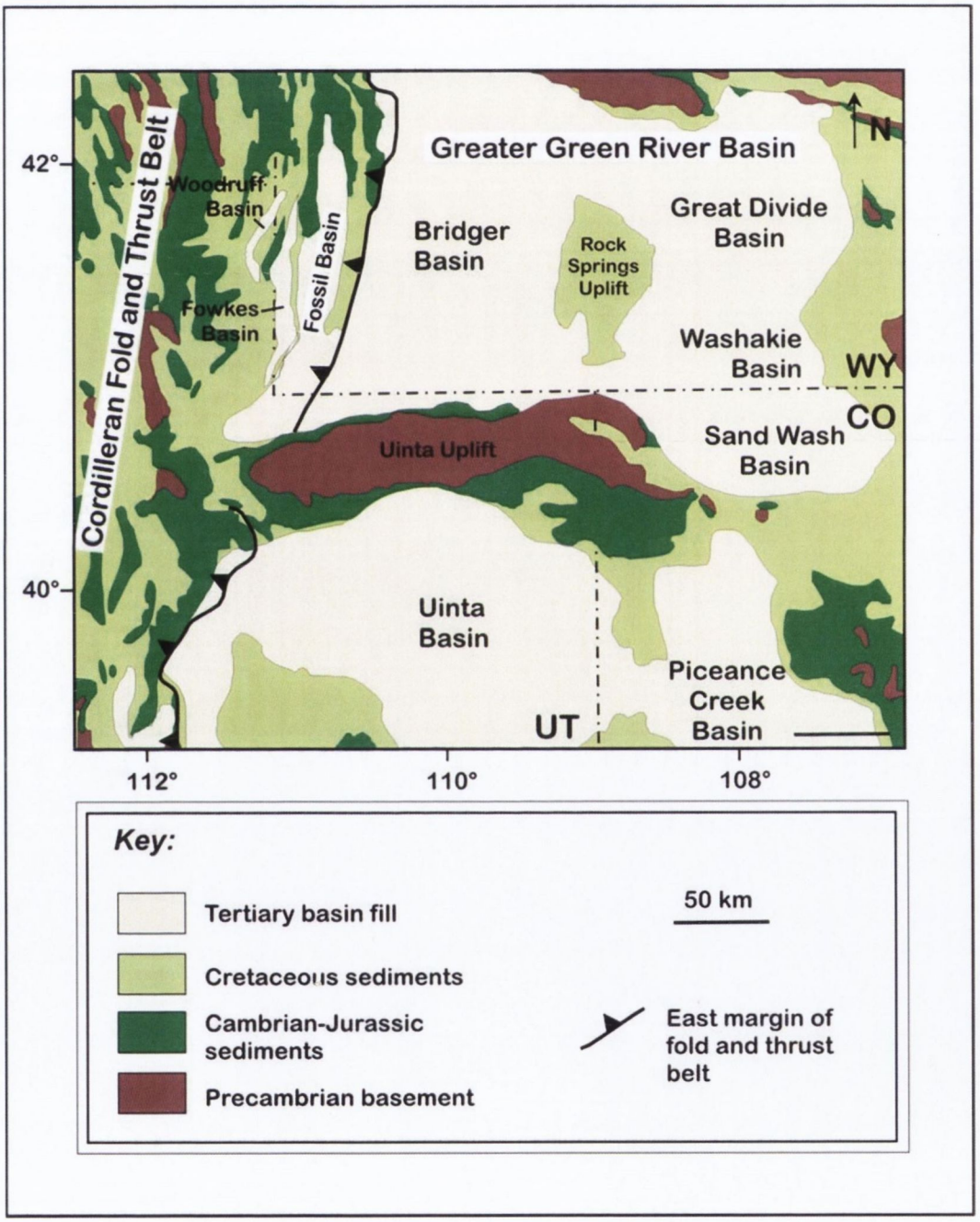

Figure 2.2: Simplified geological map showing the locations of Tertiary basins including Fossil Basin (redrawn after Smith *et al.* 2008), showing present-day state boundaries.

2.3.2 Fossil Basin Tertiary strata

Within Fossil Basin two main units are recognised as having been deposited in Fossil Lake, namely the Fossil Butte Member (60-80m thick at the lake centre) and the overlying Angelo Member (~60m thick at the lake centre), delineated by Oriel & Tracey (1970). The fluvio-lacustrine to fluctuating profundal Fossil Butte Member overlies an early stage of the alluvial Wasatch Formation and is in turn overlain by the evaporative Angelo Member thus demonstrating a gradual basin infill sequence (Smith *et al.* 2008). The alluvial Bullpen Member of the Wasatch Formation overlies all of the aforementioned members, filling in Fossil Lake (Buchheim & Eugster 1998; Buchheim *et al.* 2004). Buchheim (1994a) informally divided the Green River Formation of Fossil Lake into a lower, middle and upper unit, with the majority of the upper unit being equivalent to the Angelo Member. The lower unit is dominantly bioturbated micrite, the middle unit laminated micrite and the upper unit laminated dolomicrite and siliclastic mudstone (Buchheim & Eugster 1998). These designations reflect three distinctive phases of Fossil Lake with the lower unit characterised by localised subsidence and frequent fluvial dominated events interpreted as a balanced to over-filled lake sequence. The middle unit represents the maximum high stand of Fossil Lake marked by a distinctive climate transition to a wetter climate and balanced to over-filled lake conditions, supporting diverse fish faunas (Buchheim *et al.* 2002). The upper unit or Angelo Member was characterised by a drier climate and a hypersaline, under-filled lake devoid of life, except for a few fresh periods when isolated fish populations returned (Buchheim *et al.* 2002). Throughout the depositional history of Fossil Lake, lake size and depth were controlled by the interplay of sedimentation, precipitation/evaporation and subsidence rates (Buchheim *et al.* 2004). Quaternary uplift and erosion has resulted in the present day dissected topography of the area with occasional alluvium deposits (Chandler 2006).

2.3.3 Geological age

Palynological studies support a late Early Eocene (Ypresian, 55.8-48.6±0.2 Ma) to early Middle Eocene (Lutetian, 48.6-40.4±0.2 Ma) age for the Green River Formation in Fossil Basin (Cushman 2002). This is corroborated by mammal evolution ages which indicate a Lostcabinian age (mid-Ypresian) for the top of the Wasatch Formation and the overlying

Fossil Butte Member (Ambrose *et al.* 1997; Froehlich & Breithaupt 1998). Radiometric dating of a potassium feldspar tuff from the top of the middle unit by Buchheim & Eugster (1998) gave an age of 50.2±1.9 Ma. More recent $^{40}Ar/^{39}Ar$ dating of sanidine and biotite from a tuff layer within the Fossil Butte Member gave a similar age of 51.66±0.17 Ma (Smith *et al.* 2008), confirming the preceding age ranges. Smith *et al.* (2008) further suggest that the fluvial-lacustrine phase during deposition of the Fossil Butte Member occurred around 53 Ma, changing to fluctuating profundal by 51.5 Ma, with Fossil Lake finally entering the evaporative Angelo Member phase at 50.5 Ma. Fossil Lake was much shorter-lived than the larger lakes in the wider Green River area as well as having the smallest surface area; however it was deepest of the three lakes during much of its existence (Grande 1984).

2.3.4 Localities

In Fossil Lake the majority of the fossil fish are found in five main micritic facies within the Fossil Butte Member in the middle unit of the Green River Formation. Two of these facies were targeted for sampling in commercial fossil quarries that operate in the area, near to the present-day topographic high of Fossil Butte which lies several kilometres to the north of the main depocentre of Fossil Lake (Buchheim & Eugster 1998) as shown in Figure 2.3. As defined by Grande & Buchheim (1994), F-1 and F-2 denote open lacustrine and more marginal lacustrine facies respectively, known locally as the '18-inch-layer' (F-1) and the 'split-fish-layer' (F-2). F-1 deposits are thought to be stratigraphically above F-2 deposits by only one or two metres (Grande & Buchheim 1994), however it should be noted that on the scale of this study 2m is a large stratigraphic thickness. The open lacustrine facies (F-1) is characterised by kerogen-rich to kerogen-poor finely laminated micrites containing well-preserved fish, plant material, ostracods, gastropods and amorphous kerogen produced by algae (Biaggi & Buchheim 1999). Nearshore carbonates (F-2) consist of finely laminated kerogen-poor micrites containing well-preserved fish, ostracods and occasional vertebrate bones (Grande 1984). Both F-1 and F-2 sections are interspersed with frequent ash beds, now weathered to limonitic clays. Some differences in preservational style between the two facies were noted in the field, particularly the darker appearance of the F-1 fish. A strong bituminous odour emanates from the more

kerogen-rich beds, particularly when being broken apart during palaeontological prospecting.

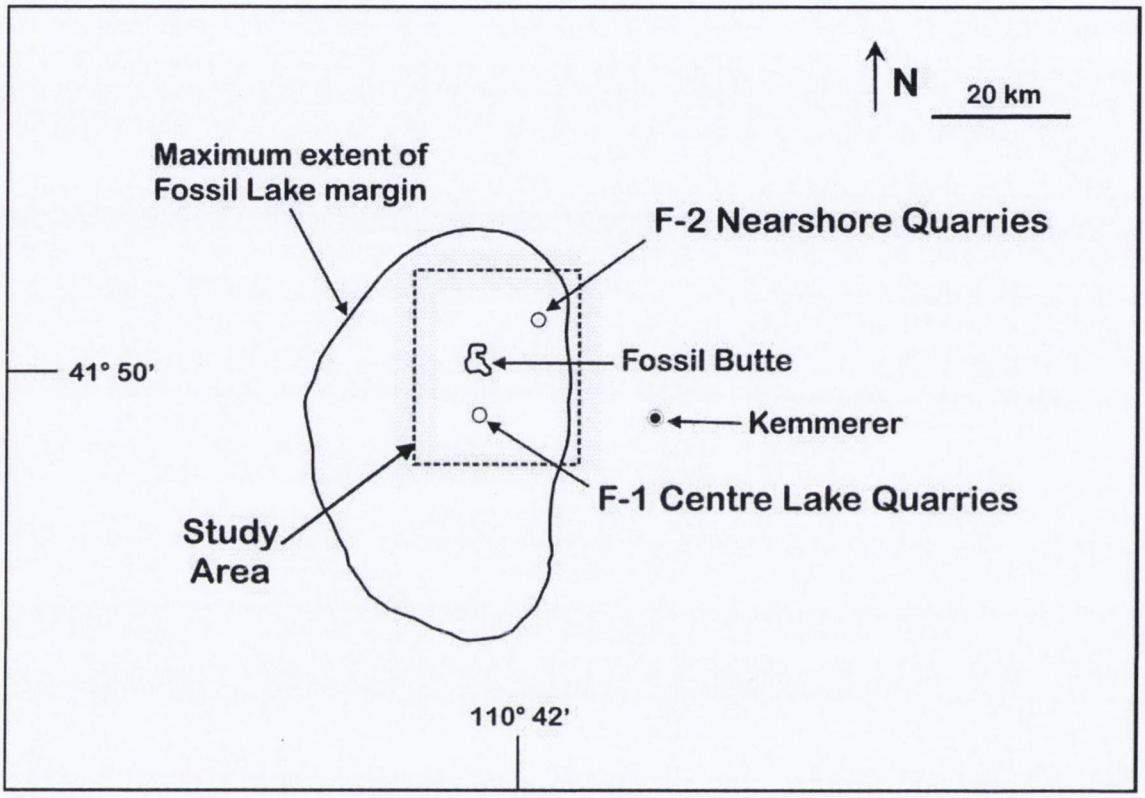

Figure 2.3: Fossil Lake, enlarged from map in Figure 2.1, showing general locations of F-1 and F-2 quarries in relation to the local topographic high of Fossil Butte (after Grande & Buchheim 1994).

Five different commercial quarries were targeted for sampling, including both F-1 centre lake and F-2 nearshore fish-bearing facies. For the locality names in this study the F-1 and F-2 terminology of Grande (1984) were used for each quarry, including a prefix of the initials of the quarry proprietor or specific locality. The locations of the five quarries labelled SH F-1, RH F-1, RH F-2, RD F-2 and CN F-2, all in the vicinity of Fossil Butte National Monument, are shown in Figure 2.4. All of these quarries are located at topographically high elevations and are accessible by four wheel drive off-road vehicles. Different quarries favour different strata depending on which are the most locally productive for fossil fish. No continuous vertical sections were available for study and although F-1 localities are thought to be stratigraphically above F-2 localities by only one

Fossil Butte Member (Ambrose *et al.* 1997; Froehlich & Breithaupt 1998). Radiometric dating of a potassium feldspar tuff from the top of the middle unit by Buchheim & Eugster (1998) gave an age of 50.2±1.9 Ma. More recent $^{40}Ar/^{39}Ar$ dating of sanidine and biotite from a tuff layer within the Fossil Butte Member gave a similar age of 51.66±0.17 Ma (Smith *et al.* 2008), confirming the preceding age ranges. Smith *et al.* (2008) further suggest that the fluvial-lacustrine phase during deposition of the Fossil Butte Member occurred around 53 Ma, changing to fluctuating profundal by 51.5 Ma, with Fossil Lake finally entering the evaporative Angelo Member phase at 50.5 Ma. Fossil Lake was much shorter-lived than the larger lakes in the wider Green River area as well as having the smallest surface area; however it was deepest of the three lakes during much of its existence (Grande 1984).

2.3.4 Localities

In Fossil Lake the majority of the fossil fish are found in five main micritic facies within the Fossil Butte Member in the middle unit of the Green River Formation. Two of these facies were targeted for sampling in commercial fossil quarries that operate in the area, near to the present-day topographic high of Fossil Butte which lies several kilometres to the north of the main depocentre of Fossil Lake (Buchheim & Eugster 1998) as shown in Figure 2.3. As defined by Grande & Buchheim (1994), F-1 and F-2 denote open lacustrine and more marginal lacustrine facies respectively, known locally as the '18-inch-layer' (F-1) and the 'split-fish-layer' (F-2). F-1 deposits are thought to be stratigraphically above F-2 deposits by only one or two metres (Grande & Buchheim 1994), however it should be noted that on the scale of this study 2m is a large stratigraphic thickness. The open lacustrine facies (F-1) is characterised by kerogen-rich to kerogen-poor finely laminated micrites containing well-preserved fish, plant material, ostracods, gastropods and amorphous kerogen produced by algae (Biaggi & Buchheim 1999). Nearshore carbonates (F-2) consist of finely laminated kerogen-poor micrites containing well-preserved fish, ostracods and occasional vertebrate bones (Grande 1984). Both F-1 and F-2 sections are interspersed with frequent ash beds, now weathered to limonitic clays. Some differences in preservational style between the two facies were noted in the field, particularly the darker appearance of the F-1 fish. A strong bituminous odour emanates from the more

kerogen-rich beds, particularly when being broken apart during palaeontological prospecting.

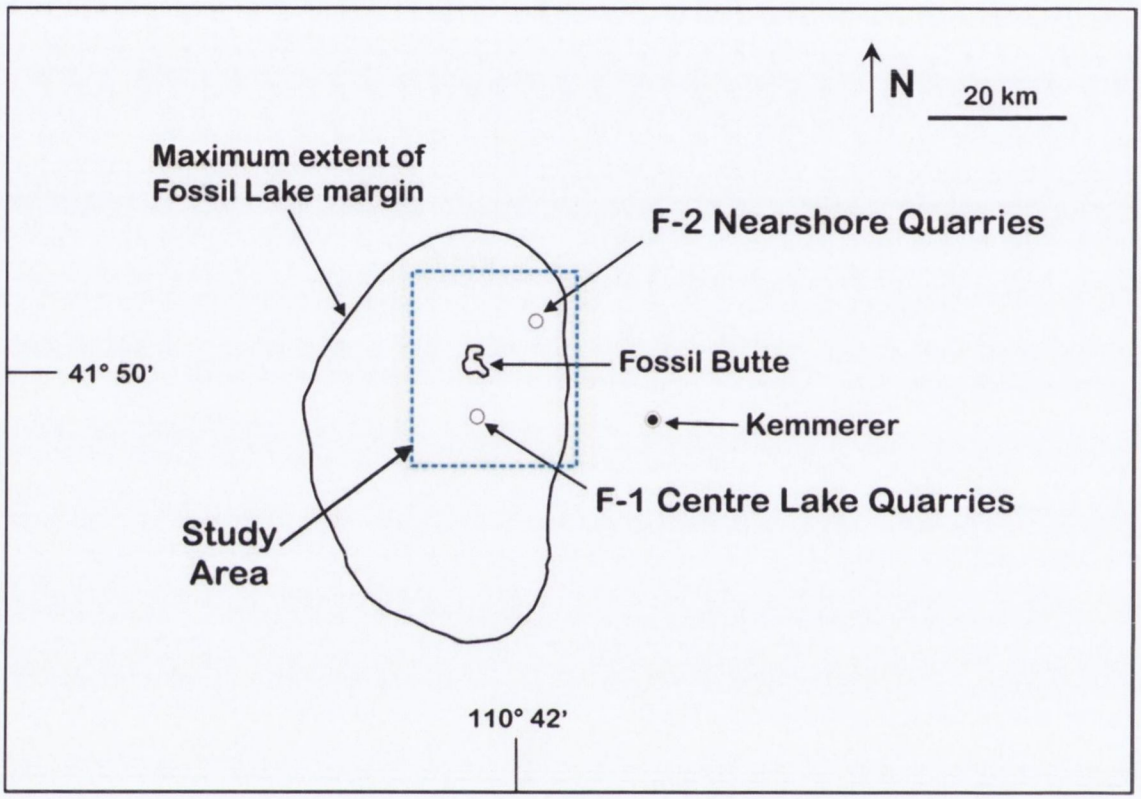

Figure 2.3: Fossil Lake, enlarged from map in Figure 2.1, showing general locations of F-1 and F-2 quarries in relation to the local topographic high of Fossil Butte (after Grande & Buchheim 1994).

Five different commercial quarries were targeted for sampling, including both F-1 centre lake and F-2 nearshore fish-bearing facies. For the locality names in this study the F-1 and F-2 terminology of Grande (1984) were used for each quarry, including a prefix of the initials of the quarry proprietor or specific locality. The locations of the five quarries labelled SH F-1, RH F-1, RH F-2, RD F-2 and CN F-2, all in the vicinity of Fossil Butte National Monument, are shown in Figure 2.4. All of these quarries are located at topographically high elevations and are accessible by four wheel drive off-road vehicles. Different quarries favour different strata depending on which are the most locally productive for fossil fish. No continuous vertical sections were available for study and although F-1 localities are thought to be stratigraphically above F-2 localities by only one

or two metres (Grande & Buchheim 1994) this could not be confirmed during the field campaign. At all of the quarries targeted for this study just a small section of the middle unit within the Fossil Butte Member is exposed, with only SH F-1 having good exposure of other strata albeit those of the upper middle unit. The majority of fish fossils collected for this study were from localities SH F-1 and RH F-2 due to their accessibility, high fossil yield and locally well known stratigraphy. Fossil fish are ubiquitous in both of these

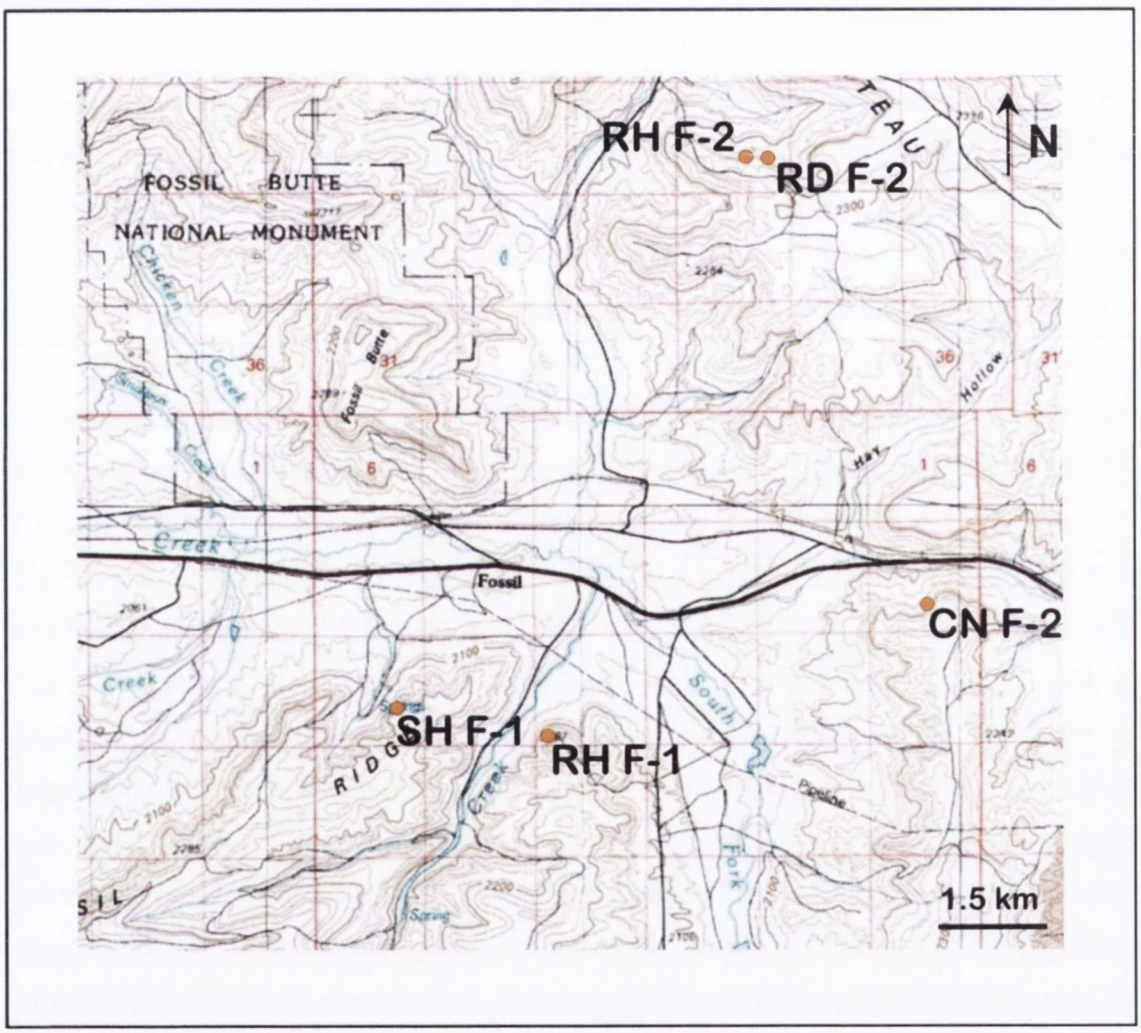

Figure 2.4: Topographic map with orange filled circles denoting the locations of quarries where samples were collected for this study. (Topographic map taken from USGS Fossil Quadrangle, Lincoln County, Wyoming available at www.topozone.com).

locations in the 18-inch-layer (SH F-1) or split-fish-layer (RH F-2) beds and these have been quarried commercially during the summer months for the past few decades. Elevations of all five quarries visited are at more than 2000m above sea level and as such the climate in this arid high desert region (see Knight 1994) precludes fossil collection at any other time of year. Access to locality RH F-1 was further restricted to the end of the summer due to eagle nesting times as directed by wildlife laws. Both localities SH F-1 and RH F-2 support thriving businesses and fossils are retrieved by hand using hammers and chisels once units have been exposed using heavy plant earth moving equipment.

2.3.5 Stratigraphy

Detailed sedimentary logging of the exposed sections in the five different quarries was carried out in Wyoming and all logs are presented in Figure 2.5 A-G. The sediments are extremely fine grained and variations in grainsize could not be distinguished in the field. Each quarry was assigned an arbitrary base to the section and all beds were measured in relation to this. In all five quarries the bedding planes and laminae appear to be horizontal. The quarries RH F-2, RD F-2 and CN F-2 have up to 2.6m of exposed split-fish-layer beds, also known as the 'lower sandwich beds' due to the frequent thin orange/red limonitic clay layers from volcanic ash fall. These clay layers of altered ash are present throughout, with a maximum thickness of 40mm in these three quarries although most are less than 5mm thick. Easily distinguished thicker ash layers have been named locally and this nomenclature is used herein. The remaining lithologies in the F-2 quarries are not readily distinguished, being consistently fine-grained, kerogen-poor, pale buff-coloured (greyish-yellow) micrites with fine laminations. There is a complete absence of any bioturbation or soft sediment disturbance in most beds. With the use of hand tools the micrite parts easily along the laminations often revealing exceptionally preserved fossil fish along with frequent coprolites and fish scales. The laminae tend to split along the centre of the fossils, meaning that the fossil fish are collected as negative and positive halves of each specimen. The exposed units are frequently jointed although slabs of up to a metre in length were retrieved from quarry RH F-2. This jointing meant that specimen retrieval was more problematic in quarry RD F-2, often leading to only partial specimens being recovered. Quarry CN F-2 was much less productive for fossil fish retrieval with

poor exposure and was frequently jointed into much smaller blocks with offsets of up to 30cm. It was possible to log the stratigraphy and measure the units between the most distinctive ash layers by removing the overburden, but the damp underlying rocks did not split easily along laminae. As such prospecting for fossil fish was discontinued in this quarry. A photograph of a typical section of outcrop at quarry RH F-2 is shown in Figure 2.6 A.

In the 18-inch-layer beds the ash layers continue but are generally much finer and less than 1mm in thickness with the exception of the 1cm thick black and white 'salt and pepper ash' layer which marks the base of this unit. The 18-inch-layer is also jointed but on a much larger scale and slabs can be retrieved that are up to several metres in length. This layer is characterised by kerogen-rich to kerogen-poor finely laminated micrites, and these are observed as frequently alternating laminae, again with notable absence of any bioturbation or soft sediment disturbance. The rocks are much harder than those in the F-2 quarries and can be split along finer partings, where well-preserved fish and plant material are frequently found, as well as many coprolites and occasional insects. However, the layers often split just above or below fossils, meaning that the specimens from the F-1 quarries are collected covered in a fine layer of hard micrite up to a few mm thick which must be removed using percussion tools and micro-abrasive blasting equipment in the laboratory to reveal the specimen. It should be noted that the F-1 fish-bearing layer is actually thicker than 18″ in the centre of the lake, usually around 22″, or 56cm, as observed in SH F-1. The base of this unit is delineated by the black and white ash layer as well as the underlying lower oil shale; a very dense, hard black kerogen-rich micrite which is followed by a thin parting known locally as the 'fly layer' due to the large volume of insects found at this level. Other beds are difficult to distinguish but can be measured reliably from these lower units, or from the upper distinctive 'top capping' which has a mottled red or purple appearance and a characteristic sheen, in order to locate the main fossil-bearing levels. Fossil fish can however be found on parting any laminae within the 18-inch-layer. A photograph of a typical section of the 18-inch-layer at quarry SH F-1 is shown in Figure 2.6 B.

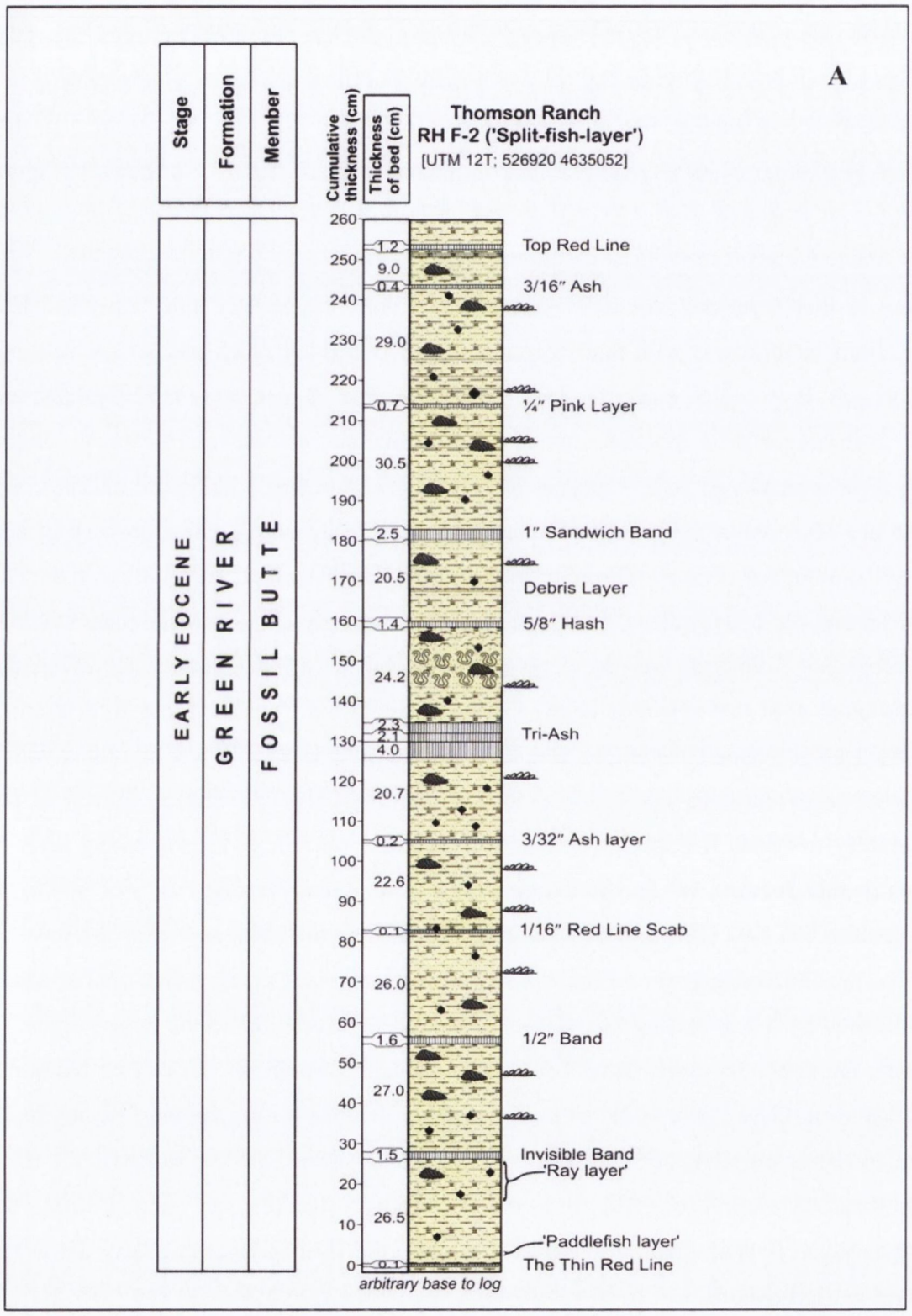

Figure 2.5: A) Stratigraphic section of the exposed split-fish-layer units in quarry RH F-2.

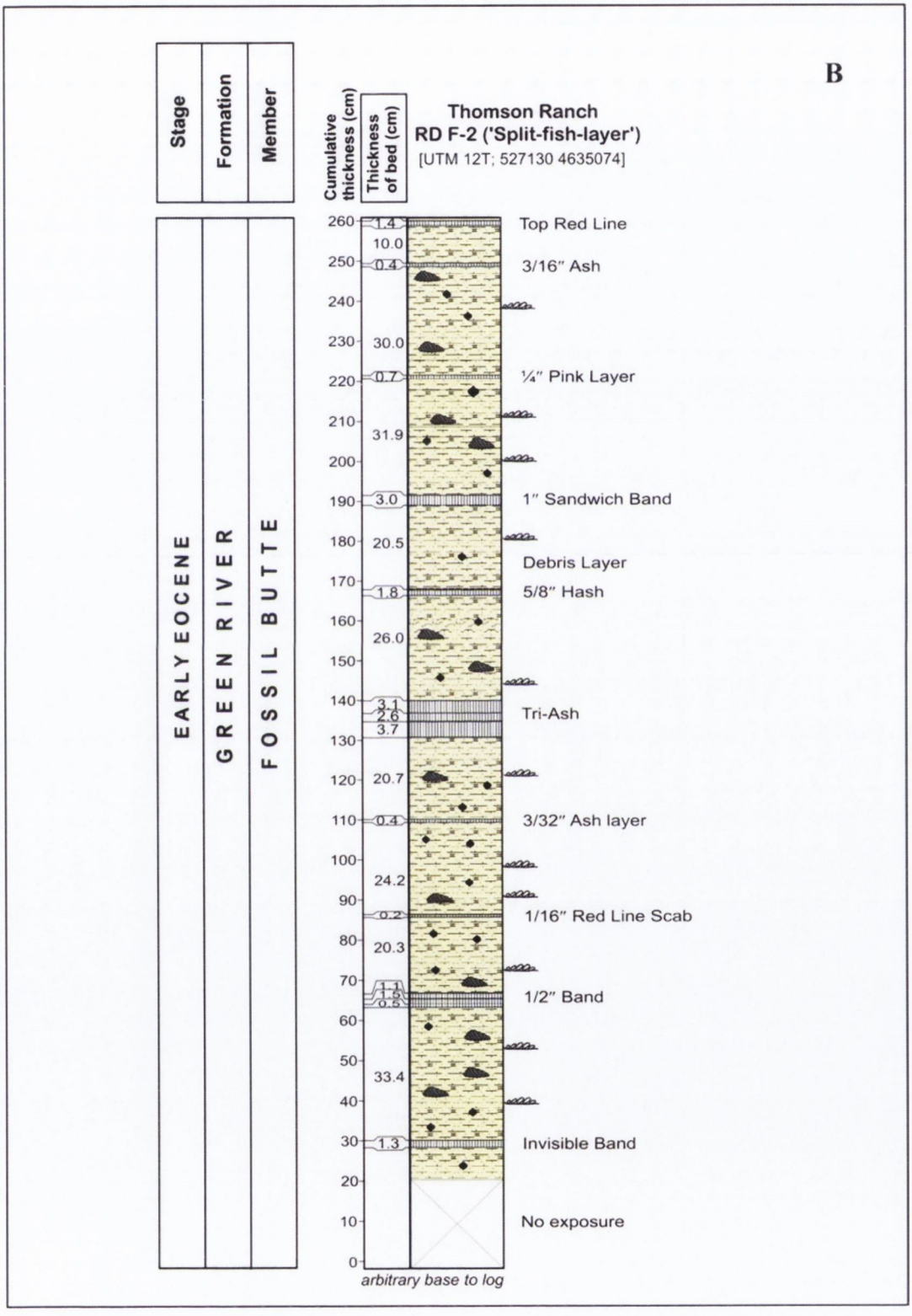

Figure 2.5: B) Stratigraphic section of the exposed split-fish-layer units in quarry RD F-2.

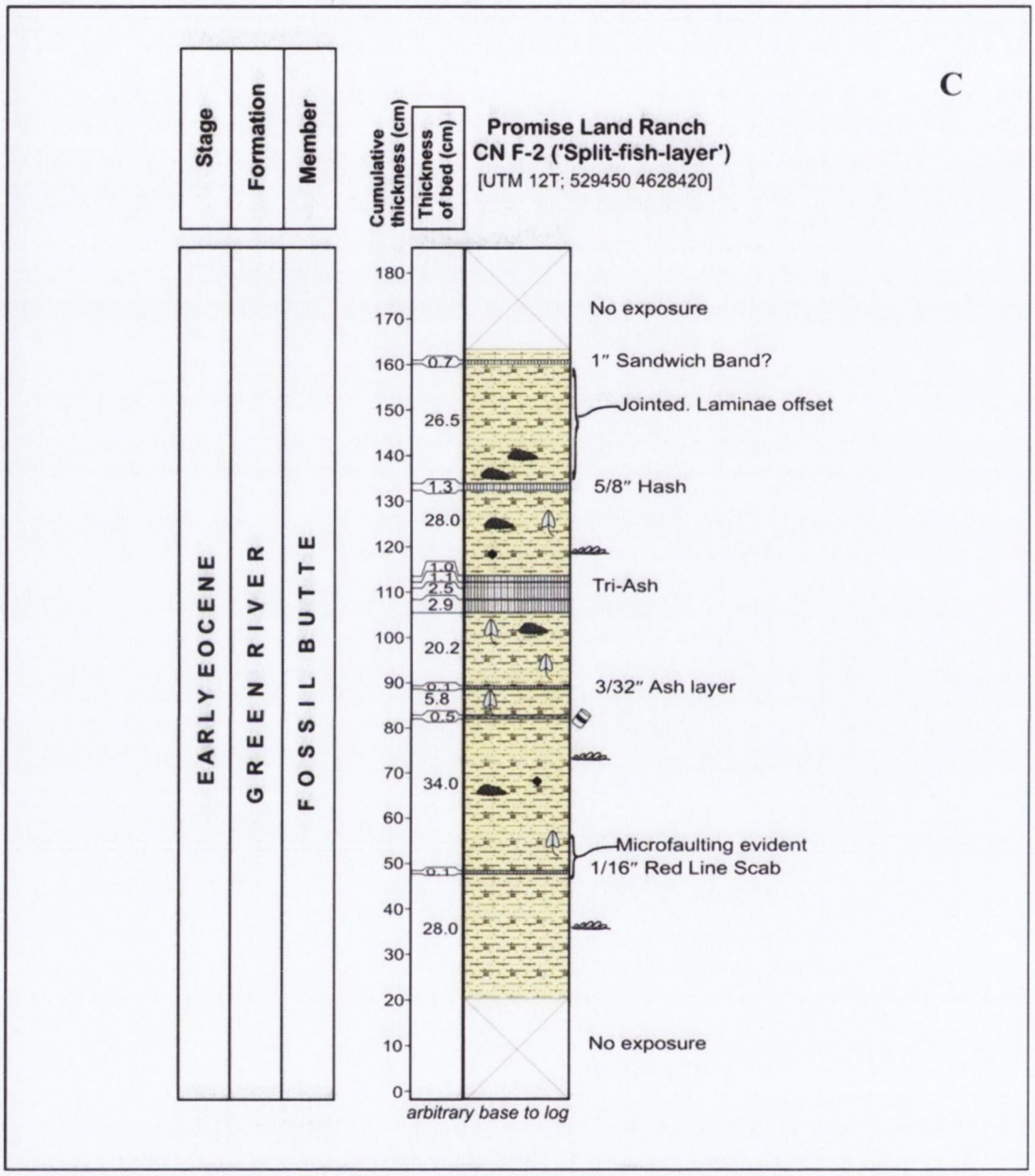

Figure 2.5: C) Stratigraphic section of the exposed split-fish-layer units in quarry CN F-2.

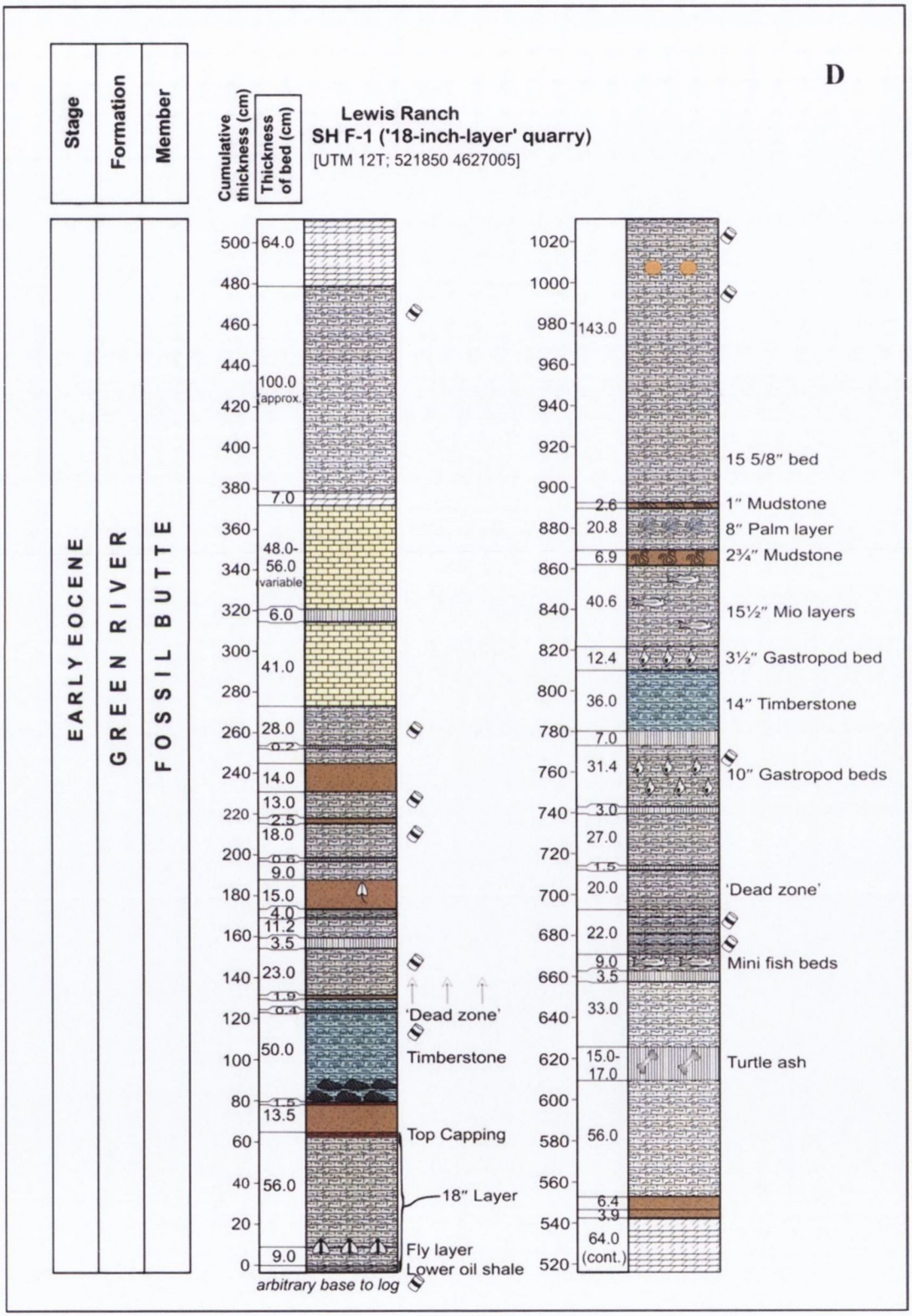

Figure 2.5: D) Stratigraphic section of all exposed strata in quarry SH F-1.

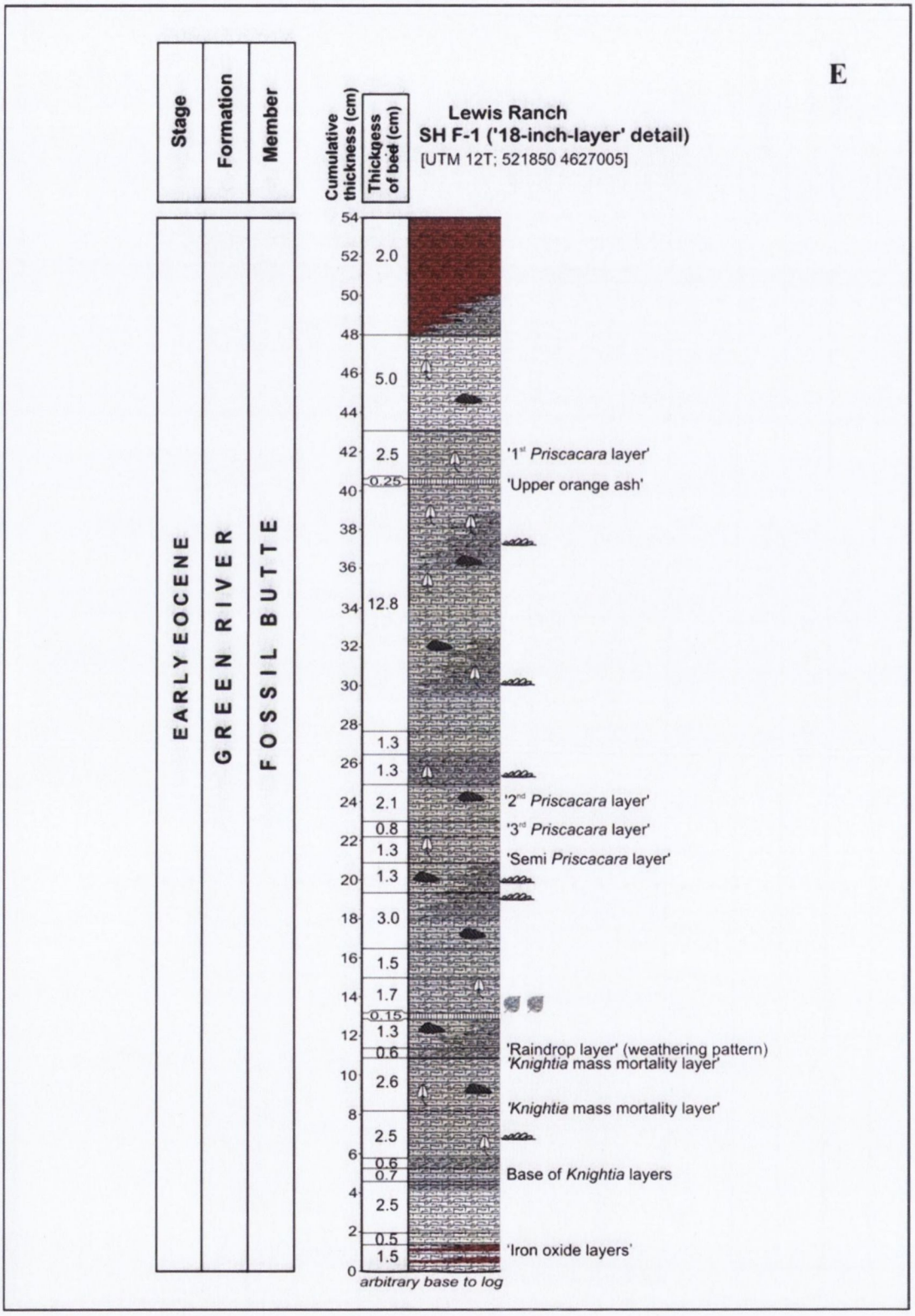

Figure 2.5: E) Stratigraphic section of the exposed 18-inch-layer units in quarry SH F-1.

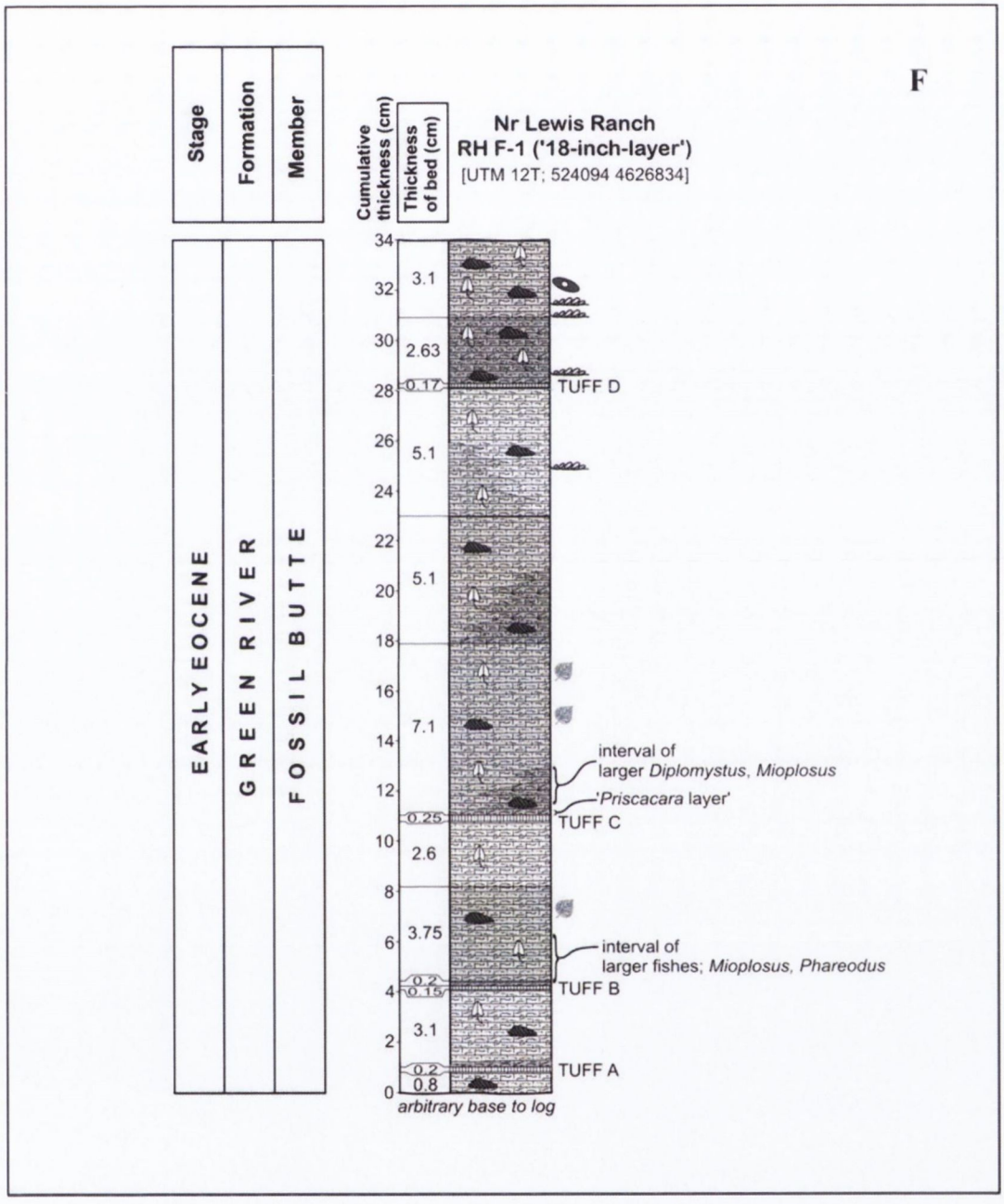

Figure 2.5: F) Stratigraphic section of the exposed 18-inch-layer units in quarry RH F-1.

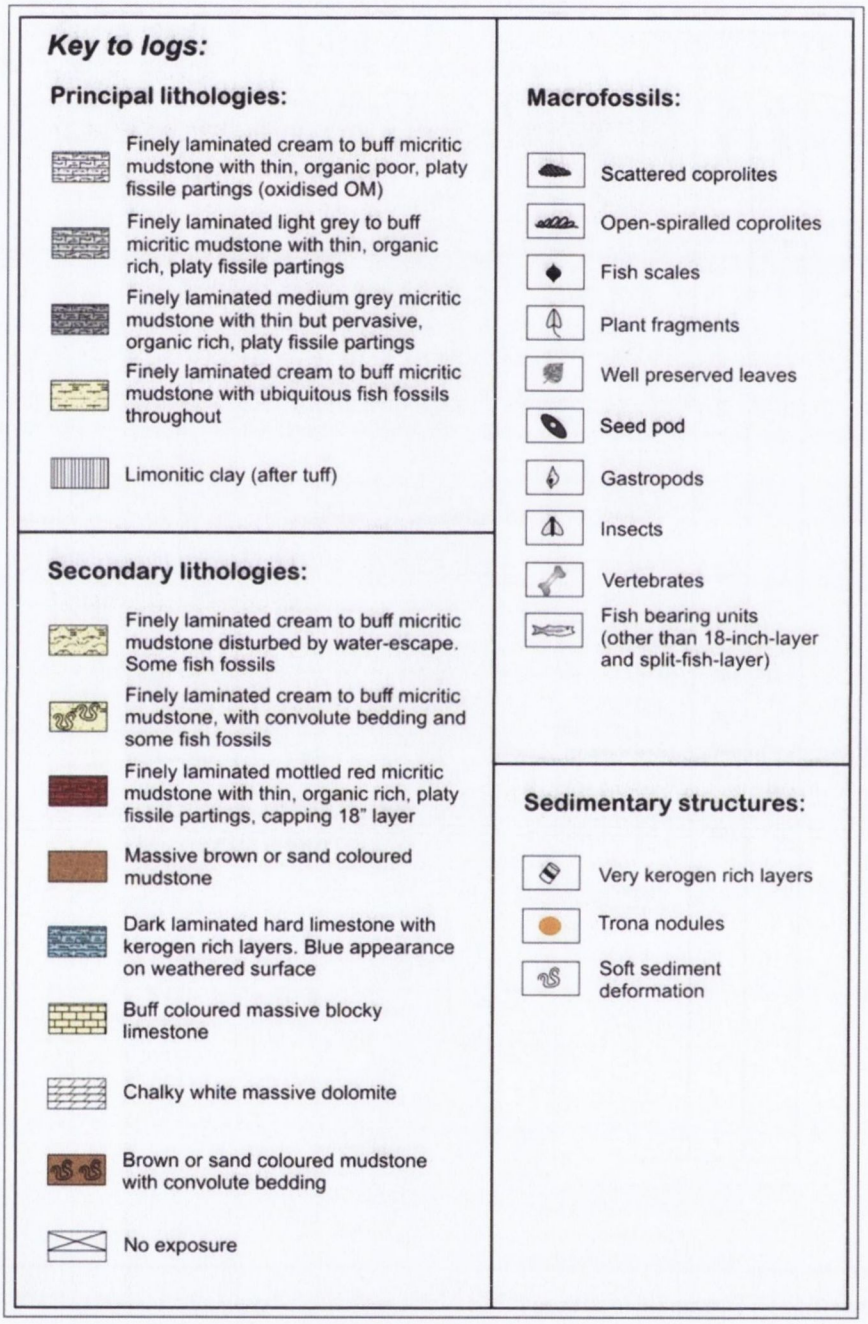

Figure 2.5 key: Key to stratigraphic sections presented in Figures 2.5 A to G.

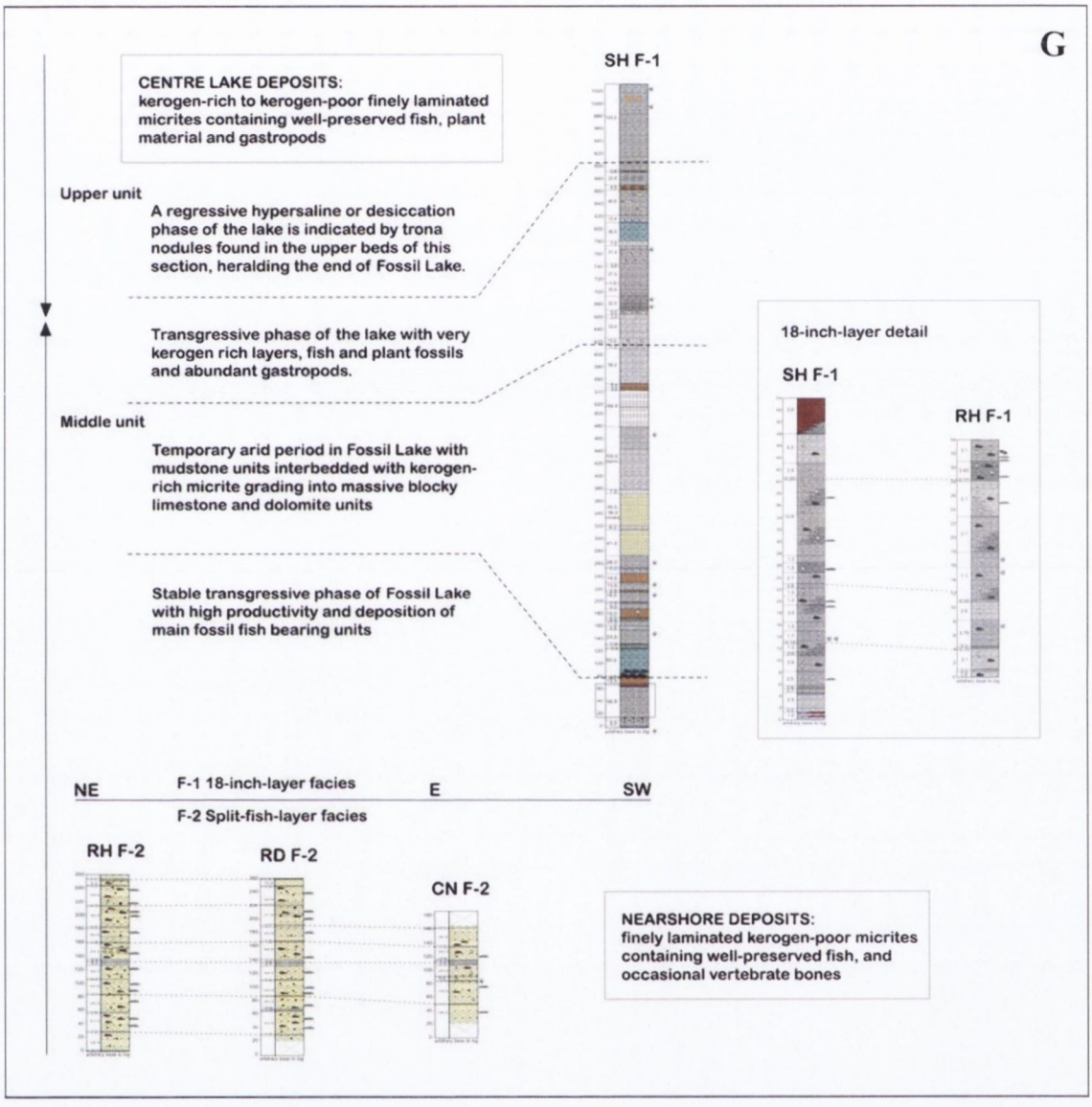

Figure 2.5: G) Stratigraphic sections of all units logged in vertical and lateral relation to one another.

In quarry SH F-1 good exposure of the 10m of units overlying the 18-inch-layer are easily accessible and were logged in detail, again using local nomenclature as shown in Figure 2.5 D. The first 5m overlying the 18-inch-layer deposits are known locally as the 'Dead Zone' deposits and yield very few fossils. This 5m section is thought to be indicative of a temporary arid period in Fossil Basin with mudstone units interbedded with kerogen-rich micrite grading into massive blocky limestone and dolomite units. Buchheim (1998)

suggests that almost total desiccation of the lake occurred during the formation of the dolomite bed. Much thicker limonitic clay layers from volcanic ash deposits are seen within these final strata of the middle unit and the initial strata of the upper unit, including a significant ash bed of 15-17cm thickness labelled here as the 'turtle ash' due to the fossil turtle material found near the ash bed by quarry workers. This ash bed is referred to as the 'K-spar tuff' marker bed by Buchheim (1994a; 1998) and Buchheim & Eugster (1998) and can be correlated basin-wide. This bed marks the onset of another transgressive phase of the lake with very kerogen rich layers, fish and plant fossils, plus abundant gastropods found in two main beds. A final regressive hypersaline or desiccation phase of the lake in this section is indicated by nodules of the evaporite mineral trona, found within the uppermost beds.

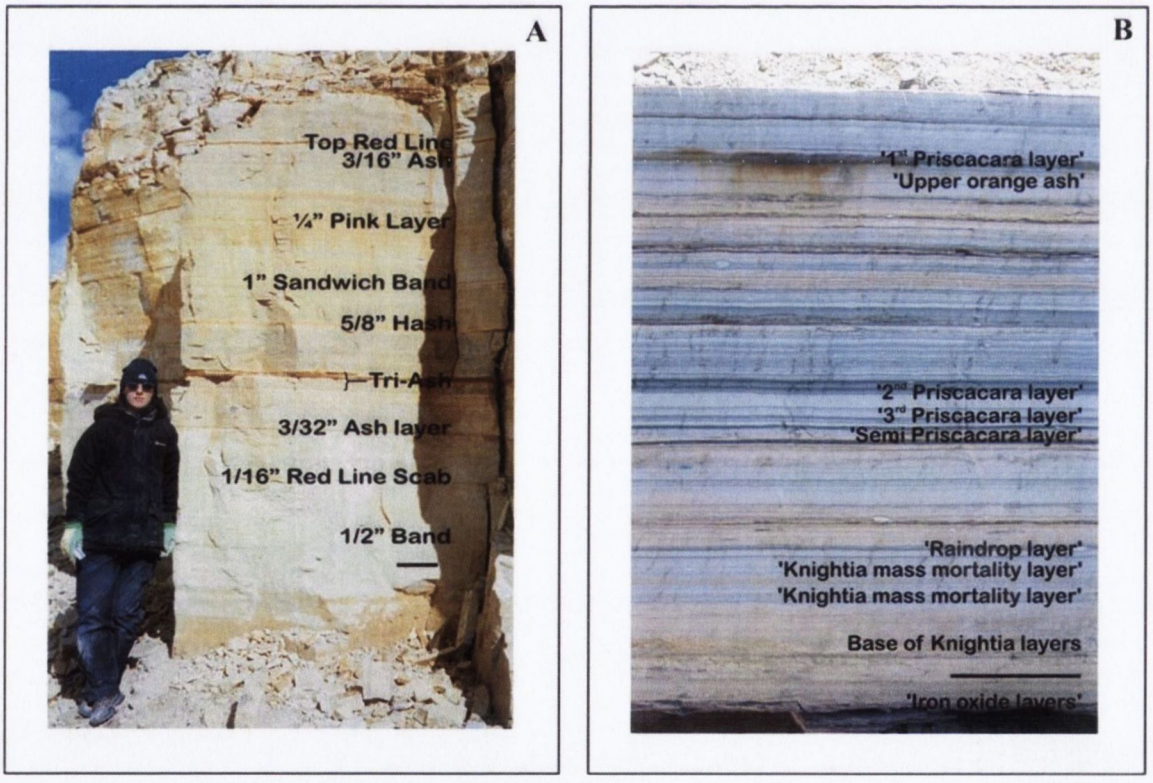

Figure 2.6: Examples of main lithological units. **A)** A typical section of the outcrop at quarry RH F-2 with prominent ash beds labelled. Scale bar 20cm. **B)** A typical section of the 18-inch-layer at quarry SH F-1 with main fossil-bearing beds labelled. Scale bar 10cm.

2.4 Micro-scale sedimentary structures

2.4.1 Composition of laminae

Historically the light and dark laminae that make up the 18-inch-layer facies and also the laminations in the split-fish-layer beds have been widely accepted as varves, with alternating light (carbonate) and dark (kerogen) bands representing summer and winter deposition respectively (e.g. Bradley 1929; Bradley 1948; McGrew 1975; Crowley *et al.* 1986). In the early model of Bradley (1929) the lake floor was considered to have been normally covered by "putrescent organic ooze" supplied by the plankton rain from the upper water mass forming dark kerogen-rich layers, with photosynthetic activity from early summer blooms of phytoplankton inducing carbonate precipitation thus providing the lighter coloured laminations. Buchheim & Surdam (1977) suggested that the kerogen rich layers, rather than originating from phytoplankton in the upper water column, may result from algal or microbial mats growing on the lake floor. Fischer & Roberts (1991) support this view suggesting that the sharply bounded, discrete nature of the carbonate laminae would not have been retained in the "putrescent ooze" suggested by Bradley (1929). They argue that the composite nature of the kerogen laminae and the occurrence of discontinuous patches of carbonate between more continuous kerogen laminae infer binding by microbes forming microbial mats. Analysis of micro-scale sedimentary structures in Lake Gosiute and Lake Uinta confirmed that many of the structures found there were formed by microbial mats (see Schieber 1999 and 2007) and this may also be the case in Fossil Lake.

2.4.2 Laminae thickness as a proxy for climatic cycles

Grande (1984) suggested that the ~4000 couplets of fine light and dark laminae making up the 18-inch-layer in Fossil Lake represent about 4000 years of deposition. Analysis of similar laminations from Lake Gosiute by Ripepe *et al.* (1991) attempted to attribute changes in laminae thickness to climatic variations. Five year and twelve year cycles were recognised within the varves and were suggested to correlate with ENSO (El Niño-Southern Oscillation) and sunspot cycles respectively, confirming much earlier work by Bradley (1929) and that of Crowley *et al.* (1986). However, it was noted that some of the richer layered oil shales did not represent annual layers, but rather were thought to

represent numerous planktonic blooms within one year (Ripepe *et al.* 1991). The alternating carbonate and kerogen-rich laminae have also been used to investigate the presence of longer climatic rhythms in the Green River Formation of Lake Gosiute and changes were correlated to the Milankovitch cycles of precession (20 ka) and eccentricity (100 ka) (Fischer & Roberts 1991; Pietras *et al.* 2003; Meyers 2008). Within the Fossil Butte Member of Fossil Lake laminae from a continuous unit correlated using enclosing ash beds were analysed from basin centre to margin along a 15km lateral section by Church & Buchheim (2002). Varves caused by annual precipitation events in open water would be expected to produce laminae of even thickness and number across the basin (Buchheim 1994a). In Fossil Lake however, laminae thickness was found to be most consistent towards the centre of the basin with large fluctuations towards the basin margin, where laminae were also found to increase in number by 134%. Church & Buchheim (2002) found no evidence for sunspot cycles and concluded that the laminations were not annual varves, but rather laminations controlled by input into the basin. Their research supports the Buchheim & Eugster (1998) model of deposition for Fossil Lake where laminae represent calcite precipitation in response to episodic inflow leading to higher nearshore sedimentation rates. Also, the ~50mm ka^{-1} deposition rate proposed by Grande (1984) for the 18-inch-layer at the lake centre, using the assumption that the laminae couplets are varves, appears to be a little too low when compared with other balanced-fill facies which have sediment accumulation rates of >100mm ka^{-1} (e.g. Carroll *et al.* 2002), therefore providing further support for the inflow model.

2.4.3 Evidence of a microbial origin of laminae

A hand specimen and photomicrographs of thin sections typical of 18-inch-layer samples collected as part of this study are shown in Figure 2.7 A to D. Light and dark laminae can clearly be seen in thin section, with the lighter layers being carbonate and the finer dark layers organic rich inter-beds. Even at low (x5) magnification it can be seen that these laminae are not flat-lying and parallel, but have a gently undulating asymmetrical nature. The dark organic rich layers have a frequently interconnecting anastomosing pattern and appear to be the cause of lenticular areas of carbonate. Observations from these thin sections and also hand specimens lead to the conclusion that the dark laminae are formed

by microbial mats on the lake floor, as postulated by Buchheim & Surdam (1977) and Fischer & Roberts (1991), which are known to create sub-millimetre to millimetre laminations in modern settings (Hagadorn & Bottjer 1997). In hand specimen an irregular pustulose relief on bed surfaces can be seen (Figure 2.7 A), and is thought to be identical to those characteristic of microbially induced sedimentary structures (MISS) formed by microbial mats on bedding planes (e.g. Hagadorn & Bottjer 1999; Noffke *et al.* 2006). Burial of a mat-covered surface by an influx of sedimentation can force the mat community to migrate upward (Hagadorn & Bottjer 1999) and this could be the cause of the anastomosing nature of the organic laminae from the 18-inch-layer. This pattern would not be expected from phytoplankton rain; instead a flat-lying and parallel sedimentation would be likely such as those seen in the sapropels of the eastern Mediterranean (e.g. Mercone *et al.* 2001). Any surface topography would be infilled by the next layer of fine carbonate particles or phytoplankton, leading to continued parallel sedimentation with little relief. In Figure 2.7 B to D the carbonate layers do not infill the relief of the palaeosurfaces but appear to be shaped by the organic layers, suggesting cohesion of the carbonate grains. Modern microbial mats use mucilaginous binding to incorporate silt and clay sized particles into the mat surface and the presence of microbes is known to substantially alter the adhesion of sediment grains (Hagadorn & Bottjer 1997). Hagadorn & Bottjer (1999) also hypothesised that microbial mats with trapped clay particles may mediate parting along mat-rich layers in sedimentary rocks, with the clays providing a post-compaction cleavage interface in lithologically homogenous rocks.

In the nearshore split-fish-layers the laminated strata are kerogen-poor and less cohesive. Photomicrographs of thin sections typical of split-fish-layer samples collected as part of this study are shown in Figure 2.7 E to H. If laminations in this area of the lake are also as a result of microbial mats then perhaps the increased production of carbonate in these areas suggested by Buchheim & Eugster (1998) would effectively dilute the volume of organic material produced. This appears to be the case, with anastomosing thin layers of organic material being finer and more widely spaced by thicker layers of carbonate. The carbonate grainsize appears much bigger in the F-2 thin sections when compared with that of the F-1 specimens, suggesting that the nearshore deposition of carbonate was in

response to episodic inflow of carbonate-rich waters leading to proximal precipitation of coarser grained material, while finer carbonate grains may have travelled further to the centre of the lake. Figure 2.7 H shows a thin section taken parallel to bedding with high relief areas of organic matter showing through the surrounding carbonate grains. At high magnification no structure can be seen in the darker organic-rich areas and it appears to be composed of amorphous kerogen. Modern microbial mat communities are typically found in nonmarine settings where bioturbating organisms are restricted (Hagadorn & Bottjer 1997) and it is thought that Fossil Lake may have provided an ideal setting for such mats to thrive.

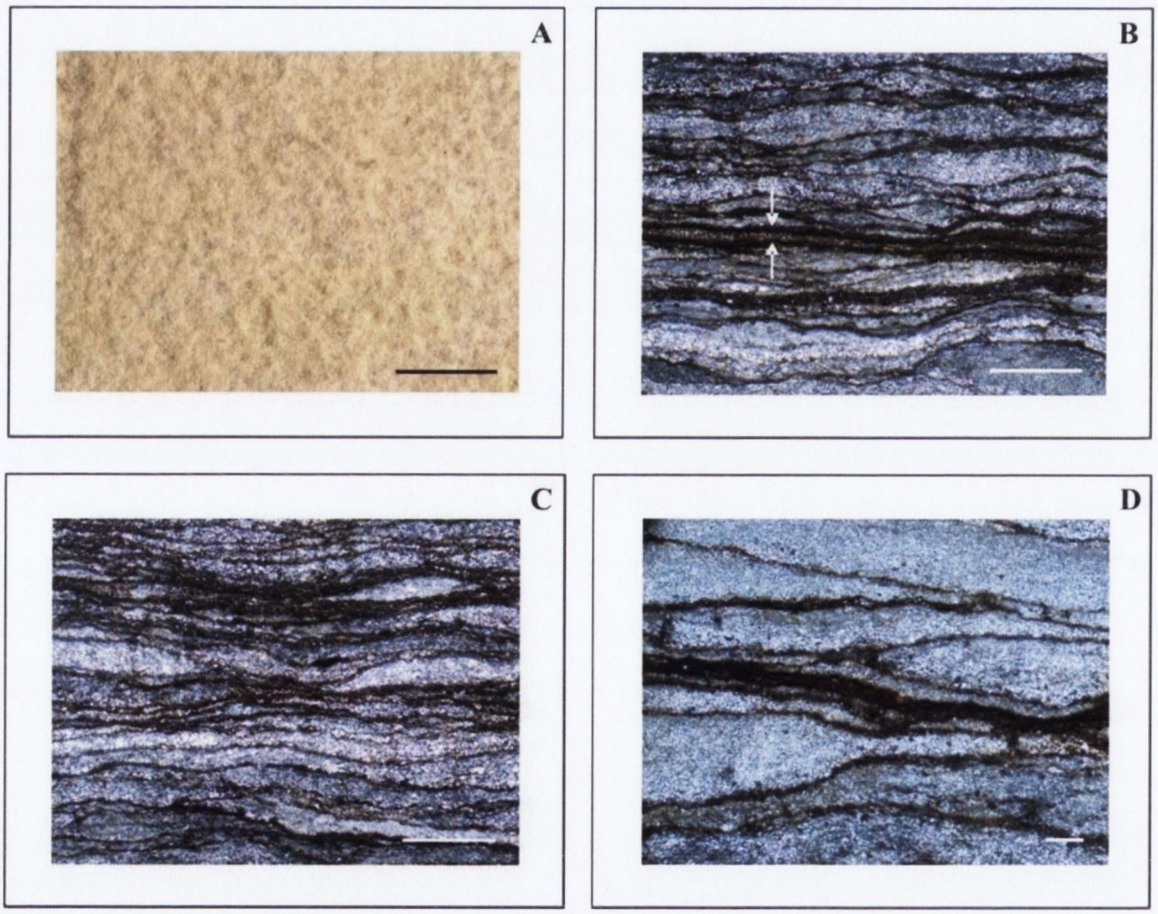

Figure 2.7: Photomicrographs of laminated strata. **A)** Hand specimen from the 18-inch-layer showing surface features on horizontal parting. Scale bar 1cm; **B and C)** Thin sections of 18-inch-layer deposits perpendicular to bedding, at x5 magnification. Scale bar 500μm. White arrows highlight a fine volcanic ash layer; **D)** Thin section of 18-inch-layer deposits perpendicular to bedding, at x10 magnification. Scale bar 100μm;

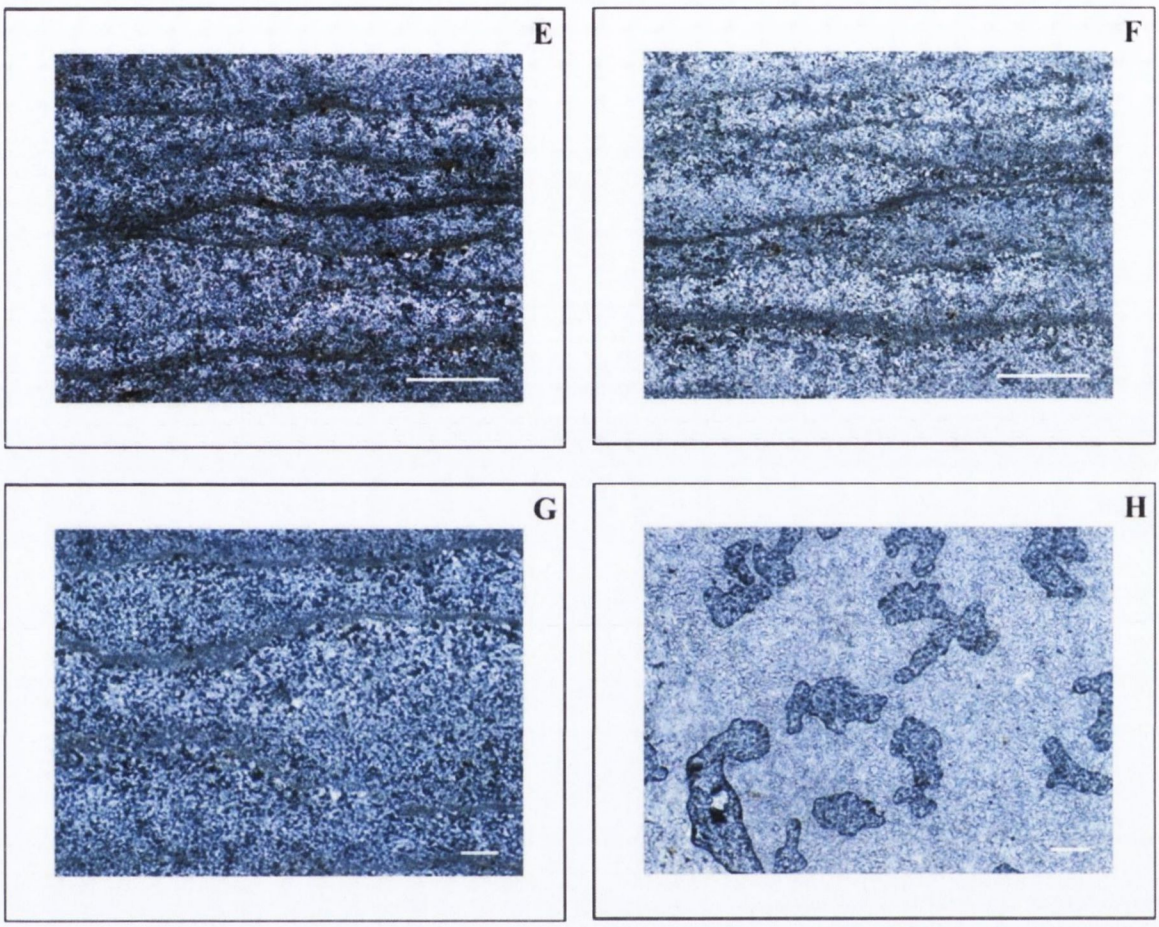

Figure 2.7 continued: E and F) Thin sections of split-fish-layer deposits perpendicular to bedding, at x5 magnification. Scale bar 500μm; **G)** Thin section of split-fish-layer deposits perpendicular to bedding, at x10 magnification. Scale bar 100μm; **H)** Thin section of split-fish-layer deposits parallel to bedding, at x10 magnification. Scale bar 100μm.

2.5 Palaeontology

2.5.1 Fossil Lake taxa

Fossils are found in all three Eocene lakes of the Green River Formation, although taxa and assemblage vary between the three. Fossil Lake strata contain an abundance of well-preserved fossil flora and fauna in the F-1 and F-2 units, in such variety that this lagerstätte is one of the most extensive known in North America (Biaggi & Buchheim 1999); examples of some of the fossils found during the field campaign are shown in Figure 2.8. Global average temperatures in the Eocene generally exceeded present values

by 3-7°C (Sewall & Sloan 2006) and this, coupled with the lower altitude of Wyoming, meant that Fossil Lake formed in a moist, subtropical climate, similar to that of the Florida everglades, USA, today (Benton *et al.* 1994). Plants include palm leaves and fronds, as well as smaller leaves from deciduous terrestrial dicotyledons and some aquatic eudicotyledons (Manchester & Kester 2002).

Figure 2.8: A montage of photographs showing some common and rare finds from the field campaign. A) Water lily leaf from RH F-1 (*Nelumbo* Adanson, 1763), scale bar 10cm; B) *Knightia eocaena* from RH F-2, scale bar 2cm; C) *Diplomystus dentatus* from RH F-2 showing positive and negative split, scale bar 5cm; D) contorted *Knightia eocaena* from RH F-2 scale bar 2cm; E) unidentified small leaf from SH F-1, scale bar 2cm; F) unidentified bird from RH F-2, scale bar 5cm; G) *Knightia eocaena* from RH F-2 scale bar 2cm; H) *Phareodus* scale from RH F-2, scale bar 1cm; I) unidentified dragonfly from RH F-1, scale bar 2cm; J) gastropod from '10″ Gastropod bed', SH F-1, scale bar 1cm; K) unidentified trionychid turtle from RH F-2, scale bar 20cm; L) disarticulated or 'exploded' fish from SH F-1, scale bar 10cm; M) small *Knightia* from 'Mini fish beds', SH F-1, scale bar 10cm. Photographs of bird and turtle courtesy of R. Hebdon.

Invertebrates include insects, ostracods, gastropods and some bivalves (Buchheim & Eugster 1998). The most common vertebrate fossil fauna are the large variety of pelagic freshwater fish species, although turtles, crocodiles, birds and some mammals have been found (Grande & Buchheim 1994). Well-preserved coprolites are extremely common in these units, as are isolated fish scales (Grande 1984). This study concentrates on common fish found in the F-1 and F-2 deposits described in Section 2.2. Grande (1984 and 2001) produced thorough reviews of the fish fauna of the Green River Formation, with some discussion of other fauna and flora, reporting that 23 species of fish are known from Fossil Lake in the late Early Eocene.

The most common fish species in the F-1 and F-2 facies are *Knightia eocaena* Jordan, 1907; *Knightia alta* Leidy, 1873; *Diplomystus dentatus* Cope, 1877; *Priscacara liops* Cope, 1877; *Priscacara serrata* Cope, 1877; *Mioplosus labracoides* Cope, 1877; *Phareodus encaustus* Cope, 1871 and *Phareodus testis* Cope, 1877. Adults of these species account for over 90% of all fossil fish finds in both F-1 and F-2 quarries each year (Grande 1984) and all were collected as part of this study. In F-1 fossil sites the small herring genera *Knightia* and *Diplomystus* account for around 70% of all fossil fish finds, with a further 20-30% comprising of *Priscacara* similar to that shown in Figure 2.9 A. Some large finds of adult *Notogoneus* Cope, 1885 have been reported but these are confined to a single bed in the F-1 quarries (pers. comm. J. Montgomery). In F-2 quarries thousands of *Knightia* are found every year similar to that shown in Figure 2.9 B, accounting for around 60% of all fossil fish finds there, with *Diplomystus* accounting for a further ~30%. Finds of *Priscacara*, *Mioplosus* and *Phareodus* typically constitute the remaining 10%. Rare fish which make up the majority of the remainder of the fish assemblage in Fossil Lake were not targeted for this study. They include *Heliobatis* Marsh, 1877; *Crossopholis* Cope, 1883; *Lepisosteus* Cope, 1877; *Amia* Jordan, 1907 and *Eohiodon* Grande, 1979, which each account for less than 1% of all fossils found per year, in either the F-1 or F-2 quarries (Grande 1984). There are several major differences in fossil assemblage between the F-1 and F-2 deposits, which are thought to represent centre lake and nearshore fauna respectively. Higher percentages of insect and plant fossils were found in the deeper water F-1 setting during collection for this study. Conversely, the

nearshore quarries are known to contain a higher proportion of fossilised terrestrial animals (notably crustaceans, amphibians, reptiles, birds and mammals), more abundant *Heliobatis* (stingrays) and a larger number of juveniles for most fish taxa (Grande & Buchheim 1994). Hatchlings of *Diplomystus* are found in the centre lake deposits and this

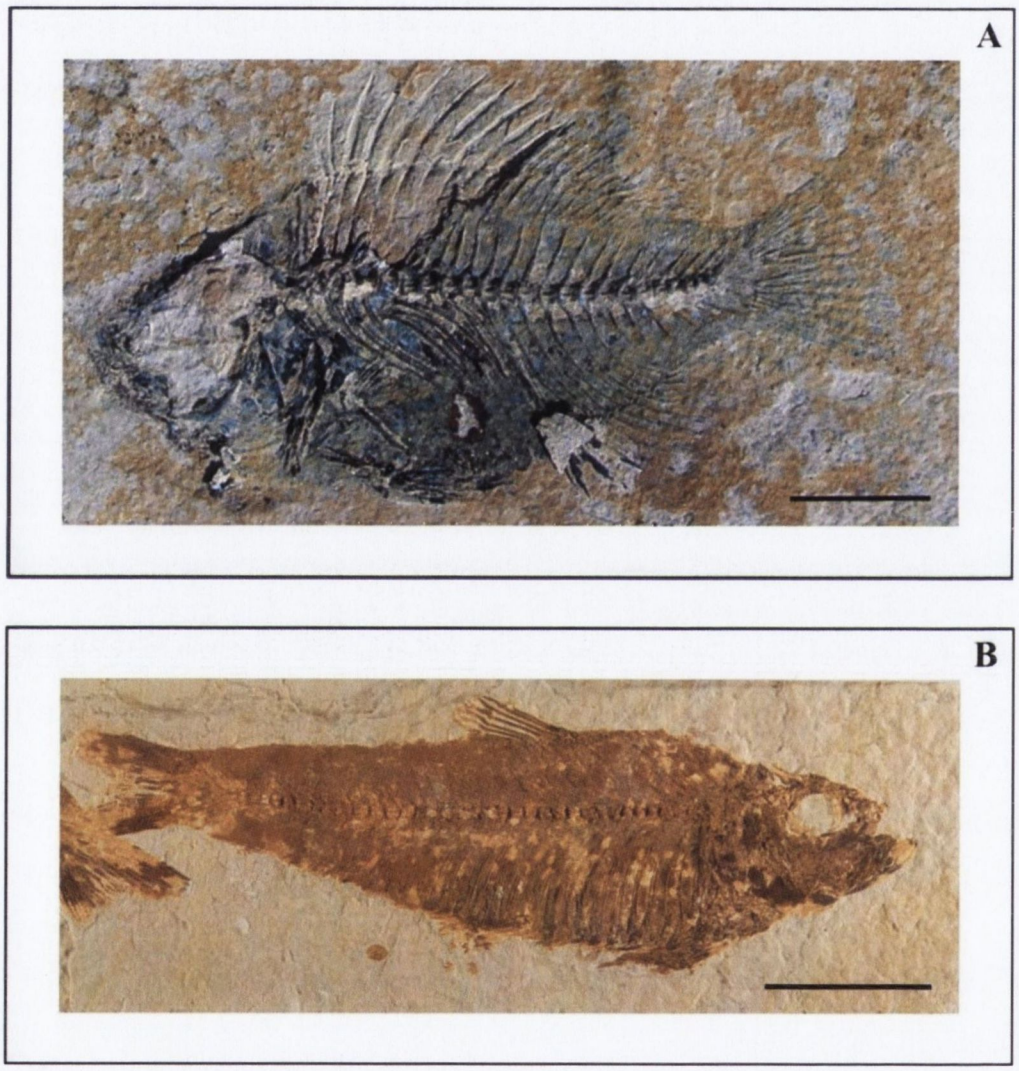

Figure 2.9: Examples of fish from centre lake and nearshore localities. **A)** A typical small *Priscacara* from an F-1 18-inch-layer locality covered by a thin film of carbonate. Brown patches on surrounding rock are attributed to weathering. Scale bar 2cm. **B)** A typical *Knightia* from an F-2 split-fish-layer locality showing excellent preservation of scales. Scale bar is 2cm.

clupeomorph may have had a different spawning pattern to most of the other fish species present; some extant clupeomorphs are known to prefer to spawn in deeper open water

(Grande & Buchheim 1994). The occurrence of only adult *Notogoneus* in the centre lake deposits and their notable absence in nearshore strata may indicate that spawning of this species occurred in surrounding streams with only fully grown adults entering the lake and living in the deeper water (Grande 1984; Grande & Grande 2008). In both the F-1 and F-2 beds fish fossils are found in mass mortality layers which can contain as many as 500 fish per square metre (Buchheim & Eugster 1998) and the majority of these horizons contain monospecific assemblages.

2.5.2 Causes of fish mass mortality events

Fossil Lake is interpreted as a deep, warm-monomictic lake which would have had thermal stratification during much of the year and only complete mixing during the winter months when surface waters cooled to a similar temperature as the bottom waters (Ferber & Wells 1995). Whether the lake was anoxic below the thermocline is unclear. The cause of the regularly occurring, possibly cyclical, mass mortalities of thousands of fish in Fossil Lake is unknown and difficult to determine, but may have been multi-factorial. Present day mass mortalities of fish in coastal zones and lakes are often attributed to the upwelling of cold anoxic bottom water due to annual changes in wind direction or seasonal temperature variation. This upwelling causes schools of fish to perish in large numbers due to hypoxia, examples of which are mainly seen in Western Europe, the Eastern and Southern coasts of the USA, and East Asia, particularly in Japan (see Selman 2007). In late summer months the Western Baltic oxygen saturation has been observed to drop from 100 to 0% saturation in less than 1h (Fischer *et al.* 1992). During one such event in 1987 over 400 000 fish suffocated in a few hours and most were found washed ashore or floating in the shallows with spread operculae, typical for death caused by asphyxiation (Fischer *et al.* 1992). This is therefore probably not the case for Fossil Lake, as no signs of asphyxiation, distress or torsion are observed in the fossil fish, and the fossils are found at lake centre localities as well as those nearshore. Oxygen depletion within the water column would also have no effect on the surrounding wildlife and would not explain the quantities of reptiles, birds, bats and small mammals found fossilised in the lake sediments. Similarly, the effects of upwelling of chemically toxic waters (for example containing H_2S released from the kerogen-rich sediments) or changes in salinity would

have had little effect on the birds and mammals living in the lake environs. As such, upwelling of oxygen depleted or chemically toxic bottom waters are not thought to be responsible for the majority of deaths in Fossil Lake. The frequent volcanic ash fall in the area is also thought to be unrelated to the fish mass mortality events; no correlation between fish fossils and ash deposits was observed in the field. In other present day cases of fish mass mortality, upwelling or inflowing nutrient rich waters instigate blooms of phytoplankton, with nutrient eutrophication contributing significantly to bloom development and support. These phytoplankton are often cyanobacteria, archaea or dinoflagellates and blooms result in the death of thousands of fish in hundreds of coastal areas and some lacustrine settings around the world today (e.g. Berman-Frank *et al.* 1994; Oren & Gurevich 1995; Heil *et al.* 2001; Siqueira *et al.* 2006). Such events were first postulated as mechanism for the fish mass mortality in Fossil Lake by McGrew (1975). The blooms can result in the death of aquatic life either because of the toxicity of the phytoplankton themselves or because of the depletion of oxygen in the water column due to phytoplankton respiration and their decomposition by bacteria, leading to hypoxia. Evidence for the presence of a toxic variety of dinoflagellate in Fossil Lake is discussed in more detail in Chapter 7 Section 7.6.2 and is thought to be the most likely cause of fish mass mortality as it would also have had an impact on other wildlife in and around the lake. Dinoflagellate blooms may have occurred annually in conjunction with the influx of nutrient rich waters during the wetter months.

2.5.3 Conditions leading to preservation of mass mortalities

Although occasional fossil fish specimens are disarticulated probably due to expulsion of internal gases, the vast majority of fish are found complete and articulated indicating that the majority underwent the same taphonomic processes. In each mass mortality layer the fish are randomly oriented in a horizontal plane within a single sub-millimetre lamination, constituting a fish bone bed. The fish are frequently preserved flattened on the bedding plane lying on their lateral surface, although specimens are occasionally found preserved lying on the ventral or dorsal surface. The preservation of large numbers of articulated specimens of a similar size and of one species is thought to represent the mass mortality of a shoal of fish over a short or instantaneous time interval. The fish are all very well

preserved with excellent morphological detail, retaining bones, teeth, scales and fins. Little soft tissue preservation is observed and specimens recovered have only a slight 3D structure, being mostly compacted in nature, but despite this the preservation of fish in this manner is still exceptional. The fossilisation of delicate coprolites such as those frequently found in the F-1 and F-2 units are rare in the fossil record and serve to further emphasise the unusual nature of the depositional environment and fossil preservation within Fossil Lake (Grande 1984). That the fish coprolites are preserved, the fish are intact and the sediment laminae undisturbed strongly suggests a complete lack of benthic organisms and scavengers in Fossil Lake, and this is also reflected in the fossil assemblage found and the sedimentary structure. Oxic sediments preserved in the geological record have massive textures without lamination, often preserving trace fossils and burrows of macro-benthos. Benthic sediments that contain interstitial oxygen are commonly bioturbated by metazoa, including multicellular burrowing organisms such as clams and worms (Peters *et al.* 2005). This lack of evidence of bottom-dwelling life indicates that Fossil Lake bottom waters were anoxic or at least prohibitive to most life forms. Bottom waters contain decay products from sinking organic matter and in high concentrations can inhibit photosynthetic growth and can be toxic or debilitating to respirors (Wilde *et al.* 1990). The absent benthos coupled with the presence of a highly diverse nekton confirms the stratification of the water column in Fossil Lake, as suggested in the seminal depositional model by Bradley (1948). Paradoxically, *Heliobatis* or stingrays have been found in the lower units of the nearshore RH F-2 quarry, although these are limited to a small bed as shown in Figure 2.5 A and may indicate a hiatus in the normal regime. Similarly *Notogoneus* are thought to have been bottom feeders but appear to be restricted to just one narrow horizon. Evidence for benthic microbial mats exists as discussed in Section 2.4; colonial microalga are known to grow in extreme conditions toxic to many other life forms, thriving due to minimal disturbance from grazers (Bauld 1981). It can be concluded, therefore, that lake bottom conditions were such that benthic microbial mats flourished with the exclusion of all other life forms due to the hostile conditions of the lake floor, although it is outside the scope of this thesis to characterise and constrain what those prohibitive conditions were. The conditions persisted even in nearshore settings, apparently uncompromised by inflow of freshwater and runoff.

In most modern instances of fish mass mortality the fish carcasses are seen floating or are washed up on the shore (e.g. Fischer *et al.* 1992). In Fossil Lake however, hundreds of fish sank to the bottom to become fossilised. The mechanism that allowed this to happen is unknown, though could be related to the vertical water density structure in the lake, which would have been dependent on temperature and chemical gradients in the water column (e.g. Wüest *et al.* 1996). Fossil Lake is thought to have been thermally stratified due to meteorological influences (Ferber & Wells 1995) but biogenically induced chemical gradients may have also existed, adding to the stability of the water column and inhibiting deep water renewal (Wüest *et al.* 1996). Fish dying near or below the thermo/chemocline may have initially sunk through the bottom waters of the hypolimnion coming to rest on the lake floor (see Whitmore *et al.* 2002). Microbial mats covering the sediment surface probably had a cohesive gelatinous nature, essentially encouraging fish to adhere to the lake floor and growing around them, encapsulating the fish in a film of calcium carbonate and preventing the fish refloating. The gas bladders of fish frequently cause them to float after death, but can escape from the carcass if the carcass is restrained in some way, as was observed during experiments with extant fish discussed in Chapter 6, thus allowing the fish to remain on the lake bottom. Modern microbial mats will grow over entire corpses within hours or at most days, creating a strongly reducing environment within and inhibiting the decay of the fish, thus leading to excellent preservation (Barthel *et al.* 1990). This encapsulation may have been the mechanism by which the fish were kept intact during permineralization of bones, scales and teeth, while the internal organs decayed. The fossil fish are preserved as fluorapatite ($Ca_5(PO_4)_3F$) as discussed in Chapter 4 and shown in Figure 4.7. Modern vertebrate bioapatites are composed of carbonate hydroxylapatite ($Ca_5(PO_4)_3OH$) mineralised on an organic framework (Lowenstam & Weiner 1989), suggesting that some diagenetic alteration has occurred in each specimen, with the hydroxyl group being chemically replaced by the fluoride ion. Microbial mats are known to be an important agent in exceptional fossilization, particularly where apatites are involved (Wilby *et al.* 1996). A high burial rate during episodic inflow of calcium-rich waters increasing carbonate production may also have enhanced this early diagenetic mineralization (e.g. Biaggi *et al.* 2000). This was probably the controlling factor in fossil preservation in the nearshore F-2 localities, being both near to inflow and having less

dense microbial mat communities as shown in Figure 2.7. The suggested depositional environment is illustrated in Figure 2.10. Despite the evidence for apparent chemical stratification in Fossil Lake it has been observed in modern settings that although this stratification can preserve sedimentary laminations it does not lead to preservation of fish, whereas preserved laminations and fish remains were reported in a non-chemically stratified lake (Britton & Buchheim 2002). The complex interplay of the different environmental factors responsible for mass mortality and fossil preservation in Fossil Lake is still little understood and requires further research.

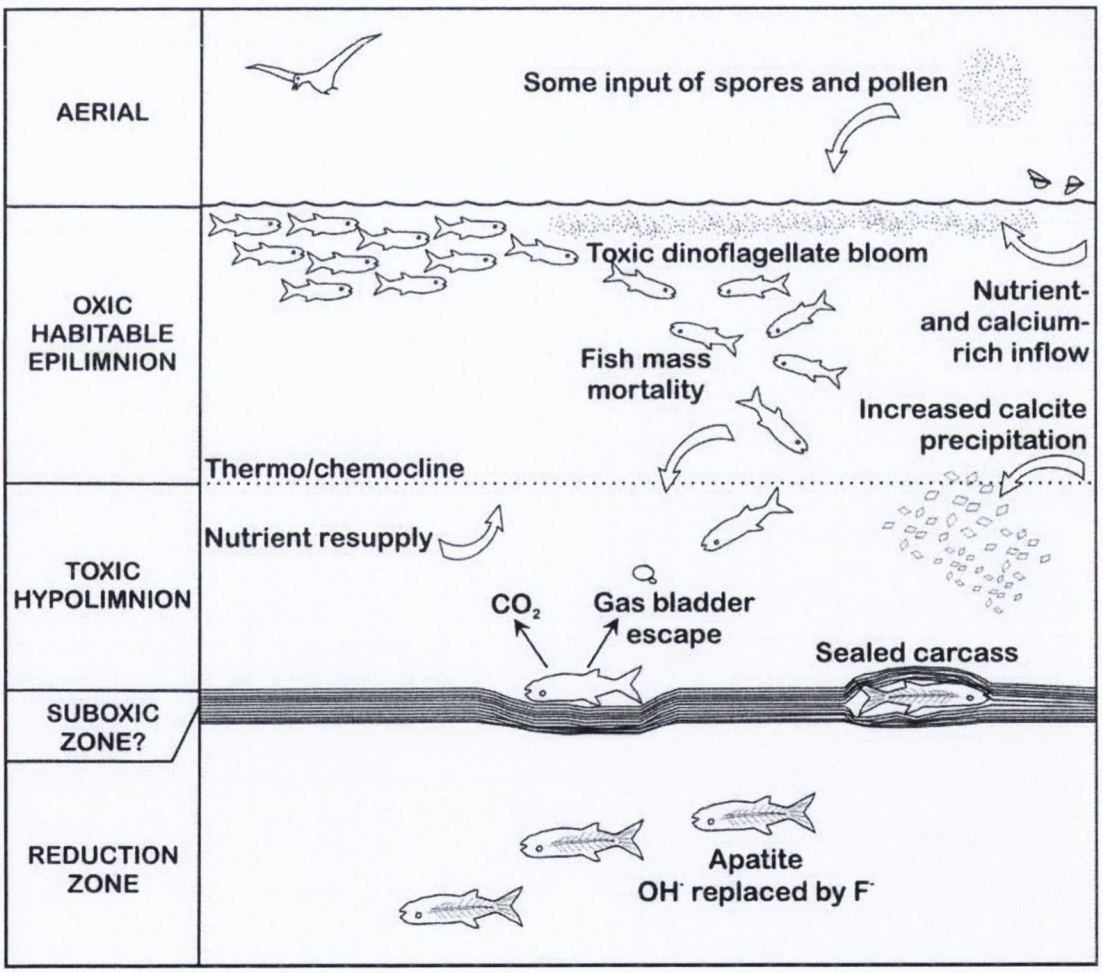

Figure 2.10: Suggested environment of deposition in Fossil Lake leading to fish mass mortalities and their preservation (redrawn after Martill 1988 and Buchheim & Eugster 1998).

2.6 Sampling procedure

Hundreds of fossil fish specimens were collected over a two-month period during the summer of 2005. The objective for the field campaign was to retrieve samples ideally from several mass mortality horizons, each with as diverse a fauna as possible in order to test the theory that original nitrogen and organic carbon isotopes from the fish were preserved and could be used to deduce the trophic structure of Eocene Fossil Lake. However, the reality in the field was that only one such slab of rock containing six different species was sourced. The field sampling strategy was altered accordingly and fish of the common species *K. eocaena*, *K. alta* and *D. dentatus* were collected throughout each succession. It was hoped that monospecific comparisons of small fish of similar size from throughout the stratigraphy would proffer information concerning changes in the lake both spatially and temporally. These fish would add to the wealth of knowledge regarding the geology and chemostratigraphy already gathered by previous authors, and compliment other data collected for this study. Whole rock samples were taken from throughout the stratigraphic column to gain a clear understanding of the processes and changes that occurred in Fossil Lake during the Eocene using more traditional geochemical methods. Samples were collected from each quarry detailed in Section 2.2.4 using hammers and steel blades or chisels. Both fossil and whole rock samples were collected from each locality for analysis. The position of each sample was measured in relation to the quarry floor, an arbitrary stratigraphic base to each log shown in Figure 2.5 A to F. The precise horizon where the fossil was found was accurately recorded to within 0.5mm and a sample number assigned to the specimen, including an abbreviation of the location name, date found and a number. All fossil specimens were identified in the field where possible, and the species and standard length noted. Standard length is defined here as the distance from the most anterior part of the fish's head to the posterior end of the vertebral column (after Grande 1984). Where fish were incomplete a common size parameter was used to extrapolate the length of the fish based on their width. Samples were then wrapped carefully in foil and sealed in polythene bags before being packed in bark chips for shipping to Ireland for preparation and analysis. The results of these analyses are presented in Chapter 5.

Chapter 3: Methods

3.1 N and C_{org} stable isotope analysis of fossil samples

3.1.1 Sampling and sample treatment

Fossil fish from the Green River Formation, Wyoming, USA, were collected from the localities detailed in Chapter 2 and transported to Ireland for $\delta^{15}N$ and $\delta^{13}C_{org}$ isotope analysis. All samples were measured, photographed and identified to species level where

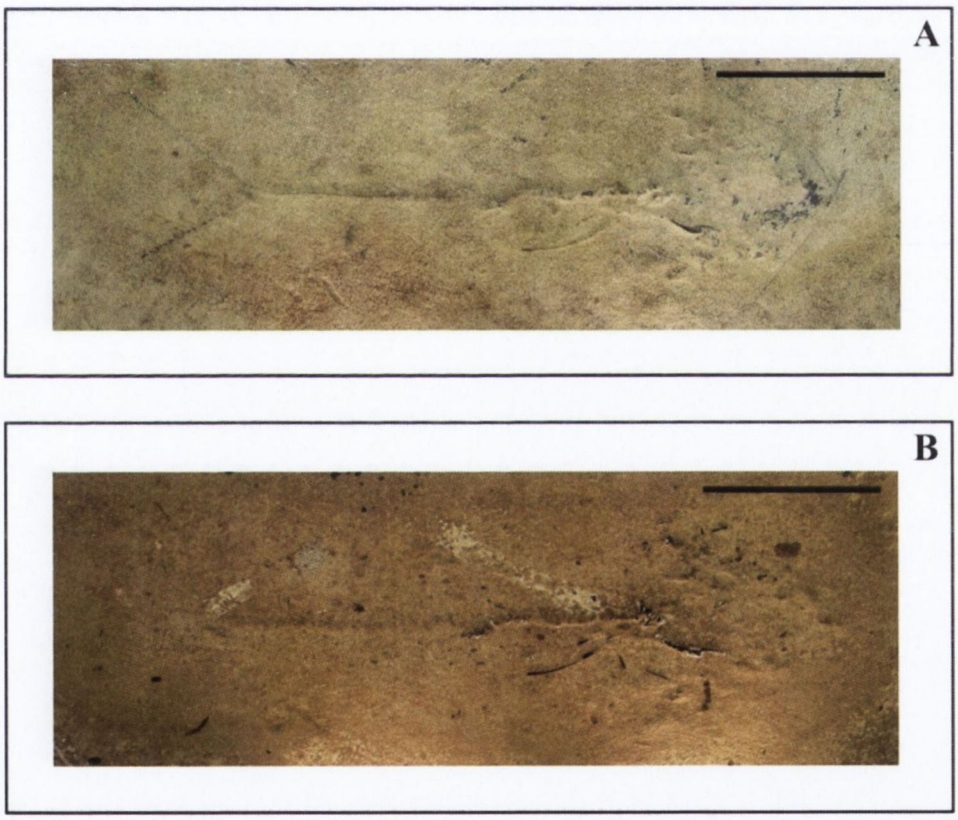

Figure 3.1: Sample preparation using acid. **A)** F-1 specimen RH290713 prior to preparation; **B)** F-1 specimen RH290713 after immersion in acetic acid for a 48 h period. Although some etching has taken place the fossil fish is still under a layer of hard micrite of a few mm in thickness. Scale bars are 10cm.

possible, prior to preparation. Fossils from 18-inch-layer F-1 quarries were retrieved covered by a thin layer of consolidated micrite up to a few mm in thickness and this had to be removed prior to analysis and in many cases before accurate species identification could be made. In the laboratory an electric Proxxon© IB/E handheld drill/grinder was

used to attempt the removal of this covering layer to reveal the F-1 fossil fish specimens, although this proved problematic. The hard nature of the micrite was such that the carborundum grinding bits used were unable to successfully cut through the micrite and an alternative method of carbonate removal was sought. A preparation technique occasionally used by preparators in Wyoming is the complete immersion of the micrite slabs in acid, and this was attempted in the laboratory. A large slab containing a fish (sample number RH290713), probably *Phareodus encaustus*, shown in Figure 3.1 A was immersed in acetic acid which was replenished several times during a 48 h period, beginning with 3M and decreasing to 2M acid. Scrubbing and rinsing to encourage carbonate dissolution was also employed. After the 48 hour period had lapsed several layers of micrite had been removed, revealing coprolites and a small fish, however the large fish was still underneath a layer of micrite as shown in Figure 3.1 B. The encapsulation of the F-1 fossils in this manner meant that most were disregarded for any further experimentation due to the absence of a practicable and efficient method for removal of the hard micrite.

The majority of the fossil fish collected from the Green River Formation for this study were from the split-fish-layer F-2 quarries with the fossil fish split into two halves and as such were readily prepared for geochemical analyses. These fish were embedded in slabs of a more poorly consolidated, softer micrite than the F-1 fossils. However, the presence of micrite powder in any sample would result in a mixed inorganic and organic carbon isotope signature and could potentially affect any nitrogen isotope analyses. In order to exclusively measure the N and $C_{organic}$ isotopic composition of the fossils, the F-2 fish collected for this study were first removed from the calcareous matrix by hand using dental tools and a scalpel under a binocular microscope. In turn each specimen was then homogenised by grinding in an agate mortar and pestle, prior to acid treatment. The powders were treated with 2M acetic acid for up to 24 hours to remove any of the calcareous cement still present whilst precluding dissolution of the powdered fluorapatite. A thorough investigation to find the best chemical treatment for this step is detailed in Chapter 4. Laboratory equipment was washed in a solution of Decon 90® surface active cleaning agent where possible and rinsed thoroughly with deionised water (DIW).

Additionally, all glassware was soaked in 10% HCl overnight and rinsed five times with DIW before use.

Sample preparation for N & C_{org} isotope analysis does not require such complex protocol as some techniques used for other geochemical analyses (e.g. Mg/Ca palaeothermometry, Barker *et al.* 2003); however, steps were taken to ensure that the preparation of the fossil fish samples was carried out in a clean environment. This entailed the design and construction of an over-pressured filtered glove box or 'mini clean lab' as shown in Figure 3.2, in order to prevent any contamination of the samples during chemical preparation. A specially designed fan system constantly delivered a gentle flow of filtered air into the Perspex box, eliminating airborne particulates from the structure. This was essential due to

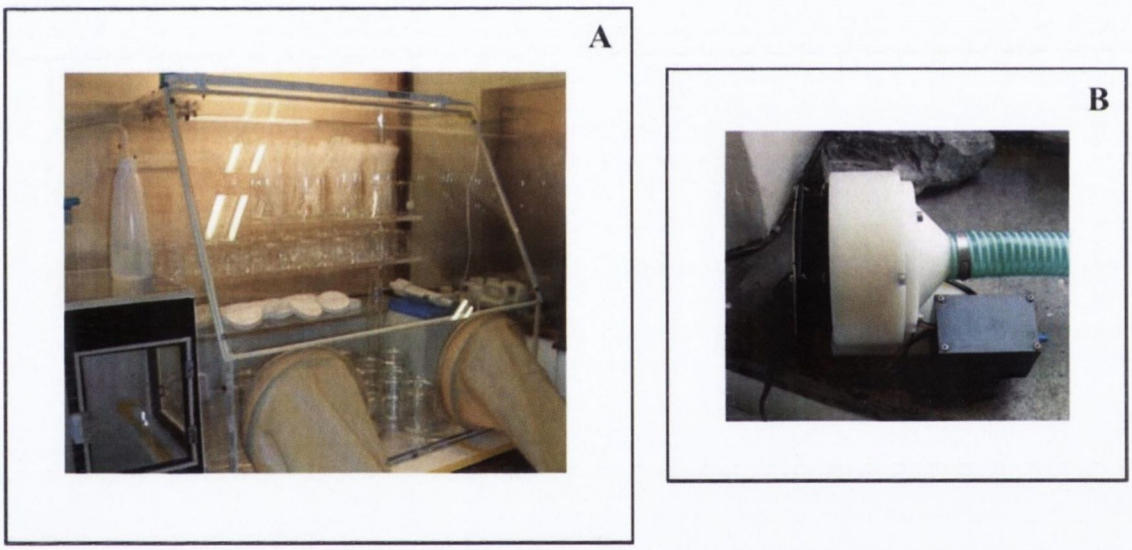

Figure 3.2: Precautions were taken to ensure minimal sample contamination. **A)** Over-pressured glove box used in laboratory preparation of fossil samples. **B)** A specially designed fan using a standard 80mm PC fan with filter attachments was sufficient to exclude airborne particulates and eliminate them from the system. This filtered air was constantly fed into the glove box.

the airborne organic matter, dust and pollution entering the laboratory through the ventilation system. On a daily basis these particulates do not interfere with most laboratory uses, but the small sample size and longer time frames involved in the fossil sample preparation meant that major contamination could be caused in this instance. With

sample quantities measured in milligrams, containing as little as 2% organic carbon and 0.02% nitrogen, particulates such as human skin flakes or soot particles could cause disruption to isotope measurements. A transfer chamber was built into the design of the box to prevent contaminants entering when samples and equipment were transferred in to, and out of, the glove box. Another problem overcome during the glove box design and realisation was that of excess static electricity due to the acrylic materials used in the construction of the glove box. This was solved by lining the box with household aluminium foil and connecting it to ground via metal water pipes in the laboratory. Natural rubber gauntlets with an 8" diameter were sourced for the glove box and replaced immediately when cracked or punctured. The interior of the glove box was cleaned intermittently with a solution of Decon 90® surface active cleaning agent and rinsed with DIW.

Fossil powders were transferred into the glove box and treated with acid to remove all traces of $CaCO_3$. Reagents used in this method were of research grade to prevent the addition of any other impurities. Approximately 40mL of 2M acetic acid was added to each sample and left to equilibrate, the majority of the solution drawn off and the procedure repeated over a 24 hour period until a stable pH was achieved. This was followed by two DIW rinses to remove any remaining acid before samples were left to dry at room temperature in the glove box. The dried, powdered samples were sealed in 8 x 5mm pre-tared tin foil capsules which were crimped to a bead using tweezers. The beads were weighed accurately using a high-precision microbalance (Sartorius MC5, ± 2μg), prior to analysis using an in-house procedure on a Thermo Delta^{plus} continuous flow isotope ratio mass spectrometer (CF-IRMS) with a CE Instruments Flash EA 1112 Elemental Analyzer™ (EA), in the Department of Geology, TCD. For a discussion of analytical precision see Section 3.1.7.

3.1.2 Delta notation and reference material

The isotope results presented in this thesis are reported in delta (δ) notation relative to the abundance of the minor isotope in an international standard. The delta scale is defined by Equation 3.1, where R is the isotope ratio in question, i.e. $^{15}N/^{14}N$ or $^{13}C/^{12}C$. Deviations

from the standard ratio are expressed using per mil (‰) notation. N is reported relative to nitrogen in air (AIR), whereas C is reported relative to a secondary standard material defined by International Atomic Energy Agency (IAEA) convention as V-PDB.

$$\delta\,(‰) = \frac{(R_{sample} - R_{standard})}{R_{standard}} \times 1000 \qquad \textbf{Equation 3.1}$$

Throughout the analyses synthetic L-alanine ($C_3H_7NO_2$), an aliphatic amino acid, was used as a working standard which can conveniently be reanalysed by other laboratories. This was originally calibrated with the Research Laboratory for Archaeology and the History of Art, University of Oxford, UK. The L-alanine used has a $\delta^{15}N$ value of -1.66‰ and a $\delta^{13}C$ value of -27.00‰ and was run repeatedly before and after, and at regular intervals during the sample runs to enable accurate calculation of any random internal machine error.

3.1.3 Instrumentation and apparatus

Use of the EA system entails loading the pre-weighed samples into an AS 200 auto sampler carousel from which they are dropped into the oxidation reactor sequentially. The EA reagents were packed according to manufacturer's instructions and the temperature conditions were maintained at a constant level: the oxidation reactor at 900°C, the reduction reactor at 650°C and the post-reactor gas chromatograph (GC) column (fused capillary column, 25m x 0.32mm i.d.) at 40°C. As each sample entered the oxidation reactor a 3 second burst of oxygen was injected which resulted in combustion at around 3000°C, converting the sample to its base elements in the gas state. Certified pure (CP) helium was used as the carrier gas which draws the sample gases through the reaction columns and traps until only CO_2 and N_2 remain. These gases are separated on a GC column and then passed on to the mass spectrometer via a Conflo III open split interface. The gases are ionised in the source and the resulting signals for each isotope recorded by ISODAT software. A typical L-alanine profile produced by the software is shown in Figure 3.3. Total run time for each sample was 640 seconds. Results for both isotope and percentage composition data were obtained for the samples.

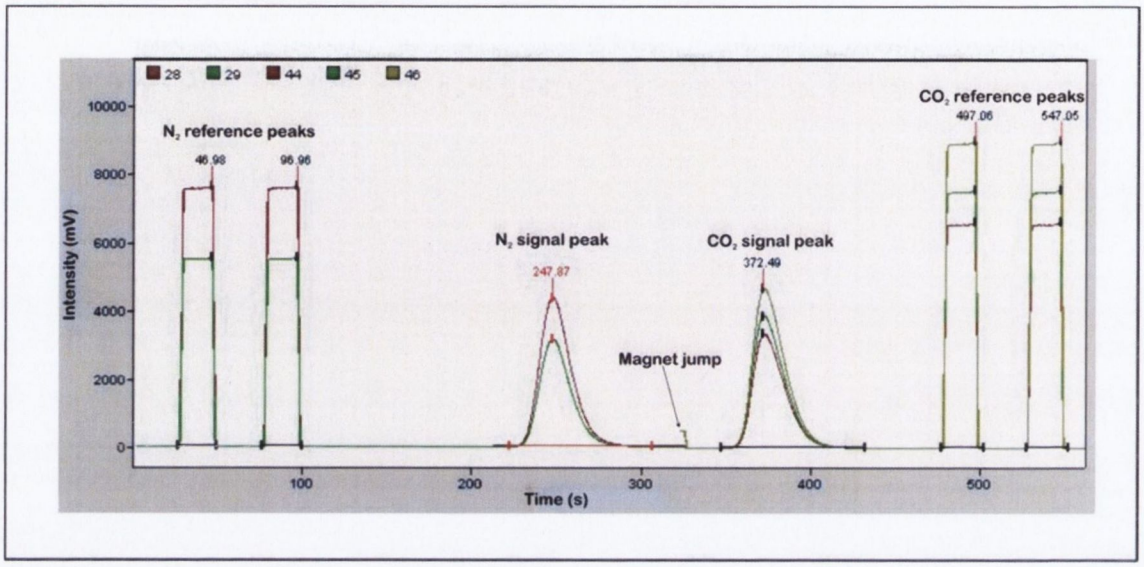

Figure 3.3: A typical profile for an L-alanine reference sample showing N_2 and CO_2 reference peaks and the measured N_2 and CO_2 peaks at 247.87 seconds and 372.49 seconds, respectively.

All samples were prepared and analysed in a random order to prevent the introduction of systematic bias. Each resultant profile was carefully examined to ensure that all results used were valid, with no sample peak interference with the reference gas profiles or magnet jump. Modern fish samples used in taphonomy experiments detailed in Chapter 6 and Cretaceous Argentinean Mata Amarilla fossil samples discussed in Chapter 8 were run in the same manner using the EA, but were not subject to any pre-treatment. Before any samples were run using the CF-IRMS system, the linearity was checked to ensure that conditions were stable and that the data produced would be robust. This entailed running a minimum of 12 samples of the L-alanine standard of various weights to ensure that the same $\delta^{15}N$ value could be achieved regardless of the peak intensity.

3.1.4 Analysis of samples with low N concentrations

Under standard operating conditions as described by the manufacturer, the Delta^{plus} should deliver linearity on peak signals between 1V and 10V (i.e. with no demonstrable sample size effects on the recorded δ values). However, this was not always possible to achieve for the N_2 peaks produced by the fossil samples. It was found that the fossil samples from the Green River and Mata Amarilla formations both contained a much higher percentage

of organic carbon compared to their nitrogen content. For modern fish specimens a C:N ratio of 3:1 can be expected (e.g. Pinnegar & Polunin 1999), however the fossil fish C:N ratios were found to vary greatly from 30:1 up to as much as 80:1. If the two elements were to be viewed on the same CF-IRMS profile whilst ensuring that the carbon values did not exceed the 10V scale, the resultant output contained an extremely small (e.g. 200mV) nitrogen signal for each sample. Various steps were taken in order to amplify the N peaks whilst maintaining the C signal. One method attempted by TCD staff and Thermo Scientific Ltd personnel was to reduce the total volume of the EA by packing oxidation and reduction reagents into a single tube. However, this meant running the oxidation reactor at 750°C and it was suspected that combustion may be incomplete at this lower temperature. The single tube was unable to contend with the usual number of samples (~300) and results began to be adversely affected after approximately 50 samples. A similar lack of capacity was encountered when attempting to run the EA with low volume twin tubes, where conventional reagents and temperatures are used with smaller volume reaction tubes. Both of these methods involve cooling the EA and repacking tubes regularly which is not practical for large numbers of samples. Another technique that can increase sample peak size is reduction of the External Carrier He flow from its standard settings. This delays the peaks and increases the peak areas, but also increases background values. The peaks also rapidly begin to tail into the magnet jump and interfere with the reference peaks and the C data was thought to be compromised. These attempts at increasing the sample N peak were considered impractical and unreliable and were therefore discounted.

A different approach concentrating on the linearity of the CF-IRMS system with the standard EA configuration was used for most fossil samples analysed in this thesis to extract palaeodietary information. By focussing on the low-signal linearity of the mass spectrometer it was possible to achieve robust data with very low sample weights and low output intensities. Repeated L-alanine standards were run with suitable weights to establish the precision of $\delta^{15}N$ values from N_2 peaks above the recommended 1000mV intensity. Once linearity was established, a series of L-alanine standards of lower weights were analysed to attain a range of N_2 peaks below the recommended intensity. These data

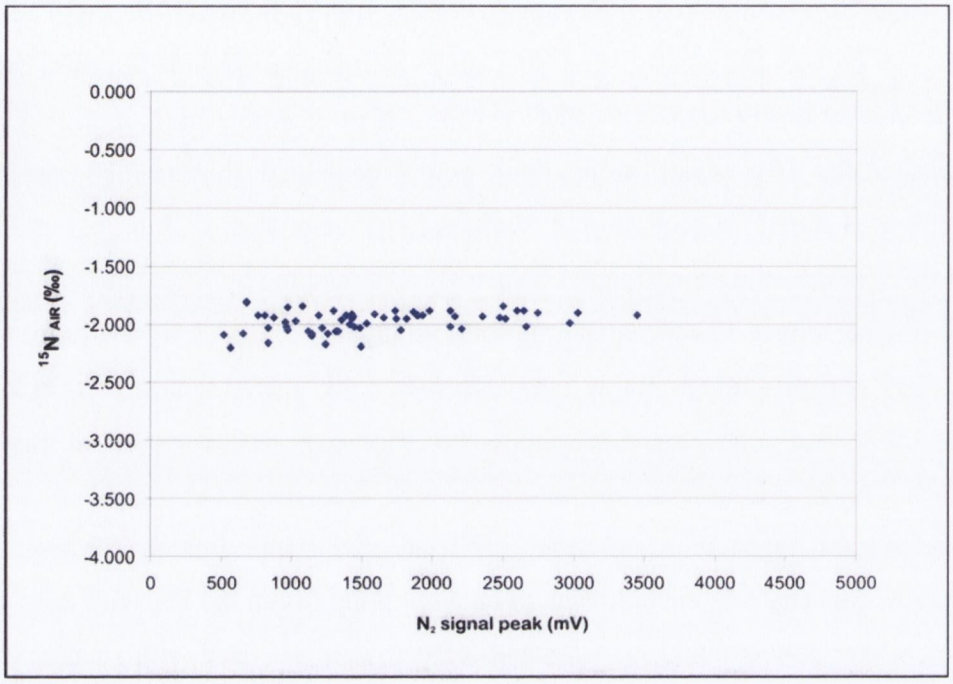

Figure 3.4: A typical graph showing the linearity of L-alanine reference samples of various weights, showing a slight deterioration in linearity below 1000mV.

were then analysed and the standard deviation calculated and a graph of $\delta^{15}N$ versus intensity (mV) drawn. An example of one such graph is shown in Figure 3.4. Once L-alanine linearity was deemed within a suitable range for running fossil samples with low peak intensities, samples of powdered fossil fish vertebrae were run repeatedly as an internal standard (sample RH260705, *Phareodus testis* Cope, 1877, which was also used in the experiments detailed in Chapter 4). This indicated that robust data could be produced from Green River fossils at peak intensities as low as 300mV, as demonstrated in Figure 3.5. Below this level the data are scattered, so all data produced with peak intensities of less than 300mV were discounted for this thesis. Excellent low-signal linearity was obtained and robust data gathered from small samples with peak intensities as low as 300mV. However, good low-signal linearity is transient and can be difficult to achieve. Optimum conditions include low contaminants in the samples, new reagents in the EA system and a young source filament. If all criteria are met the linearity can still be difficult to achieve for low intensities and can be a very time consuming task.

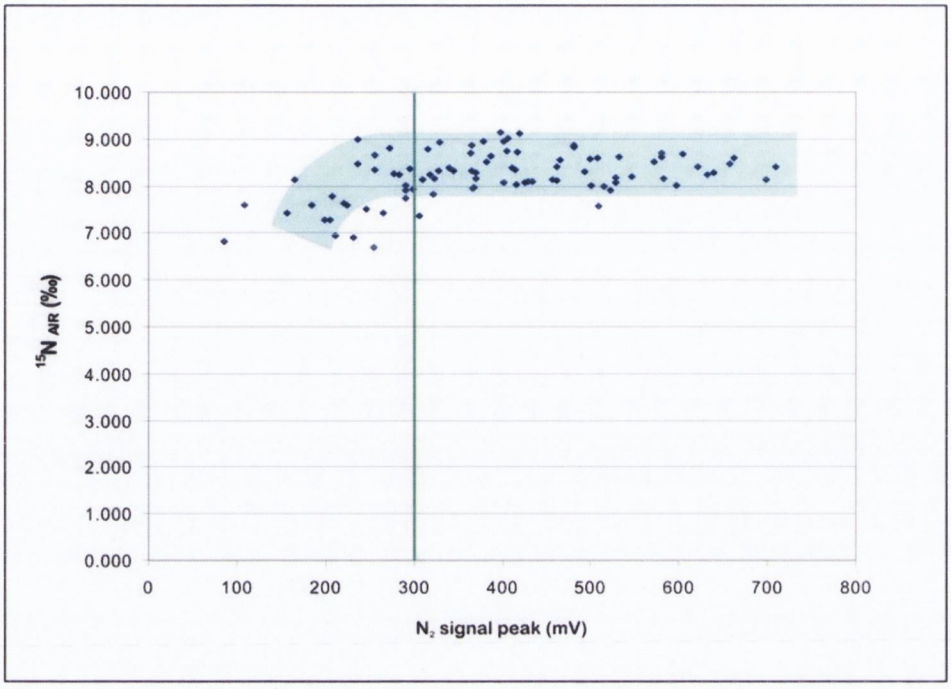

Figure 3.5: A graph showing the linearity of samples of internal standard RH260705 of various weights, showing deterioration in linearity below 300mV. Shaded area highlights the major trend observed.

3.1.5 Ascarite modification of EA

In order to overcome the difficulties of viewing both N and C on the same scale, an Ascarite II® trap was fitted to the EA to adsorb all CO_2 present so as to exclusively target the nitrogen isotopic composition of the samples and eliminate all carbon. Ascarite II® is a sodium hydroxide coated silica which rapidly adsorbs CO_2, (and other acid gases), and is used in a number of analytical and micro analytical procedures. By removing all CO_2 from the samples it was possible to run much larger samples with no interference from a large CO_2 peak, thereby achieving a much stronger signal for N_2 and reducing errors in these measurements significantly. An extra modification, using a 2m GC coil rather than the regular 3m GC coil, also improved the performance of EA when focussing on N_2 alone. However, this technique results in the loss of all C data for those samples run using the Ascarite II® trap. This was an effective method employed when running fossil samples that had not had successful complete carbonate removal, as discussed in more detail in Chapter 4.

3.1.6 Experimental amplification of N values

A further attempt was made to significantly increase the signal for the nitrogen values of each sample, thereby minimising error and maximising reproducibility. It was proposed that if a standard was added to each sample then a strong signal well within the accepted linearity of the mass spectrometer could be achieved, and the contribution to these bulk nitrogen signals by the fossil samples could then be calculated using mass balance. Approximately 0.5mg of L-alanine standard was added to each of 12 samples of homogenised prepared Green River fish RH260705. A further 12 samples of RH260705 were run with no added standard. Although the samples with added standard produced a

$$\delta^{15}N_{(bulk)} = \frac{\Sigma(\text{Standard}\,(N_{2\,(wt)} \times \%\,N) \times \delta^{15}N_{(Std)}) + (\text{Fossil}\,(N_{2\,(wt)} \times \%\,N) \times \delta^{15}N_{(fossil)})}{\Sigma(\text{Standard}\,(N_{2\,(wt)} \times \%\,N) + \text{Fossil}\,(N_{2\,(wt)} \times \%\,N))} \qquad \textbf{Equation 3.2}$$

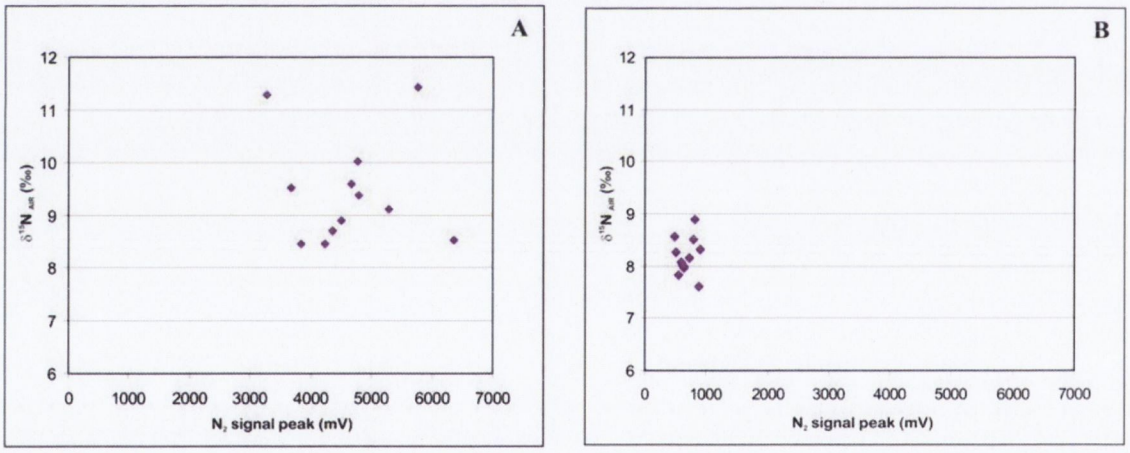

Figure 3.6: Experimental amplification of N values. **A)** Twelve replicates of sample RH260705 to which a standard was added and the $\delta^{15}N$ of each sample calculated by mass balance from the total signature. **B)** Twelve replicates of sample RH260705 which had no standard added. Although all signals are low in terms of mV the overall spread of data is much smaller.

much stronger signal (an average of 4626mV, in contrast to the unaltered sample average of 679mV), there was a slightly wider spread in the overall results. Equation 3.2 was rearranged in order to calculate the unknown entity $\delta^{15}N_{(fossil)}$ for each sample. This equation relied on the assumption that the percentage N in each fossil sample was known and constant. An average value from previous experimentation was used for this

percentage. However, after the mass balance calculations the data to remove the nitrogen values for the standard, the fossil data was extremely scattered. Although this technique of adding a standard works in theory when higher percentages of fossil nitrogen are entered into the equation, in reality the low nitrogen content of the fossil fish leads to unreliable results and henceforth this proposal was withdrawn. Figures 3.6 A and B illustrate the effects of adding a standard.

3.1.7 Data quality

All samples were handled carefully throughout collection, preparation and analysis, therefore cross-contamination is negligible. All samples were exposed to the same potential sources of contamination, for example polythene bags and aluminium foil during transportation and laboratory equipment during preparation for analysis. Powder-free latex examination gloves were used to handle all samples in the laboratory during procedures described in Section 3.1 to Section 3.3. Analytical precision is measured in terms of reproducibility, as is the precision of the analyst, therefore replicate samples and calibration standards were analysed at various points throughout the isotopic analyses. The results of these repeat analyses were used to calculate the mean standard deviation (SD) for each specimen, using Equation 3.3. The SD is shown on each graph in Chapter 5 as error bars.

$$SD = \sqrt{\frac{n\sum x^2 - \sum (x^2)}{n^2}} \qquad \textbf{Equation 3.3}$$

The results from Equation 3.3 were then used to calculate the relative standard deviation (%RSD) using Equation 3.4. The percentage RSD is quoted for the analyses in Chapters 4, 5, 6 and 8 for various techniques.

$$\%RSD = \frac{SD}{\bar{x}} \times 100 \qquad \textbf{Equation 3.4}$$

3.2 C and O stable isotope analysis of carbonate samples

The $\delta^{13}C$ and $\delta^{18}O$ values of carbonate samples were measured using the Thermo Delta^{plus} CF-IRMS via a Thermo Gas Bench II. Carbonate was scraped from horizontal layers of the soft micritic rock samples using a scalpel and 0.6mg portions of this powder were accurately weighed into round bottomed glass exetainers using a high-precision microbalance (Sartorius MC5, ± 2μg). A working standard, Cranford dolomite, and an international standard, IAEA-CO-1 Marble (157), were also weighed into other exetainers. The Cranford Dolomite used has a $\delta^{13}C$ value of -8.15‰ (±0.06) and a $\delta^{18}O$ value of -10.91‰ (±0.11). The sealed exetainers containing sample and standard mineral powders were loaded into a CTC Analytics CombiPal auto sampler with a thermostated hot block maintained at 72°C. The exetainers were flushed with CP helium then treated with >99% ortho-phosphoric acid (H_3PO_4), metered using a precision FMI acid pump. The CO_2 produced was introduced into the mass spectrometer via the Gas Bench II, using CP helium as the carrier gas. The resulting signals for C and O isotopes were recorded by the ISODAT software. All C and O isotope data were reported relative to V-PDB.

3.3 X-ray powder diffraction (XRD) analysis of samples

X-ray powder diffraction is a non-destructive analytical technique primarily used for phase identification of a crystalline material and provides information on the crystalline phases in homogenized powders. Prior to XRD analysis Green River fossil samples were prepared using the method described in Section 3.1.1, but rather than being placed in tin capsules, the dried sample was further triturated then analysed. Powdered carbonate samples and Mata Amarilla fossil samples were also analysed using XRD but no pre-treatment was necessary. The powdered samples are placed in bulk cavity mounts, loaded into a goniometer and bombarded with X-rays. The X-ray generator used was a Phillips PW1720 with a Phillips PW1050/80 goniometer and a Phillips PW3313/20 Cu k-alpha anode tube that was run under standard conditions of 40kV and 20mA. A Soller slit and a 1° divergence slit were used on the incident X-ray beam and a 1° anti-scatter slit followed by a 0.2° receiving slit were used on the diffracted beam, in front of the PW1711 Proportional Counter detector. As the sample and detector are rotated, the intensity of the reflected X-ray beam is recorded. When the geometry of the incident X-rays impinging

the sample satisfies the Bragg Equation ($n\lambda=2d \sin \theta$), constructive interference and a peak in intensity occur. The proportional counter records and processes this X-ray signal and converts the signal to a count rate. The detector controller was a Philips 1710. All measurements were taken from 3 to 40 degrees (2θ) in steps of $0.02° \ s^{-1}$. The data are output to Traces 5.20 software in order to interpret the crystalline species present in each sample, using Carleton University Department of Earth Sciences 2θ (Cu) table for common minerals and the International Centre for Diffractions powder diffraction sets 1-48 plus 70-85 from the 1998 database.

3.4 Analysis of whole rock suite and refractory elements

10g samples of powdered sediments from a profile in quarry RHF2 were sent to OMAC Laboratories Ltd, Loughrea, Ireland for inductively coupled plasma optical emission spectrometry (ICP-OES) and inductively coupled plasma mass spectrometry (ICP-MS) analysis. The samples were fused with lithium metaborate ($LiBO_2$) and lithium tetraborate ($Li_2B_4O_7$) flux in graphite crucibles at 1000°C. The resulting melt for each sample is dissolved in dilute HNO_3 and then analysed using a Perkin Elmer Optima 5300DV ICP-OES for major elements, using an internal standard. The same solutions were analysed using a Thermo X-Series ICP-MS for a suite consisting of refractory and rare earth elements that would not normally be recovered using ICP-OES alone. The samples were run in batches of 50 including blank control samples and duplicate samples. These ICP techniques combined give accurate concentrations of the major elements present, including SiO_2, Al_2O_3, CaO, MgO, Na_2O, TiO_2, Cr_2O_3, K_2O, Fe_2O_3, MnO and P_2O_5. Concentrations of refractory and rare earth elements are also given, including Ba, Ce, Co, Dy, Er, Eu, Ga, Gd, Hf, Ho, La, Lu, Nb, Nd, Ni, Pr, Rb, Sc, Sm, Sn, Sr, Ta, Tb, Th, Tm, U, V, W, Y, Yb and Zr. Loss on ignition (LOI) is given by a thermo gravimetric method.

3.5 CHN analysis of fossil and carbonate samples

Powdered samples of fossil and sediment were analysed in the Microanalytical laboratory, School of Chemistry, University of Bristol, UK. Percentage C, H and N values were obtained using a EuroVector EA3000 Elemental Analyser. The percentages of inorganic carbon present were determined using a Ströhlein Coulomat 702 Analyser. This

instrument has been modified to include phosphoric acid digestion to liberate carbon dioxide from the sample which is then measured to obtain the inorganic carbon value. Both instruments are calibrated using certified standards to ensure the accuracy of the determinations. Each sample was analysed twice giving two values for percentage C, H, N and percentage inorganic carbon (IC). Total organic carbon (TOC) present was calculated using Equation 3.5.

$$TOC = \left(\frac{\%C_1 + \%C_2}{2}\right) - \left(\frac{IC_1 + IC_2}{2}\right) \qquad \textbf{Equation 3.5}$$

3.6 Analysis of lipid biomarkers in fossil and carbonate samples

Two fossil fish samples, one sediment sample and one blank control sample underwent the following procedures to extract lipid biomarkers. The total lipids were extracted then separated to obtain neutral and acid fractions, which were further separated and derivatised as necessary for analysis by gas chromatography and mass spectrometry. The protocol used is presented here in full due to possible variations from the published literature.

NB: All glassware used in methods 3.6 and 3.7 was washed in Decon 90® surface active cleaning agent and rinsed three times with tap water and allowed to dry. The glassware was then wrapped in aluminium foil and heated to 450°C in a furnace to remove any remaining organic residue.

3.6.1 Soxhlet extraction

- 200mL of dichloromethane:methanol (DCM:MeOH) 2:1 was poured into each of four 250mL round bottomed flasks (RBFs).
- Approximately 7 pre-extracted silica anti-bumping granules were added to each one.
- The three dry, powdered samples were weighed into individual pre-extracted cellulose thimbles. Pre-extracted glass wool was placed on top to prevent loss of powder during the initial phase of extraction. Weights are shown in Table 3.1.

Sample	Pre-extracted weight (g)
Fish A / SH270701A	9.8377
Fish B / SH270701B	5.9787
Sediment / SH270701C	27.1175

Table 3.1: Pre-extracted weights of all three samples investigated using lipid biomarker analyses.

- The thimbles were placed in the chambers of the three Soxhlet extractors. A fourth Soxhlet extractor was used for a blank control sample.

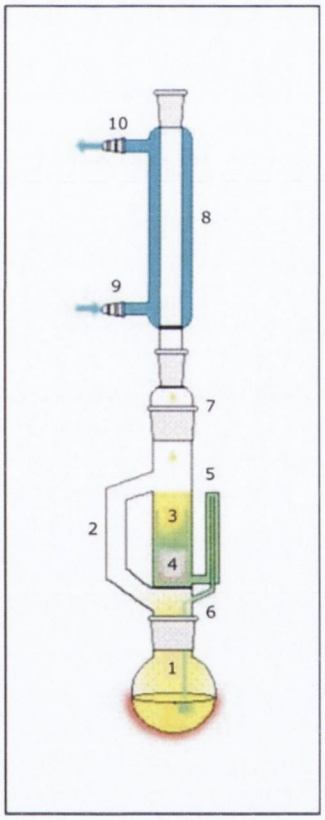

Figure 3.7: Schematic representation of Soxhlet extraction equipment. **1)** 250mL RBF with solvent (200mL of DCM:MeOH 2:1) and pre-extracted bumping granules, heated to gently boil; **2)** Distillation path; **3)** Thimble; **4)** Powdered sample with pre-extracted glass wool on top to prevent splashing; **5)** Siphon top; **6)** Siphon exit; **7)** Expansion adapter; **8)** Condenser; **9)** Cooling water in; **10)** Cooling water out.

- The RBFs were each placed in a heating element, with a Soxhlet container and attached condenser secured above (see Figure 3.7).
- The condensers and heating elements were switched to an appropriate level to allow constant gentle reflux and left for 21.5 hours. The resulting total lipid extract (TLE)

collected in the RBFs was then allowed to cool. The thimbles containing the extracted powders were covered in aluminium foil and dried in a fume hood.

3.6.2 Removal of sulphur

- Pre-extracted Cu turnings were placed in a 28mL vial and covered with 1M HCl.
- A clean stir bar was added to mix for 10 minutes using a magnetic stirrer. This process removed any surface tarnish and oxides from the Cu turnings.
- The cleaned turnings were then rinsed with:
  a) Bi-distilled DCM-extracted water (DDW) (~10x) until neutral;
  b) MeOH (3x);
  c) DCM:MeOH 2:1 (1x);
  d) DCM (3x)

  and stored in DCM.
- A small spatula-full of the now activated Cu turnings was added to the TLE in the four RBFs and left overnight (no reaction took place indicating that sulphur was not present in these samples).
- The solvent was removed from the TLE in the four flasks by means of a rotary evaporator and the TLE transferred (using DCM:MeOH 2:1) to four pre-weighed 7mL vials.
- The four 7mL vials were placed under a gentle stream of N_2 until all remaining solvent had evaporated and were then re-weighed. Weights are shown in Table 3.2.
- 10µL of a 5α-androstane 2-hexadecanol standard was added to each vial.
- The vials were capped, sealed using 3M™ PTFE tape and stored at -18°C.

Sample	TLE weight (mg)
Fish A / SH270701A	7.4
Fish B / SH270701B	53.2
Sediment / SH270701C	287.7
Blank control sample	0.1

Table 3.2: TLE weights of all three samples investigated using lipid biomarker analyses.

3.6.3 Bond Elut® column chromatography

Four Bond Elut® glass aminopropyl (NH_2) columns were used to separate two different fractions (neutral and acid fractions) from the TLE by elution using different eluents.

- The columns were prepared by washing through 12mL MeOH (2x) and 12mL dichloromethane:isopropyl alcohol (DCM:iPA) 2:1 (2x) and the eluate discarded.
- The samples and blank control sample (maximum ~5mg) were loaded onto the respective columns and eluted into 100mL RBFs. The weight of each sample used is shown in Table 3.3. Different eluents were used to extract the neutral and acid fractions from the TLE:

  - To extract the neutral fraction the samples were eluted using 12mL DCM:iPA 2:1.

  - To extract the acid fraction the samples were eluted using 12mL 2% acetic acid in ether.

- The resulting eluates were collected in eight 100mL RBFs (two per sample plus two blank control flasks) and excess solvent removed by means of a rotary evaporator. The residue was transferred (using the appropriate solvent) to eight pre-weighed 7mL vials.

Sample	Weight used (mg)
Fish A / SH270701A	7.4
Fish B / SH270701B	5.4
Sediment / SH270701C	5.9

Table 3.3: Weights of the three TLE samples added to Bond-Elut columns.

- The eight 7mL vials were placed under a gentle stream of N_2 until all remaining solvent had evaporated and were then stored at -18°C.

3.6.4 Neutral fraction protocol

3.6.4.1 Alumina column chromatography

The neutral fraction of the TLE from the three samples and the blank control sample was separated further using alumina column chromatography.

- The columns were made by plugging short glass pipettes with pre-extracted glass wool and filling with >4cm of pre-extracted activated alumina (Al_2O_3) powder (prior to use the Al_2O_3 was stored at 100°C to maintain its anhydrous form).
- The columns were prepared by washing through 1x column volume of n-hexane:DCM 9:1 and the eluate discarded.
- The samples and blank control sample were loaded onto the column and eluted into 7mL vials. Different eluents were used extract the apolar and polar fractions:
  - To extract the apolar fraction the samples were eluted using 4x column volumes of n-hexane:DCM 9:1.
  - To extract the acid fraction the samples were eluted using 3x column volumes of DCM:MeOH 1:2.
- The eight 7mL vials containing the apolar and polar fractions were kept at 40°C and placed under a gentle stream of N_2 until all remaining solvent had evaporated, then were then stored at -18°C.

3.6.5 Acid fraction protocol

The acid fraction of the TLE from the three samples and the blank control sample was treated further to release any bound fatty acids and convert all fatty acids into their methyl ester form.

3.6.5.1 Saponification

- 10µL of n-C_{19} (nonadecane, $C_{19}H_{40}$) standard was added to each of the four 7mL vials.
- 1mL of 0.5M 95% methanolic NaOH (made using DDW) was added to each 7mL vial and heated at 70°C for 1 hour.

3.6.5.2 Acidification

- The samples were acidified to pH1-2 by adding ~2mL 1M HCl to each 7mL vial.
- 2mL of n-hexane was added to each 7mL vial and mixed using a vortex mixer.
- The resultant organic layer in each vial was transferred to a clean 7mL vial.
- The remaining aqueous layer in each vial was washed with a further 2mL of n-hexane and the organic layer extracted and transferred to the new vials. This step was repeated.

- The four 7mL vials were placed under a gentle stream of N_2 until all remaining solvent had evaporated.

3.6.5.3 Methylation

- 100µL of boron trifluoride:methanol (BF_3:MeOH) was added to each 7mL vial, the vials were then capped and heated at 70°C for 30 minutes.
- After cooling 1mL of DDW was added to each vial.
- The resultant aqueous layer in each vial was washed with 2mL of DCM and the methyl ester layer extracted and transferred to a clean 7mL vial. This step was repeated twice.
- The four 7mL vials were placed under a gentle stream of N_2 until all remaining solvent had evaporated.
- The fatty acid methyl esters (FAMEs) were dissolved by adding 1mL DCM to each of the four 7mL vials.
- To remove residual water the FAMEs fraction was eluted using pre-extracted anhydrous sodium sulphate (Na_2SO_4) columns.
- The columns were made by plugging short glass pipettes with pre-extracted glass wool and filling with >4cm of pre-extracted activated Na_2SO_4 powder (prior to use the Na_2SO_4 was stored at 125°C to maintain its anhydrous form).
- The samples and blank control sample dissolved in DCM were loaded onto the columns. To extract the residual water the samples were eluted using 6mL DCM and the resultant eluate collected in clean 7mL vials.
- The four 7mL vials were placed under a gentle stream of N_2 until all remaining solvent had evaporated.

3.6.6 Trimethylsilyl (TMS) derivatisation

TMS derivatisation was necessary to replace reactive hydroxyl functional groups from the polar and FAMEs fractions with trimethylsilyl groups.

- 25µL of N,O-bis(trimethylsilyl)trifluoroacetamide (BSTFA) containing 1% trimethyl-chlorosilane was added to each of the eight 7mL vials.
- 25µL of pyridine (C_5H_5N) was added to each of the eight 7mL vials.
- The vials were capped and heated at 70°C for 1 hour.

- After being allowed to cool to 40°C the eight 7mL vials were placed under a gentle stream of N_2 until dry.

3.6.7 Gas chromatography

The apolar, polar and FAMEs fractions were analysed using gas chromatography. In GC the differences in the chemical properties between different molecules in a mixture cause these molecules to separate as the sample travels the length of the column. The interactions of the gaseous analytes with the walls of the column (coated with a stationary phase) causes the different molecules to elute from the GC at different retention times, thus facilitating the identification of individual molecules present in the mixture. The gas chromatograph (GC) used was a Carlo Erba HRGC5300 Mega Series fitted with a fused capillary column (50m x 0.32mm i.d., coated with 0.12 μm methyl silicone CPSil-5CB) and H_2 was used as the carrier gas. 1μL of Grob standard test mixture was injected on-column prior to any samples to evaluate the capillary columns (see Grob *et al.* 1978 and 1981). The twelve components in this mixture each serve as a diagnostic tool to determine the separation efficiency, film thickness, acid/base characteristics and adsorptive activity of the column and system. The results from this injection were satisfactory and the GC deemed ready for sample analyses. Prior to analysis all samples were dissolved in 50-100μL ethyl acetate (amounts used are shown in Table 3.4). For sample injection a 10μL syringe was flushed out using DCM seven times prior to, and subsequent to, use with a sample. The syringe was loaded with a 1μL air bubble, 1μL of sample and a further 1μL air bubble and these syringe contents injected on-column at 70°C. This was carried out for all twelve samples.

TLE fraction	Ethyl acetate added (μL)
Apolar	50
Polar	100
FAMEs	50

Table 3.4: Volume of ethyl acetate added to dissolve the three TLE fractions prior to GC injection.

The GC temperature program for each sample run was set as follows:

- 70°C-13°C at 20°C min^{-1};
- 130°C-300°C at 4°C min^{-1};
- Isothermal of 25 minutes at 300°C.

3.6.8 Gas chromatography-mass spectrometry

As it is not always possible to make an accurate identification of a particular molecule by gas chromatography alone, the apolar, polar and FAMEs fractions were also analysed using gas chromatography-mass spectrometry (GC-MS). These two techniques when used together allow a much finer degree of substance identification than either technique used separately. Using GC alone, multiple molecules can have the same retention time which can result in two or more molecules co-eluting leading to difficulties in identification. Combining GC with MS makes it extremely unlikely that two different molecules will behave in the same way in both. Therefore when an identifying mass spectrum appears at a characteristic retention time in a GC-MS analysis, it typically lends to increased certainty that the analyte of interest is in the sample. Prior to analysis all samples were dissolved in 50-100μL ethyl acetate (amounts used are shown in Table 3.6.4). 10μL of each of the twelve dissolved samples were loaded into crimp top auto sampler vials using a 20μL syringe flushed with DCM seven times prior to, and subsequent to, use with a sample. GC–MS analyses were made using a Thermoquest Trace GC fitted with the same column as was used for GC analyses and the same temperature program and carrier gas were employed. The GC was equipped with GC Pal (CTC Analytics) autosampler and coupled, via a transfer line heated at 300°C, to a Finnigan Trace Mass Spectrometer Plus scanning in the range of *m/z* 50–650 with a cycle time of 1s. The current was maintained at 149μA with an ion source temperature of 0.12μm 200°C and an electron voltage of 70eV. Peak assignments were made through comparison with literature mass spectra.

3.7 Analysis of amino acids in fossil and carbonate samples

Aliquots of the same powdered sediment sample and the two fossil fish samples analysed using the method outlined in Section 3.6 were subjected to the following procedure to extract amino acids. A blank control sample was also subject to the same procedure to test

the reliability of the data produced. The protocol used is presented here in full due to possible variations from the published literature.

3.7.1 Hydrolysis

- Approximately 0.1g of each of the lipid extracted samples was placed in culture tubes. The actual weights used are shown in Table 3.5.
- 50μL of norleucine standard, a crystalline α-amino acid, was added to each tube plus a blank control tube.
- 2mL of 6M HCl was added to each tube, the air evacuated using a gentle stream of N_2, before the tubes were capped and sealed using 3M™PTFE tape.
- The tubes were heated for 24 hours at 100°C before being allowed to cool slightly.
- 0.5mL of DDW was added. The tubes were then kept at 60°C and placed under a gentle stream of N_2 until dry. This step was repeated.
- 0.5mL of MeOH was added. The tubes were then kept at 60°C and placed under a gentle stream of N_2 until dry. This step was repeated.
- 1mL of MeOH was added to each of the four tubes, the tubes sealed and stored at -18°C.

Sample	Weight used (g)
Fish A / SH270701A	0.1511
Fish B / SH270701B	0.1210
Sediment / SH270701C	0.1520

Table 3.5: Weights of the three lipid extracted samples added to culture tubes for amino acid extraction.

3.7.2 Ion exchange chromatography

3.7.2.1 Preparation of DOWEX™ ion exchange resin

- A small amount of DOWEX™ resin was placed in each of two 28mL vials, 6M NaOH added and the resin left to soak overnight.
- The excess NaOH was removed by washing the resin 5 times with DDW.
- 6M HCl was added to the vials and the resin left to soak overnight.
- The excess HCl was removed by washing the resin 5 times with DDW.

3.7.2.2 Elution using ion exchange columns

- 1mL of prepared DOWEX™ resin was placed in each of four flash columns.
- The columns were washed with 2mL DDW. This step was repeated twice and neutrality of the eluate confirmed using universal indicator paper.
- <1mL of each of the hydrolysed samples were added to the columns.
- Salts were eluted from the samples using 5x 1mL DDW and the eluate discarded.
- The amino acids were eluted from the samples using 6x 1mL 2M ammonium hydroxide solution (NH_4OH) and the eluate collected in four 7mL vials.
- The vials were then heated and kept at 60°C under a gentle stream of N_2 until dry.
- 1mL 0.1M HCl was added to each vial, the vials sealed and stored at -18°C.

3.7.3 Esterification

- The vials were brought to room temperature, heated and kept at 75°C under a gentle stream of N_2 until dry.
- 1mL of fresh 2M acetyl chloride in anhydrous methanol was added to each sample.
- The vials were capped and sealed using 3M™PTFE tape, mixed using a vortex mixer and heated at 75°C for 1 hour.
- The vials were placed in an ice bath and the reagents were evaporated under a gentle stream of N_2.
- 1mL of DCM was added to each vial to remove any excess reagents and evaporated under a gentle stream of N_2 in the ice bath. This step was repeated twice.

3.7.4 Acetylation

- 1mL of acetone:trimethylamine:acetic anhydride solution 5:2:1 was added to each vial and the samples heated and kept at 60°C for 10 minutes.
- The vials were placed in an ice bath and the reagents were evaporated under a gentle stream of N_2.
- A phase separation was then carried out by adding 2mL ethyl acetate and 1mL saturated NaCl solution to each vial. After vortex mixing the organic phase from each vial was transferred to a clean 7mL vial.

- 1mL ethyl acetate was added to each of the original vials and any remaining organic phase extracted to the new 7mL vials.
- The vials were placed in an ice bath and the reagents were evaporated under a gentle stream of N_2.
- Any residual water was removed from the samples by adding 1mL DCM and the vials placed under a gentle stream of N_2 until dry. This step was repeated twice.
- 1mL DCM was added to each vial, the vials sealed and stored at -18°C.

3.7.5 Gas chromatography

The four vials of extracted amino acid residues were analysed using gas chromatography. The gas chromatograph (GC) used was a Hewlett Packard 5890 Series II fitted with a fused-silica capillary column (60m x 0.32mm i.d., coated with coated with 5% phenyl, 95% methyl, polysiloxane) and helium was used as the carrier gas.

The GC temperature program for each sample run was set as follows:

- 40°C for 1 min;
- 40°C-120°C at 15°C min^{-1};
- 120°C-165°C at 3°C min^{-1};
- 165°C-250°C at 15°C min^{-1};
- Isothermal of 15 minutes at 250°C.

Data were acquired and analysed using HP Chemstation software.

3.8 GC-IRMS stable isotope analysis of fossil and carbonate samples

Carbon isotopic ratios of individual compounds were determined by gas chromatography–isotope ratio mass spectrometry (GC-IRMS) with a ThermoFinnigan Delta S using the same column and run conditions as described above in Section 3.6.4. All C isotope data were reported relative to V-PDB and were calculated by comparison with a calibrated CO_2 gas; the uncertainties, determined by using co-injected standards, are ±0.3‰.

3.9 SEM analysis of fossil and carbonate samples

Scanning electron microscope (SEM) images of fossil and carbonate samples were obtained using a Zeiss Supra™ series variable pressure field emission SEM in the Centre for Microscopy and Analysis (CMA) at TCD. The Zeiss Supra™ is a computer controlled high resolution field emission scanning electron microscope which can produce exceptional images at low operating voltages. Samples for SEM analyses often require coating in carbon or gold to prevent the samples from becoming electrically charged due to the high operating voltages of most SEM machines. It was therefore decided that the Zeiss Supra™ SEM would be most suitable for use in this study as it produces results using uncoated samples, negating the introduction of unnecessary contaminants to the specimens and allowing for their use in further geochemical analyses. In high vacuum mode this SEM functions by scanning a focused beam of high energy electrons across the surface of each sample. The beam-specimen interaction produces a variety of signals including secondary electrons, back-scattered electrons and X-rays. The low energy secondary electrons are collected to form the standard image and the high energy back-scattered electrons provide an image with atomic number contrasts. Energy dispersive spectroscopy (EDS) microanalysis was carried out on these samples to determine their elemental composition using a PGT Spirit Energy Dispersive X-ray Analyser connected to the Zeiss Supra™ SEM. The X-rays produced in the SEM are characteristic of the elements in the sample and they may be separated out into an energy spectrum to identify the elemental composition of the sample. The X-rays were mapped back to their original position in the samples to provide a map of the distribution of the elements in the samples. The EDS detector can detect elements heavier than and including carbon and provides a quantitative analysis at a microscopic scale, for areas as little as $10\mu m^2$.

Chapter 4: Acid treatment effects on fossil fish skeletal $\delta^{15}N$ and $\delta^{13}C$

4.1 Overview

Prior to geochemical analyses fossil bones and teeth are often extracted from any surrounding lithified sediments using chemical techniques such as immersion in acid. As isotope analysis becomes more commonplace in palaeoecological investigations it is important to consider what effects chemical preparation techniques may have on the subsequent results and to constrain these effects as quantitatively as possible. In this study of ancient ecosystems with only small amounts of N and C available for analysis it was vital that variability in the data set should not be introduced as a result of protocols used during sample preparation. Here, various strengths of two weak acids commonly used during palaeontological preparation were tested to evaluate their effects on the $\delta^{13}C_{org}$ and $\delta^{15}N$ isotopic signatures of the vertebrae of a large fossil fish collected from Fossil Lake. Changes in the isotopic values occurred over time regardless of which acid was used, each causing a variable response in both $\delta^{13}C_{org}$ and $\delta^{15}N$ isotopic values. Without careful monitoring of the acidification process in a controlled environment any resulting data could confound the interpretation of an ancient food web.

4.2 Introduction

4.2.1 Introduction to fossil extraction treatments

As the geochemical analysis of fossils becomes more widespread, chemical preservation and extraction techniques of fossils need to be reviewed. In the past, the damage to fossils during retrieval, preparation and storage was an accepted downfall of the scientific process (McCrae & Potze 2007). However, modern geochemical analyses require that the fossil material be retrieved and extracted from any surrounding lithified sediment with no alteration to the fossil chemistry and that no evidence be removed, or indeed added, to the specimens. During retrieval of vertebrate specimens adhesives such as cyanoacrylates and acrylic polymers are often used in the field to ensure the integrity of the specimen. Upon arrival in the laboratory fossil preparators then use physical and chemical treatments to extract the fossil specimens from any enclosing sediments. Furthermore consolidants and

resins are often used to prevent the deterioration of specimens housed in museum collections. If geochemical data representing the original specimen are to be successfully obtained from fossils then no chemicals should be applied to the material during field collection or storage. Where possible, handling should be kept to a minimum and fossils should be stored in unreactive or inert materials such as aluminium foil which do not shed particulate matter onto the surface of the fossil specimens. During preparation or extraction from enclosing matrices mechanical methods are preferable to chemical methods, although it should be noted that the high temperatures reached due to friction with electrical drills and engraving tools may also lead to alteration of the fossil geochemistry. In the instance of retrieving fossils from calcareous enclosing sediments however, treatment with an aqueous acid or base is often the only viable option. Calcareous sediments are often extremely fine-grained and can remain in small pockets within pitted fossil bone after mechanical preparation. Chemicals are able to access these areas that mechanical tools cannot, and differentiation between matrix and fossil is more subtle and accurate (Lindsay 1987). Acid preparation also has the advantage of gradually revealing fossils hidden below the matrix surface (McCrae & Potze 2007). For geochemical analyses, particularly those involving organic carbon, it is essential to remove all traces of inorganic carbonate as this can confound any results. Incomplete removal of calcite is known to affect carbon and oxygen isotope values (e.g. Koch *et al.* 1997) although little is known of the consequences for nitrogen isotopic values.

4.2.2 The nature of this study

In this thesis the $\delta^{15}N$ and $\delta^{13}C$ isotopic signatures of Early Eocene fossil fish were investigated as a possible means for palaeoecological and palaeoclimatic reconstruction. Stable isotope analysis is used in a wide range of palaeoclimate studies and can be a very powerful tool, provided that the isotopic signatures are not chemically altered during diagenesis or sample preparation. Prior to isotopic analysis of skeletal fluorapatite from the fossil fish used in this study, pre-treatment was necessary to remove inorganic carbonate that could potentially alter the results of CF-IRMS analyses. In doing so, it was vital to avoid any chemical damage to the fossils that could result in alteration of the isotopic signatures therein. It was essential for this study that a chemical preparation

method be used to remove the calcareous matrix from the Green River fish fossils: some bones were extremely fine and fragile and mechanical retrieval was only partially successful in removing the calcareous matrix from these. In particular, fossil fish scales were very difficult to extract manually from the calcareous rock due to their delicate nature and overlapping arrangement. However, although chemical extraction was necessary to remove all carbonate, potential etching of the fossils was extremely undesirable as it may lead to alteration of the isotope values and loss of important information, and thus a suitable method was sought that would meet these requirements. It was important to identify a method adequate for removing inorganic carbonate without causing a response in the $\delta^{15}N$ and $\delta^{13}C_{org}$ isotopic values.

4.2.3 Common chemical techniques used in microfossil extraction

Chemical preparation techniques of both macro- and microfossils have been widely used since the late 19th century and the various procedures used are reviewed in texts such as Rixon (1976) and Green (2001). Many of these techniques have been developed principally for the recovery of microscopic fossils from rock samples (see Aldridge 1990 and references therein) and differ according to the rock type and composition of the microfossils. For example, studies investigating microfossils from lithified sediments use a variety of extraction techniques including harsh chemicals such as hot hydrogen peroxide (Pingitore *et al.* 1993) and sodium hypochlorite (Aldridge 1990) to release specimens from any surrounding sediment. These and other procedures can be severe and potentially lead to specimen damage. Studies using the isotopic signature of calcareous microfossils from recent unlithified sediments to investigate palaeoclimate (e.g. Barker *et al.* 2003; Elderfield *et al.* 2002; Skinner *et al.* 2003) also use chemical techniques to clean specimens prior to analysis. Such techniques often involve mechanical crushing to expose all contaminants within the microfossils, washing with methanol to remove clays, followed by hot oxidising treatment using a hydrogen peroxide solution to remove unwanted organic matter. Samples are then often polished using a weak nitric acid solution prior to analysis. These methods have also been found to be potentially destructive and can alter the chemistry of the microfossils being studied (Barker *et al.* 2003). The above examples of pre-treatment of microfossils were not deemed necessary or

suitable for this study and so were discounted as possible techniques for the safe removal of carbonate from Green River fossils.

4.2.4 Common chemical techniques used with fossil and modern vertebrates

Studies of stable isotopes from the skeletal remains of Recent vertebrates have mainly centred on the inorganic C and O isotopic values of tooth enamel from terrestrial archaeological sites. These are usually drilled and powdered before being subject to pre-treatments in order to extract bioapatite for analysis and remove the organic components. Sodium hypochlorite is commonly used for this purpose and its effects are well-documented. Zazzo *et al.* (2006) investigated the effects of NaOCl on the isotope data retrieved from drilled, powdered tooth dentine and found large differences between untreated and bleached samples. An exhaustive study of $\delta^{13}C$ values in powdered bone samples before and after NaOCl treatment by Koch *et al.* (1997) did not find such large differences, although the isotope data produced by this study had values in a region now known to show little effect from NaOCl treatment (Zazzo *et al.* 2006). However, bleaching is known to have little effect on the dissolution of calcium carbonate (Pingitore *et al.* 1993), therefore despite its effects on isotopic signatures being well defined bleaching was an unsuitable method for this study. Isotope studies of dinosaur bone in the 1990s also used samples retrieved by drilling, and bone powders were treated with a weak acetic acid solution as described by Silverman *et al.* (1952), prior to the isotopic analysis of structural carbonate (e.g. Barrick & Showers 1994; Showers *et al.* 2002). However, in these studies of dinosaur material the oxygen isotopic composition of the bone phosphate was measured after being extracted as $BiPO_4$ using a concentrated HNO_3 solution (see Shemesh *et al.* 1983 and Crowson *et al.* 1991) involving costly and complicated apparatus and no consideration was given to N isotope analyses. Balter *et al.* (2002) used a weak acetic acid to remove carbonate from hydroxylapatite within Quaternary bones and teeth by leaching under vacuum, reporting increased fractionation of $\delta^{18}O$ with time. Some studies of Recent vertebrates have investigated N and C isotopes, and although none appear to have encountered samples enclosed in a carbonate matrix, chemical treatments have been used to extract different parts of the bone for isotopic analyses. Over 20 years ago DeNiro & Weiner (1988) obtained $\delta^{15}N$ and $\delta^{13}C$ values from the organic matrix in

prehistoric bones using NaOCl to isolate the organic material from within fused aggregates of hydroxyapatite. Similarly Minami & Nakamura (2005) analysed the N and C isotopic content in Recent (>4000BP) powdered bone fragments. They tested the effects of decalcifying treatments with different strengths of HCl using modern bone for comparison and found that the HCl had a significant effect on the N isotope data, which would ultimately confound any palaeoecological interpretations. In trophic level studies of modern ecosystems using $\delta^{15}N$ and $\delta^{13}C$, washing freeze-dried powdered organisms with HCl to remove nondietary carbonate has been commonplace for many years (e.g. Rau *et al.* 1983; Fry 1988; Hobson & Welch 1992). The effects of this practise have been investigated by many other researchers (e.g. Bunn *et al.* 1995; Bosley & Wainright 1999; Pinnegar & Polunin 1999; Jacob *et al.* 2005) and have been reviewed recently in an extensive study by Carabel *et al.* (2006). The acid washing of modern organisms was found by these authors to cause fluctuations in the resulting isotope values, in particular $\delta^{15}N$, highlighting the effects of sample preparation techniques on isotope data and the potential for erroneous interpretations.

4.2.5 Objectives of this study

Despite the demonstrable effects of acid washing on stable isotopic values, it was necessary to remove enclosing carbonates from the Green River fish being studied in this thesis. It was also essential that when comparing results from the fossil fish that all samples had been treated equally during preparation and analysed under the same conditions, thereby negating any sources of random error and the introduction of any false trends to the data set. A suitable acid was required of a strength that would have minimal impact on the isotopic values while readily removing inorganic carbonate from the specimens. 1M HCl is routinely used by field geologists as a standard for determining effervescence class and readily dissolves carbonate. However, as HCl is a strong acid it was considered to have a high potential for causing textural damage to the fossils; as such other acids were considered for use in this study. Two weak acids commonly used in palaeontological preparation techniques are acetic and formic acid, and these were thought to be suitable for use in this study. Both of these organic acids are highly miscible with water, are relatively safe and easy to use and are economic when processing a large

sample set. However, when used for the extraction of phosphatic microfossils from lithified sediments as detailed in Jeppsson *et al.* (1985; 1995 and 1999), these acids were found to be potentially harmful to the fossils and therefore need careful monitoring in a controlled environment to prevent dissolution of any phosphate.

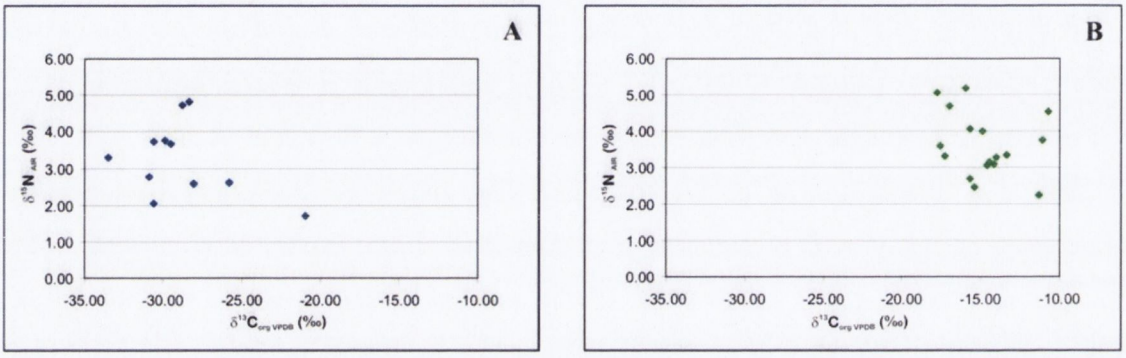

Figure 4.1: Carbonate contamination of isotope values. **A)** Typical Green River fossil N and C isotope values when all carbonate has been removed from the samples; **B)** Samples where not all carbonate residue was removed, leading to more positive C values due to inorganic carbon contamination. The $\delta^{13}C_{org}$ values are more positive by around 10‰ although $\delta^{15}N$ values do not seem to be affected.

In this investigation both buffered and unbuffered weak acids were tested in order to find the optimal technique for removing inorganic carbonate prior to isotope analysis. This was carried out prior to the preparation of any of the fossil fish samples for isotopic data acquisition presented as part of this thesis. Prior to these experiments, 1M acetic acid had been used on samples as part of a pilot study and was found to leave some carbonate residue. The inorganic carbonate residue left behind caused the organic carbon values obtained to be much more positive than expected. Previous values for $\delta^{13}C_{org}$ obtained for fossil fish during the initial research for this thesis indicated that values of -20 to -30‰ should be expected. The actual values obtained when carbonate residue was present were between -10 and -18‰. This contamination by carbonate to give more positive $\delta^{13}C_{org}$ values than expected is illustrated in Figure 4.1. 1M formic acid had also been tested on these pilot samples and had considerably depleted the amount of fossil specimen present, leading to the conclusion that fluorapatite dissolution was taking place and therefore the potential alteration of isotopic signatures. For comparison 1M acetic and 1M formic acid

were included in these experiments. The main objective was to identify an exact time limit that fossils could be safely left in acid of a certain pH before any alteration occurred.

When acetic acid is applied to carbonate sediments the result is consumption of acid and limestone, production of calcium acetate and some evaporation of water and acetic acid (Jeppsson *et al* 1999) as shown in Equation 4.1. This can result in an increase in pH and cessation of dissolution of the carbonate as all the acid becomes neutralised; this was thought to be the reason that 1M acetic acid used in preliminary studies left behind some carbonate residue. In these experiments two higher concentrations of acetic acid were tested to see whether the increased concentration of hydrogen ions would dissolve all of the carbonate whilst still leaving the fluorapatite unaffected. Conversely, the 1M formic acid used in preliminary studies had proved too aggressive; however, by buffering formic acid a higher pH can be achieved. The solution can then resist changes in pH and dissolution effects on the fossils should be minimised. Buffering has been found to decrease the risk of dissolution of phosphatic fossil material when kept at a pH above 3.6 (see Jeppsson & Anehus 1995). While formic acid can be destructive in some instances it has the advantage over acetic acid for some other localities in that it can break down dolomite, although no dolomite was present in the Green River fossil fish samples. Equation 4.2 shows the consumption of formic acid and limestone to produce calcium formate, carbon dioxide and water. In order to constrain the optimal pH and time necessary to remove all carbonate with no acid attack on the specimens, a variety of concentrations of both of these acids were tested over a logarithmic time range from as little as 1.5 hours, up to a maximum of 768 hours (32 days).

$$2CH_3COOH_{(l)} + CaCO_{3(s)} \rightarrow (CH_3COO)_2Ca_{(l)} + CO_{2(g)} + H_2O_{(l)} \qquad \textbf{Equation 4.1}$$

$$2HCOOH_{(l)} + CaCO_{3(s)} \rightarrow Ca(CHO_2)_{(l)} + CO_{2(g)} + H_2O_{(l)} \qquad \textbf{Equation 4.2}$$

4.3 Methods

In order to find the most suitable acid for pre-treatment of all fossil samples, the vertebrae of a large *Phareodus testis* Cope, 1877 specimen from locality RH F-1 (RH260705) were used to experiment upon (see Figure 4.2). The vertebrae were assumed to have a fairly uniform isotopic signature and were ground and homogenised so that each portion used in these experiments would be equal in all aspects and have the same isotopic composition at the outset. Prior to acid testing all powdered samples were examined using XRD performed at standard conditions as detailed in Chapter 3 Section 3.3 in order to identify mineral composition and to confirm that there was no phase variation between the ground, homogenised vertebrae portions. All samples were found to be comprised of fluorapatite and calcite. XRD is not quantitative, but the percentages of these two mineral phases were assumed to be similar in all samples, based on visual observations. All reagents used in these experiments were of research grade to prevent the addition of any impurities and all acid solutions were prepared using deionised water (DIW).

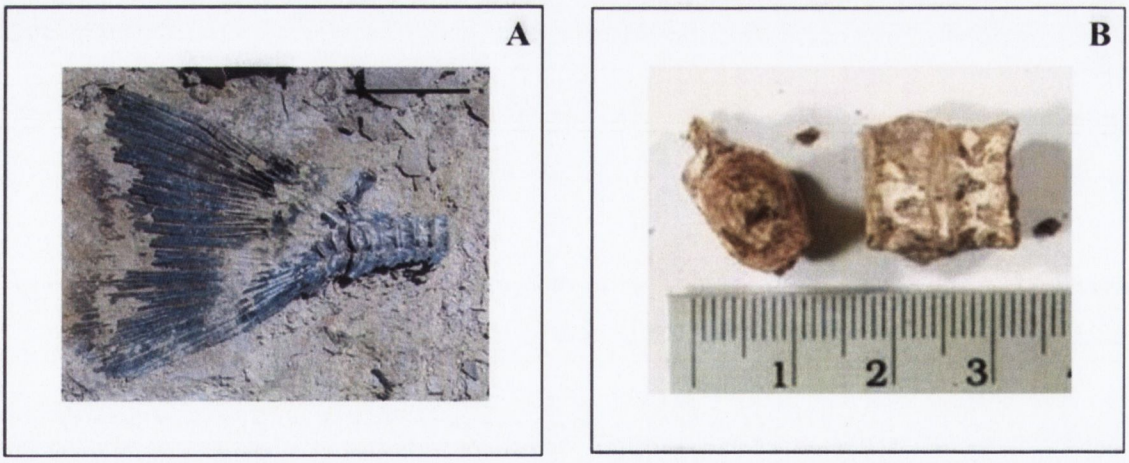

Figure 4.2: Fossil specimen used for experimentation. **A)** *Phareodus testis* RH260705 *in situ*, scale bar 5cm; **B)** Some sections of vertebrae from sample RH260705 prior to preparation.

This experiment used three concentrations of unbuffered acetic acid and three concentrations of unbuffered and buffered formic acid in aqueous solution. Details of these solutions are shown in Table 4.1. The acid dissociation constant or pK_a value for formic acid is given as 3.75 in tables in Beynon & Easterby (1996). Buffers give effective pH control when within about one pH unit on either side of the pK_a value, therefore pH 3

and 3.7 were chosen for these experiments. 1M NaOH solution was added to 1M formic acid until the desired starting pH was achieved. The pH was measured using a pHep® 4 waterproof pH/temperature tester which was calibrated immediately prior to these experiments. Temperature was not one of the monitored variables in this experiment; the pH of both acetic and formic acids are relatively unaffected by changes in temperature (Beynon & Easterby 1996). The effect of ionic strength was not considered to be significant here and no neutral salts were added. To prevent any contamination of the samples all acid treatments were carried out the clean over-pressured glove box described in Chapter 3 Section 3.1.1. Laboratory equipment was washed in a solution of Decon 90® surface active cleaning agent where possible and rinsed thoroughly with DIW. Additionally, all glassware was soaked in 10% HCl overnight and rinsed five times in DIW before use. 100mg subsamples of the powdered fossil *Phareodus testis* vertebrae were weighed into each of 60 labelled beakers using a high-precision microbalance (Sartorius MC5, ± 2μg). Replicate samples were also run to monitor reproducibility. Ten time periods on a logarithmic scale were chosen for this study, from 1.5 hours up to 768 hours. 40mL of the relevant acid was added to each beaker, the pH and time (t_0) noted. All beakers were stirred midway through the experiment ($t_{½}$) and the pH noted. After each time increment had elapsed (t_1), the pH was measured for a final time, the acid drawn off and each powdered sample rinsed twice with DIW before being left to dry at room temperature.

Description	Label	Base added	Initial pH
Unbuffered acetic acid, 1M	A1	None	2.2
Unbuffered acetic acid, 2M	A2	None	1.9
Unbuffered acetic acid, 3M	A3	None	1.9
Unbuffered formic acid, 1M	F1	None	1.6
Buffered formic acid, 1M	FB3	Sodium hydroxide, NaOH	3.0
Buffered formic acid, 1M	FB4	Sodium hydroxide, NaOH	3.7

Table 4.1: Six different acid solutions tested in this experiment

The dried samples were then accurately weighed before being re-examined using XRD to identify any overall changes in mineral composition. For the analysis of $\delta^{15}N$ and $\delta^{13}C_{org}$ content, portions of each powdered sample (1.5-16mg) were measured using CF-IRMS under conditions described in full in Chapter 3 Section 3.1.3. Samples were analysed on the same day in a random order to prevent any systematic bias in the results, and corrected to international standards with the L-Alanine working standard previously described in Chapter 3. Experimental precision based on these replicates was ±7.4%RSD for $\delta^{15}N$ and ±3.3%RSD for $\delta^{13}C$.

4.4 Results

Results of all analyses are shown in Appendix 2 and Figures 4.3 to 4.6. Results for all samples left in acid for a total of 192 hours were omitted from the graphs due to suspected contamination during deionised water rinses.

4.4.1 Variations in pH

Although very little carbonate was thought to be present within the samples when compared to the majority of the fossil samples prepared for analysis in this study, there was an immediate effect on the pH of all four unbuffered acids at t_0 when they were added to each relevant aliquot of RH260705. For acid A1 an average change of 0.65 pH units was observed, for A2 an average change of 0.75 pH units was observed and for acid A3 a change of 0.6 pH units was observed in each beaker at t_0. Similarly a change of 0.5 pH units for the unbuffered formic acid F1 was observed at t_0, whereas the buffered formic acids remained constant. Further pH measurements were taken at $t_{½}$ and t_1, and it was found that this trend towards more basic pH values continued with time. Those samples remaining in the lower molarity acetic acid for the longest time showed the most marked changes in the pH of the resultant solution. For example, samples in acid solution A1 with an average t_0 value of pH 2.85 showed an increase to pH 3.3 during the first 192 hours of the experiment, with a final t_1 pH reading of 3.7 at 768 hours, an overall observed increase of 0.85 pH units. For samples in acid solution A2 with an average t_0 value of pH 2.65, an increase to pH 3.0 was observed during the first 192 hours of the experiment, with a final t_1 pH reading of 3.3 at 768 hours, an overall increase of 0.65 pH units. For samples in acid

solution A3 with a t_0 value of pH 2.5, an increase to pH 2.8 was observed during the first 192 hours of the experiment, with a final t_1 pH reading of 3.0 at 768 hours, an overall increase of 0.5 pH units. Similarly, the solutions containing samples in unbuffered formic

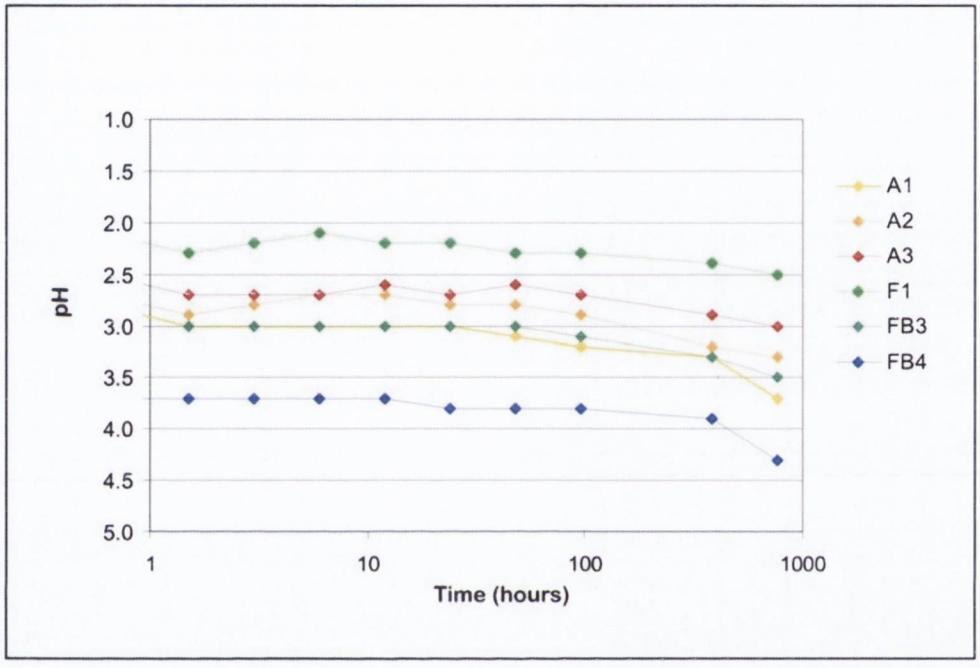

Figure 4.3: pH values at t_1 for all acids at nine intervals from 1.5 to 768 hours (time shown on logarithmic scale). Samples were treated using: A1, 1M acetic acid; A2, 2M acetic acid; A3, 3M acetic acid; F1, 1M formic acid; FB3, formic acid buffered to pH 3; and FB4, formic acid buffered to pH 3.7.

acid F1 showed an increase in pH over time. For samples in acid solution F1 with a t_0 value of pH 2.1, an increase to pH 2.3 was observed during the first 192 hours of the experiment, with a final t_1 pH reading of 2.5 at 768 hours, an overall increase of 0.4 pH units. Surprisingly the solutions containing samples in buffered formic acid also showed some changes in pH over time. Both FB3 and FB4 were stable for at least 48 hours after being added to the fossil samples, but by 768 hours after the experiment began FB3 had increased by 0.5 pH units and FB4 had increased by 0.6 pH units. The measured pH values at t_1 for each acid are shown in Figure 4.3 plotted against a logarithmic timescale and all show this gradual trend towards more basic values over time.

4.4.2 Variations in $\delta^{15}N$

In Figure 4.4 the $\delta^{15}N$ isotope values of the RH260705 samples treated with the six different acids are plotted against a logarithmic timescale. These $\delta^{15}N$ isotope values show increasing fluctuations with increasing time, particularly the profiles of those treated with the three different molarities of acetic acid. For the first 48 hours the three acetic acid treatment profiles all fluctuate between 5.5 and 7‰ before dropping sharply to a minimum at 384 hours (or 16 days), with the samples in the most concentrated acid (A3) recording a

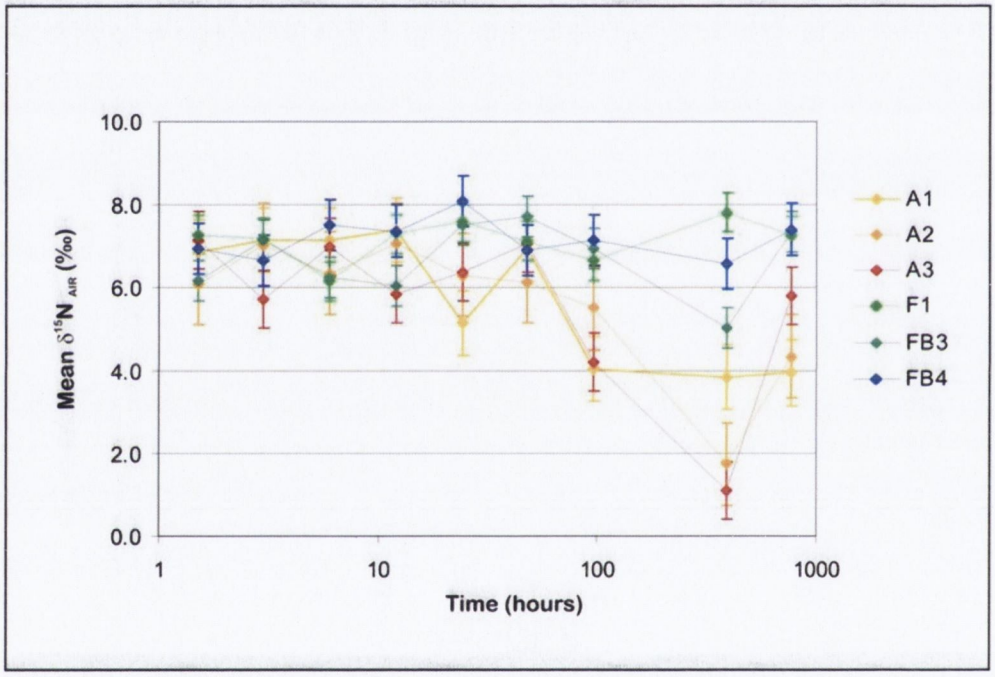

Figure 4.4: $\delta^{15}N$ mean isotope ratios for samples left in acid for a total of 1.5 to 768 hours (time shown on logarithmic scale). Error bars represent the standard deviation for each acid method. Samples were treated using: A1, 1M acetic acid; A2, 2M acetic acid; A3, 3M acetic acid; F1, 1M formic acid; FB3, formic acid buffered to pH 3; and FB4, formic acid buffered to pH 3.7.

mean $\delta^{15}N$ as low as 1.1‰ at this point. All three profiles then returned to higher values before 768 hours (32 days) lapsed, of between 4 and 6‰. The samples treated with the three formic acids all show different trends, with the unbuffered 1M acid (F1) samples showing a fluctuating profile over time with a general positive trend, and the profile of the samples treated with buffered FB3 acid being similar to the acetic acid trends. The profile

of the samples treated with FB4 acid show a general increase to the 24 hour point before decreasing to a minimum at 384 hours followed by a return to higher values. The $\delta^{15}N$ isotope values of the samples treated with F1 and FB4 show less dramatic (<2‰) fluctuations overall, staying between 6 and 8‰ at all times. The $\delta^{15}N$ isotope values for all samples, regardless of acid strength, appear to be most stable within the first 48 hours of the experiment, with larger variations occurring after this time.

4.4.3 Variations in $\delta^{13}C$

Figure 4.5 shows the organic carbon isotope signatures for samples at t_1 after treatment with each of the six acids, with time in hours plotted on a logarithmic scale. The three profiles for samples treated with different molarities of acetic acid are similar, showing an initial drop, then fluctuating between approximately -25 and -23‰. The results for samples treated with formic acid FB4 show a varying profile, with fluctuations limited to

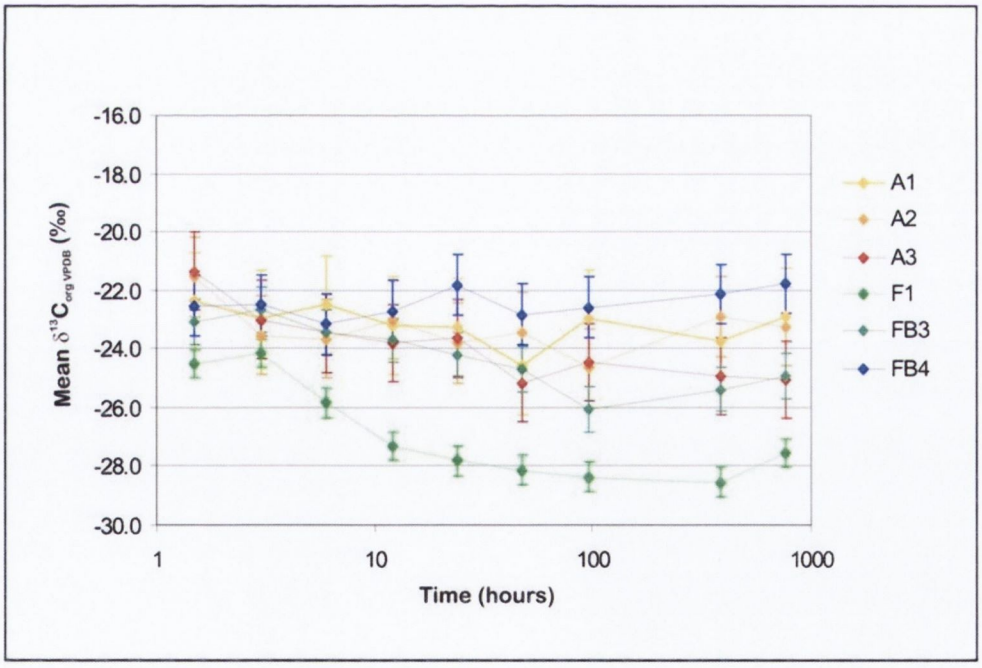

Figure 4.5: $\delta^{13}C_{org}$ mean isotope ratios for samples left in acid for a total of 1.5 to 768 hours (time shown on logarithmic scale). Error bars represent the standard deviation for each acid method. Samples were treated using: A1, 1M acetic acid; A2, 2M acetic acid; A3, 3M acetic acid; F1, 1M formic acid; FB3, formic acid buffered to pH 3; and FB4, formic acid buffered to pH 3.7.

between -23.2 and -21.8‰. Samples treated with F1 and FB3 formic acids show relatively smooth curves with an overall more negative trend over the first 96 hours, with a slight return to more positive values towards the end of the experiment. Both acids caused changes of around 4‰ in the organic carbon isotope value of RH260705 overall. However, acid F1 seems to cause the most marked changes in the $\delta^{13}C$ isotope values after just 3 hours, when compared with the isotope results for all samples treated with the other acids. The $\delta^{13}C$ isotope values for RH260705 samples treated with all other acids appear to be most stable within the first 48 hours of the experiment, with larger variations occurring after this time.

4.4.4 Variations in weight

Each beaker contained 100mg of powdered *Phareodus testis* vertebrae RH260705 at the outset (t_0). After each time increment had lapsed, the dried powder remaining was weighed. These weights are shown in Appendix 2 and Figure 4.6. The unbuffered formic acid (F1) had the most marked effect, decreasing the sample weight by 90% within 24 hours, confirming the qualitative visual assessment of preliminary studies. Buffering was found to considerably reduce this dissolution of fluorapatite and gave similar results to the acetic acid treatments. For the samples treated with the acetic acids and buffered formic acid FB3, at least 20% weight loss occurred in the first 1.5 hours of the experiment. This indicates that at least 20% of samples from RH260705 were composed of readily dissolved $CaCO_3$. Within this same time frame only 10% of the sample in acid FB4 had dissolved, indicating that the highly buffered acid lacked the capacity to dissolve $CaCO_3$ successfully. In most cases the weight of the remaining sample increased after a treatment period of between 8 and 16 days. XRD analyses were unable to detect any new mineral phases accumulating within any of the samples of RH260705 treated with the various acids. The XRD traces for all samples are shown in Figure 4.7; although no change in the overall mineral composition is observed after the acid treatments were applied for 768 hours, the presence of calcite has decreased substantially.

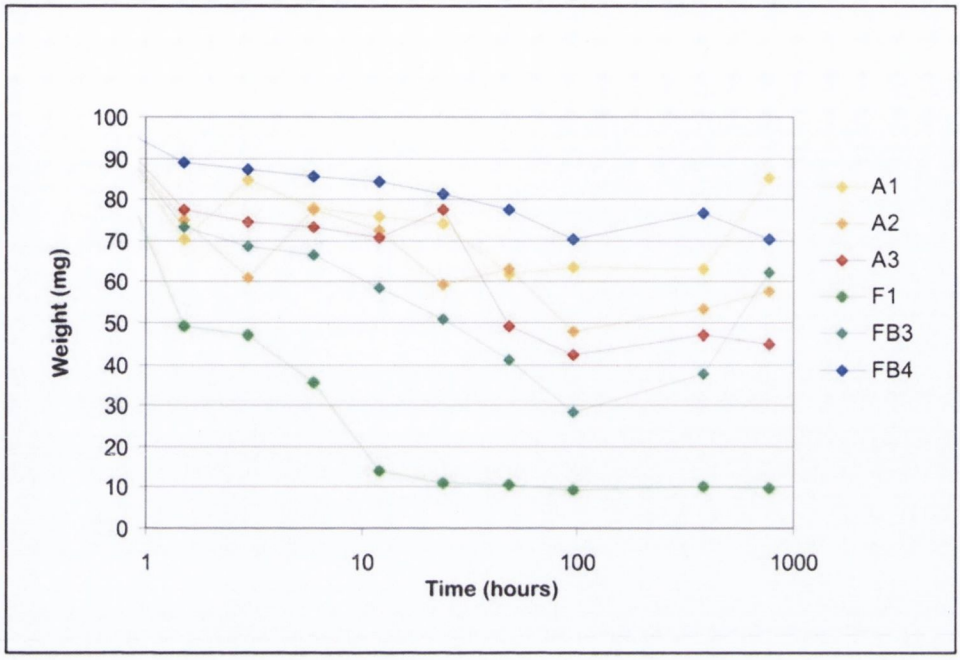

Figure 4.6: Weight at t_1 for samples at nine intervals from 1.5 to 768 hours (time shown on logarithmic scale). Samples were treated using: A1, 1M acetic acid; A2, 2M acetic acid; A3, 3M acetic acid; F1, 1M formic acid; FB3, formic acid buffered to pH 3; and FB4, formic acid buffered to pH 3.7.

4.5 Discussion

4.5.1 Variations in pH

All unbuffered solutions showed an immediate change in pH as soon as each acid was added to each sample of homogenised RH260705 vertebrae. This was due to $CaCO_3$ dissolving in the acid upon contact, thereby making the resultant solutions more basic. In the solutions treated with acetic acid this trend continued and there was an inverse relationship between the overall pH changes and the molarity of acid used over time; larger final changes in pH were observed at t_1 in those samples treated with lower molarity acids. The fewer acid ions available to react with the relatively constant amount of $CaCO_3$ present in each beaker meant that the pH quickly became more basic. Conversely, the higher molarity acetic acids allowed a less marked change because available ions were still present and the reaction shown in Equation 4.1 did not go to completion. Weaker acids with fewer ions available for reaction with $CaCO_3$ lead to the total consumption of

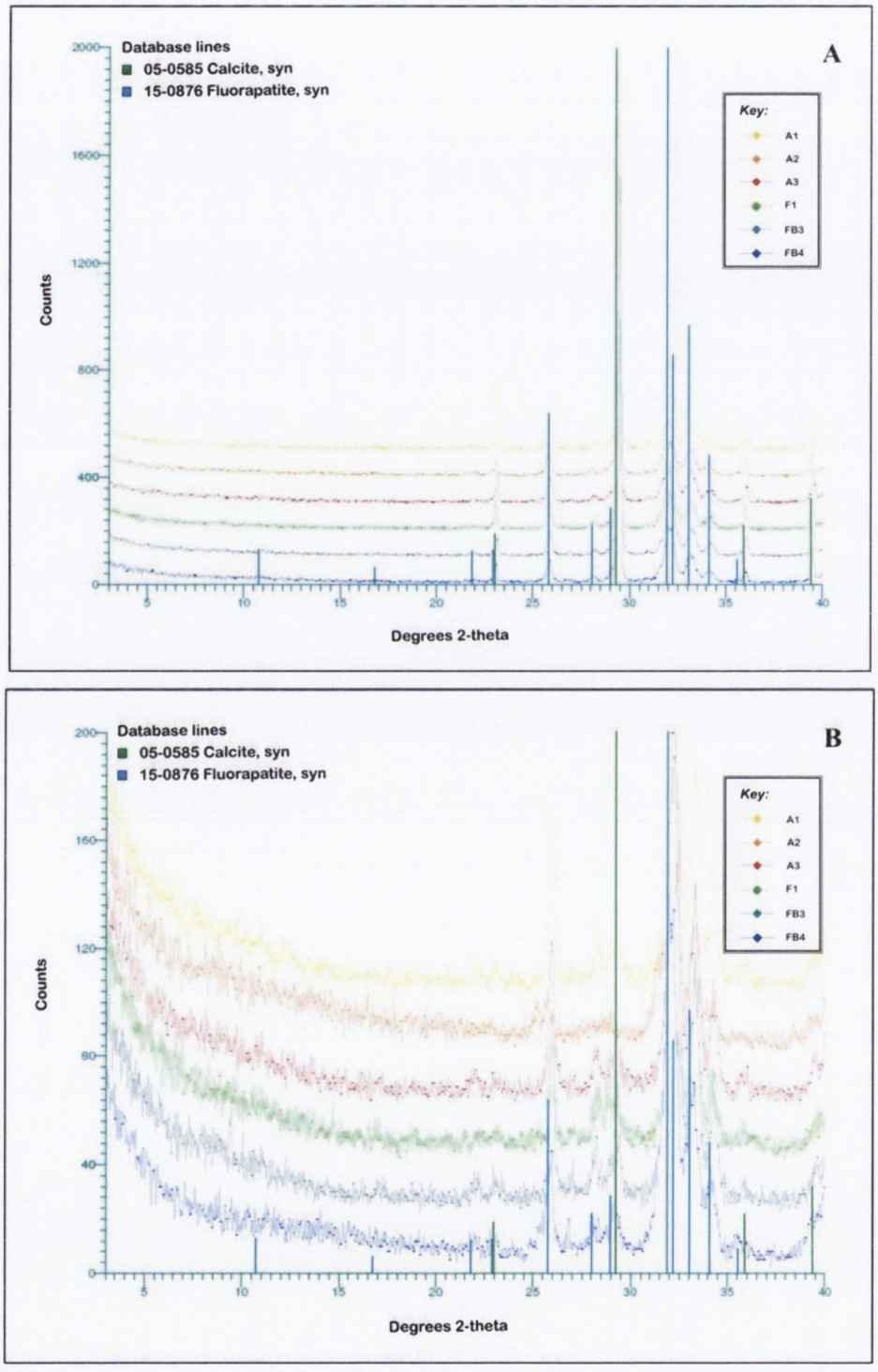

Figure 4.7: XRD traces of RH260705 aliquots **A)** before and **B)** after being treated with various acids for 768 hours. Note the change in the count scale between profiles A and B caused by the lower calcite content of the samples after treatment. Compositionally all aliquots are very similar in profile A and in profile B.

acetic acid and the production of calcium acetate, with excess $CaCO_3$ remaining in the sample. For samples containing more carbonate than those herein, unbuffered acetic acid should be changed frequently to prevent the solution becoming saturated with calcium acetate and unable to dissolve any more $CaCO_3$. Based on the findings in this chapter, the treatment of fossil samples should be adjusted according to the amount of $CaCO_3$ present. The powdered fossil vertebrae used here were relatively unaltered over a certain amount of time in the acetic acid; despite having very little $CaCO_3$ present in the samples little dissolution of the fossil powders took place. It is presumed from these findings that fossil samples containing a much higher proportion of $CaCO_3$ will have the increased ability to force Equation 4.1 to the right, with all available acid being used at a much faster rate. This indicates that the addition of acetic acid to a sample with higher $CaCO_3$ would show a much more marked increase in initial pH. Therefore, the relevant acid should be replaced at frequent intervals, within the time frame identified here as 'safe', until only an increase in pH of ~0.6 occurs after the addition of fresh acetic acid, as noted here at t_0. Once this initial pH is achieved, the fossil sample can then be safely left in the acid for less than 48 hours, as discussed in Section 4.4, without affecting the isotopic values more than shown in Figures 4.4 and 4.5.

Overall, the 1M unbuffered formic acid used in these experiments showed the smallest pH change of the unbuffered acids, just 0.4 pH units between t_0 to t_1. This indicates that more ions were available for reaction with the $CaCO_3$ in the formic acid than in any of the acetic acid solutions, probably due to its higher ionisation constant. However, the dramatic decrease in sample weight to just 10% of its initial mass after 24 hours shows that this method is wholly unsuitable when dealing with small quantities of fossil material during preparation for isotope geochemistry. The most marked changes in $\delta^{13}C_{org}$ of 4.39‰ were also observed when using this acid, further demonstrating the unsuitability of this acid for isotope geochemistry preparation. 1M formic acid when buffered to pH 3 using NaOH shows similar qualities, although not as pronounced. Although changes in pH were negligible throughout these experiments, a decrease in sample weight to ~50% of the initial mass occurred during the first 24 hours, indicating that dissolution of the fluorapatite was not halted by the raised pH. Similarly, large changes were also observed

in the $\delta^{13}C_{org}$ results, of up to 2.96‰. These indicate that 1M formic acid buffered to pH3 is also unsuitable for isotope geochemistry preparation of fossil material. Jeppsson & Anehus (1995) observed that buffering decreased the risk of dissolution of phosphatic microfossils when kept at a pH above 3.6. Here, 1M formic acid was buffered to pH 3.7, but almost 20% of the original sample still dissolved within 24 hours of adding this acid to the powdered vertebrae. The pH remained almost constant for the majority of these experiments however, and very few changes were observed in the trends of either $\delta^{15}N$ or $\delta^{13}C_{org}$. The main drawback of using this acid for fossil preparation specifically to remove $CaCO_3$ is that very little carbonate dissolution appears to take place on the timescale used here. Visual observations indicate that this highly buffered acid has a very low capacity for consumption of excess $CaCO_3$, with uptake inhibited by the volume of NaOH added. Based on these observations it is suggested that the fossil samples to be prepared for this study containing a much higher proportion of $CaCO_3$ than the vertebrae of sample RH260705 would take a matter of months to prepare using this buffered acid.

4.5.2 Variations in isotopic signature and weight

Samples of RH260705 immersed in any of the six aqueous acid solutions showed demonstrable changes in their isotopic signatures and weights over time. It is postulated that as the fluorapatite breaks down and goes into solution, as reflected in the overall weight decrease in the samples, so must some of the organic matter contained within its mineral matrix. Generally, more negative nitrogen isotope values were observed with increasing time, particularly after treatment in the acetic acids which appeared to selectively leach the heavier isotope, predominantly after 48 hours had lapsed. This suggests that the heavier isotope is preferentially released and taken into solution by the acids, thereby decreasing the $\delta^{15}N$ signature of the solid residue. Similarly a general decrease in the $\delta^{13}C$ values was observed with increasing time. Again, it can be postulated that the heavier isotope is preferentially released and taken into solution with the acid, or is used in the production of calcium acetate, calcium formate or carbon dioxide. As shown in Equations 4.1 and 4.2 there are numerous pathways for the released organic carbon atoms to take during the dissolution reactions. The heavier isotope of carbon may form stronger bonds within the new chemical species formed during these reactions and thereby

remain in solution. Alternatively the lighter isotope of carbon may preferentially remain in the organic matter within the fluorapatite lattice, or its uptake into new chemical species could be inhibited by the stronger reactivity of the heavier isotope. The overall net effect of these processes would be reflected in the decreased isotopic values shown in Figure 4.5.

The more positive upturn in both N and C isotopic signatures after 192 hours had lapsed cannot easily be explained. However, this does coincide with an increase in weight in the majority of the samples immersed in the different aqueous acid solutions. If a new precipitate or solid is beginning to form or settle out of suspension at this time then perhaps the heavier isotopes are preferentially incorporated into this new mineral species. The appearance of this proposed solid in the solutions after 192 hours is unusual in that it appears to form in both the samples treated with acetic acid and those treated with formic acid. All isotopic data for these experiments were acquired on the same day and samples were run in a random order to prevent any systematic bias in the results, so these unexplained trends appear to be real. These changes in both N and C isotopic ratios are also coupled with the measurable weight gain, proving conclusively that a solid is forming from the solution. This may be due to calcium acetate and calcium formate forming within the solutions. These are not evident in the XRD traces in Figure 4.7 B; however they may still be present in quantities that are below the detection limits of the apparatus. Only fluorapatite and calcite are shown to be present in the XRD traces, but it is unlikely that any weight increase could be due to the re-precipitation of either mineral. In order for the reactions shown in Equations 4.1 and 4.2 to operate in reverse the solutions would have had to approach a pH of 9 to enter the carbonate stability field (see Zeebe & Wolf-Gladrow 2001). The most likely explanation is the formation of calcium salts, as observed during the acid treatment of vertebrate fossil bone samples by previous authors (see McCrae & Potze 2007 and references therein), thus causing the observed weight increase in the dry powder residue post-treatment.

4.6 Conclusion

All six acid treatments affected the isotope geochemistry of the powdered *Phareodus testis* sample. Increasing the molarity of the acetic acid treatment resulted in only a small variation in initial pH at t_0 and appeared to exert little influence on isotopic signatures within the fossil fish in the first 48 hours. However, in preliminary investigations 1M acetic acid was found to leave some carbonate residue in the samples, thereby causing unwanted effects on the organic carbon isotope signature. Inorganic carbon remaining in the samples caused a variable shift in the $\delta^{13}C$ data to more positive values. The results shown here suggest that 3M acetic acid causes the most variation in the isotopic signature of the fluorapatite. A 2M solution appears to be more suitable when using acetic acid, ensuring successful carbonate removal whilst remaining an economic method for preparation of a large sample set requiring consistent results. The increases in weight and the positive changes in the isotope values after 16 days suggest that some other solid begins to form within the beakers due to the acid treatments. XRD analysis of the powder remaining after treatment did not clarify this matter, indicating that the solid formed may be present in very small quantities or may not be crystalline. The unbuffered formic acid caused the most marked changes in the carbon isotope curve and the most dissolution of the fluorapatite powder. While formic acid is very effective for removing any carbonate matrix from palaeontological samples, care should be taken if geochemical analyses are to be based on these samples. A pH of approximately 3.5, achieved by adding an appropriate base, can counteract these adverse effects. However, the higher pH means that the acid has less ability to consume $CaCO_3$ in a timely manner. By consistently replenishing the buffered formic acid it is thought that $CaCO_3$ will eventually dissolve completely over an extended time period, but this was not thought a viable technique for use in this project due to the schedule and the financial constraints.

When using a preparation treatment prior to geochemical analysis of fossils, consideration should always be given to the time period involved if the effects on the isotope geochemistry are to be negligible. The results shown in Section 4.4 suggest a time frame of less than 24 hours is the most suitable; longer leach periods lead to significant artefacts in the resulting isotopic data. If all samples are treated in exactly the same manner and for

an exact, short amount of time, then the resulting data should be robust, making direct comparison within the data set possible. A weak acid was sought for use during this research which would produce the least effect on the isotopic values and weights of the fossils to be analysed, balanced with being the most able to dissolve $CaCO_3$. Based on the findings herein 2M acetic acid, when used for a total of less than 24 hours, has the least significant effect on the isotopic values, pH and weight of the fluorapatite fossils coupled with the highest potential for dissolving $CaCO_3$ when compared to the other acids used in this investigation. Therefore 2M acetic acid should be used for the pre-treatment of fossils in the acquisition of organic isotope data and was deemed suitable for all acid digestion treatment of Green River fossil fish prior to the isotopic data acquisition reported in Chapter 5.

Chapter 5: Fossil fish analyses and chemostratigraphy of Fossil Lake

5.1 Overview

Fossil fish collected from the well-studied fossil ecosystem of the Green River Formation, Wyoming, were analysed for their isotopic signatures. The aim was to identify whether $\delta^{15}N$ and $\delta^{13}C_{org}$ values of the original fish were preserved and could be used to reconstruct trophic level in individual fish species. This could be tested by using the isotopic signatures to calculate trophic level, then by the use of direct comparison of the results to trophic adaptations of the fish inferred by observation. Various considerations are discussed and several techniques were used to assess the geochemical characteristics of the fish, including XRD and EDS microanalysis. Different preserved tissues of two fossil fish were analysed individually to assess whether the isotopic differences observed between modern fish tissues might be preserved. Six different species from one mass mortality horizon were analysed to test whether the trophic hierarchy was reflected in the $\delta^{15}N$ and $\delta^{13}C_{org}$ signatures produced. If the trophodynamics were constant in Fossil Lake then any changes in the $\delta^{15}N$ isotopic signatures of one fish species over time should reflect changing primary productivity. Large numbers of three primary to secondary consumers were analysed from throughout the stratigraphy to test whether changing nutrient levels could be reconstructed. These changes are discussed along with palaeoenvironmental implications of $\delta^{13}C_{carbonate}$ and $\delta^{18}O$ isotopic signatures and major, trace and Rare Earth Element concentrations from whole rock chemostratigraphy at locality RH F-2.

5.2 Introduction

5.2.1 Rationale

The original principal aim of this project was to collect fish fossils from a range of trophic levels in Fossil Lake, an extinct ecosystem where frequent mass mortality horizons are found. The trophic level of most species has long been established from morphological observations (e.g. Grande 1984). The $\delta^{15}N$ data from the fossils collected would therefore be analysed and compared with palaeoecological conclusions from previous studies,

through calculation of trophic level. Proving this technique in a well-documented ancient ecosystem could therefore expand the use of bulk $\delta^{15}N$ and $\delta^{13}C_{org}$ data to reveal trophic interactions of more poorly known fossil ecosystems where there are perhaps no extant equivalent species. When analysing modern aquatic ecosystems, a linear relationship has been postulated between $\delta^{15}N$ and $\delta^{13}C_{org}$ values from organisms feeding at different trophic levels, as first demonstrated by Minagawa & Wada (1984). Using $\delta^{15}N$ data, trophic level can be calculated directly using Equation 5.1 (from Pinnegar *et al.* 2002), where TL_{Ni} is trophic level in species *i*, $\delta^{15}N_i$ is the mean $\delta^{15}N$ of species *i*, $\delta^{15}N_{ref}$ is the mean $\delta^{15}N$ of the reference species and TL_{ref} is trophic level of the reference species. By choosing a reference species of a known trophic level, the trophic level of all other species in the same ecosystem can therefore be calculated using their mean $\delta^{15}N$ values. In their equation, Pinnegar *et al.* (2002) assumed a dietary isotopic shift of 3.4‰ per trophic level. However this is now widely thought to be too high for fish and a shift of 2.9‰ per trophic level is thought to be more realistic when analysing whole fish (Sweeting *et al.* 2007).

$$TL_{N_i} = \left[\frac{(\delta^{15}N_i - \delta^{15}N_{ref})}{3.4} \right] + TL_{ref} \qquad \textbf{Equation 5.1}$$

The objective for the field campaign was ideally to retrieve a variety of fossil fish species from several mass mortality horizons to test whether $\delta^{15}N$ and $\delta^{13}C_{org}$ values could be used to trace palaeo-trophic level at each stratigraphic horizon. As discussed in Chapter 2 Section 2.6, only one large slab or ash plate was collected representative of the wider ecosystem, containing 27 Green River fossil fish of 6 different species, namely *Knightia eocaena*, *Knightia alta*, *Diplomystus dentatus*, *Priscacara liops*, *Mioplosus labracoides* and *Phareodus encaustus*. Figures 5.1 A to F show representative photographs of each of these species The remainder of the fossil fish collected for this study were the small clupeomorphs *K. eocaena*, *K. alta*, *D. dentatus*, collected from throughout the RH F-2 stratigraphic section with the aim of revealing something of the palaeoproductivity of Fossil Lake. As the lake system changed over time, changes in primary productivity would have been reflected in the remainder of the ecosystem, with fluctuations in nutrient

level being coupled to changes in $\delta^{15}N$ in fish (see Section 5.2.6). All fossil fish collected and analysed for this study were adults to ensure direct comparison of trophic level.

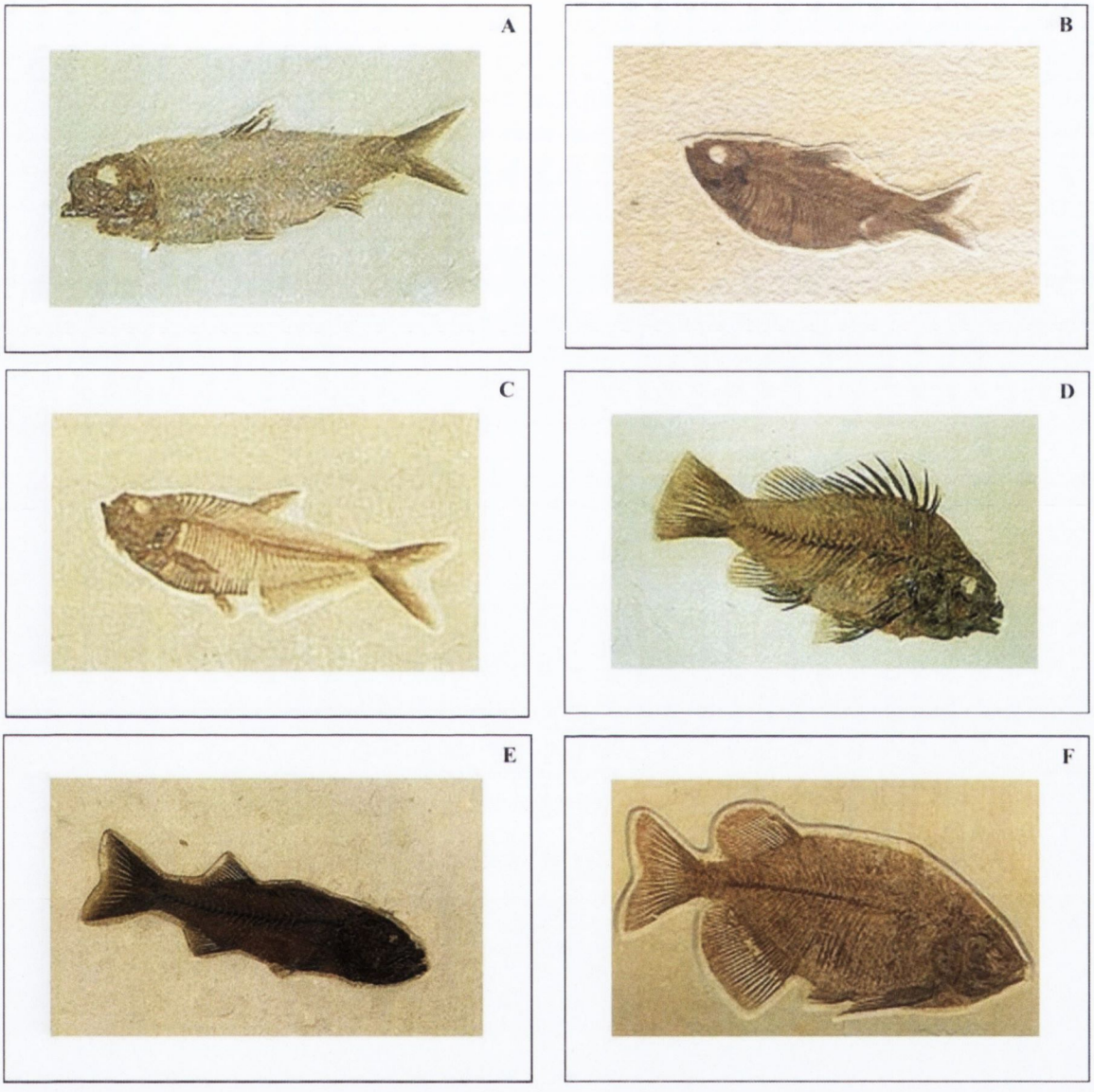

Figure 5.1: Photographs representative of fish species used for these experiments: **A)** *Knightia eocaena*; **B)** *Knightia Alta*; **C)** *Diplomystus dentatus*; **D)** *Priscacara liops*; **E)** *Mioplosus labracoides*; **F)** *Phareodus encaustus*. Photographs courtesy of R. Hebdon

5.2.2 Trophic system in Fossil Lake

The trophic adaptations of different fossil fish genera from the Green River Formation are discussed in full in Grande (1984). Of the common fish collected, *K. eocaena* and *K. alta*

are thought to have been zooplanktivores and herbivores, feeding on algae, ostracods and diatoms in the upper water column in large schools. The *Knightia* collected for this study are all between 6 and 10cm in length. *Knightia* were armed with only tiny pointed teeth, so small that they were overlooked in the original descriptions by Cope and Leidy. All *D. dentatus* collected for this study are less than 15cm and are thought to have been dominantly zooplanktivores, although larger specimens are known to have fed on small fish. *D. dentatus* has the upturned mouth typical of a surface feeder and, although armed with only very small teeth, *D. dentatus* would have been able to prey on small fish using suction feeding. *P. liops* are thought to have fed on zooplankton, algae and insects, with the presence of small pharyngeal teeth indicating a possible diet of molluscs. *Priscacara* are most commonly found in F-1 deposits and are thought to have been schooling fish like *Knightia*, with *P. liops* growing up to a maximum of around 15cm. *M. labracoides* had pointed teeth adequate to catch and hold smaller fish of up to half its own length and specimens have been reported with *Knightia* in their mouths or stomachs. *M. labracoides* grew to sizes as large as 51cm in length and are thought to have been voracious solitary predators in Fossil Lake, preying on decapods as well as small fish. Finally *P. encaustus* is

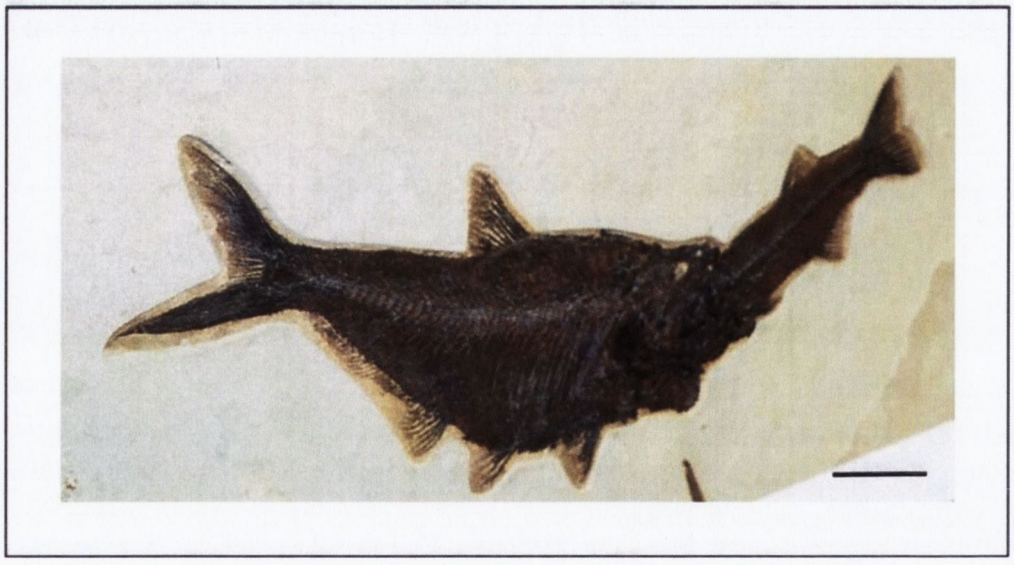

Figure 5.2: A large *D. dentatus* preserved with a small *M. labracoides* in its mouth, attesting to the voracity of *Diplomystus*. Such fossils are known locally as 'aspirations'. Scale bar 5cm. Specimen from the collection of R. Hebdon.

thought to have been the largest predator in the lake growing up to 76cm in length, with many sharp teeth attesting to a carnivorous habit. Evidence of its piscivorous diet has been reported in many specimens with percoid spines from *Mioplosus* and *Priscacara* found in their stomachs. This information from previous authors summarised by Grande (1984) gives an excellent detailed insight into the trophic system that operated in Fossil Lake and is reiterated in Table 5.1. Exceptions to this system do exist, for instance the *D. dentatus* found choking on a *M. labracoides* shown in Figure 5.2, but these exceptions are mainly seen in the extremes of size for each species.

	Maximum length (cm)	Major predator	Predator of small fish	Predator of insects	Predator of decapods	Molluscivore	Zooplanktivore	Herbivore (algae or plant eater)
Knightia	10						X	X
Diplomystus	15		X				X	
Priscacara	15			X		X	X	X
Mioplosus	51	X	X		X			
Phareodus	76	X						

Table 5.1: Trophic adaptations of the Green River fish used in this study (after Grande 1984).

5.2.3 Initial stable isotope analyses

Prior to instigation of fieldwork in Wyoming, USA, fossil fish sourced from the split-fish-layer quarry RH F-2 were purchased through a dealer in Cambridge, UK. These fish were used as a pilot study; 19 fish were removed from the surrounding matrix using the method described in Chapter 3 Section 3.1.1, 1M acetic acid washes were used to remove any remaining carbonate and ground homogenised samples containing fossil bones and scales were analysed using the CF-IRMS procedure detailed in Chapter 3 Section 3.1.3. The fish analysed were of 3 similar species of small clupeomorph, namely *K. eocaena*, *K. alta* and *D. dentatus*, and each species gave distinct isotopic signatures, indicating that reliable reconstruction of trophic structure in Fossil Lake could be possible. $\delta^{15}N$ are similar for *K. alta* and *D. dentatus* with only slightly more positive values for *K. eocaena*, although they are all presumed to be from the same trophic level. However, these three small species are

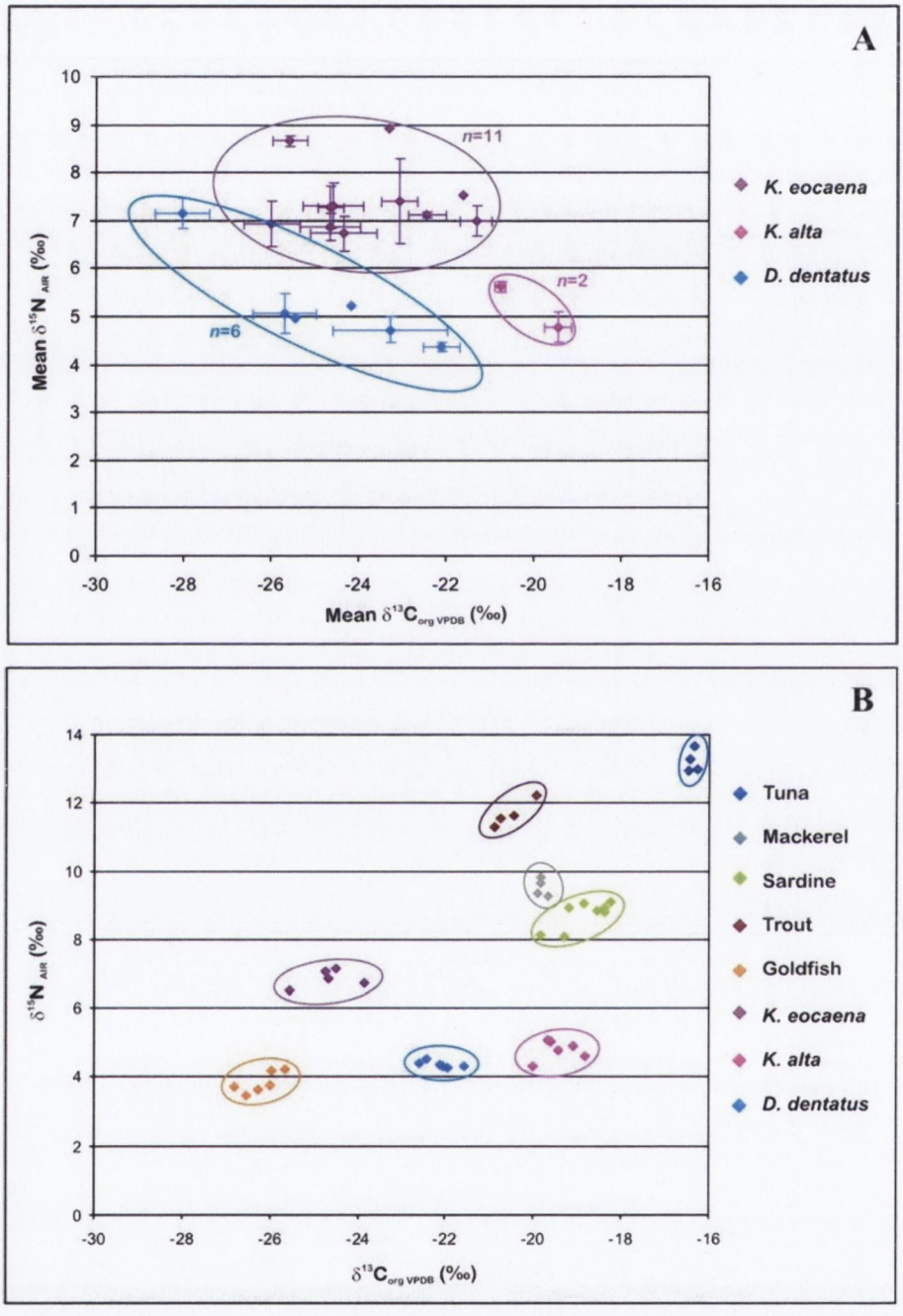

Figure 5.3: $\delta^{15}N$ and $\delta^{13}C_{org}$ results from three Eocene fossil fish species used in the pilot study. **A)** The three fossil fish species have distinct isotopic signatures, indicating reliable reconstruction of trophic structure in Fossil Lake could be possible. Data points are mean values from replicate analyses of individual fossils. NB: Error bars show the SD ($\pm 1\sigma$) for each specimen from replicate analyses of sub-samples; **B)** $\delta^{15}N$ and $\delta^{13}C_{org}$ values for replicates of fossil fish, one individual from each of the three species, plotted on a graph with replicates of muscle samples from three modern marine fish, a freshwater trout and a goldfish bred in captivity. Ellipses serve to highlight clusters of data.

clearly separated by their $\delta^{13}C_{org}$ values. Results are shown in Figure 5.3 A, and show remarkably similar values and variation to those obtained from modern fish. Of the 19 fish analysed in replicate, 3 individuals are plotted in Figure 5.3 B shown with replicate muscle samples from some modern fish. The modern marine fish plot more positive in terms of both $\delta^{15}N$ and $\delta^{13}C_{org}$, probably due to their higher trophic level and a shift in $\delta^{15}N$ and $\delta^{13}C_{org}$ owing to their provenance (e.g. France 1995). Modern freshwater trout are also likely to occupy a higher trophic level than the fossil fish did in life and this is reflected in the enrichment of $\delta^{15}N$, although $\delta^{13}C_{org}$ values appear similar. Values for the goldfish bred in captivity shown in Figure 5.3 B are more negative than the fossil fish values probably reflecting a synthetic food source. It was the successful analysis of these 19 fish using the TCD stable isotope facilities that led to the continued investigation of $\delta^{15}N$ and $\delta^{13}C_{org}$ in fossil aquatic organisms.

5.2.4 The nature of preservation in collected specimens

The fossil fish of Green River are mainly composed of fossilised bones, scales, fins and teeth, with only the imprint of some soft tissues such as the webbing between fin spines and occasionally, on careful dissection, gill filaments. Closer inspection using SEM revealed excellent preservation of micro-scale structures, although excellent preservation of structures does not necessarily imply a similar preservation of the original isotopic values (Longinelli 1996). Teeth are only visible to the naked eye in the larger fish taxa such as *Mioplosus*, *Priscacara* and *Phareodus*, an example of which is shown in Figure 5.4 A. Although teeth are thought to preserve isotopic signatures with higher fidelity than bone (e.g. Wang & Cerling 1994), the amount and volume of teeth present within the suite of collected samples was very small. As such, fossil teeth from Green River fish could not be used as a main component of this study. The preserved impression of gill filaments discovered during preparation is shown in Figure 5.4 B, suggesting rapid infill of the carcass by micrite. However, otoliths were not discovered during this dissection of the fossil fish and although they are likely to be preserved due to their hard structure they are presumed to be cemented within the bones and operculae of the fish skulls. Otolith microchemistry has frequently been used in studies of modern fish. High resolution $\delta^{13}C$ and $\delta^{18}O$ values as well as Sr:Ca and Ba:Ca ratios can be extracted from seasonal otolith

accretions to allow inference of environmental variables and therefore provenance and migration patterns of fish (e.g. Rooker *et al.* 2001; Edmonds *et al.* 2005; Ghosh *et al.* 2007). Nitrogen is not thought to be incorporated into the aragonitic otolith structure and is only associated with the gelatinous protein matrix in life, and may even be leached from this (Elsdon *et al.* 2008). $\delta^{13}C$ values from otoliths are not thought to be linked to diet (Radtke *et al.* 1996), with metabolic sources contributing to only 20-30% of the carbon deposited in otoliths (Elsdon *et al.* 2008). Otoliths were presumed present in the Green River fish, however they were assumed to contribute little to any $\delta^{15}N$ or $\delta^{13}C_{org}$ data obtained from whole ground fossil fish. Therefore, although teeth and otoliths are thought to be reliable tracers of fish habitat during life, only bones, fins and scales were available for the determination of $\delta^{15}N$ and $\delta^{13}C_{org}$ signatures of the Green River fossil fish. The likely reliability of these fossilized tissues is discussed in more detail in Chapter 6. Due to the sample size required for isotopic analyses the fossil fish were ground and homogenised and $\delta^{15}N$ and $\delta^{13}C_{org}$ data obtained for the whole fish.

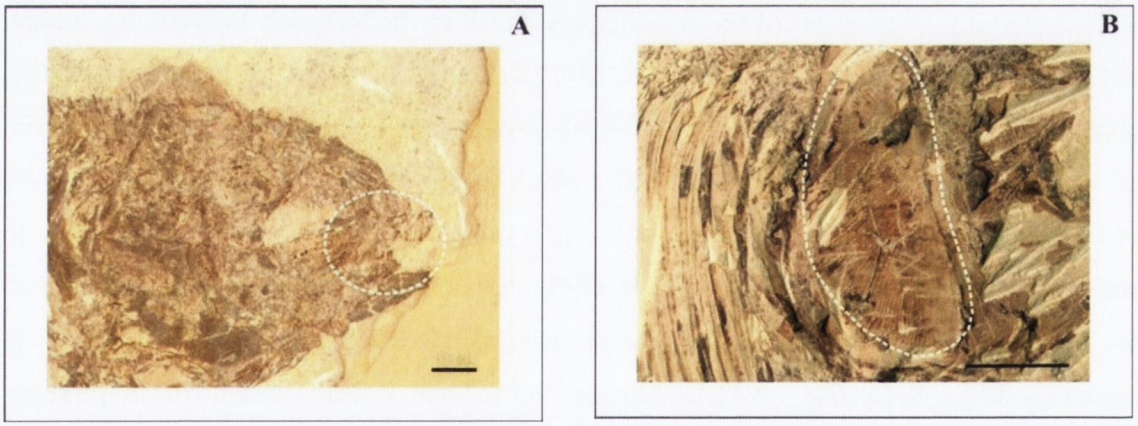

Figure 5.4: The nature of preservation in collected specimens: **A)** *Phareodus encaustus* skull showing premaxilla and dentary highlighted by dashed ellipse. Scale bar 1cm; **B)** Close up of *Phareodus encaustus* skull during preparation showing imprint of gill filaments discovered beneath the operculum, also highlighted using a dashed ellipse. Scale bar 1cm.

5.2.5 Isotopic fractionation between tissues and possible $\delta^{13}C_{carbonate}$ contamination

In modern isotopic studies of trophodynamics, whole ground fish have frequently been used, particularly when small or juvenile fish are being studied (e.g. Minagawa & Wada

1984; Sotiropoulos *et al.* 2004; Lamontagne *et al.* 2007). However, the metabolic functions of different tissues and their associated rates of turnover are known to cause differences in the diet-trophic shift within individual fish (Sweeting *et al.* 2007). Different tissues therefore have different $\delta^{15}N$ and $\delta^{13}C_{org}$ values, and whether these differences were preserved in the fossil fish was investigated using two of the larger specimens collected, plus a modern freshwater fish for comparison. Beltrán *et al.* (2009) reported that in two modern fish species $\delta^{15}N$ and $\delta^{13}C$ values were greater in tissues with higher protein and lower lipid content. Pinnegar & Polunin (1999) investigated the differential fractionation of $\delta^{15}N$ and $\delta^{13}C$ between white muscle, red muscle, heart and liver in modern fish and concluded that differences in $\delta^{15}N$ may be linked to relative abundance of different amino acids in tissues, whereas differences in $\delta^{13}C$ values may arise as a result of relative abundance of lipid within the different tissues. Removal of the lipid fraction prior to analysis of $\delta^{13}C_{org}$ in their study resulted in convergence of $\delta^{13}C_{org}$ values among tissues when compared with untreated samples, but also increased variance of within-tissue isotopic values. Moreover, lipid removal was thought to lead to poorer resolution of dietary relationships. Previous authors (Sotiropoulos *et al.* 2004; Murry *et al.* 2006; Sweeting *et al.* 2006) suggest that removal of lipids in fish tissues leads to ecologically significant shifts in $\delta^{15}N$ values. Lipid removal prior to CF-IRMS analysis was therefore not thought to be a necessary procedure for any of the analyses carried out during the production of this thesis. Neither were the tissues of any of the modern fish discussed in this thesis treated using acid: in many modern studies of aquatic ecosystems fish tissues are treated with acid to reduce contamination effects on $\delta^{13}C_{org}$ values from the inorganic carbonate component of hard structural tissues. Previous authors (e.g. Bunn *et al.* 1995; Pinnegar & Polunin 1999; McCutchan *et al.* 2003; Jacob *et al.* 2005) have found such procedures to cause fluctuations in the resulting isotope values, in particular $\delta^{15}N$, and have recommended that when selecting tissues for isotopic analyses those with low amounts of hard structural components or biomineralized tissues are desirable. The selection of hard structural components could not be avoided during this research however; the nature of most fossilized organisms is such that the biomineralized tissues are all that remain for analysis. It was therefore necessary to compare these to the hard structural components of modern fish in order to assess the preservation of $\delta^{15}N$ and

$\delta^{13}C_{org}$ isotopic signatures. This may result in some mixed inorganic and organic $\delta^{13}C$ signatures being produced and the possibility of this was taken into account when assessing the data produced. Caudal fin tissues have been reported to correlate closely to both $\delta^{15}N$ and $\delta^{13}C_{org}$ values from muscle tissue samples however (see Jardine *et al.* 2005), suggesting that not all structural components possess inorganic carbonate in quantities sufficient to produce a shift in the data produced.

5.2.6 Palaeoproductivity and palaeoenvironmental change

Small clupeomorphs collected from RH F-2 were analysed from throughout the stratigraphic section as a novel approach to assessing primary productivity in Fossil Lake. Given that primary producers preferentially utilise ^{14}N and ^{12}C from the water column (Lehmann *et al.* 2002), at times of high primary productivity the increased biomass sinks a proportionally greater amount of these lighter isotopes and this light signature is transferred along the rest of the food chain. The remaining water column therefore becomes more positive with respect to $\delta^{15}N$ and $\delta^{13}C$, and this isotopic shift is recorded in precipitated inorganic carbonate (Li & Ku 1997). At times of low primary productivity the inverse should be true, with less ^{14}N and ^{12}C being stored in organic matter (OM) and the carbonate precipitate becoming more negative in terms of $\delta^{13}C$. Changes in OM $\delta^{13}C_{org}$ from sediments in lakes have been used by other studies (e.g. Wüest *et al.* 1996; O'Reilly *et al.* 2003), but this is the first time that consumers of primary producers have been studied to infer palaeoproductivity. In Fossil Lake, *K. eocaena*, *K. alta*, and *D. dentatus* are assumed to have been primary to secondary consumers near the base of the trophic system (trophic level 2+) and should therefore record any $\delta^{15}N$ isotopic variations from primary producers over time. These fossil fish were collected on average every 2.5cm from throughout the RH F-2 succession, although some layers yielded more than one fish and in some areas a spacing of ~10cm was unavoidable between samples. All samples were collected from the same small area of the quarry wall, approximately $3m^2$ in each horizontal plane of the 2.6m vertical section. By restricting the collection area it was hoped to reduce the effects of any differential diagenesis acting in different parts of the ancient lake, and also to negate any intra-lake influences on the carbonate isotopic signatures that may result in erroneous interpretations.

In the laboratory, fossil fish were analysed for $\delta^{15}N$ values and micrite samples were collected from each rock underneath the fossil fish and were analysed for $\delta^{13}C_{carbonate}$ and $\delta^{18}O$. Carbon and oxygen isotopic data from carbonates can be used to build palaeoclimatic records throughout geological time and lacustrine carbonates, due to their wide distribution, are important archives of climate change on the continents (Talbot 1990). Palaeoclimatic research focuses to a great extent on past temperatures using variations in $\delta^{18}O$. However, stable isotope analyses from laminated lake sediments can also provide details regarding variations in moisture availability caused by changing precipitation and evaporation over time (Hammarlund *et al.* 2003). It was hoped that samples collected from Fossil Lake would allow reconstruction of short-term changes and temperature variations as well as moisture availability recorded within the carbonate-rich sediments. This is the first time that $\delta^{13}C$ and $\delta^{18}O$ data have been reported from the carbonates of Fossil Lake. Major, trace and Rare Earth Element (REE) concentrations from whole rock samples taken from throughout the stratigraphy at locality RH F-2 were also assessed as potential indicators of major hydrological events.

5.3 Method

5.3.1 Outline of analyses and initial preparation

All fossil fish collected were photographed prior to any analyses. Fossil fish on the large ash plate were covered by a thin layer of micrite which was removed roughly using a scalpel and dental tools to reveal the fish, these fish were then numbered as shown in Figure 5.5. The identifiers are prefixed with the initials AP ('ash plate') from hereon and individual photographs of each specimen are shown in Appendix 1. All small clupeomorphs collected from elsewhere in the stratigraphy were photographed without any prior preparation and these are also shown in Appendix 1, identified to species level and labelled using sample numbers allocated in the field. Fossils were then chosen at random from throughout the succession, including some from the large ash plate, and powdered samples of these fish were subjected to XRD analysis following the method outlined in Chapter 3 Section 3.3. All were found to be composed of fluorapatite giving profiles indistinguishable from those shown in Figure 4.7 A. A handful of samples were also subject to CHN analysis as described in Chapter 3 Section 3.5, to confirm that

organic carbon and nitrogen were present and therefore likely to be present in the entire suite of samples, prior to isotopic analysis. An average of ~3% total organic carbon (TOC) and between 0.01% and 0.07% nitrogen were found in the fish samples tested, whereas sediment samples contained ~7% TOC and no N. One specimen from the ash plate was selected for SEM analysis, as well as a large specimen from quarry SH F-1 for comparison, using the method described in Chapter 3 Section 3.9. These samples were broken by hand rather than ground via mechanical methods to retain any 3D structures and

Figure 5.5: The large ash plate procured for this project with 27 fish from a mass mortality event. These fish represent 6 different species from Fossil Lake, namely *K. eocaena*, *K. alta*, *D. dentatus*, *P. liops*, *M. labracoides* and *P. encaustus* and are numbered arbitrarily 1 to 27. Hammer for scale; hammer head 16cm.

prevent smearing of carbonate across the fossil surface. The samples were analysed using EDS microanalysis to identify whether differences existed in the elemental content of the fossils at a microscopic scale; results are presented in Section 5.4.2. It was hoped that these data would provide further insight into the preservation of the fossils and the

integrity of the surrounding matrix than could be provided by bulk XRD analyses alone. SEM images were also examined.

Sections of two of the larger fossil fish from the ash plate were analysed to determine whether differential fractionation of $\delta^{15}N$ and $\delta^{13}C_{org}$ signatures between tissues is preserved as described in Section 5.3.2. All fossils from the large ash plate were analysed to determine their $\delta^{15}N$ signatures, and a sample of the matrix underlying each one collected and analysed to obtain $\delta^{13}C_{carbonate}$ and $\delta^{18}O$ values to test for possible differential diagenetic alteration across the slab. Concentric rings thought to be from meteoric water reacting with the ash or limonitic clays on the surface of the slab indicate possible alteration during or post-diagenesis, therefore $\delta^{13}C$ and $\delta^{18}O$ data were hoped to identify any potential isotopic exchange. Of the remaining small clupeomorphs collected throughout the RH F-2 section, 120 were analysed in replicate to determine their $\delta^{15}N$ signatures, and the enclosing micrite from each one analysed to obtain $\delta^{13}C$ and $\delta^{18}O$ values for palaeoenvironmental interpretation and/or diagenetic control. Whole rock major, trace and REE's elemental concentrations were determined for 48 of these micrite samples, distributed evenly throughout the RH F-2 section, via the method outlined in Chapter 3 Section 3.4.

5.3.2 Preservation of differential isotopic fractionation among fossil fish tissues

Different fossilized tissues of two of the larger specimens from the ash plate, AP7, *P. liops*, and AP11, *P. encaustus*, were analysed to test whether the differential fractionation of $\delta^{15}N$ and $\delta^{13}C$ present between modern fish tissues was preserved, as described in Section 5.2.5. Different parts of the fossils were picked by hand from the surrounding carbonate matrix (e.g. scales, bones or teeth), washed in acid following the procedure recommended in Chapter 4, ground and homogenised in turn and their $\delta^{15}N$ and $\delta^{13}C$ values analysed. For comparison a freshwater rainbow trout, *Oncorhynchus mykiss* Walbaum, 1792, was sourced from a local fishmonger, dissected and different tissues analysed for $\delta^{15}N$ and $\delta^{13}C$. Portions of each sample (19.3-71.8mg of fossil samples and 1.2-6.2mg of trout samples) were measured using CF-IRMS under conditions described in full in Chapter 3 Section 3.1.3. Samples were analysed in a random order to prevent any

systematic bias in the results, and corrected to international standards using the L-Alanine working standard previously described in Chapter 3. Based on these replicates the analytical precision was ±4.8%RSD for $\delta^{15}N$ and ±0.5%RSD for $\delta^{13}C$ during analyses of the fossil samples and ±3.9%RSD for $\delta^{15}N$ and ±0.5%RSD for $\delta^{13}C$ during analyses of the modern trout samples. Results are shown in Section 5.4.1 and Appendix 2. The standard length of AP7, *P. liops*, is 158mm, AP11, *P. encaustus* is 220mm and *O. mykiss* is 270mm.

5.3.3 N and C_{org} isotopic analysis of fossil fish plus $\delta^{13}C$ and $\delta^{18}O$ analysis of micrite

Fossil fish retrieved during the field campaign in Wyoming were prepared for analysis following the protocol outlined in Chapter 3 Section 3.1.1. Due to the difficulties in specimen preparation discussed in Section 3.1.1, geochemical analyses were restricted to split-fish-layer samples from quarry RH F-2 in Fossil Lake. Carbonate removal was not successful in all samples however, despite the protocol development discussed in Chapter 4; the presence of carbonate subsequent to the treatment of samples with acid was confirmed using XRD. This was particularly true for small specimens that were difficult to separate from the matrix, where powdered fossil and matrix had been collected for acid treatment. Further immersion in acid for a longer leach period or the use of a higher molarity acid would likely cause an undesirable effect on the isotope geochemistry of the fossil samples, based on the results presented in Section 4.4. As such, CF-IRMS stable isotope analysis for the majority of fossil fish samples was carried out using the Ascarite modification described in Section 3.1.5. This technique meant that only $\delta^{15}N$ values could be collected for those samples run using the Ascarite II® trap, as all C is effectively stripped from the system by the trap. However, in doing so this method is thought to provide more accurate $\delta^{15}N$ values. In addition, following further research discussed in Chapter 6 Section 6.6.1, it is suggested here that $\delta^{13}C_{org}$ data might no longer be reliable in fossil fish. Previous studies have also found carbon to be unreliable as a tool to estimate trophic level even in some modern aquatic ecosystems (e.g. Fry 1988) and therefore the absence of C_{org} data was not deemed to be of great consequence. All fossil fish were ground and homogenised and a $\delta^{15}N$ value obtained for the whole fish by analysing portions of each (8.5-51.6mg). The CF-IRMS analyses were carried out over several

weeks and calibration standards were also analysed throughout to enable calculation of accuracy and repeatability as detailed in Chapter 3 Section 3.1.2. Analytical precision based on these replicates was ±1.7-7.1%RSD for $\delta^{15}N$. The internal standard RH260705 also measured throughout these analyses indicated a similar precision of ±2.9-6.0%RSD for $\delta^{15}N$, when considering only those results with a signal peak intensity >300mV, as described in Chapter 3 Section 3.1.4 and shown in Figure 3.5. Samples of micrite were collected from directly under each fish specimen on the large ash plate and from underneath small clupeomorph specimens from throughout the RH F-2 stratigraphy. The $\delta^{13}C$ and $\delta^{18}O$ values of these carbonate samples were measured using CF-IRMS via a Thermo Gas Bench II as outlined in Chapter 3 Section 3.2. Replicate standards analysed throughout indicate a precision of ±1.3%RSD for $\delta^{13}C$ and ±0.8%RSD for $\delta^{18}O$.

5.4 Results

5.4.1 SEM imaging and EDS microanalysis

Images taken during SEM analysis revealed exquisite preservation of hard structural components of the fossils, such as scales, bones and pharyngeal teeth. Examples of these are shown in Figure 5.6. EDS microanalysis of sub-samples of specimens AP7 and SH270701 revealed that both of the fossils were composed of fluorapatite in all areas tested, with minor amounts of other elements such as Si, Al, Mg, and Na. In occasional spectra amounts of Ba and K were also present, and some spectra from samples of SH270701 contained either S or Sc, or both. Nitrogen did not show on any of the 10μm^2 to 50 μm^2 surface areas of the fossils sampled. This may indicate that N content is below detection limits at <0.1% or N may be held in internal areas of the fossilized tissues. A typical spectrum obtained from an area of a fossil is shown in Figure 5.7 A. There is no linear connection between measured count number and concentration, i.e. peak intensity does not reflect composition, rather capability of excitation. Traversing a section perpendicular to the bedding plane of sample AP7 showed little change in the composition; the micrite appears to be composed of very pure $CaCO_3$ with only occasional Si, Al, Mg and K appearing on the spectra. A typical spectrum obtained from the micrite is shown in Figure 5.7 B.

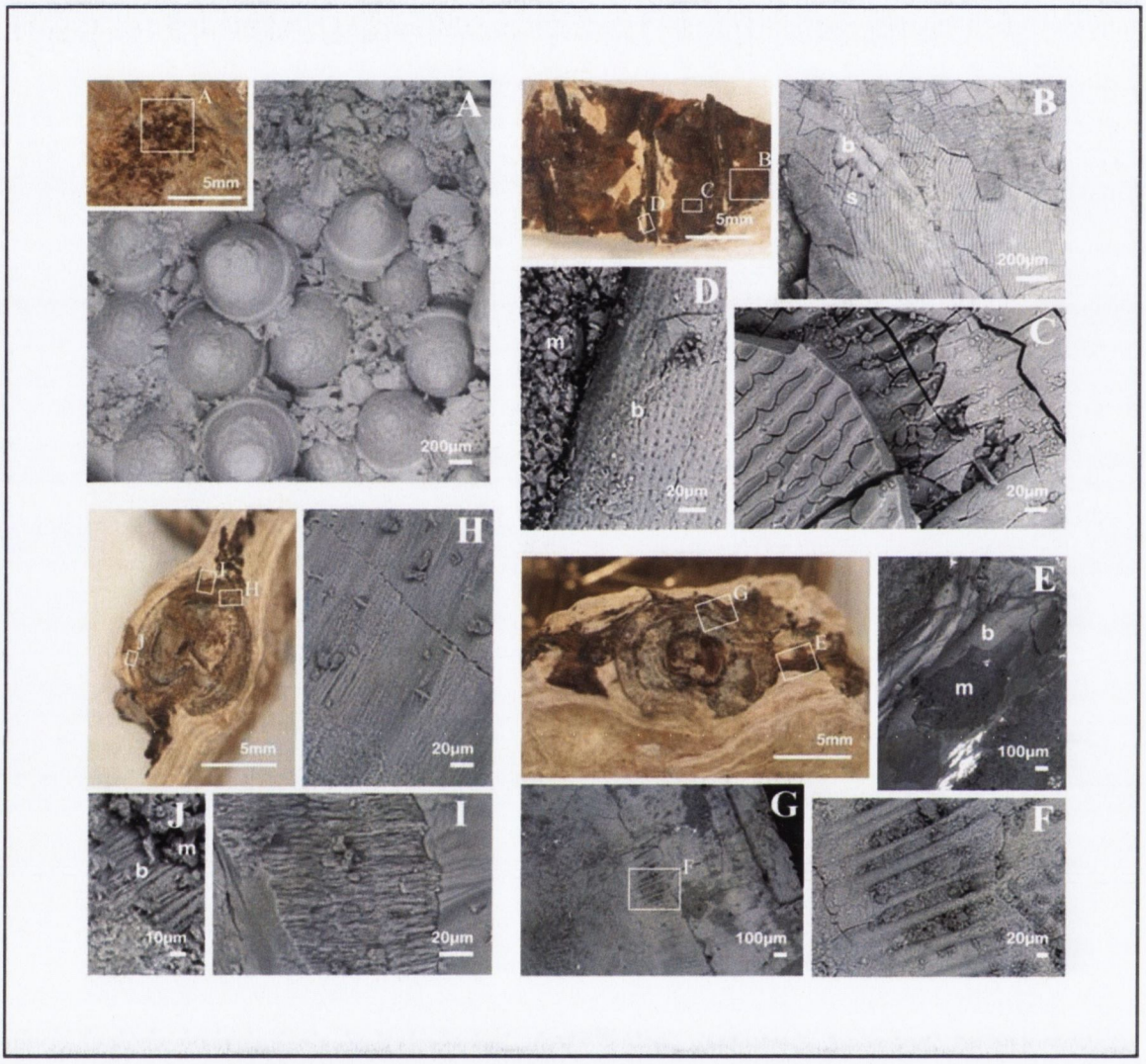

Figure 5.6: Various SEM images of samples of AP7 and SH270701: **A)** pharyngeal teeth; **B)** scales overlying rib bones; **C)** rib at high magnification; **D)** scales showing overlap; **E)** neural spine with micritic infill; **F)** close-up of vertebrae; **G)** transverse section of a vertebra showing preserved layering; **H)** to **I)** different areas of a vertebra showing preserved structures. Abbreviations: b, bone; m, micrite; s, scales.

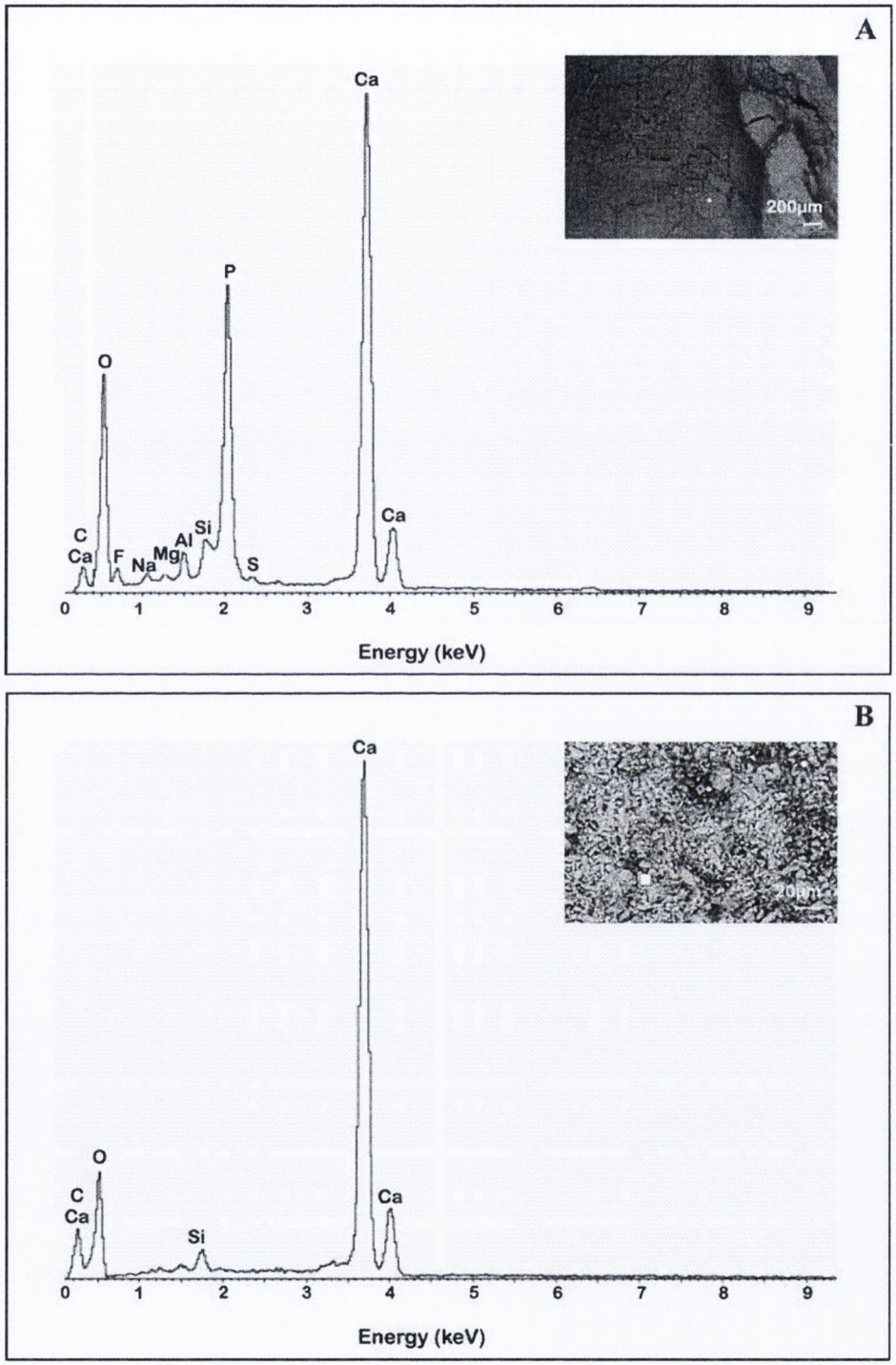

Figure 5.7: EDS spectra of **A)** fossil fish and **B)** micrite. The fossil fish are all composed of fluorapatite and the micritic matrix is calcium carbonate with few impurities. NB: there is no correlation between peak intensity and concentration.

5.4.2 Preservation of original fractionation of $\delta^{15}N$ and $\delta^{13}C_{org}$ between fish tissues

Results from the isotopic analyses of different preserved tissues of *P. liops*, and *P. encaustus*, as well as the results from body tissues of modern *O. mykiss*, are shown in Figure 5.8 and Appendix 2. Error bars in Figure 5.8 represent the standard deviation of data around the mean for each tissue type calculated individually for each fish. Not all tissues were available for sampling in both of the fossil fish specimens, but as many as possible were analysed in each. The fossil fish data show a similar overall spread to those data from the modern trout tissues, however the majority of inter-tissue variation in *P. liops* is along the y-axis, whereas the modern trout data show the most spread along the x-axis. Similarly, the larger SD from the mean is seen in the $\delta^{15}N$ data from *P. liops*, whereas the modern trout shows most intra-tissue variation in $\delta^{13}C_{org}$ results. Fewer fossil tissues were available for sampling from *P. encaustus*, but those tissues analysed show little spread in $\delta^{15}N$, constrained over a range of just 1.1‰, compared with *P. liops* results which exhibit a total range of 5.1‰ in $\delta^{15}N$ values. General trends seen between the modern trout data do not seem to be mirrored directly in the data from either fossil fish species. For example, the trout scales are enriched by an average of 1.1‰ $\delta^{15}N$ and 3.8‰ $\delta^{13}C_{org}$ compared to the trout vertebrae replicate samples, whereas the same tissues in *P. liops* also show 1.0‰ enrichment in $\delta^{15}N$, but an average 0.4‰ decrease in $\delta^{13}C_{org}$ to more negative values from scales to vertebrae. The overall pattern of variation between different body tissues in the modern trout is not replicated in the fossil specimens. The data from dorsal spines highlights this, with the datum point representing the trout spines being the most enriched in $\delta^{15}N$ when compared to the remainder of the trout tissues, although they appear to give $\delta^{13}C_{org}$ close to average. The inverse is true when regarding the *P. liops* dorsal spines however, with spines being the most enriched in $\delta^{13}C_{org}$ of all the *P. liops* tissues with a mean $\delta^{15}N$ value close to the average.

C:N ratios were determined from the percent element data also produced during the N and C isotopic analyses and are shown in Appendix 2. Data from all tissues were combined for each fish and are represented schematically in Figure 5.9. The much higher ratios seen in the fossil fish and the larger spread of data indicate losses of N to the system during

fossilisation. Absolute values attest to this, and also indicate large losses of C from the fossil fish post-mortem. The mean data from *O. mykiss* give N and C concentrations of 6.1% and 20.3% respectively, with a mean C:N ratio of 3.6. *P. liops* data give N and C concentrations of 0.02% and 0.9% respectively, with a mean C:N ratio of 54.1, and *P. encaustus* data show very similar mean percentages with a mean C:N ratio of 48.3. This average 300-fold decrease in N and 20-fold decrease in C content compared to modern fish is assumed to have occurred in the fossil fish post-mortem and may affect the resulting isotopic values. Additionally some of the C percentage is likely to be accounted

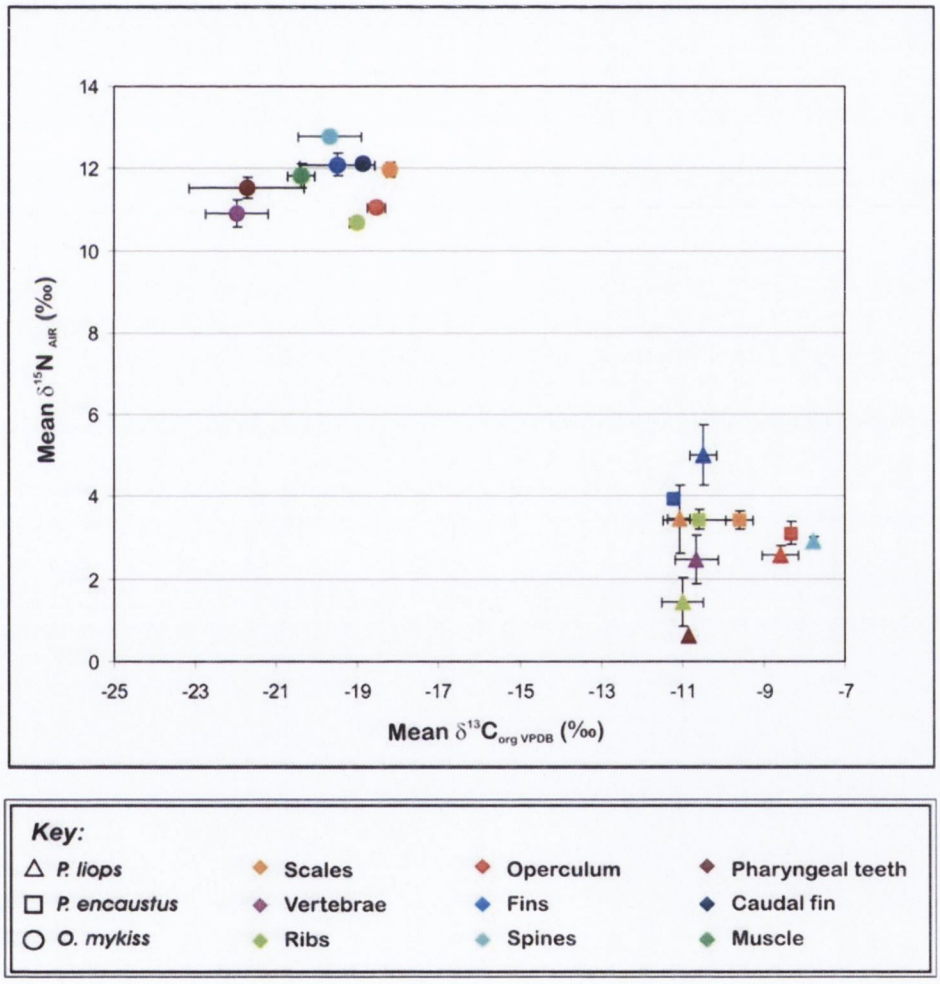

Figure 5.8: Mean $\delta^{15}N$ and $\delta^{13}C_{org}$ values for replicate samples of different tissue types from *P. liops*, *P. encaustus* and *O. mykiss*. Error bars illustrate the spread of data for each tissue type in each fish using SD from the mean ($\pm 1\sigma$).

for by inorganic C, with absolute organic C values being even lower. Overall *P. liops* scales showed the lowest C:N ratio of any tissue type, giving a mean value of 29.3, indicating the least amount of post-mortem change. The same is not true for *P. encaustus* however; its scales gave an average C:N value of 42.8, close to the overall average value of 48.3 from all tissues sampled from the specimen.

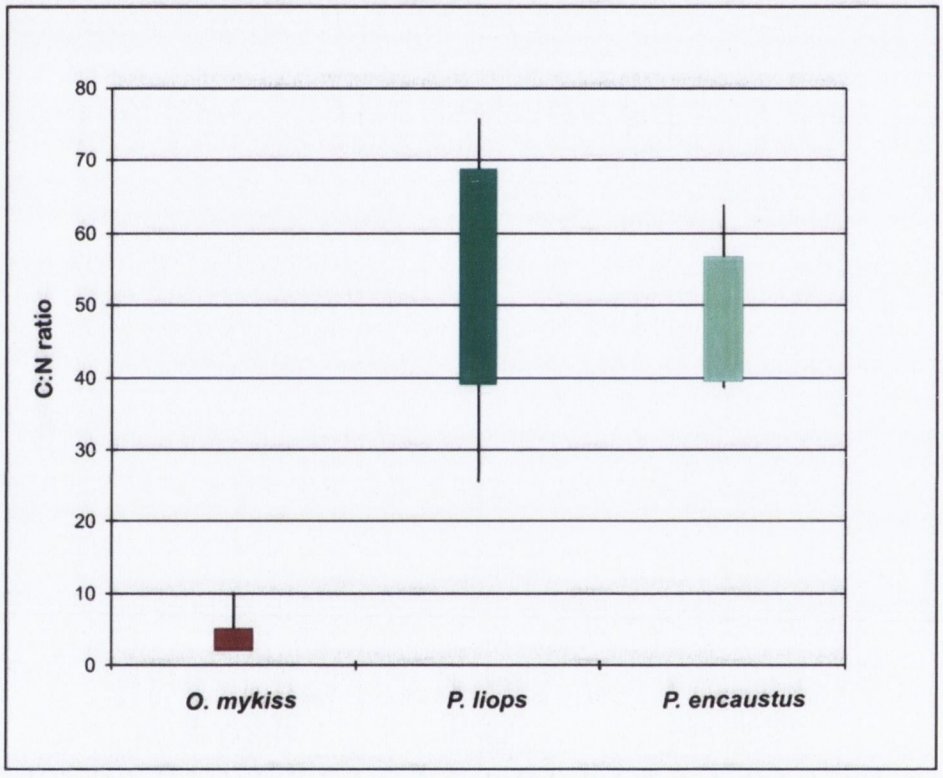

Figure 5.9: A visual representation of C:N values, showing standard deviation from the mean (solid blocks) plus maximum and minimum (bars) C:N ratios found in all *O. mykiss*, *P. liops*, and *P. encaustus* tissues.

5.4.3 Fossil fish $\delta^{15}N$ and matrix $\delta^{13}C$ and $\delta^{18}O$ from ash plate

The 27 fish from the large ash plate comprised 14 specimens of *K. eocaena*, 3 specimens of *K. alta*, 7 specimens of *D. dentatus*, and just 1 each of *P. liops*, *M. labracoides* and *P. encaustus*. *K. eocaena* AP26 was not analysed as it was overlaying *P. liops* AP7 and would have resulted in a mixed signal. 92 replicate aliquots of the remaining 26 fish were analysed for $\delta^{15}N$. Any analyses resulting in a signal peak intensity of <300mV were discounted from the results. The $\delta^{15}N$ data from each fish were then averaged and the SD calculated, and these results are shown in Figure 5.10 plotted against standard length, and

in Appendix 2. The three small clupeomorphs, *K. eocaena*, *K. alta*, and *D. dentatus*, plot quite closely together with a total spread of 4.3‰ in their isotopic signatures, from a minimum value of 3.3‰ to a maximum of 7.6‰, from fish with a range of lengths from 54mm up to 101mm. In general the highest $\delta^{15}N$ values appear to be from some of the smallest fish. The three larger species *P. liops*, *M. labracoides* and *P. encaustus* all have extremely similar $\delta^{15}N$ isotopic signatures just over 4‰ with an average SD of 0.4. Despite their size and inferred higher trophic level their values match the lowest average $\delta^{15}N$ value obtained from any of the small clupeomorphs. Consistent $\delta^{13}C_{carbonate}$ and $\delta^{18}O$ values from the micrite and ash matrix directly underlying each fish indicate no significant isotopic exchange with meteoric water during diagenesis. $\delta^{13}C$ and $\delta^{18}O$ results are presented in Appendix 2, with an average of 3.1‰ $\delta^{13}C$ (SD 0.2) and -3.3‰ $\delta^{18}O$ (SD 0.3).

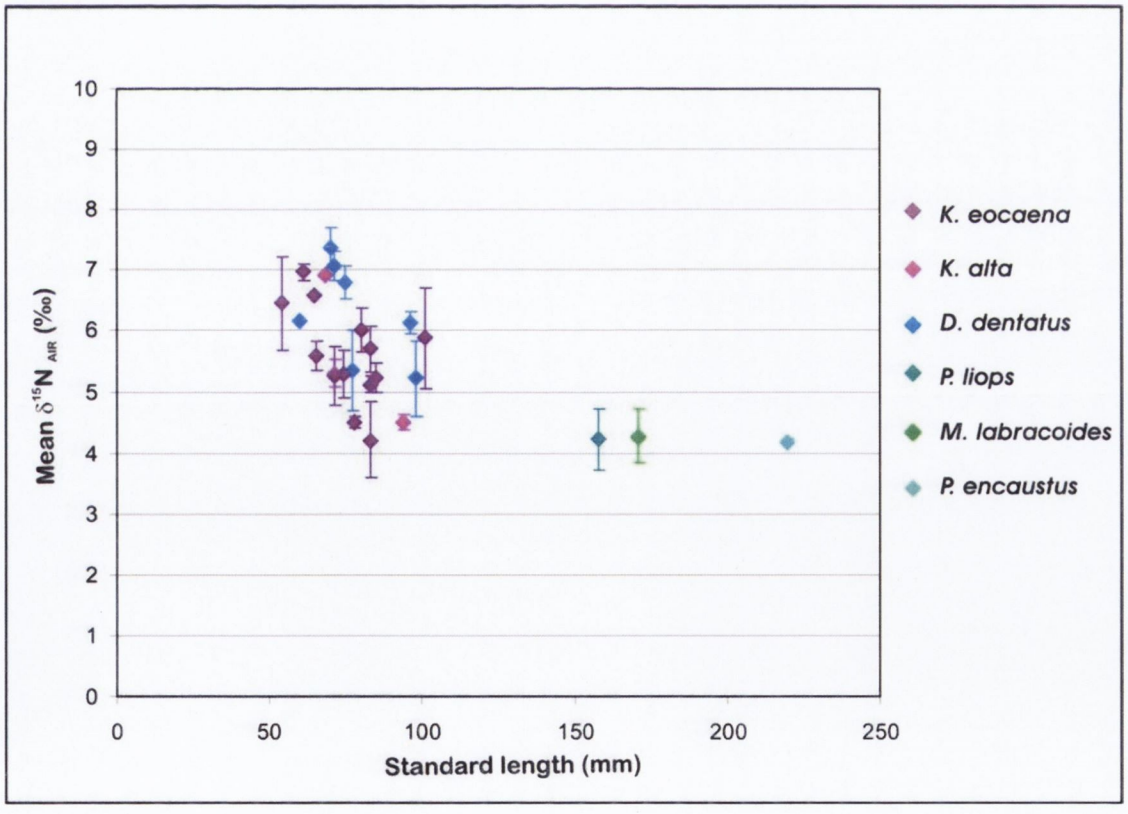

Figure 5.10: $\delta^{15}N$ values for 26 fossil fish of 6 separate species from the large ash plate, plotted against the standard length of each fish. Data points are the mean N values from replicate analyses of individual fossils. NB: Error bars show the SD ($\pm 1\sigma$) for each specimen from replicate analyses of sub-samples.

Patterns in the $\delta^{15}N$ data from the three small clupeomorphs were studied in more detail prior to the analysis of the fish collected from the remainder of the RH F-2 section. Findings from fish on the large ash plate suggest that there is no major difference in isotopic signature between the three different species, and length does not appear to exert much influence on the resulting data. Replicate analyses from all *K. eocaena* gave an average $\delta^{15}N$ value of 5.60‰, replicates from the 3 specimens of *K. alta* gave an average value of 5.57‰, and replicates from all specimens of *D. dentatus* gave an average value of 6.30‰. The average values for different standard lengths are shown in Table 5.2. That no significant differences were seen between the data produced from this horizon suggests that comparisons of the three small clupeomorphs can safely be made from throughout the entire RH F-2 succession, regardless of species type and length. Any data out with the range of that presented in Figure 5.9 may then suggest changes in the environment and productivity of Fossil Lake over time.

Standard length (mm)	**Number of replicates *n* =**	**Average $\delta^{15}N$ value (‰)**
51 to 60	3	6.3
61 to 70	10	6.7
71 to 80	29	5.7
81 to 90	12	5.1
91 to 100	13	5.3
101 to 110	3	5.9

Table 5.2: Six categories of standard length from three species of clupeomorph give similar $\delta^{15}N$ values.

5.4.4 Fossil fish $\delta^{15}N$ and micrite $\delta^{13}C$ and $\delta^{18}O$ from the RH F-2 stratigraphy

The $\delta^{15}N$ data from the three small clupeomorph species, *K. eocaena*, *K. alta*, and *D. dentatus*, collected throughout the RH F-2 stratigraphy are shown in Figure 5.11 plotted against height above quarry base. The values fluctuate over time between a minimum of -2.9‰ and a maximum of +5.9‰ over a total range of 8.8‰, more than double that observed in the same species from the ash plate. The largest fluctuations recorded occur within the first 80cm of the succession below the Red Line Scab, although this may be an

artefact due to the higher density of data produced for that section. $\delta^{13}C$ and $\delta^{18}O$ data from carbonate samples taken from beneath each fish are also plotted in Figure 5.11 and exhibit strong mutual correlation (Pearson correlation coefficient $r = 0.91$). There is no correlation between the $\delta^{15}N$ data and the carbonate $\delta^{13}C$ and $\delta^{18}O$ data ($r = 0.27$). These relationships are emphasized in Figure 5.12 A and B. The main ash layers or limonitic clays are highlighted in Figure 5.11 and these appear to exert no influence on either the fish $\delta^{15}N$ data or the whole rock $\delta^{13}C$ and $\delta^{18}O$ data. The carbonate isotopic data do not exhibit extensive shifts: $\delta^{13}C$ data fluctuates over a range of just 1.2‰ and $\delta^{18}O$ over a range of 2.3‰. The larger fluctuations in the carbonate data to more negative values are seen in the first 55cm of the section below the ½" Band, with more positive and consistent

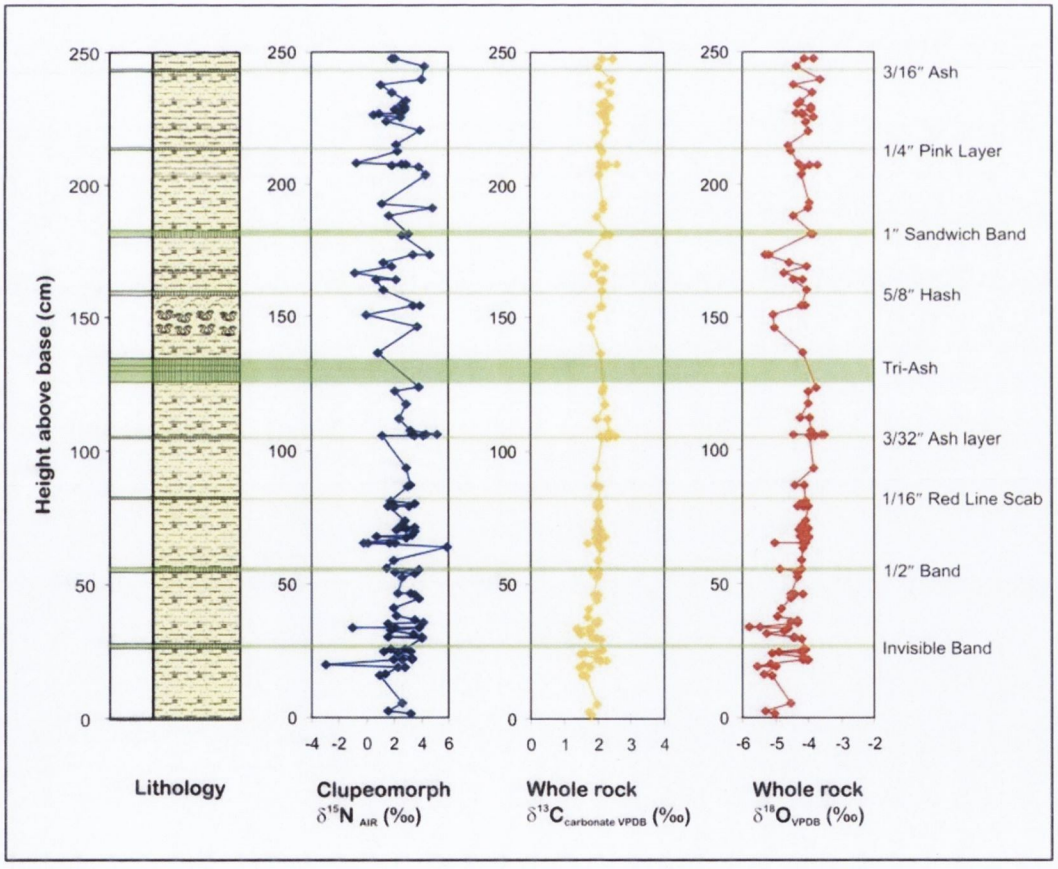

Figure 5.11: $\delta^{15}N$ values from small clupeomorph fossils collected throughout the RH F-2 stratigraphy, plotted against height above arbitrary quarry base. $\delta^{13}C$ and $\delta^{18}O$ data from whole rock carbonate samples are also shown. Main ash beds are highlighted from sedimentary log for ease of correlation.

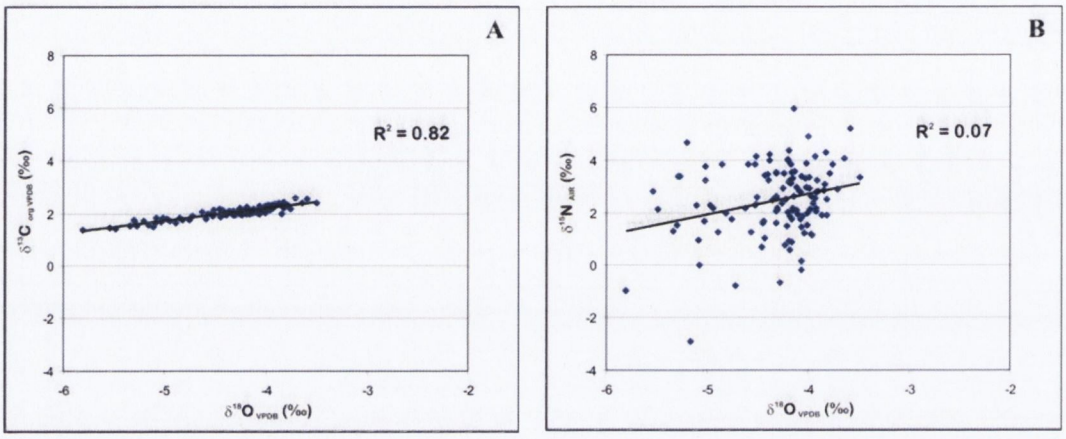

Figure 5.12: Correlation between: **A)** $\delta^{13}C$ and $\delta^{18}O$ data from carbonate samples, $R^2 = 0.82$; **B)** fossil clupeomorph $\delta^{15}N$ data and $\delta^{18}O$ data from whole rock carbonate samples, $R^2 = 0.07$.

values seen from this level to the 6.4cm Tri-Ash, around 130cm above the base of the succession. Above the Tri-Ash is a large negative excursion, a more positive excursion and another negative excursion up to the 1″ Sandwich Band at 182cm above the base. The remainder of the section shows minor fluctuations around mean values.

5.4.5 Major, trace and rare earth elements from the RH F-2 stratigraphy

Of the fossil fish collected throughout the RH F-2 stratigraphy, 120 were analysed for their $\delta^{15}N$ signatures and the underlying rock samples analysed for $\delta^{13}C_{carbonate}$ and $\delta^{18}O$. 48 of these whole rock samples were then selected randomly from throughout the section and further analysed for major, refractory and REE and the results are presented in Appendix 2 and in Figure 5.13. Samples are interspersed on average at 5cm intervals throughout the stratigraphy, though intervals were as little as 1cm and up to 11cm. This selection of samples was analysed rather than the entire suit of samples collected due to financial constraints. The results were organised into a correlation matrix to analyse relationships between the data set, and this is shown in Appendix 2. Elements with a Pearson correlation coefficient of $r > 0.9$ and $r < -0.9$ are highlighted. There is a very strong positive correlation between data from loss on ignition (LOI) and CaO, indicating that all volatile substances in the samples are intrinsically linked to CaO and can be attributed to CO_2 loss from the carbonates. LOI and CaO data accounts for 95% of the bulk rock

samples analysed, on average. None of the other elements are correlated with the LOI or CaO. MgO, MnO and Na_2O do not correlate with any of the elements in the suite, or with each other. MgO ranges from 0.5 to 4.9%, whereas MnO and Na_2O are only present in minor quantities (<1%). There is strong correlation between SiO_2, Al_2O_3, Cr_2O_3, Fe_2O_3, K_2O, P_2O_5, TiO_2 indicating a common mineral source. Most refractory elements and REE are also associated with this mineral phase; the entire suite analysed excluding Sn, Sr, U, V and W all show strong positive correlations. These remaining elements do not correlate

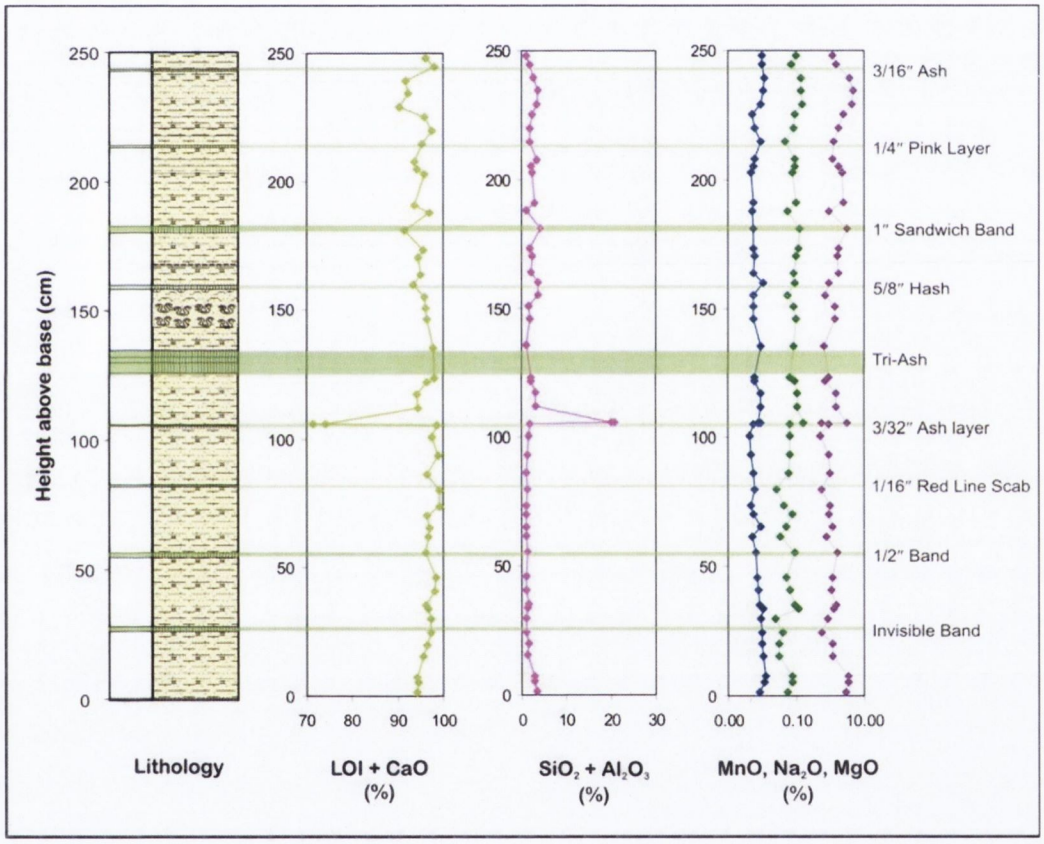

Figure 5.13: Major element data from ICP-OES analysis of whole rock carbonate samples from throughout the RH F-2 stratigraphy. Main ash beds are highlighted from sedimentary log for ease of correlation. Note the difference in scale used for different elements, including a logarithmic scale for MnO, Na_2O and MgO.

with one another and are present in small quantities (on average 0.0 to 20ppm) with the exception of Sr which is present in >1000ppm amounts in most samples. The major and trace elements associated with the mineral phase containing SiO_2 all show a strong negative correlation to LOI and CaO. Despite the lack of statistical correlation between

MnO, Na_2O and MgO and the main SiO_2-rich phase, and the lack of correlation with each other, visually all of these major oxides correspond to one another in Figure 5.13. The majority of positive and negative excursions seen in the data curves do show covariance at many intervals, and the most rapid excursions seem to be associated with the main ash layers. Other curves are likely to also correspond to ash deposition: many smaller ash layers exist between the main ones, sometimes on a sub-millimetre scale at frequencies of several per centimetre. Visually these major elements appear to have a negative correlation with LOI and CaO. There is no correlation between the $\delta^{13}C_{carbonate}$ and $\delta^{18}O$ isotope values shown in Figure 5.11 and any of the elemental data, either statistically (r = <0.3 or >-0.3) or visually.

5.5 Discussion

5.5.1 SEM observations and EDS data

Previous authors have found fossilized bacteria associated with exceptional preservation of vertebrate fossils (e.g. McNamara *et al.* 2006). This was not the case here; no fossil bacteria were observed on the surface of the fossils even at extremely high resolution. The preserved outline of any soft tissues found in Fossil Lake are not likely to be as a result of films of organically preserved bacteria therefore, but are thought to be from the impression of the fish preserved in soft sediment and rapid mineralization of tissues. There was also no evidence of fossilized algae or plankton in any of the examined sections. SEM images do show that the rib bones of the fish are highly porous, although transverse sections of vertebrae appear less so. Some infill of bones by micrite was also observed, and bones and scales were subject to cracking and fragmentation at a microscopic level. These cracks signify pathways which may have allowed alteration by meteoric water at any stage of their history, although $\delta^{13}C$ and $\delta^{18}O$ data from carbonate samples suggests little diagenetic change in Fossil Lake. Using EDS microanalysis previous authors have found fossilized microalgae to contain high levels of Si, with associated Al, Na and K (e.g. Wierzchos *et al.* 2003; Ascaso *et al.* 2005). This may indicate that although the mats of microalgae thought to be present in Fossil Lake were not physically replicated during the fossilization process, their chemical constituents may be represented, incorporated into the fluorapatite matrix. Si, Al and K were also observed in the carbonate sediments of

Fossil Lake using EDS, but with less frequency. These elements may therefore simply be an artefact of the volcanic ash associated with the sediments. Sulphate reduction has long been associated with modern benthic algal mats, with bacteria at intermediate depths of the mat anaerobically producing elemental sulphur (Doemel & Brock 1976). S was only associated with the fossil fish of sample SH270701 however, and would perhaps be expected to be more widespread were this a major mechanism operating in Fossil Lake. Sulphur has been reported to represent the biomolecular fidelity of preserved organic material by other authors: the incorporation of S into organic matter is known to enhance the preservation potential of organic compounds such as lipids and carbohydrates on geologic time scales (Sinninghe Damsté *et al.* 1998). It may be beneficial during future work to consider the concentration of S in the remnant organic matter to this end.

5.5.2 Fractionation of $\delta^{15}N$ and $\delta^{13}C_{org}$ among fish tissues

Different $\delta^{15}N$ and $\delta^{13}C_{org}$ isotopic signatures are preserved in the different tissues analysed from the fossil fish. The data from two large fossil fish presented in Figure 5.8 show a similar spread when compared to the differential fractionation of isotopes between fish tissues from a modern trout. Some of the isotopic differences seen between tissues of the modern fish are mirrored in the fossils, for instance the difference between operculum and fin data. While this is very encouraging and may indicate the preservation of original $\delta^{15}N$ and $\delta^{13}C_{org}$ isotopic signatures in the fossils, some differences do exist between the data from fossil and modern fish. For example, the overall range of $\delta^{15}N$ data for *P. liops* is greater than that seen in the modern fish and some fossil tissues show opposite trends to those seen in the modern tissues. While this may be due to natural variation among species, in the literature modern fish appear to have similar differences in isotopic signature between different tissues regardless of species (e.g. Pinnegar & Polunin 1999; Jardine *et al.* 2005; Beltrán *et al.* 2009). Although differences are not entirely consistent between modern fish tissues, general trends were observed in the data for all species previously reported. Therefore, it was assumed that isotopic relationships between different tissues should be similar in both fossil species and the modern trout. The different relationships observed between the $\delta^{15}N$ isotopic signatures of the different body tissues from fossil and modern fish may be attributed to many sources and it is not within

the scope of this thesis to characterize all possible causes. However, it is likely that most differences observed between the fossil and modern fish tissues are caused due to the high collagen and protein content in the modern fish, when compared with the fossil fish where the majority of collagen is assumed to be completely degraded (Briggs *et al.* 2000).

The fossil fish organic matter is likely to be from aggregates which have similar $\delta^{15}N$ values but dissimilar $\delta^{13}C_{org}$ values to collagen (DeNiro & Weiner 1988). Aggregate organic matter is not subject to the same diagenetic processes that can alter the isotope ratios of collagen and is thought to retain *in vivo* $\delta^{15}N$ isotope signatures in archaeological specimens (DeNiro & Weiner 1988). $\delta^{13}C_{org}$ isotopic data reported from the fossils is thought not to be valid and rather is a mix of organic and inorganic signatures. Overall, the $\delta^{13}C_{org}$ values for the fossil fish are much more positive than would be expected, by as much as 10‰. This suggests that removal of carbonate as described in Section 5.3.2 was unsuccessful, or that original inorganic carbon was still present in the matrix of the fluorapatite and was also not removed during acid washing. The contamination effects on $\delta^{13}C_{org}$ values are thought to be most likely from a mixture of carbonate carbon and remnants of the inorganic carbonate component of the hard structural tissues. The $\delta^{15}N$ data do however appear to be robust. That the spread of $\delta^{15}N$ data is larger in the *P. liops* fossil fish than the modern fish perhaps attests to some post-diagenetic exchange in the fossils, though this is not surprising from fish of such antiquity. This is again highlighted by the pattern of data between the two fossil specimens: tissues that are more enriched than other tissues in one specimen do not show the same trend in the other specimen. Nevertheless, that the overall spread of data is similar between fossil fish and the modern fish is encouraging.

5.5.3 N and C_{org} content of fossil fish

C:N ratios were much higher in both fossil fish analysed when compared with the modern trout. The low N percentage of the fossil bones indicates that collagen is very poorly preserved when using the classification of Petchey (2000). According to their categories, only non-collagenous amino acids may be present in bone with N contents of 0.02%. The significant losses of N and C from all tissues when compared to those of the modern fish

indicate post-mortem change, although this is not surprising considering the absence of any soft tissues. While percentages have decreased overall, any exchange with the surrounding burial environment signifies the potential for uptake of N and C from contaminant sources. In an open system the degradation products from the organic content of the fish post-mortem may seep and escape from the carcass, however this means that consideration must be given to the intake of contaminant N and C. If the fish were encased by an algal mat as suggested in Chapter 2 Section 2.5.3, then exchange of organic matter between fish and algal mat is entirely plausible. However, no remnant N and a high TOC content are observed in the sediment samples using CHN analysis. If any post-mortem exchange did occur between the fish and algal mats then the resulting organic matter composition was subject to different mechanisms of preservation post-burial. The results from CHN analyses and the percent element data produced during CF-IRMS analyses show that N is present in all fish and TOC content is lower than that of the sediment samples. These data suggest that the OM in the fish may be indigenous or from immediate post-mortem contamination but was preserved over geological time perhaps as pockets within the fluorapatite structure of the fossils. The suggestion that isotopic signatures may be from organic matter held within clay inter-layers (e.g. Ostrom 1994) can now be discounted as no similar preservation of organic N was found in the clay-rich layers of the sedimentary matrix formed from volcanic ash deposition.

5.5.4 $\delta^{15}N$ isotopic signatures of fish from an ancient ecosystem

The six different fossil species analysed from the large ash plate all produced $\delta^{15}N$ data as shown in Figure 5.10, however all mean values produced were very similar despite the perceived hierarchy between species. The linear stepwise relationship seen in $\delta^{15}N$ values between modern species feeding at successive trophic levels is not present in these fish and Equation 5.1 could not be employed. In the three smaller clupeomorphs, the spread of data was such that almost a full trophic level could be inferred between fish of the same size and species. The larger carnivorous predators showed lower $\delta^{15}N$ values than many of the primary to secondary consumers sampled, suggesting that the data set may not be representative of the original isotopic compositions of the fish. Sections of two of the larger fish, AP7 and AP11, were removed for separate $\delta^{15}N$ and $\delta^{13}C_{org}$ analyses presented

in Section 5.4.2, however the mean $\delta^{15}N$ isotopic signature for these constituent tissues is very similar to the $\delta^{15}N$ values obtained for the remainder of the fish and the data presented in Figure 5.10 are still thought to be representative of the whole fish. Although dietary shifts in $\delta^{15}N$ between food and consumer are known to be in the region of 2.9‰ for whole fish (Sweeting *et al.* 2007), shifts are reported to vary substantially between different consumers, with the lowest shift in those raised on invertebrate diets (1.4‰), an intermediate shift in consumers raised on plant and algal diets (2.2‰) and the highest shift in consumers raised on high-protein diets (3.3‰) (McCutchan *et al.* 2003). This further serves to highlight that the $\delta^{15}N$ data should be much higher in the three larger fish specimens analysed if they fed in a simple stepwise food chain. Initial data from small clupeomorphs *K. eocaena*, *K. alta* and *D. dentatus* shown in Figure 5.3 A suggested that distinct isotopic signatures were achievable from the fossil fish, however the largest differences between species were observed in terms of $\delta^{13}C_{org}$ rather than $\delta^{15}N$, and were larger than would be expected from trophodynamics alone.

The data presented in Figure 5.10 may reflect diagenetic changes to the $\delta^{15}N$ values over time, contamination of the fish $\delta^{15}N$ signatures by algal mat organic matter immediately post-mortem, or may reveal a complex natural system with no clearly defined trophic hierarchy, reflected in the resulting $\delta^{15}N$ values. In their seminal study of an intertidal zone ecosystem Minagawa & Wada (1984) reported $\delta^{15}N$ values that increased steadily from one trophic level to the next (Figure 1.2). Similarly, Fry (1988) reported a clear enrichment in $\delta^{15}N$ of ~1.5‰ between planktivorous fish, opportunistic generalists and piscivorous fish on the continental shelf, regardless of species. In marine systems such as these a clear relationship between trophic level and $\delta^{15}N$ isotopic signatures exists and in particular in open-water systems where the primary food source is limited to phytoplankton (Michener & Schell 1994). This clear stepwise enrichment with trophic level was also replicated at TCD as part of the pilot study for this research using pelagic marine fish, although benthopelagic and demersal feeders showed much more variability and their $\delta^{15}N$ isotopic signatures alone could not be used to predict trophic level. A mixed isotopic signal may be the result of scavenging or may be related to isotopic

differences between the primary consumers being eaten by some of these fish. In their study of Canadian lakes Vander Zanden & Rasmussen (1999) discovered that large discrepancies in isotopic signature may occur at the base of the food chain, with a mean 5‰ range in $\delta^{15}N$ (-2 to +9‰ overall) observed between different primary consumers, such as deep and shallow water dwelling zooplankton, trichoptera (caddisflies) and ephemeroptera (mayflies). This implies that fish with lower $\delta^{15}N$ signatures may have been feeding from a food chain with a relatively low $\delta^{15}N$ baseline, rather than exhibiting simply a lower trophic level. It may therefore be the case that the fossil fish with similar $\delta^{15}N$ values occupied very different trophic positions. This is a distinct possibility in Fossil Lake as the trophic baseline is unknown for the fossil species and abundant lacustrine fish species are known to have relatively low niche overlap (Mason *et al.* 2008). However, the $\delta^{15}N$ values from fossil fish presented in Figure 5.10 are thought to be from species from the same food chain, with the largest of the fish feeding on the smaller species as discussed in Section 5.2.2. The overall lack of enrichment observed in the $\delta^{15}N$ signatures suggests that some other factor may have affected the original isotopic signal post-mortem, inferring that the values are a diagenetic product of either protein break-down or contamination from external sources. If the diagenetic products obtained from the fossils are a consequence of differential loss or retention of specific protein fractions then the geochemical characteristics and interpretation of the data are entirely a function of the protein composition of the organic matrix preserved (Ostrom *et al.* 1994). Experiments were executed to clarify the likely isotopic changes immediately post-mortem and during early diagenesis using extant fish and are discussed in detail in Chapter 6. Whether the isotopes measured in the fossil fish are from original fish organic matter or are an artefact of contamination is considered and presented in Chapter 7. This work was carried out to try and characterise the origin of the $\delta^{15}N$ signal in the fish but proved inconclusive.

5.5.5 Interpretation of palaeoenvironment

The $\delta^{15}N$ data shown in Figure 5.11 provides further evidence that the nitrogen content of the fish does not completely reflect the original trophic system of Fossil Lake. If these data showed palaeoproductivity changes through time as suggested in Section 5.2.6, then a strong inverse correlation would be expected with the $\delta^{13}C$ data from the carbonates. This

is not the case, and interpretation of the $\delta^{15}N$ isotopic data relies on discovering whether the OM in the fish may be indigenous remnants of specific protein fractions or from immediate post-mortem contamination, or even contamination from late-stage diagenesis. However, the use of $\delta^{13}C$ and $\delta^{18}O$ data from carbonates is a standard method of tracking changes in environment throughout geological time. That the $\delta^{13}C$ and $\delta^{18}O$ data produced correlate strongly ($r \geq 0.7$) suggests that the carbonate precipitated in a closed-lake system where water had a long residence time (Talbot 1990). This is in agreement with field evidence for periods of high salinity and the observations of fluctuating salinity reported by previous authors (Buchheim 1994b; Buchheim *et al.* 2002). Talbot (1990) reported that closed-lake carbonates also exhibit variations of $\delta^{18}O$ over several ‰ due to large changes in water balance, which does not seem to be the case here and may suggest long-term stability in basin hydrology, or at least during the deposition of the RH F-2 succession. This may be a function of the geological and climatic setting of Fossil Lake, with steady input of run-off from the surrounding mountains and a constant annual evaporation rate related to consistent temperature gradients. The time-frame studied here is uncertain, but assuming an average sedimentation rate of 100mm ka^{-1} (after Carroll *et al.* 2002) the RH F-2 section may represent 26000 years of Eocene deposition. Unfortunately this suggested timescale is insufficient to identify large-scale variations such as Milankovitch cycles, and sampling resolution is too low to identify small-scale annual or decadal variations. Interpretations of lake volume over this suggested 26ka period can be inferred however. The RH F-2 succession sampled was the thickest available stratigraphic unit containing fossil fish throughout; further analysis of $\delta^{13}C_{carbonate}$ and $\delta^{18}O$ at high resolution from the remainder of the Fossil Lake sediments may provide more insight into the changing Eocene palaeoenvironment.

In closed-basin lakes, primary carbonates formed away from the sediment substrate are in isotopic equilibrium with lake water, and thus reflect the past variations in the isotopic composition of lake water (Li & Ku 1997). Both $\delta^{13}C$ and $\delta^{18}O$ variations are principally controlled by hydrologic balance and vapour exchange, with $\delta^{13}C$ also being influenced by palaeoproductivity (Li & Ku 1997), however covariance of $\delta^{13}C$ and $\delta^{18}O$ is unchanged during the succession analysed suggesting that palaeoproductivity remained constant in

Fossil Lake at this time. In Figure 5.11, changes in both $\delta^{13}C$ and $\delta^{18}O$ to more negative values are thought to reflect input of isotopically lighter meteoric water, with changes to more positive values reflecting periods of low recharge and continued evaporation, thereby indicating the volume changes of Fossil Lake. That no marked or sudden isotopic shifts are seen indicates a hydrologically stable phase of the lake, highlighting that fish mortality is not related to sudden catastrophic change in lake volume or increased salinity, but rather is an integral part of a closed lake in steady state. Much more extreme fluctuations have been reported from bulk carbonate $\delta^{18}O$ records from Eocene Lake Gosiute, with excursions to very depleted isotopic values (ca -15‰) being attributed inflow of snow melt (Norris *et al.* 2000), but no such extreme excursions are reported here. Following the calculations of Norris *et al.* (2000), original lake $\delta^{18}O$ isotopic values for Fossil Lake lie between -5.5 and -7.8‰. This is in agreement with their values for Lake Gosiute (-4.5 to -11.5‰) and earlier estimates for Late Palaeocene to Early Eocene meteoric waters from the Bighorn Basin, Wyoming (-5 to -14‰) from bivalves and mammal teeth (Koch *et al.* 1995). That the values presented here are more enriched than the average reported values for Lake Gosiute suggests less influence from lake inflow waters and longer residence times. The suggested average Fossil Lake water $\delta^{18}O$ values are also consistent with the findings of Fricke (2003), who reports that Eocene $\delta^{18}O$ values were higher than American rivers today, inferring a past warmer climate for the area. Calculations of palaeotemperature from past $\delta^{18}O$ isotope data are commonplace; oxygen isotope exchange equilibria between carbonate minerals and water form the basis of the oldest and most widely used type of geochemical palaeothermometer (Ghosh *et al* 2006). Temperature effects influence both the isotopic composition of rainfall (and thus that of lake inflow waters) and isotopic fractionation during carbonate precipitation, but these effects are apparently of secondary importance in closed lakes, generally being masked by the effects of hydrological balance (see Talbot 1990 and references therein). As such, calculations of palaeotemperature from the data set herein are likely to prove misleading and are not presented.

5.5.6 Interpretation of chemostratigraphy

The major and trace element data shows just two main contributors to the sedimentology of Fossil Lake, namely the carbonate and a SiO_2 and Al_2O_3 rich phase with associated oxides and trace elements. The latter of these is thought to be from ash fall from the Absaroka and Challis volcanic fields into the basin. That some of the elements found within this ash do not statistically correlate may indicate evolution of the source magma or could be a consequence of differential post-deposition alteration and production of authigenic minerals. These changes may assist with future dating of the succession, and stratigraphic correlation between different units across the greater Green River Basin. The elemental data suggest no terrigenous input into Fossil Basin from any other sources. That fluctuations in $\delta^{13}C_{carbonate}$ and $\delta^{18}O$ values do not correspond to any of the elemental volumes further confirms that the detrital input into the basin is not a function of runoff and hydrology. The data presented in Section 5.4.5 can therefore only provide information regarding the elemental composition of ash fall and reveals little regarding any palaeoenvironmental factors. The geochemistry and provenance of these tephra fall deposits is discussed in detail by Chandler (2006), who concluded that because of pervasive secondary alteration, the usefulness of major and trace element compositions of the ash beds to determine the magmatic characteristics of the volcanic ash is limited, although immobile element compositions can reveal some characteristics of the original tephras. Sample collection for this study was primarily aimed at producing $\delta^{15}N$ signatures from fossil fish, and as such ash layers were not specifically targeted for sample collection and analysis. 8 samples from the data set do correspond directly to main ash layers, but the majority of these contained trace elements and REE below detectable levels. This is probably due to the high volume of carbonate included in the samples, effectively diluting the ash content. Immobile element compositions of only 2 samples, both from the 3/32″ ash layer, could be assessed in terms of provenance. Ta, Yb, Nb and Y immobile elements indicate a volcanic arc granitic origin using the tectonic discrimination scheme of Pearce *et al.* (1984). This is in agreement with the findings of Chandler (2006).

5.6 Conclusion

Different $\delta^{15}N$ and $\delta^{13}C_{org}$ isotopic signatures were found to be preserved within the different tissues analysed from two large fossil fish and the data set produced was comparable to different tissues of a modern freshwater fish of similar size. C:N ratios indicated a substantial loss of organic matter from the biogenically mineralized tissues of the fossil fish over geological time, although this was expected from fish of such antiquity. $\delta^{15}N$ signatures were measured from whole fish at one stratigraphic level, representing 6 species that would have fed at successive trophic levels of the same ecosystem during life. Their trophic adaptations have long been studied and their feeding positions are well-known by palaeontologists. The bulk $\delta^{15}N$ data retrieved did not reflect the trophic level of the fish and may be an artefact from contamination or a diagenetically altered original signature. That bulk N isotopes can be extracted from Eocene fossil fish is remarkable, and further work is necessary to characterize the nature of the organic material in which the N is preserved. EDS microanalysis, XRD and CHN analysis confirmed that organic matter was present within the fluorapatite structure of the fossils. SEM imaging revealed excellent preservation of histological features at high resolution but did not suggest that the fish were exceptionally preserved due to bacterial biofilms. Throughout the deposition of the split-fish-layer beds at quarry RH F-2, little disruption to hydrological balance or environment is inferred. This steady state is attested to by $\delta^{13}C$ and $\delta^{18}O$ data from carbonates which show no major changes over time and their covariance throughout indicates a stable closed-basin lake. As $\delta^{15}N$ no longer appears to reflect trophodynamics, inferences regarding palaeoproductivity throughout the succession could not be made. Detrital input into the basin appears only to be from ash fall and run-off over similar deposits, and analysis of elemental data confirms provenance of the tephra from volcanic arc tectonics in the Absaroka and Challis fields to the north.

Chapter 6: Experimental modelling of post-mortem isotopic variation

6.1 Overview

The nitrogen and carbon isotope composition of organic matter has been widely used to trace biogeochemical processes in both marine and lacustrine environments. However, as bones and other hard parts of organisms become fossilised, alteration occurs at all scales from the macroscopic to the nanoscopic level. To accurately evaluate the information extracted from fossilised bones and scales of fish in order to reconstruct palaeodiet and palaeoclimate, a study of diagenetic modification of bulk N and C_{org} isotopes in extant fish was required. It was crucial to consider potential alteration of the primary isotopic signature by bacterial degradation in the water column and during early diagenesis in the sediments. Conditions were simplified and the effects of the different variables of temperature, salinity and oxygen level on extant fish were explored and changes in their $\delta^{15}N$ and $\delta^{13}C$ signatures monitored over a period of six months. Through these laboratory-based taphonomy experiments described herein, a better understanding of how isotopic signatures may vary in different tissues after death and during early diagenesis was gained.

6.2 Introduction

6.2.1 Previous work

For centuries the science of taphonomy has been carried out in order to study the transition of organic remains from the biosphere into the lithosphere via the process of fossilization, from death to diagenesis (see Martin 1999). Many taphonomic investigations of vertebrates have focused on observing bone preservation to answer archaeological questions regarding early human habits and practices via various bone concentration and alteration factors, for example, percussion, burning, gnawing and digestion, transport, weathering, and soil corrosion (for extensive reviews see Denys 2002 and Fernández-Jalvo *et al.* 2002a). Previous archaeometric taphonomy experiments have mainly focussed on these morphological degradation features of bone in soils over time (Child 1995; Fernández-Jalvo *et al.* 2002b); however, the importance of modelling of physico-chemical changes in this field of research is becoming more widely recognised (see Hedges 2002

and Lee-Thorp & Sealy 2008). By limiting the number of variables in test situations, experimental taphonomy in the laboratory also helps to isolate factors that are important in the formation of fossil assemblages, and to build models to test the effects of these factors in natural situations, a technique used increasingly in archaeology (Denys 2002).

Experimental investigations of invertebrate and vertebrate faunas pertaining to palaeontological situations have primarily been aimed at interpreting morphological features in fossil faunas. Invertebrates are now known to decay through the same stages (albeit at different rates) regardless of the circumstances (i.e. variations of salinity, oxygen and temperature) and a great deal has been revealed regarding mineralization processes (see Briggs 1995). Much experimental work has been done using extant invertebrate organisms as an analogy for the enigmatic soft-bodied faunas found in Precambrian and Cambrian fossil assemblages (e.g. Butterfield *et al.* 2007), to attempt to interpret the morphology of these fossils and to identify the conditions under which the soft tissues were mineralised (see Briggs 2003). Recently Sansom *et al.* (2008) investigated the decay of extant organisms to constrain anatomical interpretations and distinguish phylogenetic characters from taphonomic artefacts in early chordates. Similarly, Liu *et al.* (2008) used laboratory studies of extant organisms to help recognize post-mortem changes in the morphology of Ediacaran biota and to differentiate potential taphomorphs, while Raff *et al.* (2006) used experimental taphonomy to investigate the preservation of Ediacaran embryos and larvae. Several authors have explored the effects of decay and early diagenesis on extant vertebrate organisms, documenting both large and small scale morphological features. For example, Davis & Briggs (1998) carried out taphonomic experiments comparing the disarticulation and weight loss of bird carcasses in brackish and marine environments as an analogy for the preservation of fossil avifaunas in various lagerstätten, including the Green River avifauna of Fossil Lake. To investigate the fate of keratinous tissues in birds and mice, McNamara & Orr (2008) used a series of different experimental conditions to analyse differences in fidelity of various structural tissues. Small scale morphological and histological features in vertebrate specimens are often examined using a combination of scanning electron microscopy (SEM) and transmission electron microscopy (TEM) (Martill 1991; Turner-Walker & Syversen 2002; Reiche *et al.*

2002). The aforementioned research, along with similar investigations, has helped to constrain the post-mortem and post-burial effects of different taphonomic pathways, highlighting the effects of microbial activity, permineralization and authigenic mineralization in the process of fossil formation (see Briggs 2003).

Geochemical investigations regarding stable isotopic change during the decay, burial and diagenesis of vertebrates have mainly focussed on $\delta^{13}C$ and $\delta^{18}O$ of bone and tooth bioapatite in the archaeological and palaeontological record (e.g. Wang & Cerling 1994; Sharp *et al.* 2000; Lee-Thorp 2002; Zazzo *et al.* 2004; Tütken *et al.* 2008). Balzer *et al.* (1997) investigated the changes in nitrogen and organic carbon stable isotopic composition of bone collagen and individual amino acids. They concluded that bacterial decomposition of collagen is accompanied by changes in N and C_{org} isotopic abundances, which could interfere with interpretation of the original isotopic values of the native material. However, these experiments were inoculated using soil bacteria and are not analogous to the freshwater setting of Fossil Lake, nor the bulk isotopic measurements obtained herein. There has been little further study reported regarding the taphonomy of vertebrates relating to their N and C_{org} isotopic signatures. Lehmann *et al.* (2002) investigated the alteration of N and C_{org} isotopes in organic matter during early diagenesis, but focussed on the microbial degradation of algae. They document a depletion of ^{15}N in anaerobic conditions and a continuous decrease in $\delta^{13}C$ values in all incubations. These two N and C_{org} isotope studies alone indicate that modifications of the isotopic signatures do take place during early diagenesis, confirming the necessity for further experimental taphonomic investigation for the interpretation of N and C_{org} isotopic signatures of fossil vertebrates.

6.2.2 Outline

In this study, real-time experiments were conducted in the laboratory to document the N and C_{org} isotopic variation in modern fish after death, during bacterial degradation and early diagenesis, to investigate whether the N and C_{org} isotope values observed in Chapter 5 could be preserved original signatures. The experiments were designed to document first order patterns of isotopic modification and conditions were simplified versions of

complex natural systems. Extant fish were used in these experiments replicating various scenarios of the conditions postulated for Fossil Lake during the late Early Eocene in order to interpret the role of fossilisation in any alteration of the isotopic signatures. Although undoubtedly many diagenetic processes are long term, a number of processes critical to fossilisation are known to operate on a laboratory timescale (Pfretzschner 2004). By simplifying conditions and exploring the effects of changing variables, the most important factors that would have acted on the Green River fish and influenced preservation were explored. Various models have been proposed by previous authors to explain the fish preservation in the Green River Formation, but there is considerable disagreement with regard to depositional environment (Whitmore *et al.* 2002). That coprolites are also preserved with the fish of Fossil Lake suggests an exceptional combination of circumstances and mineralization may have been mediated in the presence of microbial films as discussed in Chapter 2 Section 2.4.3. Although the exact depositional environment of the fossil fish is unknown, several scenarios were recreated in microcosm and the effects of each on the isotopic signatures of extant fish evaluated. These scenarios involved three main variables and the exclusion of all other external influences. Using a series of 250mL clear, wide mouth screw-top jars with a layer of sediment and one fish in each, filled with water as shown in Figure 6.1, the potentially different patterns in the isotopic signatures during decay could be investigated over time. Each fish was only sampled once, at the end of the appropriate time period. Ten sampling days were chosen using a logarithmic timescale that was realistic in terms of early diagenetic processes. Samples of bone and scale tissue from fish in each scenario were tested to monitor change, as an analogy for the isotopic signatures of the fossil fish measured previously and described in Chapter 5. Muscle tissue was also analysed at each sampling interval where possible. Common goldfish *Carassius auratus auratus* Linnaeus, 1758 were chosen as the experimental taxon because they are readily available and bred in captivity. The imported goldfish used in these experiments were carefully sourced so that they would all be at the same stage of ontogeny, all grown in the same controlled water mass and all fed on the same food source. This ensured that the stable isotopic signatures of all the fish would be as similar as possible to each other at the outset. Crucially, the capability of the most

likely preserving environments to have caused alteration to the N and C_{org} isotopic signatures after death and during early diagenesis of the fossil fish was examined.

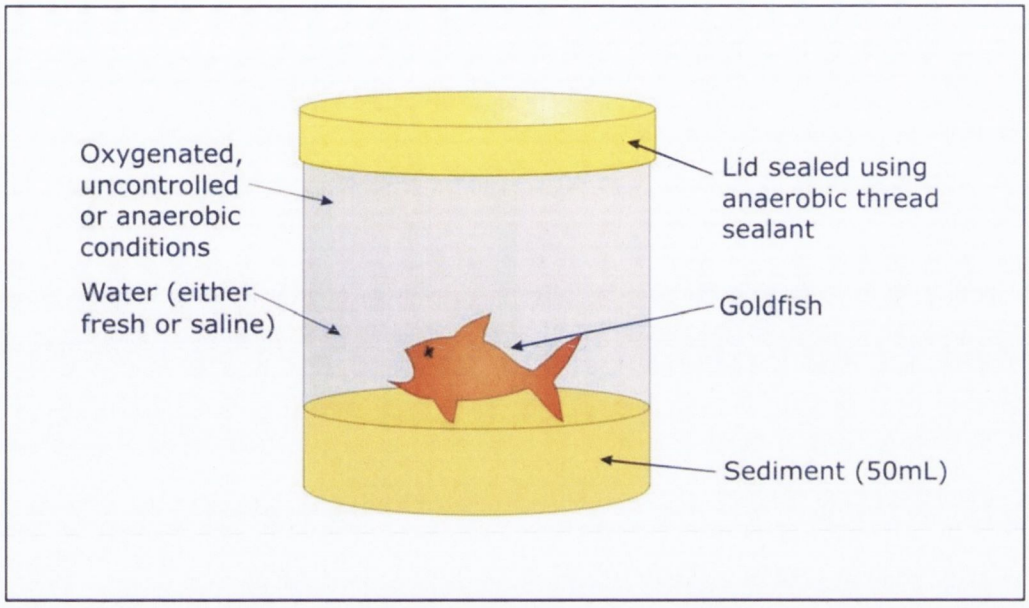

Figure 6.1: To recreate the possible conditions experienced in Eocene Fossil Lake to investigate post-mortem changes in N & $C_{organic}$ isotope signatures in fish, a series of microcosm experiments involving extant fish were devised.

6.3 Experiment design and rationale

6.3.1 Independent variables

In order to replicate a range of possible environmental conditions that may have existed within Fossil Lake, several combinations of variables were contemplated. Firstly, and perhaps most importantly, the temperature of the lake bed during the late Early Eocene was considered, as temperature is a primary control on decay (Davis & Briggs 1998). Whilst global Eocene temperatures are known to have been much warmer than today (e.g. Zachos *et al.* 1994; Pearson *et al.* 2001; Huber and Caballero 2003; Pearson *et al.* 2007), Fossil Lake would have been at a relatively high altitude broadly similar to its current elevation (Chase *et al.* 1998; Norris *et al.* 2000) and thus would have experienced cooler air temperatures than the regional sea-surface average. Palaeobotanical analyses of the intermontane Green River Basin flora suggest a mean annual temperature of 18-21°C, with temperatures during the colder months dipping to an average of just 13°C, while

remaining above 5°C (Wing & Greenwood 1993; Greenwood & Wing 1995; Wilf 2000; Prothero 2006). However, average temperatures may have been cooler at the sediment-water interface and are likely to have been subject to less interannual variation. Fossil Lake is interpreted as a deep, warm-monomictic lake that would have had thermal stratification during much of the year and only complete mixing during the winter months (Ferber & Wells 1995). Warm-monomictic lakes are subject to many variables that affect their stratification such as mixing rates, vertical dimensions of layers, layer temperature and the temporal duration of stratification, basin morphometry, as well as local hydrology and meteorological conditions (Kim & Kim 2006). Light penetration, measured as Secchi depth, also influences thermal stratification and is related to algal biomass and abundance of planktivorous fish (Mazumder *et al.* 1990). Although the changing seasonal air temperature is thought to exert the most influence on lake temperatures (Leopold 2000), estimating the likely temperature of the lake floor in Eocene Fossil Lake is unfeasible without further geochemical analyses and data collection beyond the scope of this study. Two distinct temperatures, 10°C and 20°C, were chosen for the experiments detailed herein, based on the mean annual air temperatures reported by previous authors.

Although Fossil Lake was part of a freshwater terrestrial lake system in the Rocky Mountains, it was clear from field observations that during certain periods of the late Early Eocene the lake became hypersaline, as discussed in Chapter 2 Section 2.3.5. As such, the influence of salinity on physical decay and the preservation of isotopic signatures was the second variable chosen to be explored. In Fossil Lake the trona bearing units and salt-pseudomorphs seen in the field were restricted to the non-fish bearing upper unit or Angelo Member, in agreement with previous work by Buchheim *et al.* (2002). This is thought to be due to a restriction of inflow leading to a hypersaline-alkaline phase of the lake resulting in these evaporitic facies (Loewen *et al.* 2003). It has been widely reported that due to later climatic variations the other two lakes in the Green River Formation, Lake Uinta and Lake Gosiute, were both subject to prolonged periods of hypersalinity, exacerbated by their shallow depths coupled with increased evaporation levels as a result of their larger surface areas (Bradley & Eugster 1969; Surdam & Stanley 1979; Pietras *et al.* 2003; Smith *et al.* 2008). Although the majority of fish collected for this study are

thought to be from an entirely freshwater setting, an investigation of salinity was deemed useful for future isotopic studies of trophic level in fossils, particularly in relation to that discussed in Chapter 8. Seawater has long been known to affect physical decay rates in experiments, inhibiting decay rate by limiting the survival of the bacteria usually active during decay (Schäfer 1972; Briggs & Kear 1994). Conversely, other authors have found that increased salinities substantially increase decay due to the oxidation of organic matter by sulphate-reducing bacteria (Hof & Briggs 1997). As such, both fresh deionised water (DIW) and artificial seawater (ASW) with a salinity of 35‰ were used in these experiments to monitor for changes in the isotopic composition of the fish carcasses as a result.

It is unclear whether Fossil Lake was anaerobic, disaerobic or fully oxygenated below the thermocline. Evidence suggests that certainly the sediment-water interface may have been anoxic as no scavenging or intensive bacterial decay appears to have acted on the fish prior to fossilisation, although this could have been due to chemical toxicity of the water mass, as discussed in Chapter 2 Section 2.5.2. However, due to algal blooms, large amounts of organic matter may have accumulated on the lake bed causing depletion of oxygen and formation of rotting gyttja muds. Oxygen level was therefore the third variable explored within this series of experiments on modern fish. Previous authors have investigated the role of oxygen level in the preservation of fossils (see Martin 1999), including experiments specifically in relation to the preservation of the fish of Fossil Lake (Whitmore *et al.* 2002). Traditionally anaerobic decay has been viewed as one of the main factors in creating exceptionally preserved faunas (e.g. Seilacher *et al.* 1985); where oxygen is available calcium carbonate deposition will dominate, whereas in a closed system calcium phosphate deposition has been found to replicate soft tissues within two weeks (Briggs & Kear 1993 and 1994). However, several authors have reported rapid decay during experiments despite complete anoxia (see Martin 1999). In their laboratory experiments to observe taphonomic processes in fish, Whitmore *et al.* (2002) found little difference in decay rates despite varying the oxygen concentration in the water and surmised that the fish decayed from the inside out, probably by anaerobic decay, regardless of the oxygen level of the surrounding water mass. The previous body of work

investigating taphonomy in the laboratory thus seems inconclusive in relation to the effects of oxygen level on the physical decay of organisms. To investigate the impact of different oxygen levels on the isotopic composition of extant fish during bacterial degradation and decay, three contrasting oxygen levels were selected, namely fully oxygenated, anoxic and 'uncontrolled' (beginning fully oxygenated, sealed and allowed to go anoxic).

Other variables that could have been investigated to evaluate their effects on rate of decay and isotopic signature, such as pressure, light, sediment grainsize, sediment type and pH were beyond the scope of these experiments. These parameters were controlled, monitored and kept constant as far as possible so no impact from them would be reflected in the decay rates of the extant fish or the geochemical analyses. The twelve combinations of the three variables of temperature, salinity and oxygen level chosen for experimentation are shown in Figure 6.2.

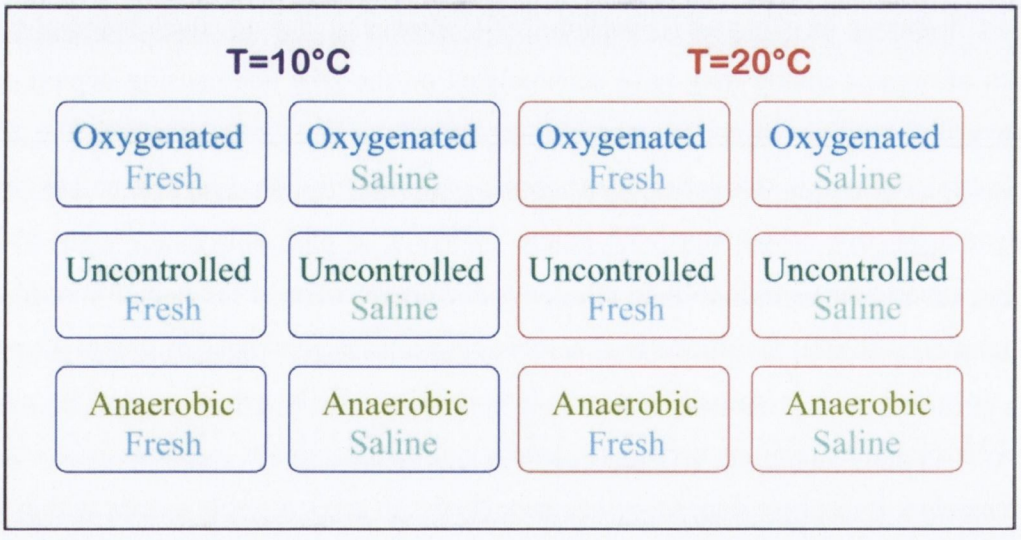

Figure 6.2: Twelve possible combinations of the three independent variables chosen for these experiments.

6.3.2 Time scale and sampling intervals

The effects of the three different parameters were to be measured over a time period chosen to reflect the most intensive period of post-mortem change. Previous studies documenting physical decay and preservation of morphological features discussed in

Section 6.2.1 used observation periods between several weeks and 18 months, although the reasoning behind their choice of time periods was not reported. Davis & Briggs (1998) documented that breakdown of the soft tissues, initiated by autolysis, was evident in the first two days of their experiment before bacteria had gained access to the deeper tissues. They found that birds decayed within 70 days, and often much faster at higher temperatures, to produce results analogous to fossil lagerstätten. Taphonomy experiments by Briggs & Kear (1993) found that mineralization of shrimps commenced within 2 weeks post-mortem and increased in extent for at least 4 to 8 weeks. Pfretzschner (2004) reports that microbial activity on bone fades after about six months in decay experiments under laboratory conditions. Successive stages in bone diagenesis are also discussed by Pfretzschner (2004), with three subdivisions of the early stage of diagenesis lasting over a year, until microbial activity finally ceases as collagen is replaced by apatite and other minerals, after which time an abiotic late diagenesis decay phase begins. In their investigation of N and C_{org} isotopes in bone diagenesis, Balzer *et al.* (1997) terminated incubation periods when microbial invasion of the mammal bones was deemed to be complete after 8 to 18 months. Limitations on the study detailed herein meant that it was possible to carry out the experiments for a maximum period of 6 months, with the final sampling taking place at 192 days. This maximum time period was divided up using a logarithmic scale and eight other sampling days chosen: day 1, 2, 4, 8, 16, 32 and 64. As the majority of changes relating to microbial decay were expected to occur during the first two weeks of the experiments an extra sampling day was added on day 12. This gave ten sampling intervals, t_1 to t_{10}, when fish carcasses would be dissected and their N and C_{org} isotopic compositions analysed.

6.3.3 Method of euthanasia

Another consideration in the experiment design was the method of euthanasia to be used with the extant fish (see recommended methods outlined in Close *et al.* 1997). The goldfish were to be killed immediately upon arrival at Trinity College after transportation from the UK to minimise the overall distress to the animals. Accepted physical methods of fish euthanasia may have affected the overall rate of decay of the internal tissue and the isotopic composition of the fish, by altering the surface area and condition of the animal

available for chemical exchange with the water and sediment. Standard chemical methods of fish euthanasia also presented problems for this study as most affect the pH of the water and/or the water temperature, and therefore may have interfered with these controlled closed-system experiments. In order to keep the fish physically intact and to minimise possible effects on the isotopic composition of the fish while maintaining the controlled conditions of the experiment, a different method of euthanasia was sought. Carbon dioxide poisoning was deemed to be the most humane method of euthanasia and the only suitable procedure to ensure rigorous scientific results. This non-standard method of fish euthanasia likely caused minimal suffering and was approved by the Trinity College Bio Resources Ethics Committee. The official approval documentation is included in Appendix 2 of this thesis. Storing and, in particular, freezing of carcasses prior to experimentation (as employed by Davis & Briggs 1998) is known to affect bone porosity and therefore degradation rates (Robinson *et al.* 2003). The goldfish were therefore euthanized and the experimentation begun immediately to negate any possible interference from such extra preparation methodologies.

6.3.4 Storage of extra samples

At the end of each time interval all fish to be dissected were sampled for bone, muscle, and scale tissue; these samples were then prepared for stable isotope analysis and analysed immediately as each chosen time period came to a close. However, to protect against possible equipment failure during the automated analysis and in anticipation of future repeat analyses, extra sub-samples were taken from each fish and frozen at -18°C as a precautionary measure. Whether using freezing as a long-term storage option was appropriate or not was investigated thoroughly prior to the commencement of these experiments. Due to the nature of isotopic analyses, marine and freshwater species collected by biologists in the field are usually preserved until they can be analysed in the laboratory, usually by freezing, drying or storing in preservatives. Adding chemical preparations has been found to substantially alter the isotopic signatures during short-term storage (e.g. Bosley & Wainright 1999; Kaehler & Pakhomov 2001; Arrington & Winemiller 2002), thus freezing aquatic organisms in the field has become standard practise (e.g. Hobson *et al.* 2002; Connolly 2003; Mill *et al.* 2007; Wang *et al.* 2009).

Colleagues in the Department of Zoology, TCD, also use this practice; fish and invertebrates retrieved onboard research vessels from around the coast of Ireland are immediately frozen until such time that they can be analysed using the Department of Geology stable isotope facility. Previous authors have investigated the effects of freezing and assessed the likelihood that alteration of the N and C_{org} isotopic signatures could occur over time periods of up to 3 and 21 months and have confirmed that freezing does not change isotopic signature in fish during long-term storage (Kaehler & Pakhomov 2001; Sweeting *et al.* 2004). As such, storage of samples by freezing was deemed suitable for these experiments. Analysing samples immediately as each fish was dissected proved to be unproblematic with all equipment and procedures functioning correctly. It was therefore not necessary to run the frozen samples of scales, muscle and bone collected throughout the experiments as security. However, subsequent to the end date of these experiments, the frozen samples from each time period were analysed for their N and C_{org} isotopic signatures and were treated as replicates.

6.4 Method

6.4.1 Preparation

A series of 147 250mL clear, wide mouth screw-top jars were used for these experiments. The jars were prepared by soaking in 10% HCl overnight, rinsed five times with DIW, dried in the over-pressured filtered glove box (shown in Chapter 3, Figure 3.2 A) and labelled before use. As well as written labels a colour coding system was devised for ease of sample recognition using adhesive coloured labels to represent the different conditions to prevail inside each jar. Approximately 50mL of dry sediment was then added to each jar and 200mL of water of the appropriate salinity added. The sediment used in these experiments was a fine carbonate powder produced by grinding up rocks sourced from the F-2 quarries. The rock specimens were devoid of fossils after undergoing the treatment described in Chapter 3 Section3.1.1. They were crushed using a Retsch KG mechanical crusher, powdered using a Tema® laboratory disc mill, and sieved in a 500μm brass sieve to ensure that any larger particles remaining were omitted. Half of the jars received 200mL of DIW and the other half 200mL of ASW. Salinity S=35 ASW was prepared for these experiments using a method adapted from that used by Ramette *et al.* (1977) and the

composition is given in Table 1. Analytical grade reagents were used to prevent impurities and contaminants entering the system. The jars containing sediment and water were then removed to either a refrigerator or incubator and allowed to equilibrate to the required temperature. A domestic Zanussi ZERT6646WH larder fridge was used to keep the 10°C samples at a constant temperature and a Labheat™ RLSD01501 150L Refrigerated Incubator was used to maintain a constant 20°C for the remaining jars. Jars for replicate samples were also prepared.

Solute	***m***	**mol kg^{-1}**	**M.W.**	**g kg^{-1}**	**g dm^{-3} (25°C)**
NaCl	0.42664	0.41168	58.4428	24.061	24.625
Na_2SO_4	0.02926	0.02823	142.0431	4.011	4.104
KCl	0.01058	0.01021	74.5513	0.761	0.779
$CaCl_2.6H_2O$	0.01077	0.01039	219.0757	2.276	2.331
$MgCl_2.6H_2O$	0.05518	0.05325	203.3027	10.826	11.080
			g salt	35.055	
			g H_2O	964.945	

Table 1: Composition of *S*=35 artificial seawater (after Ramette *et al.* 1977).

Upon arrival in the laboratory the goldfish were put in a 20L plastic bucket filled with water. The water was sparged with a constant stream of CO_2, the bucket covered and left for a period of 30 minutes. Post-mortem, the fish were individually measured and photographed and any physical differences noted. All 147 goldfish used in this study were sampled at the outset by removing a small section of scales from behind the anal fin and the initial N and C_{org} isotopes values of these were measured and recorded as a control using CF-IRMS via the procedure outlined in Chapter 3 Section 3.1.3. The 250mL jars were then brought to the appropriate oxygen level. A third of the jars were anoxic from the outset, a third were 'uncontrolled', beginning oxygenated and allowed to go anoxic, and a third kept oxygenated by sparging with air for the duration of the experiment. The water in the jars that were to be kept anoxic was sparged with certified pure (CP) argon in an argon box for 20 minutes to purge all oxygen prior to the fish being introduced. Argon was chosen rather than nitrogen as used by previous authors (e.g. Briggs & Kear 1993) to

prevent any possible interference with the nitrogen isotope exchange and the free nitrogen cycling within the sealed jars. Two Interpret AV4 Airvolution filtered aquarium pumps were used to constantly aerate the oxygenated jars throughout the course of the experiment. A series of interconnected silicon tubes fed the filtered air directly into each

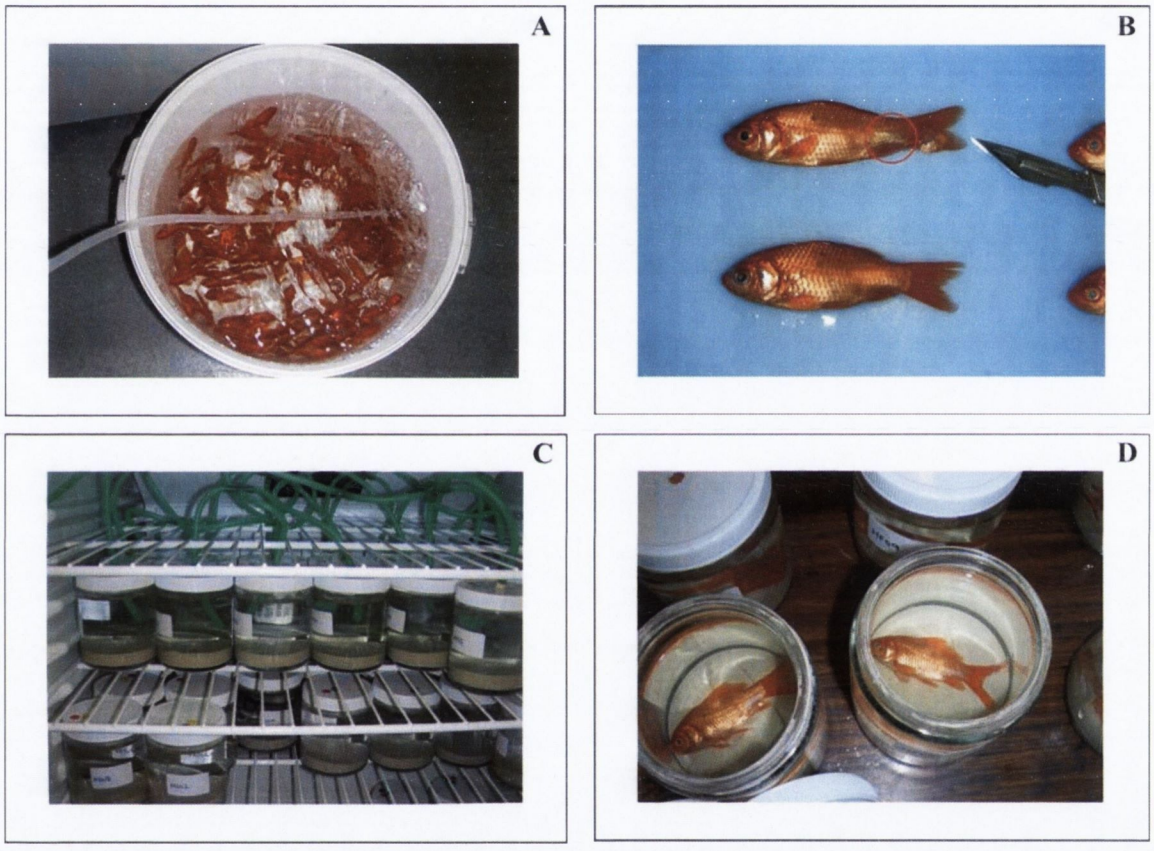

Figure 6.3: Some of the preparation procedures used: **A)** Goldfish were euthanized for the experiments by CO_2 poisoning; **B)** A sample of scales was taken from each fish from behind the anal fin, post-mortem; **C)** 147 jars were prepared and brought to temperature in a refrigerator or an incubator. A network of silicon tubing ensured that the oxygenated samples would have a constant stream of filtered air delivered throughout the experiments; **D)** The goldfish were placed into individual jars, weighted with a cover slip and the jars sealed using anaerobic thread sealant.

individual jar through holes specially drilled in the jar lids using an electric Proxxon© IB/E handheld drill. The tubing was fitted so that oxygen would bubble into the water approximately 1cm below the water line at a slow but constant flow rate. Once the jars were labelled, prepared and brought to the necessary temperature and oxygen level, then

the fish could be added. The fish were not buried but positioned on their lateral surface resting on the sediment; to prevent refloating of the carcasses, a cleaned glass microscope slide coverslip was placed on top of each fish. Each jar was then sealed with Swagelok SWAK®, an anaerobic thread sealant that was tested prior to these experiments and found to have no adverse chemical effect. All fish to be kept in anoxic water were placed in the jars and the jars sealed while still in the argon box. As the jars were sealed the time (t_0) was noted, before all jars were returned to the refrigerator or incubator as appropriate. Replicate jars were also prepared in duplicate and triplicate for most sampling days to observe variation in isotopic exchange within the same set of conditions. Figures 6.3 A-D illustrate some of the preparation procedures described in this section.

6.4.2 Sampling and analysis

Ten sampling intervals were chosen using a logarithmic timescale, from 24 h up to a maximum of 192 days. As each time period came to a close (t_1-t_{10}) the appropriate set of jars were opened and sampled. The pH and temperature of the water was measured using a pHep® 4 waterproof pH/temperature tester which was calibrated regularly during these experiments. Each goldfish was handled using powder-free latex examination gloves and any loose sediment rinsed from the carcass using DIW or ASW as appropriate before the fish was dissected in a cleaned glass Petri dish using a fresh scalpel blade and cleaned tweezers. As shown in Figure 6.4, a sample of scales was taken from the caudal area, any remaining skin removed and a sample of white muscle taken from beneath. A section of the caudal vertebrae was then extracted from each fish and any soft tissue separated and removed from the bone. The muscle and vertebrae were both cut into smaller sub-samples ready for analysis and a portion of the scales, muscle and bone was taken and stored at -18°C as a precautionary measure. Portions of each fresh sample (~2.5-4.5mg) were then weighed accurately using a high-precision microbalance (Sartorius MC5, ± 2μg) and sealed in tin capsules. Samples were not subject to any kind of drying or homogenising procedure as is sometimes used in trophodynamic studies involving N and C_{org} isotopes; these methods are frequently employed when biological samples are sent away for analysis off-site (e.g. Kaehler & Pakhomov 2001; Mill *et al.* 2007). The N and C_{org} isotope signatures of the fresh sub-samples were then measured by CF-IRMS using the

procedure outlined in Chapter 3 Section 3.1.3, and C:N ratios were determined from the percent element data also produced during these analyses. Samples from each fish were run immediately after dissection and analysed in a random order to prevent any systematic bias in the results. Throughout these experiments calibration standards were analysed to enable calculation of accuracy and repeatability as detailed in Chapter 3 Section 3.1.2. Experimental precision based on these replicates was ±6.2%RSD for $\delta^{15}N$ and ±0.8%RSD for $\delta^{13}C$. Replicate samples of vertebrae, muscle and scales were also analysed from each fish.

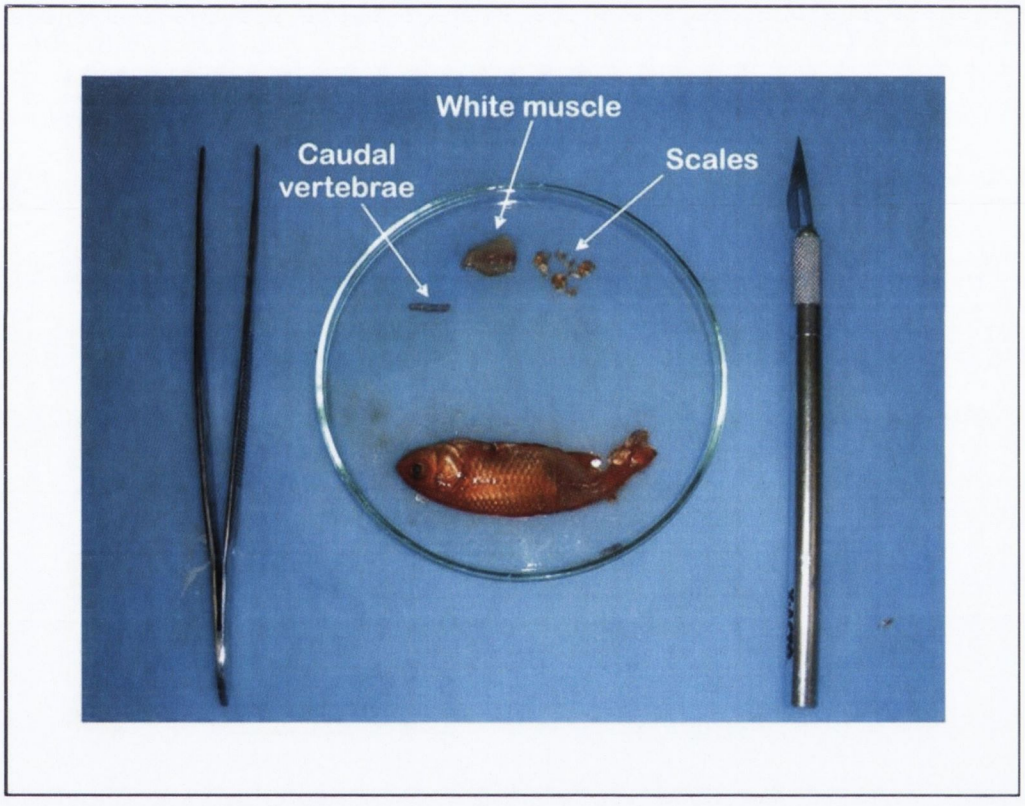

Figure 6.4: On sampling days each of twelve fish, plus replicates, were dissected and scales, muscle and caudal vertebrae were sampled. These were further sub-sampled and analysed using CF-IRMS.

At the end of all time periods as the goldfish carcasses were being sampled, a portion of sediment and a water sample was collected from the jar. The sediment was collected from directly underneath the decaying fish and dried at 40°C overnight prior to analysis of carbonate carbon and oxygen isotopes. Portions of each sediment sample (0.5-0.7mg)

were weighed accurately into cleaned glass exetainers using a high-precision microbalance (Sartorius MC5, ± 2μg). The $\delta^{13}C$ and $\delta^{18}O$ values of these carbonate samples were measured using CF-IRMS via a Thermo Gas Bench II as outlined in Chapter 3 Section 3.2. Replicate standards analysed throughout the procedure indicate a precision of ±1.1%RSD for $\delta^{13}C$ and ±1.2%RSD for $\delta^{18}O$. Water samples were filtered using Whatman® glass microfibre filters, then aliquots analysed using calibrated HANNA instruments® single parameter photometers HI-93733 and HI-93728, together with the recommended HANNA instruments® reagents, in order to determine the level of nitrate and ammonia in each water sample. Replicate aliquots were measured to ensure accuracy. Samples were diluted as necessary, some by as much as a factor of 20, in order to ensure results were in the range of the ammonia photometer.

A labelling system for the 147 jars used was devised using the three independent variables: hot or cold (H or C), fresh or saline (F or S), oxygenated, anoxic or uncontrolled (O, A or U) and time period (1 to 10). For example, a sample kept at the high temperature, in fresh, anoxic water for a period of 12 days (t_5) would be labelled HFA5. The results are shown in tables in Appendix 2 and in Section 6.5 and follow this labelling system. It should be noted here that on sampling day 16 (t_6) of these experiments a sharp temperature decrease of ~6°C in the incubator samples was observed: an engineer was called immediately and a mechanical problem rectified. This should be accounted for when analysing the data produced on this date. Subsequently temperatures in the incubator were monitored closely and found to be reliable.

6.5 Results

6.5.1 N and C_{org} isotope data from fish samples

Results of all N and C_{org} isotope analyses from day 1 to day 192 are shown in Figure 6.5. The majority of data points represent an average of measurements from three different sub-samples (n=3) of the vertebrae, muscle or scales unless otherwise stated. Any obvious outliers were removed and discounted from analysis of data in this results section. The results were corrected to international standards using the L-Alanine working standard previously described in Chapter 3, and were also corrected using the control samples of

scales analysed prior to the experiments (t_0). An average from the N and C_{org} isotope data of the control samples was taken and the difference between the starting values of each fish removed to correct them to the same starting value. All subsequent isotope data was corrected using the individual factor calculated for each fish, thus ensuring that direct comparison between fish would be accurate. In Figure 6.5 the mean $\delta^{15}N$ isotope values of the 12 fish dissected at the end of each of the 10 time periods (t_1-t_{10}) are plotted against their mean $\delta^{13}C_{org}$ values. The results from vertebrae, muscle and scales plot in distinct areas of each graph and are highlighted using a purple, green or orange ellipse, respectively.

Similar isotopic data were gained from the fish on day 1 (t_1) as on day 2 (t_2) of the experiments, with only minor fluctuations in $\delta^{13}C_{org}$ values after 48 hours had lapsed. The vertebrae $\delta^{15}N$ values are constrained between 3 and 4‰ in a <1‰ range, whereas their $\delta^{13}C_{org}$ values show a 3.2‰ range between -28.6‰ and -25.5‰. Muscle values cluster more tightly for both $\delta^{15}N$ and $\delta^{13}C_{org}$, and are slightly more enriched in the heavier isotopes of both N and C. Scales show the most similar isotopic signatures when comparing all fish with a <1‰ range in both $\delta^{15}N$ and $\delta^{13}C_{org}$, around 3‰ and -24‰ respectively. The graphs for day 4 (t_3) and day 8 (t_4) show a slightly greater spread in $\delta^{15}N$ values in all tissues, particularly with regards to muscle, although the scale sample values remain largely unchanged from day 1. After day 12 (t_5) of the experiments the muscle sample data start to spread to more negative values, and the previously constant scale sample data show a larger range in $\delta^{15}N$, although still <1‰. This trend in the scale and muscle samples appears to be reversed slightly on day 16 (t_6) however, although the muscle samples continue to show more variation and the vertebrae samples show an almost 4‰ spread in their $\delta^{13}C_{org}$ values, between -30‰ and -26‰. These data do not show any significant effects caused by the change in temperature at t_6 due to incubator failure. On day 32 (t_7) the samples of vertebrae from all 12 fish show a range of 1.3‰ in their $\delta^{15}N$ values and a continued ~4‰ spread in their $\delta^{13}C_{org}$ values. Muscle was very glutinous in nature and difficult to sample at this stage, showing obvious signs of physical decay. The spread in data mirrored this decay: the 1.9‰ range in $\delta^{15}N$ data and 3.1‰

range in $\delta^{13}C_{org}$ values is larger than the spread of data seen in muscle values on previous sampling days, with the ellipse of data points now overlapping that of the vertebrae data points.

By day 64 (t_8) only vertebrae and scales were available for sampling, as the muscle had decayed to such an extent in almost all cases that samples could no longer be retrieved. All $\delta^{15}N$ data from both vertebrae and scale samples are constrained between 2.8 and 4‰, a range of just 1.2‰, whereas $\delta^{13}C_{org}$ values for the vertebrae show a spread of 4.5‰ and scales 1.2‰. On day 128 (t_9) the range of nitrogen data is similar, with both vertebrae and scales showing a range of <1.2‰, and the majority of data points falling between 3‰ and 4‰. The ~4‰ range of $\delta^{13}C_{org}$ data for the vertebrae samples appears to have had a slightly negative shift overall when compared to the graphs from previous sampling intervals, however the majority of data still plots between -30‰ and -26‰. The $\delta^{13}C_{org}$ values for the scales shows the biggest range seen so far in the experiments of 1.3‰. On the final day of the experiments, day 192 (t_{10}), physical decay had desecrated the fish available for sampling and data points represent an average of just two analysed samples (n=2). The spread of $\delta^{13}C_{org}$ values for the vertebrae plot between -29.4‰ and -24.5‰, a range of almost 5‰, with some of the most positive $\delta^{13}C_{org}$ values obtained during these experiments. However, the majority of $\delta^{15}N$ values are still between approximately 3 and 4‰. $\delta^{15}N$ values for the fish scales plot similarly, with only one datum point outside this range, although the $\delta^{13}C_{org}$ values show the biggest range for the scales in these experiments of 2.7‰. Overall the C_{org} isotopic signatures of the vertebrae and scales have spread along the y-axis of the graphs in Figure 6.5 during the ten sampling days; the initially discrete ellipsoids of data have stretched towards each other and finally overlap on day 192, although little has changed in terms of their N isotopic signatures.

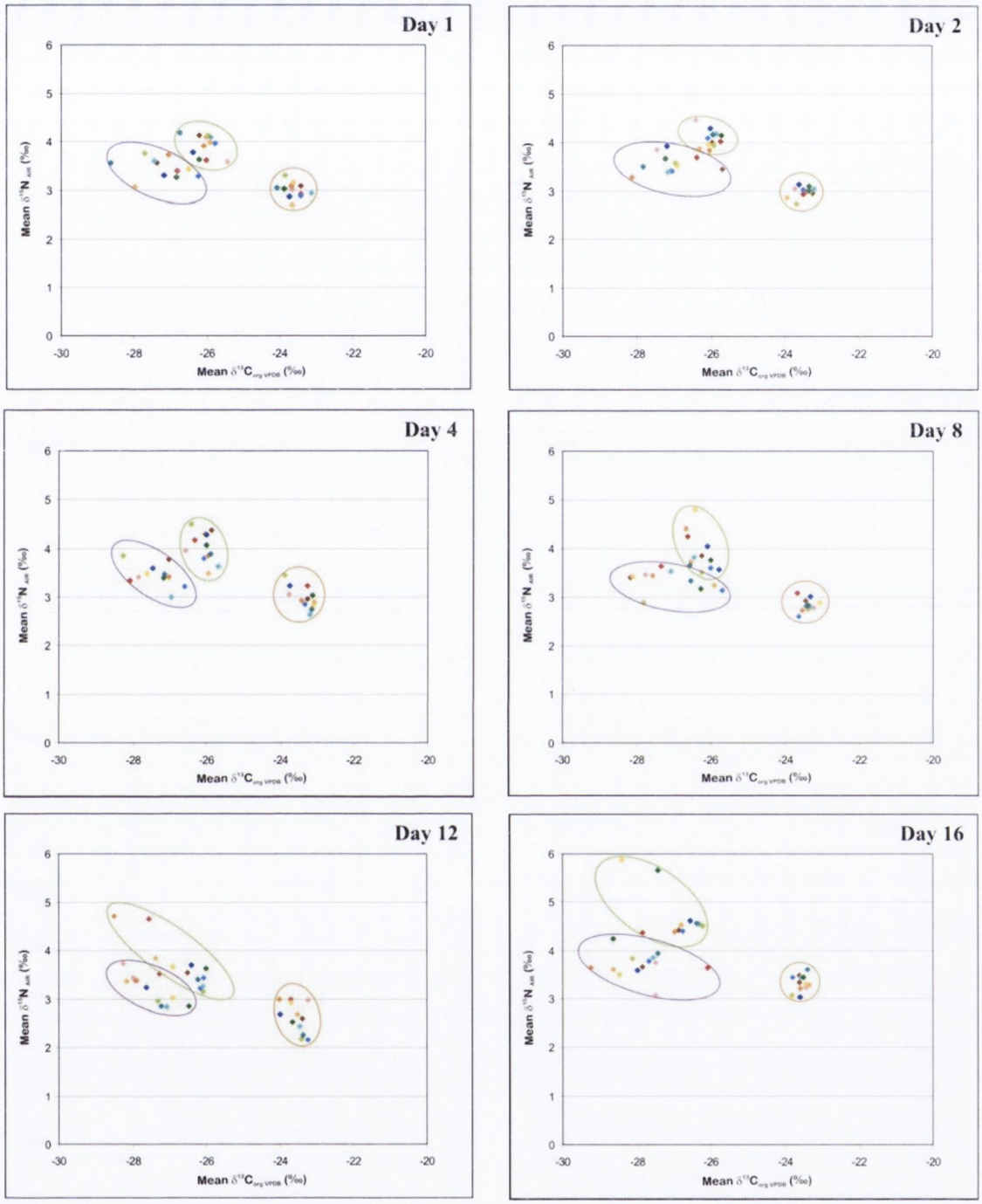

Figure 6.5: Graphs showing the $\delta^{15}N$ and $\delta^{13}C_{org}$ mean isotopic ratios for the vertebrae, muscle and scales analysed on each of 10 sampling days, 1 to 192. NB: note the difference in scale between axes. Vertebrae, muscle and scale samples are highlighted using purple, green and orange ellipses, respectively

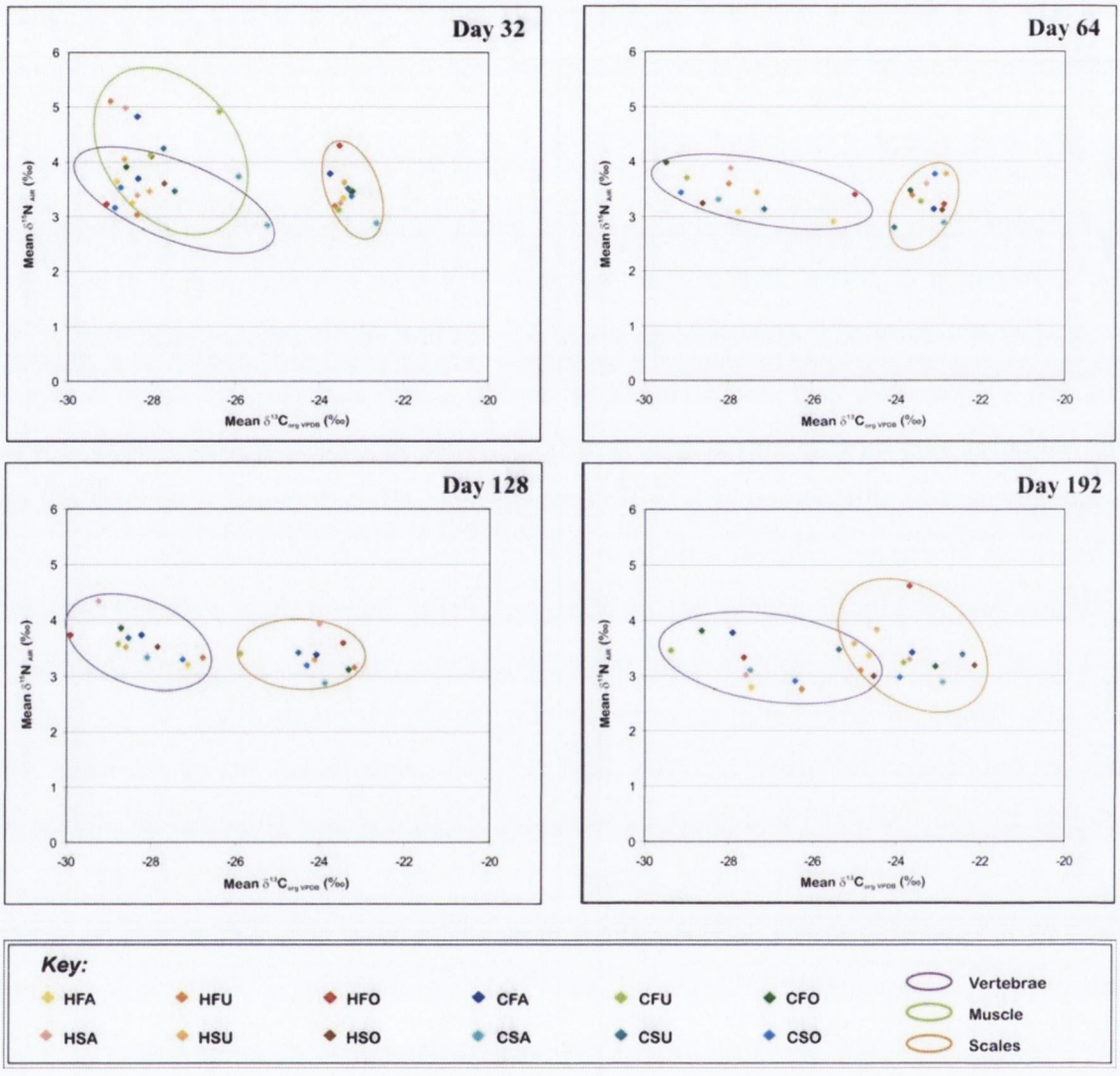

Figure 6.5 continued: Graphs showing the $\delta^{15}N$ and $\delta^{13}C_{org}$ mean isotope ratios for the vertebrae, muscle and scales analysed on each of 10 sampling days, 1 to 192. NB: note the difference in scale between axes.

In Figure 6.5, no particular combination of the three independent variables appears to cause more alteration to the isotopic signatures of the fish than any other. In Figure 6.6 A to C, the $\delta^{15}N$ and $\delta^{13}C_{org}$ isotope ratios for the vertebrae and scales analysed from the twelve different fish on day 192 are plotted individually and highlighted to represent the three independent variables chosen for study in these experiments, namely temperature, salinity and oxygen level. Superimposed on these graphs are ellipses representing the ranges of N and C_{org} isotopic data seen in the vertebrae and scales on day 1 of the experiments. By plotting the data in this way it was hoped that any trends caused by the

different variables would easily be recognised. In Figure 6.6 A the data points are coloured to reflect whether the data were from a fish kept at a temperature of 10°C or 20°C. Although the data from the vertebrae on day 192 have spread further than the bounds of the grey ellipse that represents day 1, there is no discernable trend. However, when making a comparison of the data range from the fish scales on day 192 and day 1 on the same graph, it appears that the least change has occurred in the isotopic signatures of the fish scales kept in cold water (10°C). The majority of the data points plotting out with the ellipse representing the data range on day 1 are from the hot, or 20°C, samples. In terms of $\delta^{13}C_{org}$, some are more positive and some are more negative, and just a few of the data points show enrichment in $\delta^{15}N$. In Figure 6.6 B the data points are coloured to reflect whether they were from a fish kept in fresh DIW or ASW. Again, it is not possible to decipher any trends in the isotopic ratios of the vertebrae caused by the two different conditions shown on this graph. The data from the fish scales is again mixed, however there are a cluster of ASW data points that have been enriched by up to 1‰ $\delta^{13}C_{org}$ on day 192 when compared to the data cloud from day 1. Figure 6.6 C shows the data points from fish kept in oxygenated, 'uncontrolled' or anoxic conditions. Here there are no discernable trends in the data spread of either the vertebrae or scales. As there was no quantifiable response due to the three independent variables, statistical analyses of these results were not performed.

Eleven jars were replicated in duplicate or triplicate in these experiments. The jars to be replicated were chosen at random and were from all time periods except t_5. All fish were dissected at the end of the appropriate time period and analysed in conjunction with the regular samples for N and C_{org} isotopes and their C:N ratios were calculated. Results are shown in Appendix 2. Fish from these replicate sample jars kept under the same conditions as the main jars showed variable responses but were not significantly different from the fish in the main jars. The amount of variation between replicates did not increase with increasing time or due to different combinations of the three main variables. This indicates that all results are reliable and reproducible.

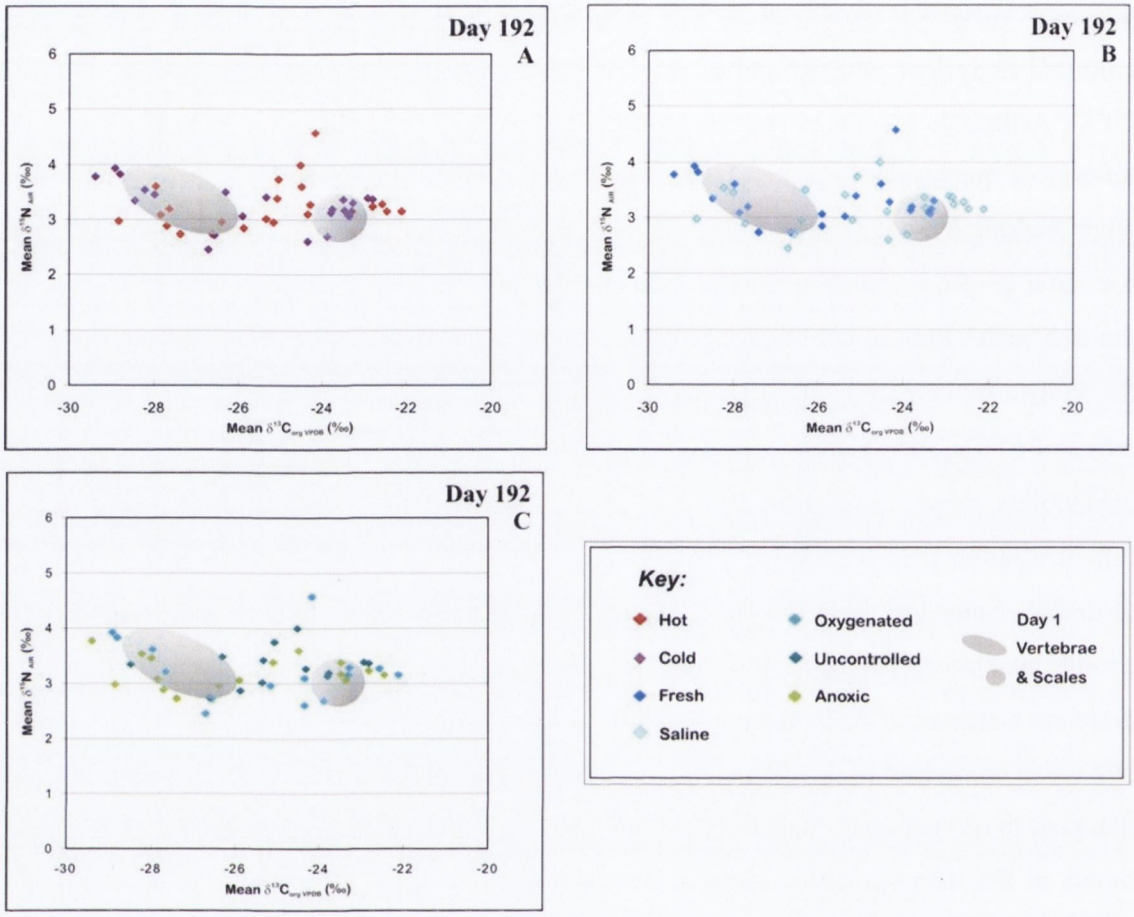

Figure 6.6: Three graphs showing the spread of vertebrae and scales isotopic data for day 192, with the data range at day 1 indicated using grey ellipses. As the fish decayed over time the three variables of temperature, salinity and oxygen level caused no obvious trends in the isotopic signatures: **A)** The effects of hot (20°C) or cold (10°C) conditions; **B)** The effects of fresh or saline (S=35) water; **C)** The effects of oxygenated, 'uncontrolled' and anoxic conditions.

6.5.2 C:N ratio data from fish samples

C:N ratios determined from the percent element data produced simultaneously with the isotopic measurements are shown in Figure 6.7 A to C. Each datum point shown in Figure 6.7 represents an average of the three sub-samples (n=3) measured for each tissue type, from one fish at one time interval (t_1-t_9), except the samples taken on day 192 (t_{10}) which are an average of two sub-samples (n=2). In Figure 6.7 A, the C:N ratios for the vertebrae samples are shown on the y-axis plotted against days on a logarithmic scale on the x-axis. A large range is seen in the C:N ratios at day 1 (t_1), between the lowest ratio of 3.7 and the highest ratio of 7.0. The results fluctuate within this range from day 2 (t_2) to day 12 (t_5),

however on day 16 (t_6) the data ranges between 5.0 and 10. 3. The data points are spread quite evenly between these two end-points and none of the three variables seem to be responsible for causing higher or lower values. The data continue fluctuating, apparently randomly, with the largest range in data occurring on day 128 (t_9): here a low of 3.7 was recorded and a high value of 16.7. On the final day (t_{10}) a range between 4.4 and 12.6 was observed. The C:N ratios from the muscle values are shown in Figure 6.7 B and are better

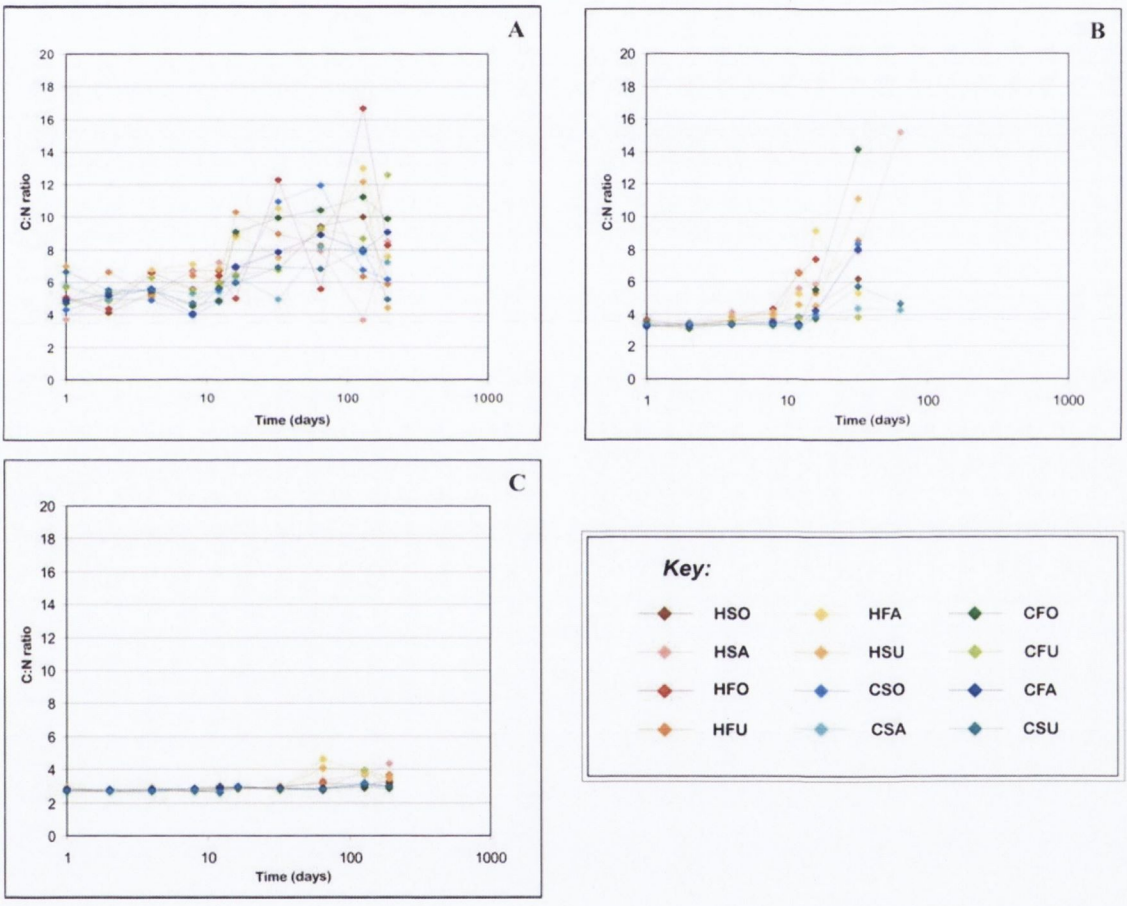

Figure 6.7: C:N ratios were determined from the percent element data produced simultaneously with the isotopic measurements: **A)** C:N data for all vertebrae samples plotted against time; **B)** C:N data for all muscle samples plotted against time; **C)** C:N data for all scale samples plotted against time.

constrained at the outset. From day 1 (t_1) until day 8 (t_4) the majority of values are between just 3.5 and 4, beginning to spread on day 12 (t_5) with a range between 3.2 and 6.7. After day 12 the majority of ratio values rise, remaining above 3.8, with some rising steeply to a ratio of over 14. The C:N ratios from the scale samples taken from each fish

throughout these experiments are shown in Figure 6.7 C and are all fairly constant at ~2.7 until day 32 (t_7). On day 64 (t_8), although the majority of ratios remained at ~2.8, two samples gave values of >3 and two samples gave values >4. These were all samples kept at 20°C and either uncontrolled or anoxic in terms of oxygen level, but varied in terms of salinity. On day 128 (t_9) and 192 (t_{10}) the majority of samples had C:N ratios of ~3, with just two samples on each day having C:N ratios of nearer to 4. Again, these samples were all from the anoxic or uncontrolled oxygen level batch, one of the four samples was in fresh water kept at 10°C and the remaining three in saline water kept at 20°C.

6.5.3 C and O isotope data from sediment samples

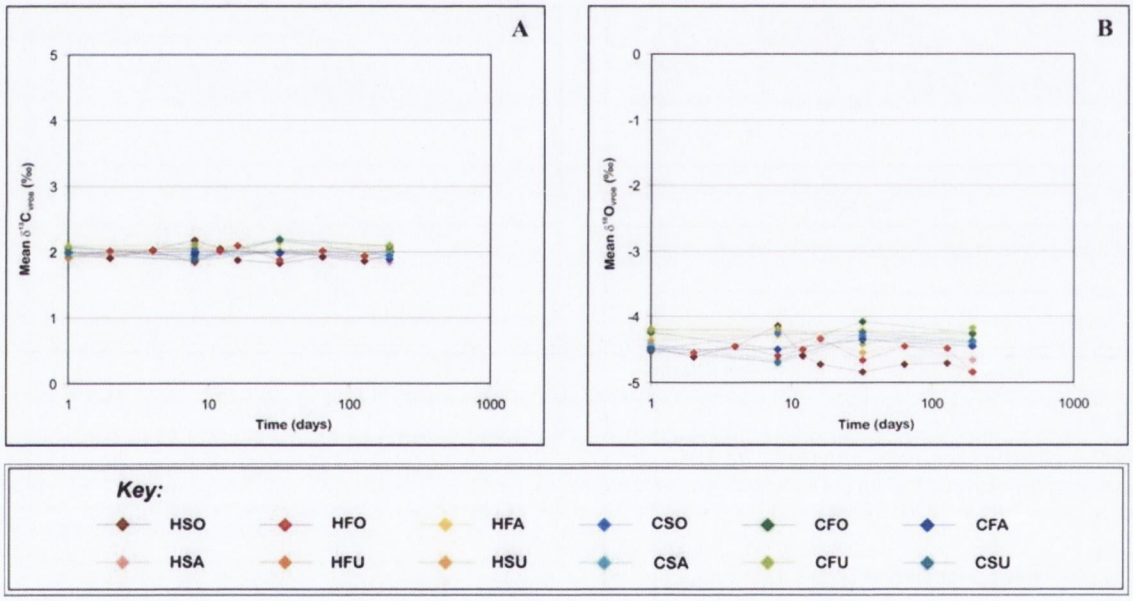

Figure 6.8: Sediment **A)** $\delta^{13}C$ and **B)** $\delta^{18}O$ data from samples collected from underneath the decaying fish throughout the experiments.

The $\delta^{13}C$ and $\delta^{18}O$ values of carbonate samples were measured from just four sampling periods, t_1, t_4, t_7 and t_{10}, due to the time and expenditure involved in analyses. Two exceptions were made: samples labelled HSO and HFO were analysed from all ten sampling periods. The results of these analyses are shown in Figure 6.8 A to C and data points represent the result from one sample analysis (n=1). Error was calculated as the average difference from the mean of replicate analyses of the same sample. This was just

0.03 for $\delta^{13}C$ and 0.05 for $\delta^{18}O$, and as such error bars could not be added to the data points. Figure 6.8 A shows the $\delta^{13}C$ values for the dried sediments plotted against time in days, from day 1 (t_1) to day 192 (t_{10}), on a logarithmic scale. All values at t_1 are clustered tightly between 1.9‰ and 2.1‰, and this continues throughout the entire experiment with the biggest data range of only 1.8‰ to 2.2‰ found on day 32 (t_7). Similarly, the oxygen isotope data for the sediments in Figure 6.8 B shows tightly constrained values between –4.2‰ and -4.5‰ at t_1. Again, the biggest range of data is seen on day 32 (t_7) but is still a small range of values between just –4.1‰ and -4.8‰.

6.5.4 Temperature, pH, nitrate and ammonia data from water samples

Water temperatures were measured as each jar was opened at the end of the relevant time period, prior to the water being extracted and filtered. In the incubated samples, including the cooler readings due to incubator failure at t_6, temperatures ranged from to 10.5 to 21.6°C (mean = 18.6°C, SD = 3.0), whereas refrigerated samples ranged from to 9.7 to 16.5°C (mean = 12.1°C, SD = 1.4). pH values ranged from 5.9 to 9.0, typically demonstrating a drop in pH in the first two weeks of the experiment then remaining quite constant in jars kept in the same conditions. For example, water in jars marked CFA gave a pH reading of 8.0 at the end of t_1, values then fell steadily until t_6 when a reading of 6.6 was given, with values from the four remaining sampling days, t_7 to t_{10}, fluctuating slightly between just 6.7 and 6.9. All data are listed in tables in Appendix 2.

Readings from the nitrate photometer were given as mg/L of nitrate-nitrogen in each filtered water sample. This was multiplied by a factor of 4.43 to convert each result to mg/L of nitrate. Ammonia results were given as mg/L of ammonium ions, and were multiplied by a factor of 0.944 to convert the readings to mg/L of ammonia. Nitrate (NO_3^-) and ammonia (NH_3) data from all water samples are shown in Figure 6.9 A and B, and data points represent the results from individual aliquots (n=1). In Figure 6.9 A the nitrate data all plot close to zero at t_1, with a maximum value of 6.7mg/L. On day 2 (t_2) the nitrate values from four of the samples kept at the higher temperature of 20°C show an increase, ranging between 7.5mg/L and 21.3mg/L. This continues for the next three sampling intervals (t_3 to t_5), with five of the 20°C samples reaching nitrate values of up to 60mg/L.

Samples kept at the colder temperature of 10°C remain <5mg/L until day 8 (t_4) when increases of up to 12.9mg/L can be seen, and show further increases of up to 26.1mg/L on

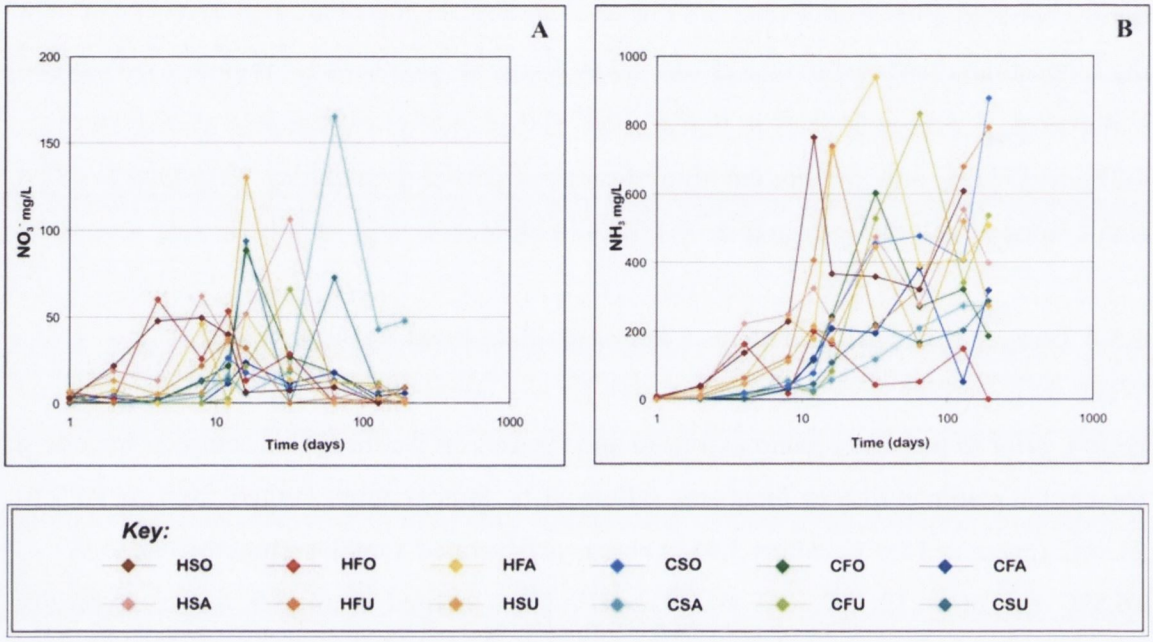

Figure 6.9: Samples of water from within each jar were measured at the end of each time period: **A)** Nitrate (NO_3^-) data plotted against time; **B)** Ammonia (NH_3) data plotted against time.

day 12 (t_5). On day 16 (t_6) eight of the data points are spread evenly between a minimum of 4.9mg/L and a maximum of 31.5mg/L of nitrate. Two 20°C samples, HSA and HSU, show higher concentrations of 51.4mg/L and 130.2 mg/L respectively, and two 10°C samples, CFO and CSU, show high nitrate values of 88.6 mg/L and 93.5 mg/L respectively. From day 16 onwards, the majority of samples show an overall gradual decrease in nitrate level, with 11 of the 12 samples on day 192 (t_{10}) giving values of <10mg/L. However, there are some notable exceptions to this trend. Nitrate values from water samples of HSA on day 32 (t_7) show a peak of 105.9mg/L, before returning to just 2.2mg/L on day 64 (t_8). Water samples from CFU also show a maximum peak on day 32, at 65.6mg/L, and return to almost zero on day 64. On day 64 two peaks are outlying the cluster of data from all other samples, namely data points CSU with a value of 72.7mg/L, and CSA with a value of 165.7mg/L. On day 128 (t_9) all samples gave values of <12mg/L nitrate with the exception of the CSA samples which remained ~45mg/L until the end of

the experiments. In Figure 6.9 B ammonia data from all water samples are shown plotted against the logarithmic timescale. All samples tested on day 1 (t_1) gave concentrations of <10mg/L of ammonia. The data points then rise fairly consistently until day 8 (t_4), with the bigger increases in ammonia values seen in the samples kept at 20°C. The samples kept at 10°C show a range of values between 28.8 and 55.1mg/L on day 8, whereas the samples kept at 20°C mainly range between 111.2mg/L and 246.5mg/L ammonia. For the remainder of the experiments the ammonia data show large fluctuations, from a minimum of 0.0mg/L up to a maximum of 939.8mg/L. After day 12 (t_5) there are no discernable trends or patterns in this data set that can be attributed to the independent variables of temperature, salinity and oxygen level investigated in these experiments. The data appear to fluctuate randomly.

6.5.5 Visual assessment of decay experiments

The aim of these experiments was not to quantify morphological degradation over time but simply to document the chemical changes occurring, and in particular any changes in the N and C_{org} isotopic signatures of the fish. However, on the final day of the experiments, day 192, all jars were photographed prior to removal and dissection of the fish. Photographs were also taken of the fish after removal to a Petri dish and any interesting points noted. Examples of these are shown in Figure 6.10 A to F. On opening some of the jars, it was noted that a black 'scum' had formed on the surface of the water as shown in Figure 6.10 A, in particular samples CFA, CSA and CSO. This had been noted during at previous sampling intervals for jars kept in these conditions, and also CFU at t_9. This skin on the surface of the water was thicker and darker in some instances than in others. Occasionally fish had broken free from the glass coverslip and floated to the surface. In these instances the black scum had also grown on the area of the fish touching or protruding above the meniscus. These blackened scales were not measured for their isotopic composition, and all instances of refloating were noted and considered when analysing the data set. In a large number of the jars throughout the experiments it was noted that although the fish remained on the sediment surface, the gas bladder had escaped

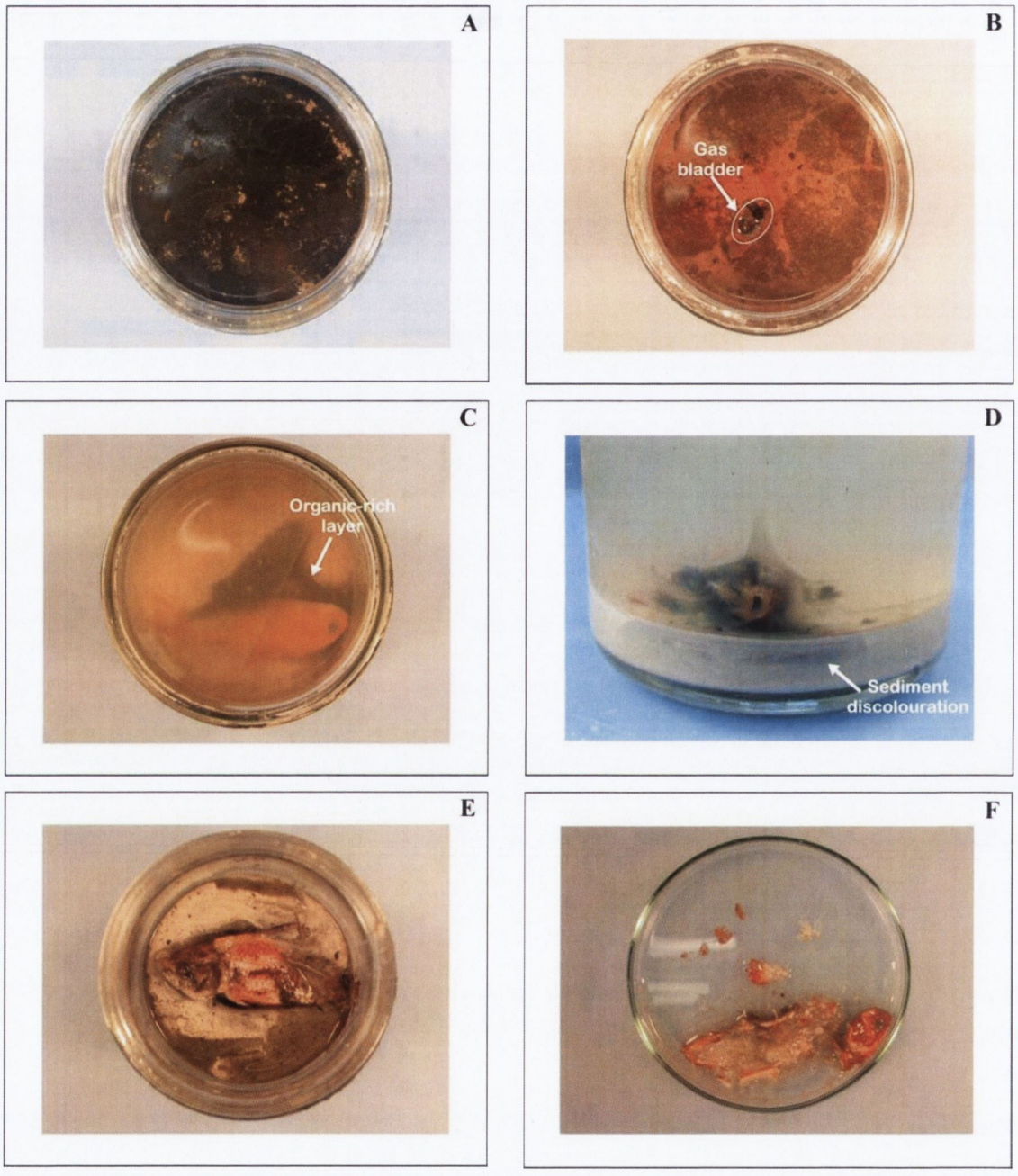

Figure 6.10: Visual assessment of fish specimens during experiments: **A)** A black 'scum' formed on top of the water in some of the jars; **B)** Escaped gas bladder floating on the surface of the water; **C)** A black organic-rich layer exuded onto the sediment next to the fish; **D)** Black organic-rich layer penetrating into the sediments and surrounding the fish carcass; **E)** Some fish remained in their entirety as the water was removed and the fish was rinsed and sampled *in situ*; **F)** Many fish were in a fragile state and difficult to sample on day 192.

from the fish and floated, as shown in Figure 6.10 B, without causing any obvious disruption to the fish carcass. In some jars a black organic-rich layer had formed on the sediment next to the fish as shown in Figure 6.10 C, and was assumed to be the product of bacterial degradation and autolysis resulting in liquefied internal organs which then seeped from the carcass. Figure 6.10 D shows how this bacterial film penetrated down into the sediment and affected the area directly around the carcass. It was this darkened sediment directly beneath the fish that was sampled for C and O isotopic analysis. In general, fish at t_{10} appeared to be fairly intact until the water was disturbed in the jar. It would then become apparent that the fish were extremely fragile and removing the fish from the jar for washing in DIW or ASW proved problematic. In some cases, like that shown in Figure 6.10 E, the fish remained in its entirety as the water was removed and the fish was rinsed and sampled *in situ*. In other instances it was necessary to retrieve as much of the fish as feasible using a cleaned, domestic desert spoon while minimising water disturbance, due to the advanced degradation state of the carcass. These fish were extremely difficult to sample and were rinsed carefully and transferred to a Petri dish for sampling, as shown in Figure 6.10 F. This is the same fish as shown in Figure 6.10 C, demonstrating the delicate nature of a fish carcass that appeared to be robust before any disturbance took place. Over the course of the experiments the only real trend observed in the physical decay process was that the samples kept in the incubator at 20°C appeared to decay faster than those kept in the refrigerator at 10°C. This was expected as microbial activity increases exponentially with temperature (Child 1995); previous authors have long since noted the link between increasing morphological degradation and increasing temperature (e.g. Swift *et al.* 1979).

6.6 Discussion

6.6.1 Assessment of data from fish

Overall the nitrogen and organic carbon isotopic data from the fish showed increasing variation as the experiment progressed. The initially discreet clusters of data for the three different tissue types gradually showed increasing disparity, particularly in terms of the C_{org} data. The range of $\delta^{13}C_{org}$ isotope data for the goldfish vertebrae increased from 3.2 to 4.5‰ over the six-month period, indicating increasing isotopic exchange between the bone and the surrounding environment. In trophodynamic studies, a stepwise enrichment

of just 1‰ $\delta^{13}C_{org}$ is reported between species from the same ecosystem at successive trophic levels (DeNiro & Epstein 1978), therefore the $\delta^{13}C_{org}$ data from the goldfish would no longer be reliable for such a study. This finding has implications for future studies using bulk C_{org} isotopic data from bone. The spread in $\delta^{13}C_{org}$ isotope data did not appear to be as a direct result of any of the three variables of temperature, salinity or oxygen level. The range observed in C_{org} data may be due to the differential decay of proteins and molecules within the tissues, leading to preferential loss of isotopically distinct fractions. In bone, collagen often breaks down more quickly than the non-collagenous proteins (NCPs) and this may be reflected in the C_{org} data as NCPs have very different signatures to collagen, although their $\delta^{15}N$ values are similar (Masters 1987; DeNiro & Weiner 1988). These experiments were necessarily crude, and the complex interplay of processes acting together and possibly outweighing each other, such as $\delta^{13}C_{org}$ fractionation during break-down of complex compounds versus preservation of isotopically distinct compounds (Lehmann *et al.* 2002), cannot be identified. These changes in $\delta^{13}C_{org}$ may also be attributed to successive loss of lipids from within the tissues, or may be due to the impact of varying amounts of inorganic carbonate contamination from within the hard structural components of the fish (see Pinnegar & Polunin 1999). Few changes occurred in the N isotopic data in these experiments over time regardless of the combination of conditions, with the vertebrae and scales both maintaining an approximately 1‰ range in the data throughout, indicating little isotopic exchange with the water and sediment. In modern settings, species feeding at successive trophic levels show an average enrichment of 2.9‰ $\delta^{15}N$ in consumer tissues over food source (Sweeting *et al.* 2007), indicating that the 1‰ range in this data would not affect trophic reconstructions.

The fluctuating general increase of C:N ratios with time in the vertebrae and muscle indicate increasing losses of N to the surrounding environment, with the scales appearing to be much more stable in terms of their C:N ratios. Bone porosity, and hence freedom of access of water to the internal skeleton, is thought to be responsible for the fluctuating C:N values in the vertebrae. The initial porosity of bone is known to be an important factor in determining the rate of chemical alteration and therefore degradation (Robinson *et al.* 2003). Previous authors have reported chemical microenvironments developing in

bone to create an essentially closed system (Trueman *et al.*2003), but this was not the case here. The apparent fluctuations in C:N ratios in the vertebrae data may represent differential rates of decay between the different fish specimens caused by permeation of water and microorganisms into the bone matrix at slightly different times. This could be due to slight differences in bone porosity between fish specimens at the outset, or a more aggressive initial bacterial attack in some of the microcosms. The onset of hydrolysis of the collagen fraction and the tunnelling of bacteria into the bone would then have occurred at different rates. The increasing C:N ratios in the fish are not thought to be as a result of the bacterial biomass colonising the tissues; bacterial biomass is known to have a C:N ratio of between 4 and 5 (Lehmann *et al.* 2002). Masters (1987) reports that preferential preservation of NCPs in diagenetically altered bone will increase C:N ratios. A low N content in bone suggests the breakdown of collagen; the N percentage of bulk bone is often measured in archaeological studies to assess the amount of remaining protein and therefore the extent of preservation or degradation (e.g. Petchey & Higham 2000; Tütken 2008). The labile muscle tissue experienced the fastest rate of change both physically and chemically, probably due to autolysis assisting increased microbial decay (Child 1995), releasing N to the surrounding water column. Internal organs often experience a greater degree of putrefaction due to the presence of gut flora (Child 1995). The spread of this microflora into the caudal region may have further accelerated decay of the muscle to be sampled, effectively decaying the fish from the inside out as also observed by Whitmore *et al.* (2002). Many of these questions could be answered with further study and analysis of organic molecules, SEM and TEM imaging and identification of the bacterial assemblage present in each jar. However, the aim of these experiments was not to define the catabolic and microbial processes occurring in the fish, but merely to identify patterns in post-mortem bulk N and C_{org} isotopic variation as an analogy for the Green River fossil fish.

These experiments demonstrate that the N isotopic signatures are reliable for at least the first 6 months of decay in all tissues and in all the simulated environments. However, many of the goldfish studied here surpassed the amount of physical decay observed in the Green River fossil fish within the first few days. Martill & Harper (1990) closely studied

the decay of an extant fish over one week as an analogy for fish from the Santana Formation, Brazil, and concluded from observations of the tissue structure that decay in the fossil organisms must have been halted after just 4 hours. It is not possible to estimate from the experiments herein how long the physical decay of the fish in Fossil Lake may have taken as numerous agents are known to retard decay rates prior to fossilization (see Briggs 1995). The by-products of microbial metabolism can create a microenvironment within the decaying organism, exceeding microbial tolerance levels and encouraging rapid mineral growth, for example by changing pH and Eh conditions (Trueman *et al.* 2003). Also, the presence of a microbial mat as described in Chapter 2 Section 2.4.3 may have accelerated the onset of mineralization. Briggs & Kear (1993) state that the optimal closed conditions to promote mineralization observed in the laboratory would also prevail where organisms are rapidly overgrown by microbial mats, halting the normal loss of soft tissue morphology within a matter of weeks. Overgrowth by a microbial mat would also inhibit disarticulation and the hostile conditions thought to have existed at the bottom of Fossil Lake would have impeded scavenging and some bacterial attack. Rapid burial is also thought to halt bioerosion and lead to the stabilisation of carcasses (Davis & Briggs 1998; Trueman & Martill 2002) but burial was not accounted for in the experiment design here as sedimentation rates in Fossil Lake are estimated at just 50 to 100mm ka^{-1}, as discussed in Chapter 2 Section 2.4.2. If decay and bioerosion were impeded and mineralization accelerated it is quite possible that the Green River fossil fish did not undergo the same extent of degradation seen in these experiments, and therefore it can be assumed that the degree of post-mortem isotopic change would be less.

6.6.2 Assessment of sediment and water data

It was not possible to measure the nitrogen and organic carbon isotopic variation in the bulk carbonate sediments used in these experiments. Instead, the inorganic $\delta^{13}C$ and $\delta^{18}O$ values were measured to monitor for any chemical exchange. These values remained constant throughout however, bearing no reflection of the increasing amounts of organic matter and bacterial growth in the sediment with time. If similar experiments were repeated, extracting particulate organic carbon and nitrogen from the sediments as described by Lehmann *et al.* (2002) and analysing the $\delta^{15}N$ and $\delta^{13}C_{org}$ should provide

more insight. The evolution of individual biochemical fractions was not considered, however, biochemical concentrations from other incubation experiments indicate the relative enrichment of lipids in residual particulate matter with ongoing decay (Lehmann *et al.* 2002), and this may also be true here. Similarly the $\delta^{15}N$ and $\delta^{13}C_{org}$ variation was not measured in the water samples collected from these experiments due to the complexity of this procedure. Instead, nitrate and ammonia data were collected with the aim of constraining the cycle of nitrogen movement within the microcosm jars, as a proxy for bacterial degradation rate of proteins. The increasing C:N ratios observed in the fish over time indicate the loss of amino acids (Derenne *et al.*1998) and thus the removal of nitrogen to the water or sediment, with neither preferential liberation of ^{14}N nor ^{15}N observed in any microcosm (*contra* Lehman *et al.* 2002). In the presence of aerobic bacteria, the breakdown and oxidation of organic matter leads to the production of ammonia and in turn nitrate, which is broken down by anaerobic bacteria to nitrite, leading to the production of nitrogen, thus continually feeding the cycle through Equations 6.1 to 6.5.

Aerobic ammonification	$N2 \rightarrow 2NH_3 + H_2$	**Equation 6.1**
Aerobic nitrification	$NH_3 + O_2 + 2H \rightarrow HNO_2 + 4H$	**Equation 6.2**
Aerobic nitrification	$NO_2 + H_2O \rightarrow NO_3^- + 2H$	**Equation 6.3**
Anaerobic nitrate reduction	$NO_3^- + 2H \rightarrow NO_2^- + H_2O$	**Equation 6.4**
Anaerobic denitrification	$NO_2 \rightarrow NO \rightarrow N_2O \rightarrow N_2$	**Equation 6.5**

Ammonification is the process whereby organic forms of nitrogen are converted to ammonia. Amino acids are broken down by a series of enzymes in both aerobic and anaerobic environments into carbon dioxide, ammonia and hydrogen sulphide or sulphate (Child 1995). Total ammonification should be slowed with a lack of oxygen (Williams 2006), but this does not appear to be the case as shown in Figure 6.9 B: water from anoxic

and 'uncontrolled' jars show high concentrations of ammonia. However, this may indicate that anaerobic nitrite ammonification was taking place. Aerobic nitrification is accompanied by a drop in pH and this was observed in these experiments. The drop in pH witnessed in the first two weeks is similar to that seen by Briggs & Kear (1993), who linked the pH change to the mineralization of shrimps in their laboratory experiments. However, no mineralization is thought to have occurred here, rather the fall in pH is attributed solely to aerobic nitrification. The initial increases in nitrate shown in Figure 6.9 are coincident with decreases in pH readings for the majority of the microcosm jars. This ammonium oxidation suggests that levels of oxygen were perhaps still within the threshold for aerobic nitrification to take place at the start of the experiments as both the anaerobic and 'uncontrolled' jars produced high nitrate readings. By the end of the experiments nitrate levels in the majority of water samples had returned to concentrations similar to those recorded at the outset, indicating that nitrate production had diminished and all nitrate had been consumed by denitrification. The denitrification process shown in Equation 6.5 is accompanied by a reduction of oxidizable organic matter and only occurs in strictly anaerobic conditions (Williams 2006). Without the presence of oxygen the nitrogen cycle is halted at this point and Equation 6.1 can no longer proceed. It is possible however, for microenvironments to develop that are anaerobic within oxic regions and thus denitrification can occur locally (Williams 2006). The fact that ammonia was still being produced in these experiments after nitrate production had ceased suggests anaerobic ammonification may have been taking place and that the bottom waters had become anoxic regardless of the intended conditions. This is in agreement with Pfretzschner (2004), who reported that in bone diagenesis experiments the redox potential sank within two days and remained low for several months, with oxidants (oxygen, nitrate, nitrite and others) being depleted in the surrounding solution. This occurred even when oxygen from the air had free access to the water in which the bone samples were stored (Pfretzschner 2004).

6.6.3 Limitations of the data set

Although all parameters were tightly controlled in these experiments, there were some inconsistencies that may have affected the outcomes. The design of these experiments

used small fish as an analogy for *Knightia eocaena* and due to this size limitation could only be sampled once when a time period had lapsed. This necessitated the use of one fish per sampling period for each set of conditions. The goldfish used in these experiments were sourced carefully to be as similar as possible at the outset; however there were some minor variations in size between them. Any variation in starting isotopic composition was accounted for and subtracted from all results shown in Figure 6.5, but some variation in degree of degradation is likely to have occurred due to their size differences. Standard length was measured as defined in Chapter 2 Section 2.6, with the fish having a minimum length of 39mm and a maximum of 68mm. Although the majority of the fish were closer to the mean length, there was also a discrepancy in that some fish appeared to be more robust or 'fatter' than others. These are thought to have been more resistant to decay, based on notes taken throughout the experiments. Qualitative zooarchaeological observations over many years have suggested that, for equivalent burial conditions, the bones of different taxa degrade at different rates, and that, even within a single skeleton, systematic variation often occurs (Robinson *et al.* 2003). This variation is linked to the size of bones, for example a long human bone will lose only 5% to 15% collagen within one year whereas a small rodent bone would lose all proteins during this time frame (Pfretzschner 2004). The preservation of soft tissue is also thought to ultimately be controlled by anatomical and physiological factors (McNamara *et al.* 2009). It is entirely possible that the bones and muscle of the smaller fish may have been more susceptible to microbial attack and degradation and hence may have skewed the overall results somewhat. Temperature variations must also be taken into account here, although the majority of samples were kept close to the average readings. The temperature fluctuations were similar to those reported by other authors in taphonomy experiments carried out in the field (e.g. Davis & Briggs 1998) and demonstrate the difficulty of maintaining artificial simulations in the laboratory.

Very few experiments combine different agents to fit more closely to the complexity of most fossil bone accumulations (Denys 2002). Here just three independent variables were observed, with the exclusion of all others, chosen to represent different possible scenarios for the bottom water of Eocene Fossil Lake. Many procedures used in other experiments

were considered and discounted during the experiment design. Previous authors have inoculated experiments with a natural bacterial consortium and yeast to promote rapid degradation (e.g. Briggs & Kear 1993 and 1994; Lehmann *et al.* 2002) and have found this essential to generate precipitation of minerals (Briggs & Kear 1994). Other authors have used advanced imaging and chemical protocol to investigate the microenvironments forming within bone during diagenesis (e.g. Martill 1991; Reiche *et al.* 2002; Pfretzschner 2004). Isotopic analysis of bulk organic material can only provide a first approximation in understanding the processes occurring during decay and early diagenesis. The ability to document geochemical changes in individual proteins as a function of time and depositional environment would provide significant insight into specific mechanisms that occur during early diagenesis (Ostrom *et al.* 1994). In a more complex study such procedures would be recommended, however this study was simplified to investigate merely the likelihood of isotopic fractionation during decay of fish. Only the first stages of decay and very early diagenesis could be replicated in the laboratory and a steady state had not been reached in any of the microcosms at t_{10}. Pfretzschner (2004) states that early diagenesis is not complete as long as organic compounds are present in bone, with the first stage of early diagenesis, including intensive microbial activity on the bone, taking around one year. Whether extending the time frame for such experiments offers a more valuable insight into diagenetic isotope exchange is doubtful. Many parameters operating in the late stage diagenesis of Fossil Lake with potential for isotopic exchange are unknown and cannot be replicated, such as the composition of circulating groundwater during dissolution or reprecipitation processes. Late stage possible isotopic evolution limits the extrapolation of the current data set due to the unknown magnitude of change that could occur under these different circumstances. The validity of extending proxies such as these experiments back to the past is dependent on the absence of any significant postdepositional interactions between fossil material and the burial environment (Zazzo *et al.* 2004) over millions of years. The most important issue to consider before making predictions from the data set presented herein however is not whether the findings can be extrapolated back in time but rather the validity of scaling microcosm experiments as a predictor of geochemical behaviour in a whole lake setting (Carpenter 1996). These experiments should be viewed as a first understanding of the complex interplay of factors

affecting post-mortem isotopic exchange in fish, in order to stimulate the development of further theory and research.

6.7 Conclusion

Changes in the nitrogen and organic carbon isotope ratios of decaying fish are thought to result from several complex processes including organic matter degradation and bacterial growth, as well as the systematic variation occurring between different tissue types. The $\delta^{13}C_{org}$ isotopic signature of all tissues, particularly the vertebrae and muscle, underwent significant alteration during post-mortem decay and early diagenesis. The $\delta^{15}N$ isotope values showed much less fractionation in all measured tissue types, although loss of N to the surrounding water and sediment was indicated by the increasing C:N ratios observed. Temperature, salinity and oxygenation conditions do not appear to have a direct impact on the magnitude or the direction of alteration in bulk isotopic signatures from the goldfish. These results indicate that $\delta^{15}N$ values from scales, and to a lesser extent vertebrae and muscle, are reliable for at least six months post-mortem. A steady state did not appear to be reached in any microcosm; bacterial and chemical degradation of the fish is thought to have continued until the final sampling day ended the experiment, and therefore obscuring of the N isotope signal may still occur out with this time frame. However, the extent of degradation seen in the goldfish far surpassed that seen in the fossil fish, therefore it can be assumed that decay was halted in Eocene Fossil Lake by some other factor or a combination of factors not present within these microcosm experiments. Significant processes and conditions occurring in Fossil Lake are unknown, for example the suite of bacteria involved in decay and fossilization, and these cannot be reproduced in the laboratory. These experiments offer a first approximation regarding the alteration of N and C_{org} isotopes in bulk measurements during post-mortem decay and early diagenesis.

Chapter 7: Biomarkers in Green River fossil fish and sediment samples

7.1 Overview

Given that nitrogen and organic carbon isotopes are present in Green River fossils, one of the fundamental questions posed by this research concerns the nature of the organic matter in which they are preserved, and whether these bulk isotopes are from original fish organic matter. Organic biogeochemical analyses were carried out in collaboration with the University of Bristol in order to assess the composition and preservation of the organic matter from which the N and C_{org} isotopes were measured. Total nitrogen and organic carbon content were found to be significantly higher in the fossil fish samples when compared with the surrounding sediment. Biomarkers were successfully extracted from the fish and these were quantitatively and qualitatively different to those from the surrounding sediment, confirming the presence of organic carbon in the 50 million year old fossil fish.

7.2 Introduction to biomarkers and their preservation potential

7.2.1 Preservation of biomarkers

During diagenesis organic compounds tend to be transformed to more stable products which have a higher preservation potential and are known as biomarkers (Briggs *et al.* 2000). The term 'biomarker' can refer to any kind of organic molecule indicating the existence, past or present, of living organisms (Peters *et al.* 2005). Biomarkers are usually complex molecular fossils derived from biochemicals, particularly lipids, and are often used in the petroleum industry to interpret the characteristics of crude oil and source rock including their maturation history. Biomarkers are potentially useful because all domains of extant life have signature membrane lipids which become hydrocarbons in the sediment during diagenesis, and these can be found wherever the record is sufficiently well preserved (Summons *et al.* 1999). Once recovered, this molecular debris can provide information on the type of organic matter present in the rocks, environmental conditions during deposition, diagenesis and catagenesis, and degree of biodegradation (Peters *et al.* 2005). Biomolecules may be listed in rank order of decay resistance (e.g., lipid > carbohydrate > protein > nucleic acid) and, by implication, preservation potential,

although this is a generalisation (Briggs *et al.* 2000). The preservation potential varies considerably with molecular structure, depositional environment and diagenetic history (Eglinton & Logan 1991), plus the preservation potential of biomolecules can be greatly increased if incorporated into structural tissues (Briggs *et al.* 2000). The preservation of low molecular weight (LMW) carbohydrates, proteins and DNA sequences appears to be limited to organic material of archaeological or Recent age, due to their susceptibility to hydrolysis within 10 Ma or less (Bada *et al.* 1999). Conversely, lipids have a much higher preservation potential and can be used to study organic material from several orders of magnitude further back in time. These enduring biomolecules are commonly hydrocarbons and, as such, are hydrophobic and have low chemical reactivities (Briggs *et al.* 2000). The amount of information that can be extracted from biomarkers is approximately inversely proportional to their preservation potential.

7.2.2 Lipid preservation

Lipids are the fat-like components of cell membranes, an essential element of all living organisms. Lipids can be defined as fatty acids and their derivatives (and substances related biosynthetically or functionally to these compounds) and can be classified as described by Fahy *et al.* (2005). Some types of lipid molecules are found only in specific groups of organisms and serve as biological markers for these groups, albeit in an altered state, in the geological record. Modification of lipid-based compounds follows relatively straightforward pathways, resulting in the loss of side chains or functional groups until simple, long chain hydrocarbons are produced (Schweitzer 2004). However, the carbon skeletons of some lipid molecules are so resistant to degradation that they can remain almost intact for billions of years. While some alteration will occur, significant functional groups or patterns can be retained, allowing the source of the hydrocarbon molecule to be identified. For example, 2-methylhopanes have been detected in organic sediments from the Pilbara Craton, Western Australia, which have been dated to 2.7 Ga (Brocks *et al.* 1999 & 2003). The detection of these abundant biomarkers in the ancient Australian sediments confirms the antiquity of the domain Bacteria to >2.7 Ga. Cyanobacteria, the only known bacterial clade capable of oxygenic photosynthesis, produce 2-methylbacteriohopanepolyols (2-MeBHPs) which are preserved in the sedimentary record

as 2-methylhopanoids (Summons *et al.* 1999). The presence of 2-methylhopane was accordingly thought to constrain the age of the oldest cyanobacteria and was assumed to coincide with the advent of oxygenic photosynthesis, although this is now disputed: Rashby *et al.* (2007) demonstrated that an anoxygenic photoautotroph was capable of generating 2-MeBHPs, concluding that the potential origins of sedimentary 2-methylhopanoids could be more diverse than previously thought. Their experimentation with extant bacteria shows how complex interpreting lipid biomarker information extracted from the geological record can be if our knowledge of the behaviour of modern species, and indeed fossil species, is lacking. If the data regarding modern species upon which the interpretation of the biomarker suite is based is incomplete, then interpretations are limited. However their experimentation also confirms that the lipid biomarkers extracted from such ancient sediments are a reliable source of information, irrespective of interpretation.

7.2.3 Protein preservation

Proteins preserved under favourable conditions have been studied in archaeological materials for many years, although over thousands of years they hydrolyse to smaller peptides and free amino acids. Amino acids are ubiquitous in all forms of life and valuable information can be preserved in the archaeological record. The greatest contribution of proteins to archaeology has been in the field of palaeodietary reconstruction using stable isotope techniques (Briggs *et al.* 2000). In bioarchaeology, the chemical analysis of human bone to assess dietary variability is now commonplace (e.g. Macko *et al.* 1999; Richards *et al.* 2000; Jim *et al.* 2004). Dietary information is recorded as elements and amino acids liberated during food digestion are incorporated into bone mineral, collagen and noncollagenous bone proteins throughout a vertebrates' lifetime, thus allowing the study of past diet composition (Pate 1994). Whether any useful information can be extracted from amino acids in the fossil record is somewhat uncertain. Bada *et al.* (1999) presented a brief review of different fossil samples and the amino acids found therein, reporting that original amino acids and their racemisation products are likely to be preserved for less than a few million years. Bada *et al.* (1999) reported that amino acids present in a biomineral matrix are generally contained until they undergo hydrolysis, after

which time they may be lost to the surrounding environment or undergo decomposition. As a result, the total amino acid content of a fossil decreases with time, although secondary amino acid contaminants may be introduced into the biomineral matrix from percolating groundwater, and also during alteration and recrystallisation of the inorganic components of the biomineral. The amino acids may then undergo Maillard-type reactions (see Maillard 1917) which could result in the incorporation of both original components and contaminants into a humic acid-like material and could thus be preserved over longer periods of geological time (Bada *et al.* 1999). These processes mean that fossil specimens may contain endogenous and exogenous components preserved in the form of high molecular weight (HMW) geopolymers.

7.3 Previous investigations of biomarkers preserved in macrofossils

Historically, lipids have usually been investigated as chemical fossils in sedimentary units to establish the origin and fate of organic matter and as an indicator of maturation history throughout geological time (Briggs *et al.* 2000). Increasingly palaeontologists are applying new technologies to try and gain more information from macrofossils, including at the molecular level. These multidisciplinary non-traditional techniques could shed new light on the evolutionary relationships and behaviour of extinct organisms. Well-preserved biomolecules have the potential to allow taxonomic relationships to be defined based on lipid profiles and other endogenous molecular information. Over the past two decades lipids have been used to extract information from artefacts of archaeological age, in particular bones, plant materials and resins (Evershed *et al.* 1999). The structural diversity of lipids is fundamental to their usefulness in archaeology because it allows lipid structures and distributions to be related systematically to specific source organisms (Briggs *et al.* 2000). Although lipid investigations of artefacts found at archaeological sites are now commonplace, few lipid investigations have been carried out on macrofossils of geological age due to the assumed exchange of biomarkers with surrounding sedimentary units over millions of years.

Organic geochemical analyses of macrofossil lipids to date have mainly centred on Tertiary lacustrine deposits, with particular focus on the Miocene Clarkia deposit of

northwestern Idaho, USA, and the Oligocene Enspel deposits in western Germany. The 17-20 Ma Clarkia fossil leaves are exceptionally preserved and have been the subject of many studies of ancient biomarkers (e.g. Niklas & Brown 1981; Logan *et al.* 1993; Huang *et al.* 1996; Lockheart *et al.* 2000; Otto *et al.* 2004). Good preservation of lignin macromolecules has been observed and the presence of hopanoid and terpanoid acids confirms the presence of original plant material within the Miocene fossils. The preserved lipids were even found to show distinct taxon-specific patterns for the leaves of different genera (Briggs *et al.* 2000). Yang *et al.* (2005) investigated fossil leaves from various species of the genus *Metasequoia* Miki, 1941, sourced from three different lacustrine deposits of Tertiary age including the Clarkia formation. While all three localities show excellent preservation, a continuum of diminishing preservation was observed at the microscopic level using SEM, and this was reflected at the biochemical level in the results of pyrolysis-gas chromatography-mass spectrometry (py-GC-MS). Late Paleocene-Early Eocene leaves from Ellesmere Island, Canada, were found to have superior preservation when compared with the Miocene Clarkia deposits, despite their considerable age (Yang *et al.* 2005). This suggests that depositional environment plays a critical role in biomarker biodegradation, rather than longevity alone. Stankiewicz *et al.* (1997) subjected Oligocene macrofossils from Enspel to SEM and py-GC-MS analyses but, rather than investigating palaeoflora, fossil beetles were examined. Although epicuticular leaf wax alkanes have a higher preservation potential than the constituent lipids of animals, preservation of chitin was confirmed in these 25.8 Ma fossils based on the associated lipid biomarker assemblage. More recently Gupta *et al.* (2007) carried out an investigation of angiosperm and gymnosperm leaves as well as fossil weevils from Enspel using tetramethylammonium hydroxide (TMAH) assisted pyrolysis. They document the presence of aliphatic components present in both the plant and insect remains not observed in the enclosing sediment, suggesting an endogenous origin for these compounds which may be the result of *in situ* polymerisation during diagenesis. Gupta *et al.* (2007) also found polysaccharide and protein moieties in the Enspel fossils indicating an extremely high level of molecular preservation. Claims of surviving DNA in Miocene Clarkia plant material (e.g. Golenberg 1991; Sidow *et al.* 1991) have now been discredited, and only fragments of proteins are thought to survive into the fossil record.

Despite evidence indicating that the breakdown of amino acids occurs rapidly on a geological timescale and that exchange with the local environment can often occur, research is still continuing in this field. Asara *et al.* (2007) sequenced ancient collagen peptides from well-preserved mastodon and dinosaur bones, made possible by advances in mass spectrometry technology. Subpicomolar quantities of fragmented proteins and peptide sequences can now be identified and this significant shift in the lower limits of detection has led to the contradiction of the existing theoretical preservation limits for protein fragments, based on predicted degradation rates (Asara *et al.* 2007). The protein sequences discovered have subsequently been used to infer evolutionary relationships using molecular phylogenetic analyses (Organ *et al.* 2008). However, the validity of this ancient protein research has been hotly contested and many organic geochemists and biologists are sceptical about the data interpretation (see Buckley *et al.* 2008a). Most studies of ancient proteins have not focussed on sequencing however, and chiefly concentrate on immunological response (Westbroek *et al.* 1979; Schweitzer *et al.* 2002; Avci *et al.* 2005). Schweitzer *et al.* (2007a) presented molecular and chemical analyses of Cretaceous dinosaur bone which was found to contain "fibrous, flexible and apparently original tissues" after partial demineralization. However, this fibrous bone matrix was found to be morphologically altered over time when compared with vessels and/or osteocytes (Schweitzer *et al.* 2007b) and has recently been interpreted as a post-burial biofilm creating endocasts within the bone (Kaye *et al.* 2008). Protein or protein-like components were found to comprise around 1% of the bone samples, and are suggested to have been preserved in micro-environments within the bone (Schweitzer *et al.* 2007b). In immunochemistry studies these were found to produce antibody responses similar to modern avian collagen (Schweitzer *et al.* 2007a). Salamon *et al.* (2005) propose that relatively well preserved DNA is occluded within clusters of intergrown bone crystals that are resistant to disaggregation by the strong oxidant NaOCl. They demonstrate that these clusters provide a privileged niche within fossil bone, preserving pockets of original proteins that are far better preserved than any proteins remaining in the bone as a whole.

7.4 Biomarker study of Fossil Lake sediments and fish bones

Over the past forty years shales from the wider Green River basins have been subjected to many organic geochemical analyses (e.g. Eglinton *et al.* 1966; Murphy *et al.* 1967; Balogh *et al.* 1971; Cooper & Evans 1983; Kawamura *et al.* 1986; Collister *et al.* 1992), particularly the more mature oil shales far to the east of the current field area. However, to date no biomarker investigations of the individual Green River fossils have been carried out. It is thought that molecular level investigations may aid a better understanding of the fossilisation process leading to their exceptional preservation. Fossil Lake is likely to be an ideal location for biomarker analyses owing to the highly favourable conditions for preservation of organic compounds in both the sediments and the fossil fauna. Decay and burial in terrestrial as opposed to marine, and anoxic rather than oxygenated conditions, appear to enhance preservation of biomacromolecules, as well as the presence of biominerals (Briggs 1999). In settings such as Fossil Lake, with slow deposition of fine-grained marl in suspected anoxic conditions, organic matter would have settled out of suspension becoming concentrated and preserved, possibly in concentric patterns in quiet deep water (Huc 1988). Well-preserved fossils of Tertiary age can retain diagenetically modified biomarkers and biopolymers for which a product-precursor relationship with the original biological materials can still be identified (Briggs *et al.* 2000). However, fidelity of the external morphology does not necessarily imply that the original chemistry is intact. By using organic geochemical techniques it was hoped that original intact biomarkers would be found within the Eocene fish of Fossil Lake and that these would be significantly different to biomarkers found within the sediment samples. The characterisation of the fossil fish biomarkers could be instrumental in discovering where the N and C_{org} isotopes measured previously (see Chapter 5) are held chemically and where they originate from. This information is fundamental to the interpretation of all bulk isotopic data from the fossil fish presented in this thesis.

In collaboration with the Organic Geochemistry Unit (OGU) at the University of Bristol, UK, biomarkers were chemically extracted from both the sediment and fossil fish to evaluate the extent of molecular preservation and to understand what microbial processes may have been occurring in the sediment at time of deposition. One sediment sample and

two fish samples from the same bedding plane were analysed, as well as a blank control sample to monitor the accuracy of the methods used and the legitimacy of the results produced. The head of a large *Phareodus* Leidy, 1873 from locality RH F-1 (specimen RH270701) was labelled Fish A, the vertebrae of another large *Phareodus* from below the surface of the same slab labelled Fish B, and a sediment sample from the ~1.5cm thick slab was also analysed. Photographs of samples prior to any treatment are shown in Figure 7.1. Both fish samples were removed from the surrounding sediment by hand and subject to acetic acid pre-treatment as recommended in Chapter 4. All three samples were ground to a fine powder prior to analysis using an agate mortar and pestle. CHN analysis was carried out on small aliquots of each powdered sample, as detailed in Chapter 3 Section 3.5. Biomarkers were extracted from all three samples and separated into apolar and polar neutral fractions, fatty acids (analysed as methyl esters) and amino acids. These individual fractions were then subjected to GC analyses, and some to GC-MS and GC-IRMS. The full protocols used and details of instrument conditions are described in Chapter 3 Section 3.6 to Section 3.8.

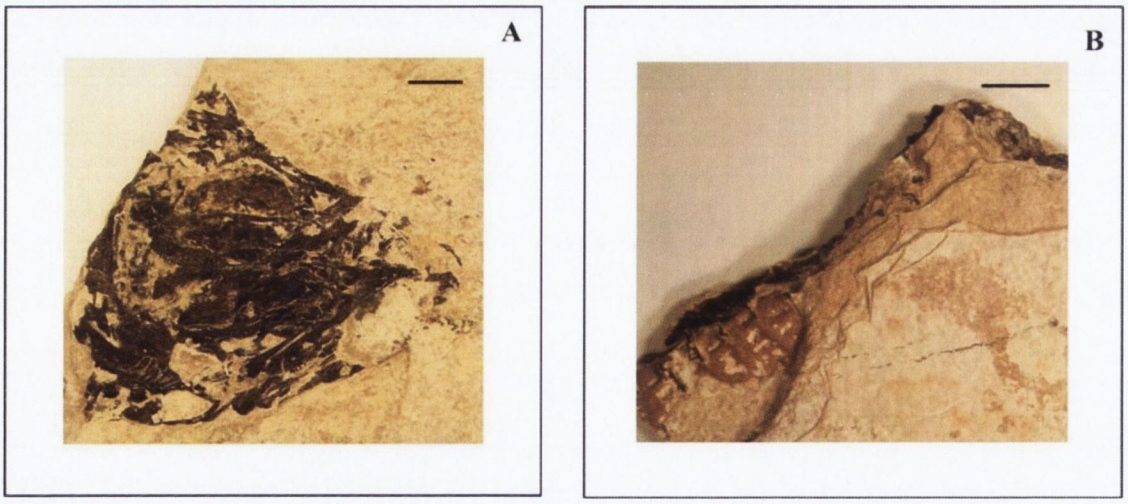

Figure 7.1: Samples from slab RH270701 prior to treatment. **A)** Fish A and **B)** Fish B. Scale bars are 1cm.

7.5 Results and interpretation

7.5.1 CHN analyses

The percentage of organic carbon found in the sediment sample was very high and indicates that, as suggested by the distinct odour, the darker layers of sediment are

composed of kerogen, similar to the oil shales reported from other units in the wider Green River area (see Figure 7.2). The percentage of organic carbon in Fish A was much lower, with Fish B being slightly higher than the sediment sample. There was no indication of any nitrogen present in the sediment samples, however nitrogen was found in both fish samples as shown in Figure 7.2. These findings confirm that the nitrogen isotopes measured in this study do not originate from the sediment and must therefore be endogenous to the fossil fish samples.

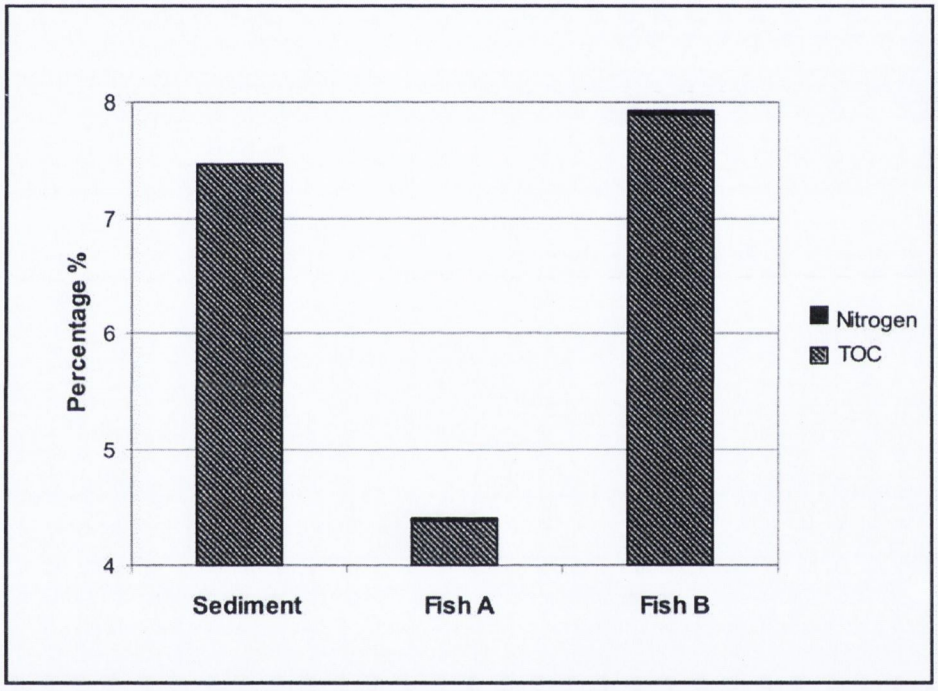

Figure 7.2: CHN results for all three samples showing organic carbon and nitrogen values. Nitrogen is not present in the sediment but is present in small amounts in both fish samples.

7.5.2 Fatty acid methyl esters (FAMEs)

The FAMEs profiles showed quantitative and qualitative differences between the sediment and the fossil fish; these profiles are presented in Figure 7.3. Fish A and Fish B profiles were very similar. The sediment profile showed a monomodal distribution with a high abundance of HMW straight-chain fatty acids maximising at n-C_{28}, with the even-over-odd predominance indicating a terrestrial source. This distribution of these long-chain (i.e.

C_{20}–C_{32}) fatty acids with an even dominance is associated with higher plant input (e.g. Bull *et al.*, 1998). Fatty acids released from the fossil fish showed a bimodal distribution with lower abundances of HMW fatty acids and a prevalence of the LMW homologues. A stronger even-over-odd predominance was observed in all regions of the profile with respect to the sediment sample. The abundance of LMW fatty acids in the fish profiles may indicate an endogenous source from within the original fish or could result from bacterial alteration or *in situ* polymerisation during diagenesis. All samples demonstrated the presence of hopanoic acids, although the abundances were much lower in the fish samples compared to those in the sediment. The presence of hopanoic acids prescribes a bacterial origin, although precursor organisms cannot be distinguished from these results.

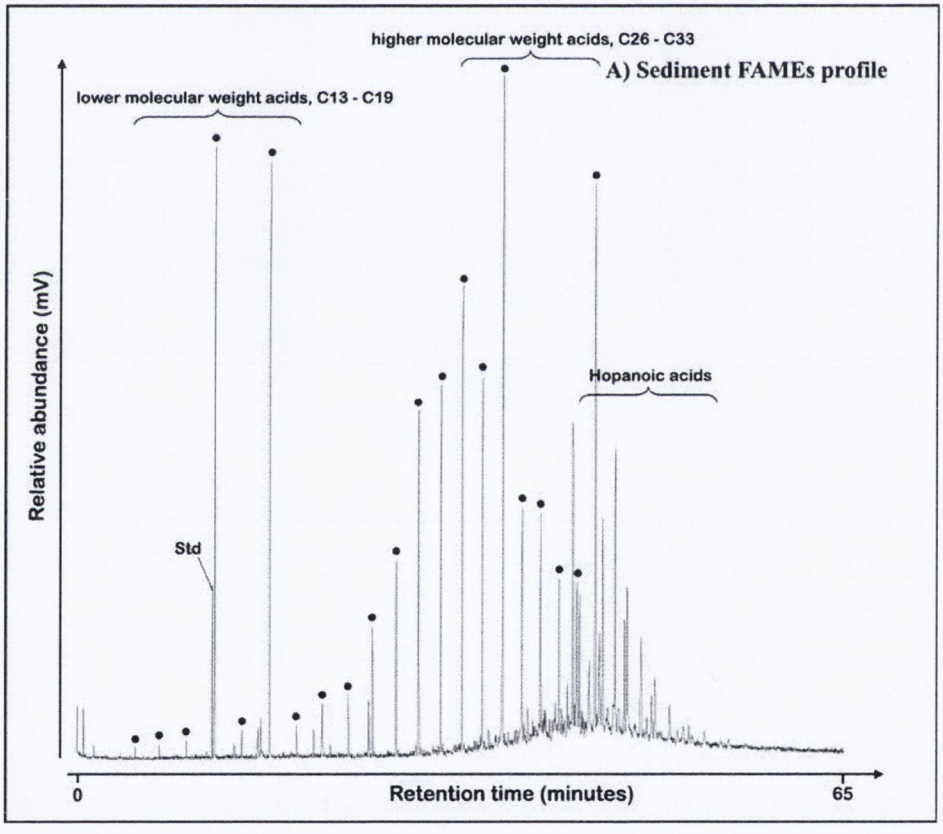

Figure 7.3: FAMEs profiles for. **A)** sediment, **B)** Fish A and **C)** Fish B samples. Filled circles indicate straight chain fatty acids, even-over-odd predominance; Std indicates the nonadecane ($C_{19}H_{40}$) standard.

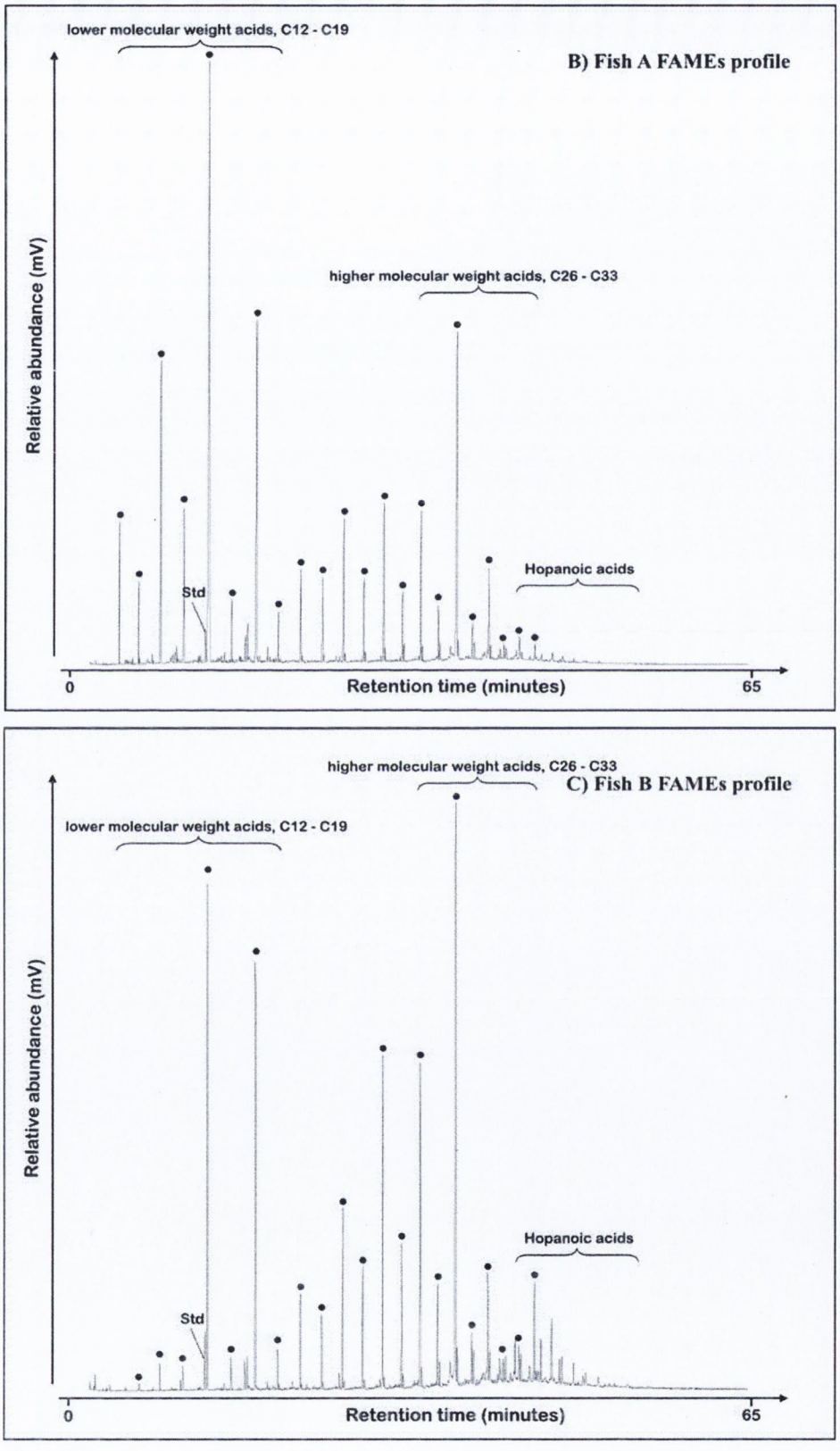

Figure 7.3: continued.

7.5.3 Apolar fraction

Apolar fractions showed that *n*-alkanes, steranes, hopanes and hopenes were present in both fish and sediment profiles. Hopanes and hopenes originate from a bacterial source and may be the degradation and rearrangement products of bacteriohopanepolyols (BHPs) (Sugden *et al.* 2005). The absence of 2-methylhopanoids in the apolar fractions suggests a lack of cyanobacteria in Fossil Lake at time of deposition. Hopenes are not commonly found preserved in sediments due to their reactive double bond, thus their presence suggests that the sediments are thermally immature. Overall the sediment apolar fraction profile does not show any significant differences to those of the fossil fish. All apolar fraction profiles are shown in Appendix 2. Further characterisation of the apolar profiles revealed that one of the most abundant steranes present was dinosterane, which is usually a minor component. Dinosterane is a diagnostic lipid originating from unicellular protists of the Division Dinoflagellata. Evidence for dinoflagellates in abundance at time of deposition was present in all three samples, an example of which is shown in Figure 7.4.

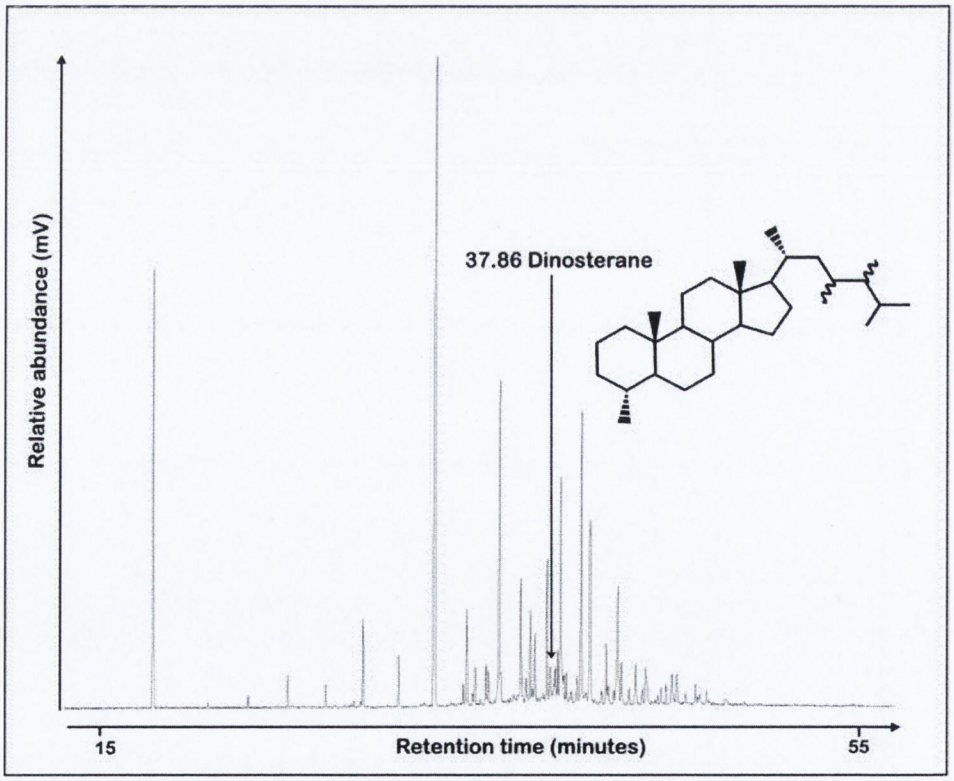

Figure 7.4: Dinosterane is shown to have eluted from the apolar lipid fraction for the sediment sample at 37.86 minutes. Dinosterane structure redrawn from Moldowan *et al.* (2001).

7.5.4 Polar fraction

Little information can be gleaned from the polar fraction profiles produced for the sediment and fossil fish samples, although there is a slightly different distribution between the sediment and fossil fish profiles. All polar fraction profiles are shown in Appendix 2. *n*-alkanols and sterols such as cholestanol and cholesterol were observed but no significant conclusions can be drawn from these as they are ubiquitous in natural systems. The even-over-odd predominance of alkanols suggests a terrestrial plant wax source. Sterols and stanols are widely distributed in living organisms therefore source assignment of individual homologues can be difficult to determine with any accuracy (Volkman 1986). However, cholesterol is primarily an animal sterol and may be derived from the original Eocene fish. There was a distinct lack of archaeol in all polar fraction profiles, suggesting the absence of the Domain Archaea in Eocene Fossil Lake.

7.5.5 GC-IRMS data

GC-IRMS analyses were carried out in an attempt to ascertain whether there was a consistent difference in C_{org} isotope values between the LMW fatty acids from Fish A and HMW fatty acids from Fish A and the sediment sample. Distinct isotopic signatures would support the theory that LMW fatty acids in the fish sample originated from a different source to the HMW acids and could be related to the original organic chemistry of the Eocene fish. The results from these compound-specific isotope analyses proved to be inconclusive however: the LMW compounds had a $\delta^{13}C$ value of -29 to -30 ‰ and the HMW compounds had a $\delta^{13}C$ value of -30 to -32‰. These differences are too small to be significant and allochthonous terrestrial input cannot be distinguished from an aquatic source on isotopic grounds alone.

7.5.6 Amino acid data

Organisms almost universally have the same 20 or so different α-amino acids making up their proteins (Eglinton & Logan 1991). The sediment sample and Fish A and B were expected to have only some surviving α-amino acid units with short chain lengths due to their age and the poor preservation potential of such biomolecules. Although some results were obtained for all three samples, the blank control sample that was run simultaneously

and subjected to the same protocol also produced results. Unfortunately this implies that the sample data may also be compromised and as such the results were deemed invalid. All four profiles are included in Appendix 2.

7.6 Discussion

7.6.1 Robustness of results

Samples of the solvent extractable lipids have shown that the Fossil Lake fish samples and their enclosing sediment contain abundant functionalised compounds of biological origin, indicating a high degree of preservation even after a 50 Ma period of burial. From CHN analyses and the FAMEs profiles it appears that the fish contain an extra organic matter component not found within the sediment. Whether this is organic matter related to the original fish biochemistry or a taphonomic artefact cannot be established from the current data set. The presence of nitrogen and LMW fatty acids could reflect an endogenous constituent or could represent post-mortem bacterial ingestion of the soft tissues of the fish. If the N isotope values presented in Chapter 5 are from a secondary process of bacterial ingestion then the original difference in isotopic signal between species should be reflected and assumptions of trophic level from the data would therefore still be valid. The endogeneity of the nitrogen and LMW fatty acids cannot be verified at present. HMW fatty acids and hopanoids found in sediment samples and to a lesser extent in the fish samples could reflect a common origin, or may be sediment-derived and have migrated into the fish samples. The high organic matter content of the enclosing sediment would favour contamination of fossil molecular signatures if such a migration was to occur (Gupta *et al.* 2007).

Detailed paleodietary information from compound specific stable isotope investigations of proteins or biomarker approaches using lipids has previously been obtained only from materials of Pleistocene or younger age (Briggs *et al.* 2000). Despite ostensible degradation of the primary biomacromolecules, N and C_{org} bulk isotopic data have been obtained here from an Eocene palaeocommunity. In archaeological studies, isotopically derived dietary information is thought to have been recorded within the chemical structure of skeletal collagen and other proteins (Pate 1994). Briggs *et al.* (2000) noted that the

reliability of the isotopic information obtained depended on the quality of the molecular preservation of collagen, although even under favourable conditions such as cool or dry deposits, little intact collagen would remain in bones after 10-30 k.y., with just minor amounts surviving up to 100 k.y. (Jones *et al.* 2001). The isotopic data retrieved from Fossil Lake and other Tertiary settings (Schweizer *et al.* 2006 and 2007) challenges this established and widely accepted scientific reasoning. Either intact collagen or proteins are preserved in the fossil fish bones to provide these results, or the isotopic data are from another source. Lipids and their functional groups can still retain significant chemical information from once-living organisms and may preserve the palaeodietary isotopic data within their enduring hydrophobic biomolecules. It was hoped that lipids and amino acids extracted from the Green River Formation fossils would provide information to confirm the chemical origin of their ancient isotopic signatures. Unfortunately this has not been possible within the time constraints of this project and the data gathered thus far has proved inconclusive, but promising.

7.6.2 A mechanism for mass mortality in Fossil Lake

As discussed in Chapter 2, the fossil fish collected from the Green River Formation appear to have accumulated at the bottom of a deep, stratified, warm-monomictic lake (Ferber & Wells 1995). Although the amorphous kerogen layers are thought to be the product of algal mats (see Chapter 2 Section 2.4), possible algal blooms in the surface waters may have contributed to the kerogen-rich laminae after these events. The high C_{org} and kerogen content of the sediments may support this theory. The characterisation of organic matter presented in this chapter has provided information on the original assemblage of micro-organisms in Fossil Lake during the late Early Eocene allowing the refinement of this theory. Two main groups of micro-organisms can now be discounted. Cyanobacteria are distributed globally in freshwater and marine environments and may form blooms which are often toxic to other organisms (Siqueira *et al.* 2006). However the absence of 2-methylhopanoids in all FAMEs profiles suggests a complete lack of cyanobacteria in Fossil Lake at time of deposition, thus ruling out these bacteria as a possible mechanism for the mass mortalities of fish. These organisms also cannot be responsible for producing the algal mat structures shown in Figure 2.7. Based on field evidence of occasional

elevated salinities it was also speculated that Archaea, known extremophiles, may cause blooms toxic to fish such as those reported in the Red Sea at the present day (e.g. Oren & Gurevich 1995). However, this theory can also be discounted due to the distinct lack of archaeol in all polar fraction profiles.

The presence of dinosterane in the apolar fractions indicates an abundance of dinoflagellates at time of deposition and thus presents a possible mechanism for the mass mortality horizons in Fossil Lake. Today these flagellate protists are mostly marine plankton but are also common in freshwater habitats, existing both as free-living algae and symbiotic zooxanthellae that inhabit various host invertebrates. The earliest fossils confidently determined to be dinoflagellate cysts date from 240 Ma (Fensome *et al.* 1996), although not all living species of dinoflagellate produce preservable cysts as part of their reproductive cycle, and the origin of the group is thought to be much older. Organic geochemical techniques have helped to identify the characteristic biomarkers for dinoflagellates in the fossil record (e.g. Summons *et al.* 1987; Summons *et al.* 1992). Moldowan *et al.* (2001) used a biomolecular approach to search the geological record for taxonomically restricted dinosteroids and, assuming that the steroids found were derived exclusively from the dinoflagellate-restricted sterols, concluded that the lineage of dinoflagellates is rooted in the Precambrian. Today many different species of dinoflagellate exist, both with toxic and non-toxic forms (John *et al.* 2003), and a toxic variety present in Fossil Lake could explain the regular mass mortalities of the ancient fish. Previous organic geochemical investigations of the Green River shales have mainly focused on the kerogen content of the shales in the wider basin, particularly the Washakie Basin corresponding to Eocene Lake Gosiute, and dinosteranes have also been reported there (Summons *et al.* 1987; Horsfield *et al.* 1995).

At the present day dinoflagellate blooms are known to take place in warm, monomictic lakes such as Lake Kinneret, Israel (Berman-Frank *et al.* 1994) and Lake Berryessa, California, USA, (Herrgesell *et al.* 1976), although they are most common in coastal marine areas such as that off the coast of Florida, USA (see Fleming *et al.* 2005 and references cited therein). Depending on the dinoflagellate species present, these blooms

can cause fish kills, are known to cause respiratory distress to humans and can affect marine mammals and birds, often resulting in death. After an extremely prolific dinoflagellate bloom off the coast of Florida in 1946/47, Gunter *et al.* (1948) made detailed observations and reported that fish were killed in numbers greater than 50 million, as well as turtles, marine mammals and birds. These episodes are now known as Harmful Algal Blooms (HABs), and although usually much less severe, occur on an approximately annual basis. Toxic blooms such as these could not only explain the regular accumulation of large amounts of fish carcasses in Eocene Fossil Lake, but could also account for the death of turtles, insects, bats and birds and other creatures living in and around the lake system due to associated respiratory problems and consumption of toxic water and organisms. The presumed toxicity to all other life-forms would prevent scavenging of these deceased organisms and could then be a factor in their preservation potential.

7.7 Conclusion

Organic biogeochemical analyses were carried out to determine the origin of the organic matter containing the $\delta^{15}N$ and $\delta^{13}C_{org}$ isotopic signatures in the Green River fossil fish, and in particular, whether the organic matter is related to the original fish biochemistry or a diagenetic artefact. Although these analyses have proved inconclusive, the solvent extractable lipids demonstrate that the fish samples and the enclosing sediment contain abundant functionalised compounds of biological origin, indicating a high degree of preservation. From the CHN analyses and FAMEs profiles it is suggested that the fish contain an extra organic matter component not found within the sediment. Whether this is organic matter related to the original fish biochemistry or a diagenetic artefact cannot be established from the current data set and further research is required. Apolar and polar fraction profiles showed little difference between fish and sediment samples, and the results from amino acid identification were deemed invalid. GC-IRMS analyses failed to identify isotopic differences between LMW and HMW compounds. One of the most significant findings from this research is the information retrieved from the apolar fractions regarding the original assemblage of micro-organisms present in Fossil Lake. Toxic dinoflagellate blooms can now be postulated as a causal mechanism for the recurring fish mass mortalities preserved throughout the succession.

Chapter 8: N and C isotopes in the Cretaceous Mata Amarilla fossils

8.1 Overview

In Chapter 5 the results of nitrogen and organic carbon isotope results from fossil fish of the Green River Formation, Wyoming, were presented and discussed. These Eocene fossil fish are well-preserved in the micritic muds of an intermontane, lacustrine setting, which has proved a viable testing ground for the organic stable isotopic investigation of a palaeoecosystem. However, whether this N and $C_{organic}$ isotope technique for investigating palaeoecology could have a wider application ideally also needed to be explored, particularly in relation to older fossil assemblages with different styles of preservation. The Santa Cruz Province of Argentina provided an excellent opportunity to further test this isotopic investigation and to research a different extinct aquatic community. The Mata Amarilla Formation in the Austral Basin of southern Patagonia contains countless fragments of bones, scales and teeth from vertebrates of the upper Cretaceous, thus presenting an exceptional opportunity to attempt to use N and C isotopes to gain valuable insight into a much older, little known fossil community with a different diagenetic and taphonomic history to that of the Green River Formation.

8.2 Introduction

In Chapters 1 to 7 the preservation of stable isotopes in fossil fish from the Green River Formation, Wyoming have been discussed. Although N and C isotopic signatures were measured from within the organic matter present in the skeletal fluorapatite it is doubtful that these signatures entirely reflect the original isotopic composition of the fish. In the taphonomic study described in full in Chapter 6 it was found that bulk N and C isotope signals degrade with time in the bones of extant fish but that their scales maintain a more reliable record of the original isotopic signatures. The dense hard tissues of older fossils such as teeth are also thought to preserve isotopic signatures with higher fidelity than bone (Wang & Cerling 1994). *In vivo*, neither the mineral (hydroxyapatite) nor organic (collagen) phases of enamel and dentine are re-metabolised once deposited, and so the isotopic signatures of the body during the animal's lifetime become archived within the tooth (Mendes *et al.* 2007). In isotopic studies of prehistoric teeth, the enamel is thought to

be more resistant to degradation and chemical alteration than dentine, thus preserving the most intact isotopic record of the consumer's diet (Zazzo *et al.* 2000). In a recent study of bacterial degradation of bone, dentine and enamel using SEM, Stathopoulou (2008) found evidence of microbial and fungal activity in fossil and recent bone and dentine samples, but no such destruction was evident in enamel samples. It is thought that the low organic content of enamel coupled with the larger crystallite size and the absence of voids in its structure prohibit the bacterial and fungal activity observed soon after burial in extant bone and dentine samples (Stathopoulou 2008). Most samples of dentine were found to have some trace of microbial activity, but not as much as bone, with the dentine retaining its original structure, showing most alteration at the enamel-dentine junction and adjacent to the pulp cavity (Stathopoulou 2008). Providing that adult teeth are sampled, a record of the original $\delta^{15}N$ and $\delta^{13}C$ and therefore trophic level of an organism could thus be preserved with high fidelity in tooth enamel. Enamel and similar substances are therefore likely to be the most desirable fossil materials for sampling when attempting to reconstruct trophodynamics.

The opportunity to study an ancient fossil aquatic ecosystem with well preserved teeth and scales as well as some bone fragments was provided by the Mata Amarilla Formation in the Santa Cruz Province of Argentina. The aim of this final aspect of the research was to test whether viable $\delta^{15}N$ and $\delta^{13}C_{org}$ values could be gained from this fossil ecosystem for trophic level reconstruction using those hard parts perceived to be more reliable than bone. The Mata Amarilla Formation and the immediately underlying Piedra Clavada Formation constitute a clear example of a deltaic system that was active during the Cretaceous in southern Patagonia (Goin *et al.* 2002). In recent years, a number of sedimentological, ichnological and palaeontological studies have been carried out on both formations in the Tres Lagos area which have provided a detailed insight into the palaeoecological characteristics of these units within an extra-Andean region of the Austral Basin (see Goin *et al.* 2007 and references therein). The Mata Amarilla Formation is an ideal study site for this research due to the abundance of teeth and scales and the loose, friable nature of the siliclastic lithology both aiding specimen retrieval. The absence of carbonate lithologies in

the delta system eliminates the major difficulties of sample preparation identified in the Green River fish as discussed in Chapter 4 of this thesis.

8.3 Location and geological setting

The study area is located in the south west of Santa Cruz Province, Argentina, as shown in Figure 8.1, within the Austral Basin (= Magallanes Basin) of southern Patagonia. The Austral Basin is located on the southern edge of the South American Plate, and its history

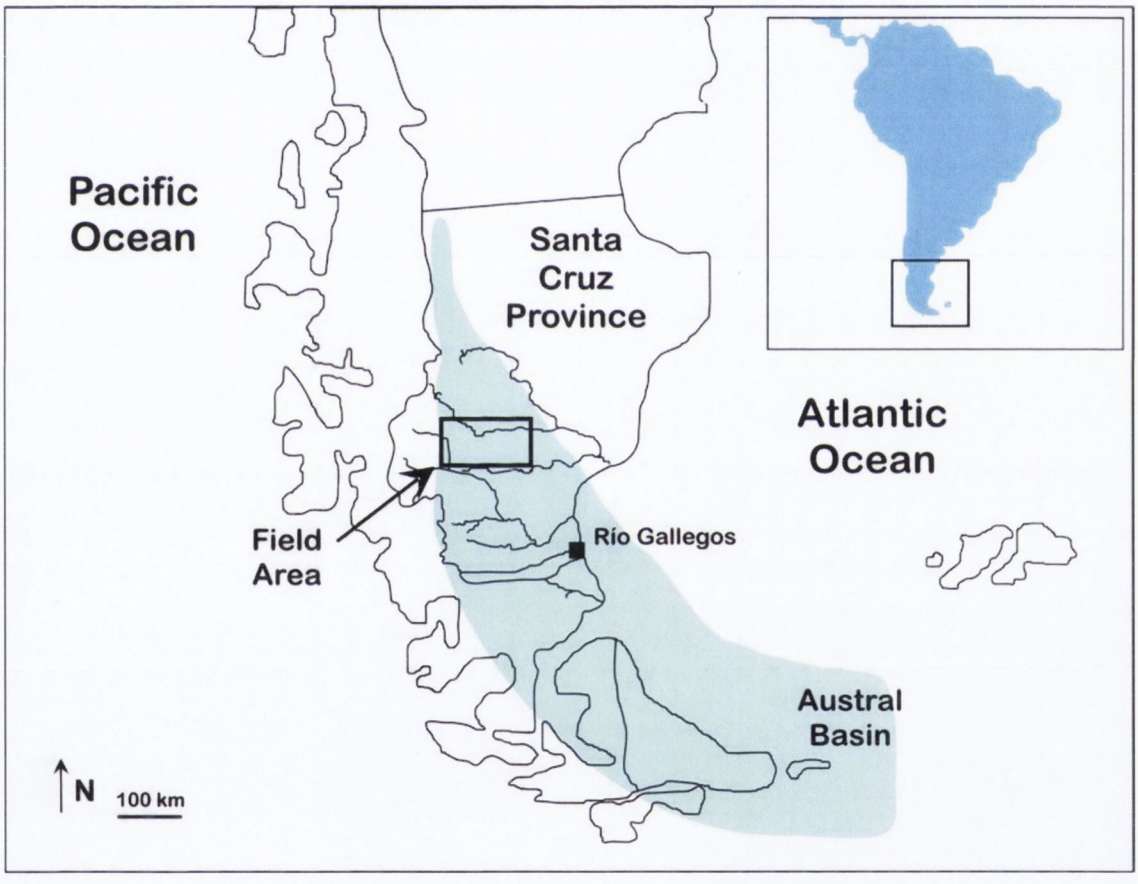

Figure 8.1: Map showing location of the field area of interest in the Santa Cruz Province, Argentina (redrawn after Iglesias *et al.* 2007). The extent of the Austral Basin is shown in pale blue.

is linked to the Triassic break-up of south-west Gondwana which resulted in the formation of a small marginal sea behind a developing magmatic arc (Iglesias *et al.* 2007). This marginal sea is thought to have closed during the mid-Cretaceous: Andean compressional tectonics related to South Atlantic spreading caused the inversion of previous extensional

structures and the beginning of a retro-arc foreland phase in the Austral basin during the Late Cretaceous (Franzese *et al.* 2003). Within the field area towards the eastern margin of the basin, the sedimentary facies comprises the Late Cretaceous deposits of the Piedra Clavada, Mata Amarilla and La Anita Formations (Iglesias *et al.* 2007). At the base of the section, the conformable units of the Piedra Clavada Formation are interpreted as the product of a tide-dominated shallow marine setting (Poiré *et al.* 2004a). From the Piedra Clavada Formation to the Mata Amarilla Formation, strong environmental changes are observed, ranging from prodelta facies to a fluvial system, all overlain by the conformable prograding delta facies of the La Anita Formation (Poiré *et al.* 2004a).

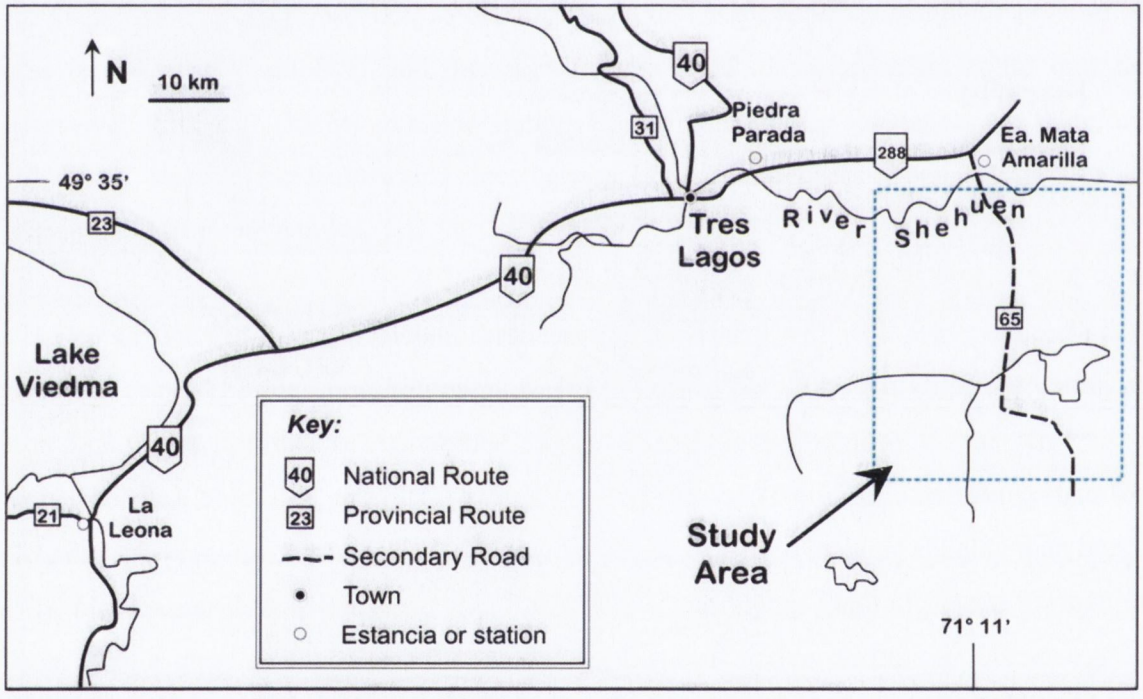

Figure 8.2: Map showing location of the study area near the town of Tres Lagos and Estancia Mata Amarilla (redrawn after Iglesias *et al.* 2007 and Cione *et al.* 2007).

The study area is located to the east of the town of Tres Lagos, just south of the River Shehuen, as shown in Figure 8.2. Extensive outcrops of all three formations are easily accessible in this sparsely populated area, although this study concentrates solely on the Mata Amarilla Formation which is easily identified in the field by its repeating units of dark grey, light grey and whiter lithologies that give the outcrops a striped appearance (see

Figure 8.3). On closer inspection this repeating sequence is comprised of dark and light grey massive argillaceous mudstones, intercalated with whitish massive sandstones. The argillaceous mudstones are composed of abundant quartz, with some feldspars and smectite and minor illite and kaolinite (Goin *et al.* 2002). Some of the mudstone layers are blackish and carbonaceous, containing many plant fragments with well-preserved cuticles (Cione *et al.* 2007). The sandstones are arenaceous with beds of up to 4m in thickness, featuring trough cross-bedding with a unimodal distribution (Goin *et al.* 2002). Shelly lag deposits are present in the lower section of the formation, and both continental and marine fossil faunas (invertebrates and vertebrates) are found throughout (Poiré *et al.* 2004a).

Figure 8.3: An outcrop of the Mata Amarilla Formation seen from a distance. The formation consists of repetitively interbedded units of dark and light grey mudstones and massive whitish sandstones.

The main units are shown as a stratigraphic column in Figure 8.4, including the location of the bone bed where the majority of fossils for this study were sourced from. The stratigraphy is well known and an overall change in palaeoenvironment from a tide-dominated delta to a fluvial system has been inferred, representing a shallowing-up succession (Poiré *et al.* 2004b). There is no abrupt lithological change however, rather a

transition in depositional setting from a sub-aerial delta complex and delta plain in the lower section to a very low-energy fluvial system featuring large lacustrine bodies in flood plains within the upper units (Iglesias *et al.* 2007). The Mata Amarilla Formation is dated as Cenomanian-Coniacian (99-87 Ma) based on ammonites found in associated marine facies (Riccardi & Rolleri 1980). The earliest date is corroborated by megaspore analyses of the immediately underlying Piedra Clavada Formation which suggest an Albian-Early Cenomanian age (Villar de Seoane & Archangelsky 2008).

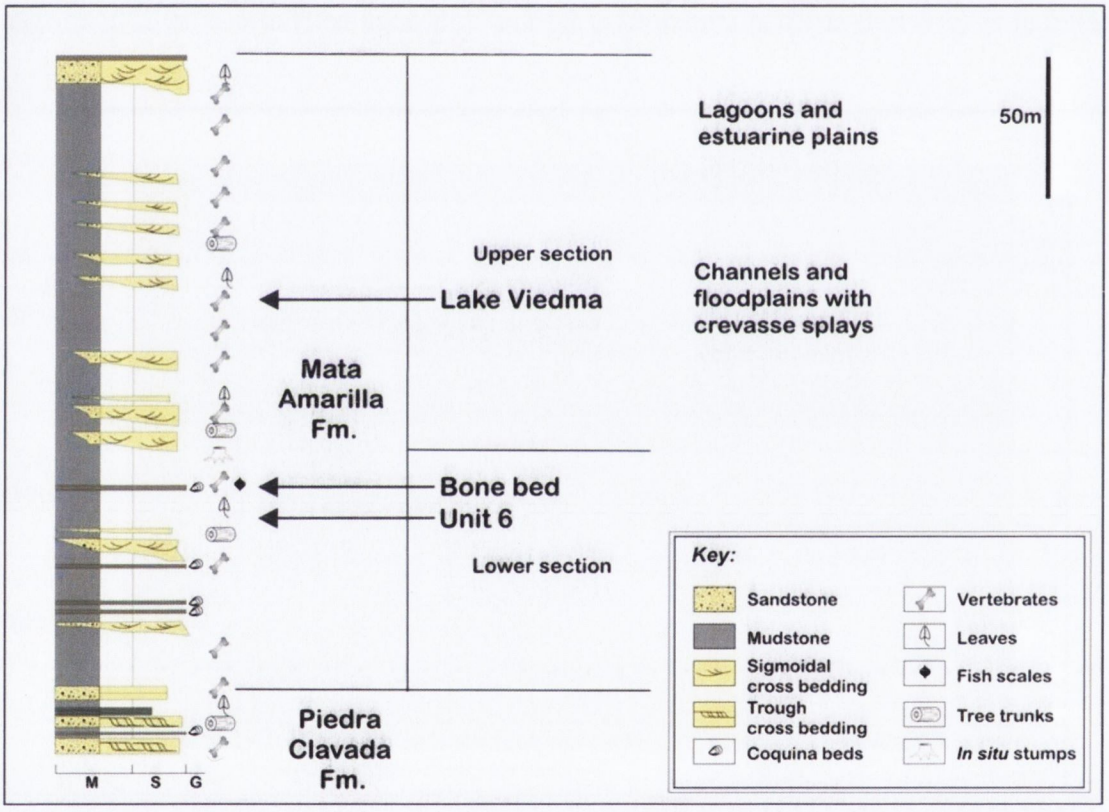

Figure 8.4: Schematic stratigraphic section of the Mata Amarilla Formation in the Tres Lagos area showing the location of the bone bed (redrawn after Poiré *et al.* 2004a, Iglesias *et al.* 2007 and Cione *et al.* 2007).

8.4 Palaeontology and palaeoenvironment

8.4.1 Macrofauna

The Mata Amarilla Formation is rich in fossil remains of a varied Late Cretaceous fauna and flora. Invertebrate fossils are found throughout the formation, with some intervals comprising molluscan beds in the lower section of the formation. These coquinoid beds

appear to be autochthonous with valves *in situ*, being unbroken, mostly articulated and showing little abrasion. The coquina levels yield *Eriphyla*, unidentified small oysters and trigonid bivalves, as well as gastropods (Poiré *et al.* 2004a). These beds are considered to represent sporadic marine transgressions in the lower section of the formation (Goin *et al.* 2002; Poiré *et al.* 2004b). Stromatolites are also found in the lower section of the formation (Iglesias *et al.* 2007) and may represent hypersaline lagoons or embayments within the delta complex. Internal casts of the gastropod *Turritella* are often found on the surface of the Mata Amarilla Formation released by weathering and also represent a marine influence in the area.

Vertebrate fossils are found throughout the entire succession, and are mainly fragmentary in nature, particularly small fragments of tetrapod bone which have so far eluded identification (Poiré *et al.* 2004a). Dinosaur bones and teeth from various levels in the succession are often weathered out at the surface as fragments and as such have proved impossible to identify to species level, but most are thought to be from sauropod dinosaurs (Goin *et al.* 2002). Fragments of crocodiles and bony plates of turtles are also frequently found throughout the succession (Goin *et al.* 2002). Despite many of the fossilised turtle carapace fragments being no more than a few square centimetres, it has been possible to assign most to the family Chelidae, although not to individual species (Goin *et al.* 2002). Chelid turtles are well-known fresh water reptiles found exclusively in South America and Australasia and their presence supports a marginal (fluvio-marine) depositional setting for these sediments (Perea *et al.* 1996). Lungfish dental plates have been found in abundance and were assigned to the genus *Atlantoceratodus* by Cione *et al.* (2007). Their preservation ranges from fragments to complete dental plates and some lungfish bones, as described by Cione *et al.* (2007). Actinopterygii are represented in the fossil assemblage by fragments of holostean archaic bony fish, related to the extant bowfin and gar of North America. Rhomboidal ganoid scales of fish possibly belonging to the heavily armoured Family Lepisosteidae and hemispherical palatal teeth from *Lepidotes* of the Family Semionotidae abound (Goin *et al.* 2002). While *Lepidotes* are known to be highly euryhaline (Billon-Bruyat *et al.* 2005), fossil lepisosteids seem to have consistently lived in nonmarine environments with only two notable exceptions (see Freidman *et al.* 2003

and references therein). In other units, lamniform shark teeth and other indeterminate shark teeth are found (Poiré *et al.* 2004a), indicating marine incursions into the continental deltaic system. These are found with Pachycormyformes fish teeth, also indicators of a marine environment (Kear 2007).

8.4.2 Macroflora

Fossil macroflora are found throughout the Mata Amarilla Formation and main occurrences are noted on the stratigraphic column in Figure 8.4. Of four conspicuous plant-rich levels, three of these levels bear leaf impressions and the fourth consists of a petrified forest in a sandstone horizon, containing coniferous tree stumps in life position with trunk diameters of up to 1.2m (Iglesias *et al.* 2007). Angiosperm leaves and twigs as well as ferns and conifer fragments are very well preserved in the leaf-bearing units, with leaves frequently having preserved cuticles. These are documented and described in full in Iglesias *et al.* (2007) who report that angiosperms dominate the flora, accounting for approximately 80% of species, providing the first evidence of an angiosperm-dominated macroflora in the southwest Gondwana region. Some of the leaves exhibit an exquisitely preserved record of insect bite damage (Poiré *et al.* 2004a), which is most common in the geological record on leaves of Cretaceous age and confirms the presence of a thriving insect community in the area (Stephenson & Scott 1992). Permineralised coniferous logs are rare, but are found in horizontal positions throughout the stratigraphy (Poiré *et al.* 2004a).

8.4.3 Suggested palaeoenvironment

This once thriving non-deciduous palaeoflora suggests a subaerial delta and flood plain with herbaceous/shrub angiosperm and fern vegetation and a canopy of tall conifers (Iglesias *et al.* 2007) which may have looked similar to a modern subtropical forest. Analysis of megaspores from the underlying Piedra Clavada Formation suggests a climate of elevated temperature and high humidity (Villar de Seoane & Archangelsky 2008) and it is likely that this regime persisted during the deposition of the Mata Amarilla sediments. Evidence of fungal activity suggests high temperatures and high relative humidity (Iglesias *et al.* 2007), with the presence of numerous herbivorous insects evidenced by the

preserved leaf damage also suggesting elevated temperatures (DeLucia *et al.* 2008). Shallow freshwater lakes possibly interconnected by surface waters within the delta complex would have been teaming with lungfish and bony fishes, along with turtles and crocodiles that possibly fed on the fish. On land long-necked sauropod dinosaurs would have had an herbivorous diet, browsing on the angiosperm understorey and possibly stripping needles from tall conifers (Dodson 1990). Although tetrapod bones from Mata Amarilla are unidentified it is likely that small mammals and reptiles would have lived in the forested area and around the lakes, feeding on insects and plants or by predation on other small tetrapods. The fine-grained sediments containing bivalves, gastropods, shark teeth and stromatolites suggest periodic marine incursions into the area or possible coastal lagoons.

8.5 Samples for isotopic analyses

8.5.1 Sample locations

The majority of samples for this study were found in the bone bed labelled on the stratigraphic column in Figure 8.4 at the locality identified as Tres Lagos 1 (3LAG1) by Cione *et al.* (2007). Shark teeth and Pachycormyformes fish teeth were collected from slightly higher in the stratigraphy but within the same unit (angiosperm unit 6 in Poiré *et al.* 2004a), and dinosaur bones were found south of Lake Viedma. As such, only the samples from within the bone bed can be directly compared with one other for any diagnosis of trophic level, but all samples were subject to isotopic analyses to see if the different faunal and skeletal elements would be viable for future trophic level studies of fossils. The samples collected are listed in Table 8.1. Samples were extracted from the poorly consolidated siliclastic sediments and were not subject to any cleaning procedures. Samples were identified to species level where possible at the Departamento Científico Paleontología Vertebrados, Museo de La Plata, Argentina, by Francisco J. Goin and Alberto L. Cione. Their diagnoses are detailed in Table 8.2.

Description	Sample labels	Location	Quantity
Dipnoi tooth plates	AI1 and AI2	Bone bed	8
Lepisosteiformes scales	LS1	Bone bed	4
Semionotiformes palatal teeth	SP1	Bone bed	4
Turtle carapace fragments	TP1 to TP5 (A and B)	Bone bed	5
Shark teeth	ST1 to ST4 (A to C)	Unit 6	4
Pachycormyformes tooth	PT1 (A and B)	Unit 6	1
Dinosaur bone fragments	DB1 and DB2 (A and B)	Lake Viedma	2

Table 8.1: Samples collected from the Mata Amarilla Formation, Argentina, for use in this study.

Table 8.2 shows the description and a photograph of the specimens used for this study. It also highlights where different components of various specimens were drilled during sample collection for isotopic analyses.

8.5.2 Sample preparation

Specimens were examined using a stereo-microscope and any surface contamination removed by hand where possible, or avoided when sampling. The samples collected were powdered and homogenised. Due to the sample size required for analysis it was necessary to combine some of the smaller elements together into one sample. The eight lungfish tooth plates were divided into samples AI1 and AI2, AI1 being the first four pictured in Table 8.2, and AI2 being the second four. Under the microscope the specimens making up sample AI1 appeared slightly more porous, suggesting a higher chance of alteration or contamination. Samples AI1 and AI2 were ground to a fine powder using an agate mortar and pestle. The four cf. Lepisosteidae indet. scales (hereafter referred to as Lepisosteidae) were combined into one sample labelled LS1 and also ground to a fine powder using the mortar and pestle, as were the four Semionotiformes palatal teeth which were labelled sample SP1. The five fragments of turtle carapace were sampled individually using a diamond-tipped dental drill, each in two main areas: area A being the more dense outer carapace area and area B being the inner more porous area with suspected contamination. The powders of each of the turtle samples TP1A and TP1B through to TP5A and TP5B were collected into clean microcentrifuge tubes. The four shark teeth were treated

individually and labelled ST1 to ST4: ST1 and ST2 being the larger cf. *Cretolamna appendiculata* and ST3 and ST4 the two small *Carcharias* teeth. Samples ST1 and ST2 were drilled using the dental drill and separate portions collected into microcentrifuge tubes: A being the enamel, B being the inner tooth or dentine and C being the base of the tooth or trabecular dentine, as indicated in Table 8.2. Samples ST3 and ST4 were smaller and as such were each homogenised whole, again using the agate mortar and pestle, to ensure sample volumes were ample for analysis. The Pachycormyformes tooth was drilled using the dental drill and enamel removed and labelled sample PT1A and the inner tooth or dentine drilled and labelled sample PT1B. The two dinosaur bones DB1 and DB2 were also drilled using the dental drill, with samples DB1A and DB2A being taken from the outer area of the bone fossil and samples DB1B and DB2B taken from the inner central part as indicated in Table 8.2.

All sample powders were subject to XRD analysis following the method outlined in Chapter 3 Section 3.3, and were found to be composed of fluorapatite. Small amounts of quartz registering in the analyses of some of the samples are thought to be from the background siliclastic sedimentation, or possibly from the silica cavity mount used for the XRD analyses. Turtle carapace and dinosaur bone samples were also subject to CHN analysis as described in Chapter 3 Section 3.5, to confirm that organic carbon and nitrogen were present and therefore likely to be present in the entire suite of samples, prior to isotopic analysis. N and C isotopic values were obtained following the method described in Chapter 3 Section 3.1.4. Due to the higher percentage of N in this fossil sample set when compared with that of Green River, robust data with peak signal values above the recommended 1000mV were easily obtained. No pre-treatment was necessary as no carbonate was present to interfere with the $\delta^{13}C_{org}$ signature. Samples were analysed in a random order to prevent any systematic bias in the results, and corrected to international standards with the L-Alanine working standard previously described in Chapter 3. Experimental precision based on these replicates was ±7.5%RSD for $\delta^{15}N$ and ±1.9%RSD for $\delta^{13}C$. Results are presented in Section 8.6 and Appendix 2.

8.5.3 Sample identification

Taxonomy	Photograph of samples
Dipnoi tooth plates Subclass: Dipnoi Müller, 1844 Family: indet. Genus: *Atlantoceratodus* Cione *et al.*, 2007 Species: *Atlantoceratodus iheringi* Ameghino, 1898 ***Atlantoceratodus iheringi***	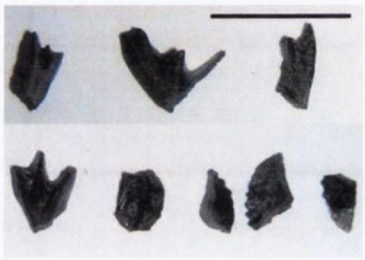
Lepisosteiformes scales Subclass: Actinopterygii Cope, 1887 Infraclass: Neopterygii Regan, 1923 Order: cf. Lepisosteiformes Hay, 1929 Family: cf. Lepisosteidae Cuvier, 1825 **cf. Lepisosteidae indet.**	
Semionotiformes palatal teeth Subclass: Actinopterygii Cope, 1887 Infraclass: Neopterygii Regan, 1923 Order: Semionotiformes Arambourg & Bertin, 1958 Family: Semionotidae Woodward, 1890 Genus: *Lepidotes* Agassiz, 1832 ***Lepidotes* indet.**	
Turtle carapace fragments Order: Testudines Linnaeus, 1758 Suborder: Pleurodira Cope, 1865 Family: Chelidae Lindholm, 1929 **Chelidae indet.**	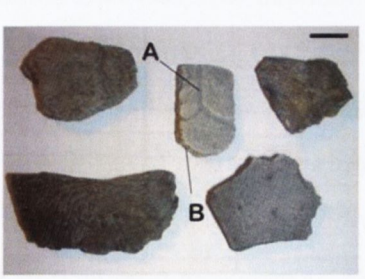

Table 8.2: Specimens prepared for use in this study: identification and photographic record. Scale bars are all 1cm long.

Taxonomy	Photograph of samples
Shark teeth Class: Neoselachii Compagno, 1977 Order: Lamniformes Berg, 1958 Family: Cretoxyrhinidae Glyckman, 1958 Genus: cf. *Cretolamna* Glyckman, 1958 Species:cf *Cretolamna appendiculata* Agassiz, 1843 **cf. *Cretolamna appendiculata***	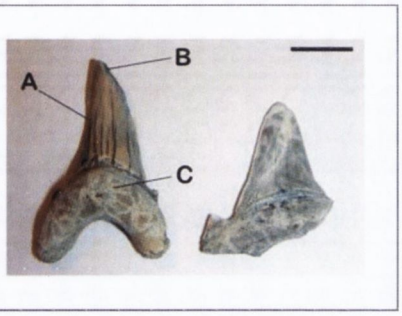
Shark teeth Class: Neoselachii Compagno, 1977 Order: Lamniformes Berg, 1958 Family: Odontaspididae Müller and Henle, 1839 Genus: *Carcharias* Rafinesque, 1810 ***Carcharias* indet.**	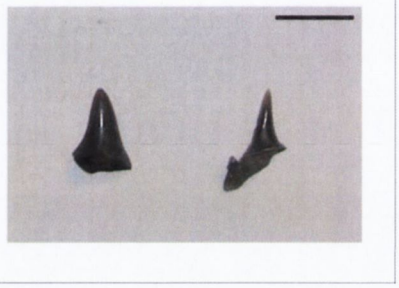
Pachycormyformes tooth Subclass: Actinopterygii, Cope, 1887 Order: Pachycormyformes Berg, 1940 Family: Pachycormidae Woodward, 1895 Genus: *Protosphyraena* Leidy, 1865 ***Protosphyraena* indet.**	
Dinosaur bone fragments Subclass: Saurischia Seeley, 1888 Order: Sauropodomorpha Huene, 1932 Infraorder: Sauropoda Marsh,1878 **Sauropoda indet.**	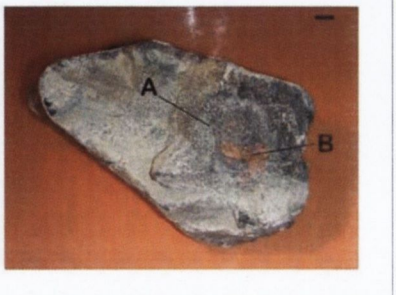

Table 8.2 continued: Scale bars are all 1cm long.

8.6 Results of N and C isotope analyses

8.6.1 Freshwater samples from the bone bed locality

The isotopic signatures of lungfish from repeat analyses of samples AI1 and AI2 show little difference in $\delta^{15}N$ values but there is a shift of just over 1‰ in the $\delta^{13}C$ values (see Figure 8.5). While this would be unexpected for such similar elements from the same species, possible contamination due to the more porous nature of AI1 samples could account for this shift. Repeat analyses of the Lepisosteidae scales (sample LS1) resulted in a tight cluster of data points with a standard deviation of just 0.04 for $\delta^{15}N$ and 0.06 for $\delta^{13}C$. A slightly wider spread was seen in data from the Semionotiformes palatal teeth (sample SP1). The lungfish, Lepisosteidae and Semionotiformes samples all show similar $\delta^{15}N$ values but are spread into distinct areas of Figure 8.5 by their different $\delta^{13}C$ values. The turtle samples show a wide range of values, both between the outer and inner samples (A and B) taken from individual fragments, and between the five different fragments analysed (TB1 to TB5). TP1A and TB2A have $\delta^{15}N$ values around 4.5‰ and $\delta^{13}C$ values between -12 and -13‰. Their counterparts from the inner part of the turtle plate fragments, TP1B and TP2B, have similar $\delta^{15}N$ values of around 4.5‰, however a negative shift is seen in the $\delta^{13}C$ values. Repeat analyses of TP1B show a spread of data points between approximately -16 and -19‰ $\delta^{13}C$, whereas the TP2B data points are clustered around -16.5‰ $\delta^{13}C$. Samples taken from turtle fragment TP3 show the inverse of this relationship, with repeat analyses of sample TP3B showing more positive values than those of TP3A. While average $\delta^{15}N$ values for both samples are just over 6‰, $\delta^{13}C$ values are approximately -13‰ for TP3A but as high as -8‰ for TP3B. Only one set of N and C data was obtained for turtle fragments TP4 and TP5. These are plotted on Figure 8.5 and show a difference between the outer and inner samples (A and B), with slightly more negative values in terms of $\delta^{13}C$, however the differences are not as marked as those of samples TP1A and TP1B, and TP2A and TP2B. Both samples TP4 and TP5 show more positive $\delta^{15}N$ values in samples taken from the centre of the turtle plate (B) when compared with the samples taken from the dense outer layer (A).

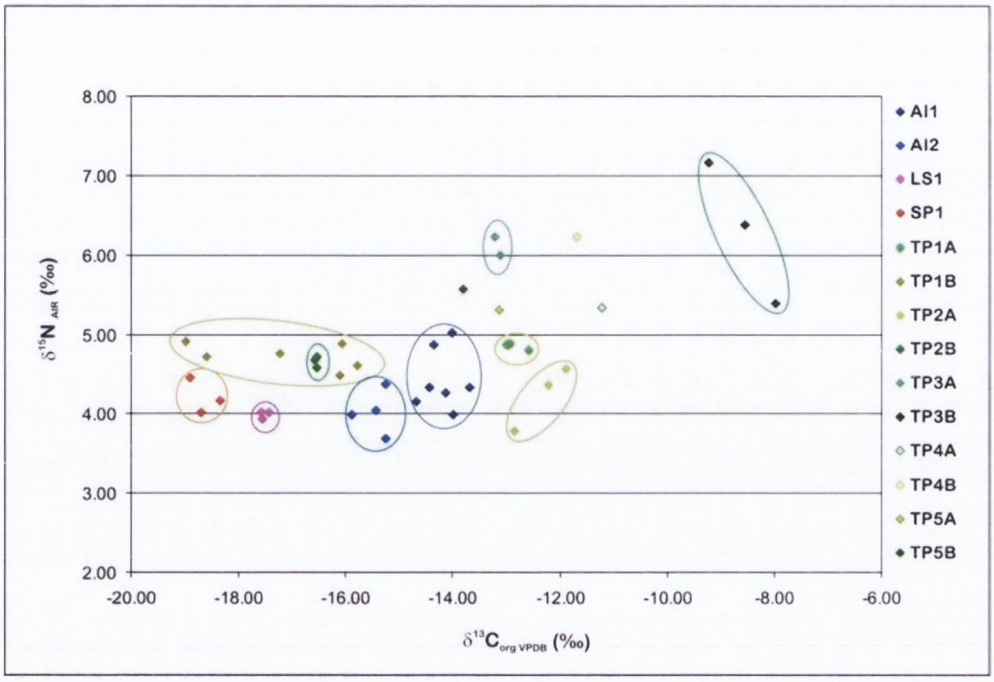

Figure 8.5: N and C bulk isotope results for samples from the bone bed. AI are Dipnoi tooth plates; LS are Lepisosteidae scales; SP are Semionotiformes palatal teeth; TP are turtle carapace fragments. Ellipses highlight data points from repeat analyses of one sample.

8.6.2 Marine samples from unit 6

The majority of the shark tooth bulk isotopic signatures for $\delta^{13}C$ are between just -7 and -8‰, whereas $\delta^{15}N$ values show a much wider +7‰ spread with a minimum of 2.5‰ and maximum of 9.8‰. There is no consistent difference between the different elements of tooth samples ST1 and ST2, where enamel, tooth infill and tooth base were drilled and analysed separately (labelled A, B and C, respectively). While ST2 shows a ~1.5‰ shift in $\delta^{15}N$ values between ST2A and ST2B, then another ~1.5‰ drop to ST2C, the values for $\delta^{15}N$ of ST1 do not follow the same order. ST1A and ST1C have similar N values around 9‰, whereas ST1B is lower with an average value of 7‰. Two smaller shark teeth which were ground and homogenised in their entirety due to their small size were ST3 and ST4, with ST3 having very little trabecular dentine present at the base. The results are encircled in Figure 8.6 using a solid line. There is a large difference in isotope values between these two small shark teeth: ST3 has an average $\delta^{15}N$ of 8‰ and an average $\delta^{13}C$

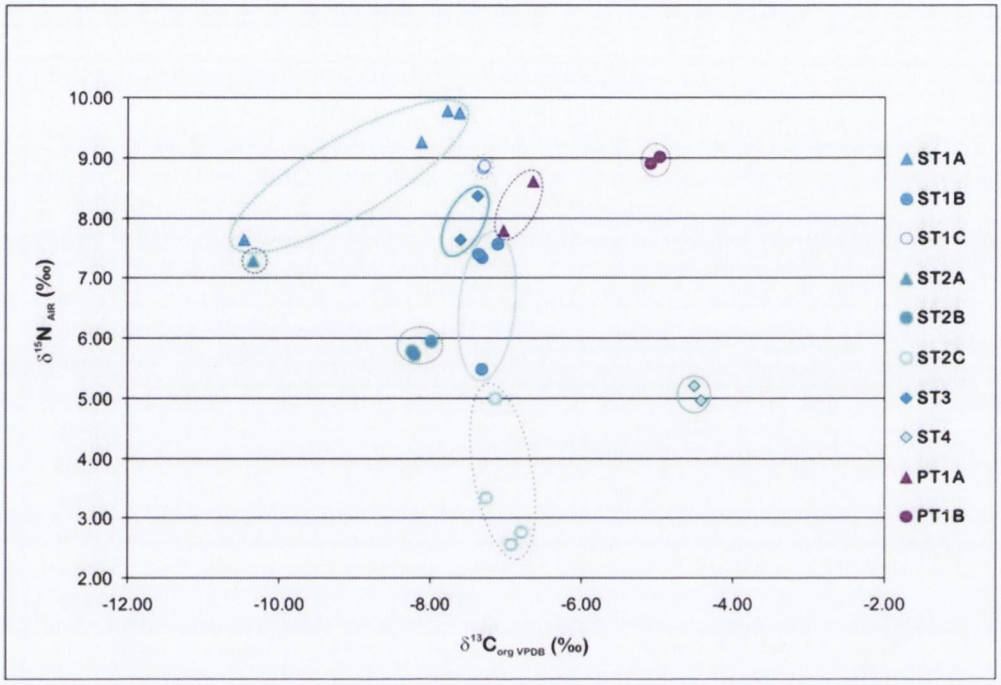

Figure 8.6: N and C bulk isotope results for samples from unit 6. ST1 and ST2 are cf. *Cretolamna appendiculata* shark teeth with samples labelled A enamel (filled triangles), B inner tooth or dentine (filled circles) and C the base of the tooth or trabecular dentine (open circles); ST3 and ST4 are *Carcharias* indet. shark teeth ground whole; PT are Pachycormyformes tooth samples of *Protosphyraena* with PT1A being enamel and PT1B being inner tooth or dentine. Ellipses highlight data points from repeat analyses of one sample. Note the different scale of this graph compared to 8.5.

value of -7.5‰, whereas ST4 has a lower average $\delta^{15}N$ of 5.1‰ and a more positive average $\delta^{13}C$ value of -4.5‰. The large fish tooth, PT, or *Protosphyraena* tooth, gave fairly similar $\delta^{15}N$ values regardless of whether enamel or tooth infill was measured (A and B respectively), however the differences in C value are more significant, with an average difference of 1.8‰. The enamel values are more negative than the inner tooth values, similar to the pattern seen between $\delta^{13}C$ data for ST1A and B, and also between ST2A and B. The actual values obtained for sample PT1A are very similar to those obtained for ST3, although slightly more positive in terms of $\delta^{13}C$.

8.6.3 Dinosaur bone samples from south of Lake Viedma

Individually, dinosaur bone fragment samples show little spread in terms of C isotope values from repeat analyses, but all show an approximate 1‰ spread in their N isotope

values. Dinosaur sample DB1A from the outer edge of the bone fragment gives more positive results than sample DB1B from the centre of the bone in both N and C values. DB1A has an average $\delta^{15}N$ value of 1.25‰ and an average $\delta^{13}C$ value of -16.9‰ whereas the average $\delta^{15}N$ value for DB1B is 0.07‰ and its average $\delta^{13}C$ value is -17.9‰. This trend is not seen from repeat analyses of the two samples taken from dinosaur bone fragment DB2, however. Although the N values are more positive for sample DB2A than DB2B, the inverse is true of the C values. In these samples, DB2A has an average $\delta^{15}N$ value of 3.5‰ and an average $\delta^{13}C$ value of -16.6‰ whereas DB2B has average $\delta^{15}N$ value of 2.34‰ and an average $\delta^{13}C$ value of -15‰.

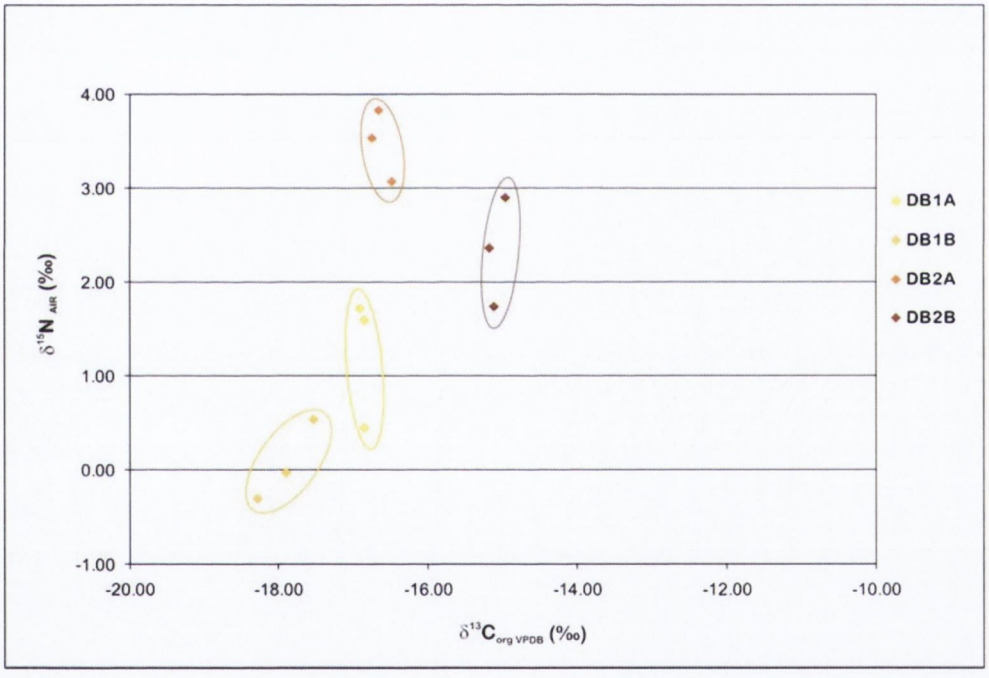

Figure 8.7: N and C bulk isotope results for dinosaur bone fragments DB1 and DB2 found south of Lake Viedma. Samples marked A represent the outer edge of the bone whereas those marked B are from the inner, densest part of the bone. Ellipses highlight data points from repeat analyses of one sample. Note this graph has a different scale to 8.5 and 8.6.

8.6.4 Comparison of N and C isotope results from all samples

The average N and C isotope data from all samples shown in Figures 8.1 to 8.3 above are shown together in Figure 8.8, with error bars used to illustrate the standard deviations from replicate analyses of each sample. While these samples are not all from the same

specific unit and therefore spatially not within the same ecosystem, some comparisons and observations can be made. On a graph showing trophic level, the enrichment of isotopes within an ecosystem would be expected to show a stepwise increase to more positive values at the upper right hand corner of the graph. From these data presented in Figure 8.8 this general trend is observed. The fragments of dinosaur bone plot at the bottom left hand side of the graph, indicating a low trophic level, with the freshwater fish plotting just above them. The turtle plate fragments have been grouped together and encircled as either

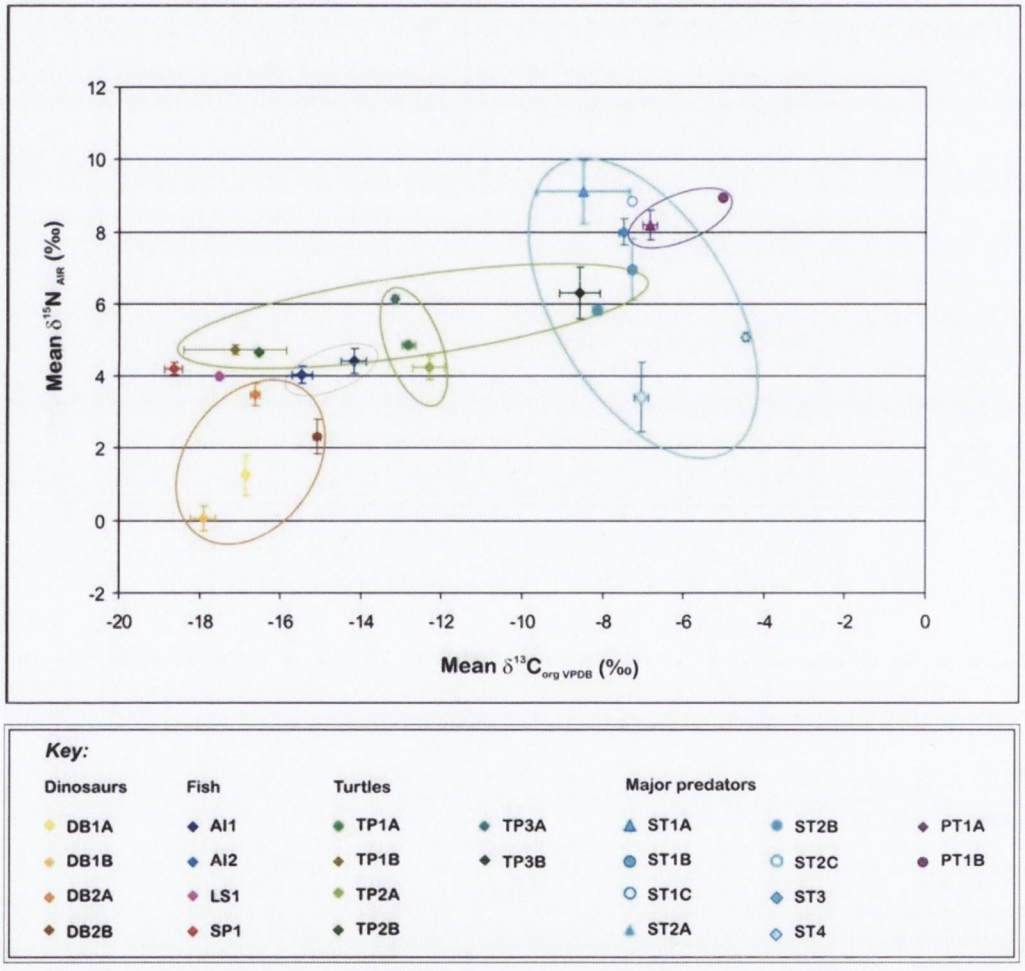

Figure 8.8: Average N and C isotope data for all samples analysed from the Mata Amarilla Formation. AI are Dipnoi tooth plates; DB are dinosaur bone fragments; LS are Lepisosteidae scales; SP are Semionotiformes palatal teeth; ST are shark teeth; TP are turtle carapace fragments; PT are Pachycormyformes tooth samples. Ellipses group data points from repeat analyses of samples from the same order or genus. NB: Error bars represent SD ($\pm 1\sigma$) from repeat analyses of each sample.

outer dense material (A) or inner more porous material (B). The results from the more dense part of the carapace all group within the smaller ellipse. With the exception of sample TP2A, both of the groupings appear higher in $\delta^{15}N$ than the freshwater fish by a small margin, with TP1A to TP3A and TP3B also being more positive than the fish in their $\delta^{13}C$ signatures. Finally the marine shark and fish teeth samples plot highest to the right hand side of Figure 8.8. Their values are fairly similar, with the Pachycormyformes tooth samples having slightly higher $\delta^{13}C$ signatures than the majority of the shark samples.

8.6.5 C:N ratios of all samples

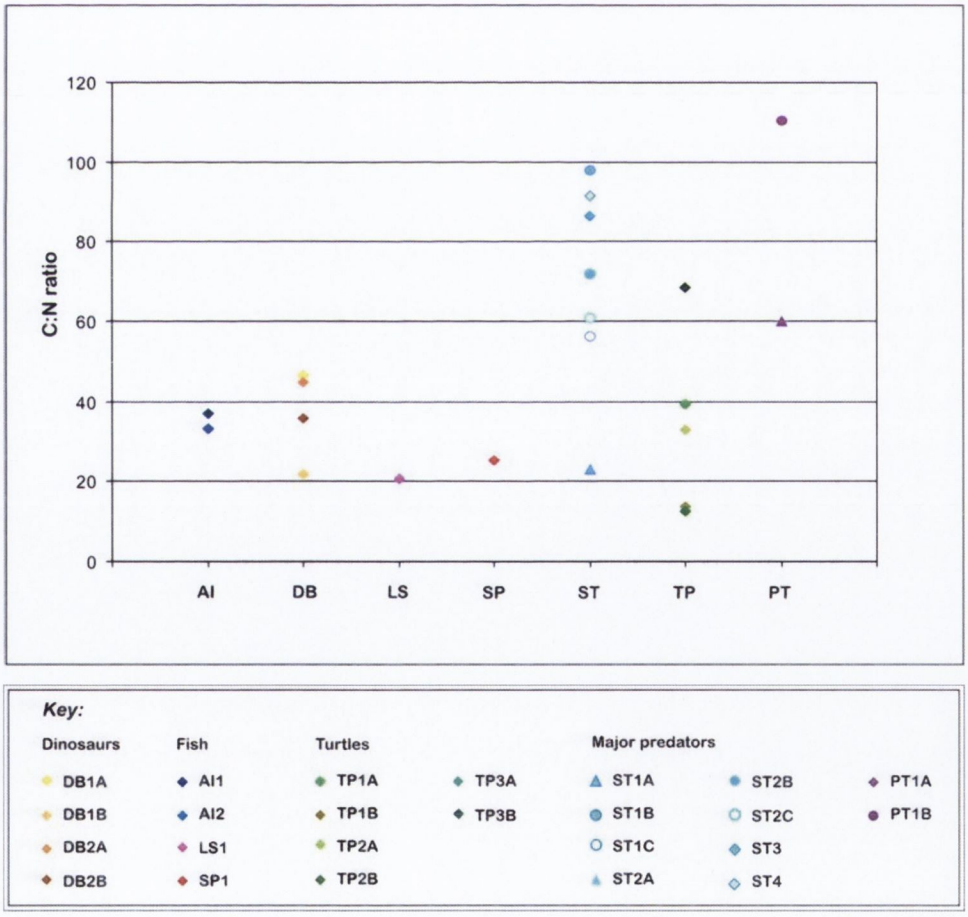

Figure 8.9: C:N ratios for all samples analysed from the Mata Amarilla Formation. AI are Dipnoi tooth plates; DB are dinosaur bone fragments; LS are Lepisosteidae scales; SP are Semionotiformes palatal teeth; ST are shark teeth; TP are turtle carapace fragments; PT are Pachycormyformes tooth samples.

C:N ratios determined from the percent element data produced simultaneously with the isotopic measurements of all samples collected from Argentina are shown in Figure 8.9. The lungfish tooth plate samples both have quite high ratios of around 35, and the four dinosaur bone fragment samples have a spread of values between 21.9 and 46.6. Lepisosteidae scales, Semionotiformes palatal teeth and shark tooth enamel all have values below 25. The remainder of the shark tooth samples are spread between 56.2 and 98. The majority of C:N ratios of the turtle carapace fragment samples are spread between 12.6 and 39.3, with sample TP3B being much higher at 68.5. Finally the Pachycormyformes tooth samples are very high, with the enamel sample PT1A having a C:N ratio of 60 and the inner tooth sample PT1B ratio being 110.3.

8.7 Discussion

8.7.1 Possible diagenetic alteration

Isotope data presented in Section 8.6 appears to suggest that information regarding trophic level may be preserved in the vertebrate fauna of the Mata Amarilla Formation. However, the effects of any diagenesis must be taken into account. Modern vertebrate bioapatites including bone, dentine, and enamel are composed of carbonate hydroxylapatite ($Ca_5(PO_4)_3OH$) mineralised on an organic framework (Lowenstam & Weiner 1989). That all samples in this study were found to be composed of fluorapatite ($Ca_5(PO_4)_3F$) suggests that some diagenetic alteration has occurred in each sample, with the hydroxyl group being chemically replaced by a fluoride ion. All specimens analysed in this isotope study would originally have been carbonate hydroxylapatite: as well as the bones and the teeth analysed, the ganoid Lepisosteidae scales are composed of bone covered with the enamel-like substance ganoin (Grande 1984) which is similar to enamel in its chemistry and structure. Also, despite morphological differences, the Semionotiformes teeth from the palatine comprise of a similar microstructure to the oral teeth of other fish with an outer enamel layer and an infill of dentine (Gillette 1999) and would also have originally been composed of carbonate hydroxylapatite. This apparent chemical replacement indicates that diagenetic alteration of the mineralised structure has taken place, but alteration of the underlying organic framework cannot easily be verified. The N and C isotope values presented in Section 8.6 are all thought to originate from preserved organic matter within

the mineralised hard tissues and evaluation of whether these isotopic signatures are original or altered cannot easily be confirmed.

8.7.2 Assessing robustness of data

In studies of oxygen isotopic signatures in bioapatites of geological age several methods exist for probing the degree of post-mortem isotopic alteration (Stanton-Thomas and Carlson 2004). While the majority of those are not applicable here, the comparison of bone and/or dentine to enamel from the same individual should give some insight into the degree of alteration. Since bone and dentine are more readily altered than enamel, isotope variability between these different bioapatite structures should indicate the effects of diagenesis. In this study the individual elements of the larger shark teeth ST1 and ST2 (cf. *Cretolamna appendiculata*) and the large fish tooth PT1 (*Protosphyraena*) do not show consistent differences in the isotopic composition of the enamel when compared with that of the dentine. Trabecular dentine sampled from the base of the shark teeth was expected to be unreliable due to its porous nature; however repeated analyses of sample ST1C produced results similar to the enamel samples labelled ST1A from the same tooth. This method for evaluating degree of diagenesis does not appear to be applicable to this study owing to the inconsistency between the results from enamel, dentine and trabecular dentine of different teeth. This test also operates on the assumption that little or no change has occurred in the isotopic signature of any enamel, whereas the apparent replacement of hydroxyl ions by fluoride ions in this study suggests otherwise. Other studies show that both N and C isotopic ratios can vary between different body parts of extant mammals, with collagen from dentine and bone showing as much as a 2-3‰ difference in each (Balasse *et al.* 1999). Carbon isotope ratios in the bioapatite of enamel are also known to vary by a similar amount, and may reflect dietary variability during the formation of the tooth (Zazzo *et al.* 2000). This effectively means that any differences in N and C isotope values between enamel and dentine of the same individual cannot be simply attributed to diagenesis but may be a factor of the range of the original isotopic signatures owing to internal variability in the individual when the teeth and other hard tissues were laid down. Analysis of oxygen isotope values from the same samples may be a more reliable indicator of diagenesis for this test. Another suggested method for evaluating the degree of

diagenesis at least qualitatively would be to examine the samples using SEM prior to preparation. The method employed by Stathopoulou (2008) to assess whether there is evidence of microbial activity in the bone, dentine and enamel of each specimen could be a very useful tool in future studies. Stanton-Thomas & Carlson (2004) also suggest using SEM as a measure of degree of diagenetic alteration; the physical preservation of micro-scale crystalline structure in bone, dentine and enamel is thought to be a prerequisite to preservation of original isotope values of the bioapatite. Unfortunately, examining the samples used herein at high resolution was beyond the scope of this project.

8.7.3 A possible insight from C:N ratios

In Chapter 6 taphonomy experiments are described in detail. During these experiments using extant fish it was noted that as physical decay occurred and isotopic signatures began to drift, the C:N ratio of the samples began to increase owing to the loss of nitrogen. This is proposed here as a method for identifying the degree of biodegradation and diagenesis and therefore reliability of the bulk N and C isotope values. It follows that with smaller C:N ratios then the alteration of N and C isotopic signatures is less likely, and conversely larger C:N ratios indicate results that should be treated with caution as the isotopic signatures may be unreliable. A trend of increasing C:N ratios with decreasing collagen yield has similarly been discussed in studies of specimens of archaeological age where collagen extraction techniques are used (e.g. France *et al.* 2007). The averaged C:N ratios from repeat analyses of each of the Mata Amarilla fossil samples presented in Figure 8.9 may offer an insight into the degree of alteration and exchange of N and C isotopes with their surroundings during diagenesis. All values are relatively high when compared with those of the extant fish presented in Chapter 6; however some are much higher and more inconsistent than others. In Chapter 6 the majority of C:N values were around 3, with ratios over 10 (up to a maximum of 17.01) in vertebrae indicating a high degree of degradation and loss of nitrogen from the system. However, the pharyngeal teeth of a modern freshwater trout (discussed in Chapter 5) were found to give higher C:N ratios of around 10, with the underlying bone giving values of almost 12, despite all other body parts having values of around 3. All data points from the fossil samples of the Mata Amarilla Formation have values of 12.6 or above. Apart from samples TP2B and TP1B

with values of 12.6 and 13.7 respectively, the suit of samples with values between 20 and 25 that include DB1B, LS1, SP1, ST1A and ST2A could tentatively be considered as the least altered by diagenesis. Interestingly, sample AI2 which was expected to be more reliable than AI1 on account of the lower surface porosity of tooth plates seen under the microscope has a lower C:N ratio than sample AI1 as predicted. However, the inner, more porous area of most turtle carapace fragments surprisingly gave much lower C:N ratios than those of the denser outer area originally assumed to be reliable on account of its dense hard nature. The exception to this is sample TP3B which consistently gave much more positive isotope results than expected, with a very high C:N ratio of 68.5 indicating that substantial alteration may have taken place in this sample, either simply by loss of original organic matter or replacement of organic material by post-mortem bacterial or fungal growth. The *Protosphyraena* tooth samples showed a marked difference between the C:N ratios of enamel (PT1A) and dentine (PT1B), being slightly more than those between shark tooth averages. While this indicates that the enamel samples are again the most reliable, sample PT1A still has a very high C:N ratio of 60, suggesting that care should be taken in the interpretation of the isotopic data. As a proxy for diagenetic change this method of using C:N ratios can only be used as a first approximation at this point in time, showing relative reliability within a data set.

8.7.4 Expected isotopic differences in the data set

Zazzo *et al.* (2000) checked for isotopic alteration during diagenesis by looking for expected isotopic differences between ecologically distinct taxa. In Figures 8.5 to 8.8 the Mata Amarilla fossils show the overall expected segregation in their isotopic signatures for their respective trophic levels. Despite their large body mass, sauropod dinosaurs would be expected to exhibit the lowest $\delta^{15}N$ values and most negative $\delta^{13}C$ in the assembled data set due to their solely herbivorous diet, and this is the case as shown in Figure 8.8. The freshwater lungfish and bony fish would be expected to have little variation between their $\delta^{13}C$ values and perhaps slightly different $\delta^{15}N$ due to variation in diet. Extant dipnoans are known to have an essentially carnivorous diet in early life including invertebrates, frogs and small fish, maturing fully into opportunistic omnivores which also consume plant material (Kemp 2002). The ganoid fish *Lepidotes* is thought to

also have had an omnivorous diet, although ecomorphologically the palatal dentitions with their hemispherical occlusal surface are typical of fish with light durophagous diets (e.g. decapods) (Buscalioni *et al.* 2008). The other ganoid fish of interest here from the Family Lepisosteidae are thought to be exclusively carnivorous. Robertson *et al.* (2008) report a diet of small fish and insects for various extant species living in the rivers, floodplains and oxbow lakes of Texas, USA. These fish were found to consume prey in proportion to their availability, opportunistically feeding on aquatic and terrestrial invertebrates as well as maintaining a highly piscivorous diet. The N and C isotopic data produced from the three freshwater fossil fish analysed for this study do not show much variation in $\delta^{15}N$ values: it is likely that these consumers shared a small number of common food resources and therefore trophic level. The probably exclusively carnivorous Lepisosteidae has an average $\delta^{15}N$ of 0.2‰ lower than the omnivorous Semionotidae, which in turn gives almost identical values to the fossil Dipnoan samples. The fish do show differences in their average $\delta^{13}C$ signals by 1-3‰, and this could be original variability or it may represent some loss of data during diagenesis. Extant Chelidae species are opportunistic omnivores and, like the fish, are predominantly carnivorous, eating a variety of prey items including crustaceans, insects and fish (Fowler & Cubas 2001). Large extant turtles tend to eat larger prey items than do small extant turtles (Georges 1982) and this may explain some of the spread seen in the data from different turtle carapace fragments in Figure 8.5. If TP1B and TP2B are the most reliable samples from the data set in terms of their low C:N ratio, then they plot as expected: they are very similar to the fish specimens in terms of their $\delta^{15}N$ and $\delta^{13}C$ signatures.

The two large shark teeth, ST1 and ST2, are identified as potentially being from the extinct species of cretoxyrhinid *Cretolamna appendiculata* which are thought to be exclusively carnivorous. These large and presumably ferocious marine predators would have had a varied prey, and in the Late Cretaceous Western Interior Seaway of America are thought to have fed primarily on teleostean fishes and soft-bodied invertebrates (e.g. squid) (Shimada 2006). Repeated analyses of tooth enamel from ST1 place this shark at the highest trophic level of the organisms analysed here: $\delta^{15}N$ data average 9.1‰ and $\delta^{13}C$ average values of -8.5‰. ST2 tooth enamel gave values 1-2‰ lower than this, but very

little sample was obtained for this tooth and only one analysis was possible, so this may not be wholly representative. The smaller shark teeth ST3 and ST4 are from the extant genus *Carcharias* and gut content analyses have shown that the species *Carcharias taurus* Rafinesque, 1810 feeds largely on teleosts and elasmobranchs, with cephalopods being taken to a lesser extent (Smale 2005). Smaller individuals were found to take similar prey taxa to larger (>2m) individuals, although the larger predators broadened their trophic niche to include a greater variety of elasmobranchs and more active prey. ST3 gave average $\delta^{15}N$ values of 1.1‰ less than ST1A, suggesting that the trophic levels were similar. However, the small size of ST3 meant it was ground whole to produce enough sample for analysis and the inclusion of dentine may have reduced the reliability of the isotope data produced, as attested to by its high C:N ratio. Tooth ST4 gave much lower $\delta^{15}N$ values, 4‰ lower than ST1A, however this specimen was also ground and homogenised and includes dentine and a large proportion of root, again giving a high C:N ratio and therefore is deemed unreliable. Averaged data from *Protosphyraena* tooth enamel, PT1A, gave $\delta^{15}N$ values 1‰ lower than ST1A with a more positive result for $\delta^{13}C$, although again the high C:N ratios of these replicate samples indicate a possible unreliability. Very little is known about the diet of this extinct primitive swordfish of the Late Cretaceous, although a carnivorous diet is inferred for the >2m-long predators. Extant swordfish are known to feed on teleosts and cephalopods (Potier *et al.* 2007), thus occupying a similar trophic niche to extant *Carcharias*, and data from the Mata Amarilla specimens seem to indicate that this may have been the case in the Late Cretaceous with *Protosphyraena* and *Carcharias* giving similar isotope values. Mature modern swordfish are known to have few natural enemies, with the exception of large sharks and sperm and killer whales. The data presented in Figure 8.6 and 8.8 suggest that the large sharks in this ecosystem did not prey on *Protosphyraena*, however.

8.7.5 Possible causes of variation in the data set

This comparison of isotopic signatures from fossils found within the same formation but at slightly different levels in the stratigraphy must be treated with caution. In archaeological settings chronological differences in N and C isotope signatures in bovine bone collagen have been found to vary by as much as 10% over just a few thousand years

(Richards & Hedges 2003). If alteration of signatures has occurred within the Mata Amarilla Formation due to diagenetic processes then it is likely that the degree of alteration could be different within different units. Migration of organic matter from the enclosing sediments could occur providing a mixed isotopic signature, and as such comparisons between different units could prove problematic. Similarly, if the N and C isotope values presented in this thesis are from a secondary process of post burial bacterial ingestion, then the presence of different bacteria in freshwater and marine units would lead to differential alteration. Although no stepwise enrichments of $\delta^{15}N$ between different trophic levels with approximately 3.4‰ per trophic level are seen, a general increasing trend of N values within the hierarchy of carnivores is present. Recent research is revealing that trophic enrichment of isotopes may vary due to metabolism and specific amino acid composition of consumer tissues in life as well as diet quality and growth rate, therefore the expected 3.4‰ enrichment in $\delta^{15}N$ may be subject to large discrepancies (Mendes *et al.* 2007 and references therein). Also, in marine communities, trophic level is expected to be higher for larger individuals of the same species (Jennings *et al.* 2002), so there are many different variables to be taken into account here. However, direct comparisons within the above data set do appear to be viable based on the expected isotopic differences between ecologically distinct taxa, and N isotope ratios are thought to be indicative of trophic position within the Late Cretaceous fauna. Assuming that the $\delta^{13}C$ values are original and not diagenetic, they appear rather more positive than expected from modern ecosystem studies and data gathered from modern fish species presented in this thesis. This enriched signal may be a result of more enriched atmospheric $\delta^{13}C$ values during the Late Cretaceous, thus causing a corresponding positive shift in $\delta^{13}C$ of Cretaceous plants (Stanton-Thomas & Carlson 2004) and a continued enrichment up the food chain.

8.8 Conclusion

This study confirms the potential of using N and C bulk stable isotope ratios from hard tissues of animals of geological age to determine trophic level and palaeoecology of an extinct ecosystem. Here, bone, dentine and enamel from eight different taxa were investigated and produced promising results. Despite many possible causes of variation in

$\delta^{15}N$ and $\delta^{13}C$ isotopic composition of animals both during life and diagenesis, the data appears to be robust based on expected isotopic differences between ecologically distinct taxa. For the future, the $\delta^{18}O$ and $\delta^{13}C$ isotopic composition of the inorganic fraction of dense hard tissues could also be investigated to provide complementary information regarding physiology, palaeoenvironment and palaeotemperature. In other palaeoecological studies this has proved to be a robust technique (e.g. Zazzo *et al.* 2000; Stanton-Thomas & Carlson 2004). While the Mata Amarilla Formation has provided an excellent testing ground for the use of N and C bulk isotope ratios to determine trophic structure in a community of geological age, the main taxa from the bone bed were found to be very similar. It is suggested that all four would have occupied a similar trophic niche and this overlap means that their isotopic ratios are all similar. A future test of this bulk technique would be to identify a unit of geological age bearing numerous teeth and fossilised hard tissues of creatures from many different trophic levels. If this were possible then clearer conclusions could be drawn from their isotopic analyses as to whether this is a robust method of investigation for fossils of geological age. However, the possible effects of diagenesis would have to be evaluated for each individual palaeocommunity. Such evaluation is crucial to the reliable interpretation of bulk isotope signals from any fossil bioapatites. Preservation of original chemistry and therefore isotopic signatures in fossil bioapatite cannot be assumed. A combination of the analysis of C:N data, SEM work and evaluation of the expected trophic levels may go some way to resolve degree of diagenesis in an individual palaeocommunity.

Chapter 9: Summary of main findings and implications for future work

9.1 Research outcomes

9.1.1 Main findings

The primary aim of this PhD project was to investigate the potential of using nitrogen and organic carbon isotopes to reconstruct the feeding habit of individual taxa within, and by extension, the trophic structure of, an extinct aquatic community. Bulk N isotopes were obtained from all 165 Eocene Green River fossil fish specimens analysed and this in itself is remarkable for fish of such antiquity. However, corresponding $\delta^{13}C_{org}$ data could not be generated for the majority of these fish. The enclosing sediments are rich in organic carbon but there is no nitrogen, proving that the N isotopic data is solely from within the fluorapatite structure of the fossil fish. The significance of the data set remains unclear however, as $\delta^{15}N$ data is not consistent with the trophic levels inferred from other evidence. The six different species of fish analysed from the same bedding surface can reasonably be considered to have formed part of the same food chain. Although some would have had similar diets others are generally considered to have fed at successive trophic levels. The smaller taxa, *Knightia eocaena*, *Knightia alta*, *Diplomystus dentatus*, and *Priscacara liops*, are thought to have fed primarily on plankton in the upper water column, although the different species potentially had some variation in their dietary preferences, including insects and possibly molluscs (Grande 1984). Two of the larger species from this bedding plane, *Mioplosus labracoides* and *Phareodus encaustus* are known to have been voracious piscivores from palaeontological evidence. *M. labracoides* would have preyed on the smaller fish such as *Knightia* and *D. dentatus*, whereas *P. encaustus* would have been a major predator in the lake feeding on all the smaller fish as well as the larger *P .liops* and *M. labracoides* (Grande 1984). This clear distinction between the diet of the smaller fish species and the larger predators is not reflected in the $\delta^{15}N$ isotopic signatures of the fish however; rather the largest fish from the highest trophic level exhibited some of the lowest $\delta^{15}N$ values. Different tissues of the larger fossil fish analysed did retain different $\delta^{15}N$ values with little overlap comparable to those of an extant freshwater fish, perhaps suggesting different preservation potential of isotopic values in different tissues. Assuming inferences of trophic level among Green River fish

from previous studies are robust, the most plausible conclusion is that the $\delta^{15}N$ data obtained is largely an artefact, either of post-mortem contamination or as a result of diagenetic fractionation of the original signature. The Cretaceous Mata Amarilla Formation of southern Argentina contains a diverse, albeit fragmentary, record of biomineralized tissues such as scales and teeth of fish and sharks, as well as turtle carapace fragments and dinosaur bones. The eight taxa analysed confirm that the N and C_{org} bulk isotopes ratios from biomineralized hard tissues of animals of this age are robust, and have the potential to record the trophic level of individual taxa, on which basis the palaeoecology of the ecosystem can be reconstructed in part. Paradoxically, despite being considerably older, this set of isotope results appeared to define trophic level with greater clarity than those from the Green River fish and exhibit the expected trend of isotopic enrichment with increasing trophic level. However, in retrospect this fauna was not ideal for proving this technique beyond doubt as several taxa were opportunistic omnivores from the same horizon, lacking clear distinction of trophic level. Secondly, the suite of samples analysed were from differing palaeoenvironments from successive lithological units and were therefore not strictly from within the same ecosystem; some compromise of the isotopic signatures as a result of differences in environment, including the taphonomic history, cannot be excluded. Beyond the results of these two studies the exercise has identified, and in many cases resolved, several methodological issues relating to the preparation and isotopic analysis of fossil material.

9.1.2 Analytical problems and caveats

Difficulties in preparation of samples from F-1 localities as described in Chapter 3 Section 3.1.1 reduced the initial the sample set considerably, hindering the identification of possible spatial changes in the isotopic signal from Fossil Lake. However, the fossils collected from multiple bedding surfaces of the RH F-2 quarry proved sufficient to allow a study of any temporal change in the isotopic signatures, as well the comparison of trophic level and isotopic values from the six species collected from the same bedding surface. Despite an extensive study focussing on the carbonate removal from samples detailed in Chapter 4, it transpired that the carbonate matrix surrounding the fossils was not removed successfully from all samples using the protocol devised. As such, CF-IRMS stable

isotope analysis was carried out using the Ascarite modification described in Chapter 3 Section 3.1.5 and only $\delta^{15}N$ data retrieved for the majority of Green River fossil fish, rather than $\delta^{15}N$ plus $\delta^{13}C_{org}$ data as initially planned. This restricted the interpretation of the data to aspects relating to trophic level only and inferences regarding potential food sources could not be made. The taphonomy experiments presented in Chapter 6, designed to investigate whether changes including fractionation of $\delta^{15}N$ and $\delta^{13}C_{org}$ isotopic signature post-mortem in extant fish occur, revealed that scales are likely to be the most reliable tissues when sampling fossil fish. However, due to the very low N concentrations of the fossils, large volumes were required for CF-IRMS analysis necessitating the analysis of a mixture of both bones and scales from the Green River fossil fish. This is not ideal and may have compromised the resulting data. Similarly, for analysis of the organic matter as described in Chapter 7 a skull and vertebrae were selected for analysis due to the large sample size required and may reflect a higher exogenous component than scales from the same fish. Finally, the data presented from the Argentinean material in Chapter 8 are not representative of one ecosystem but are thought to span successive marine, freshwater and terrestrial environments. This was taken into account when analysing the resulting data set.

9.1.3 Implications for future studies

The successful removal of any carbonate matrix using an appropriate weak acid is essential prior to analysis of $\delta^{13}C_{org}$. Following the experiments described in Chapter 4, all samples for analysis should be treated in an identical manner and immersed in acid for an exact, short amount of time, to ensure that the resulting data are robust and that direct comparison within the data set can be made. Based on the results therein, 2M acetic acid, when used for less than 24 hours, had the least significant effect on the isotopic values, pH and weight of the fluorapatite fossils yet the highest potential for dissolving $CaCO_3$ when compared to the other acids used in the investigation. In future studies 2M acetic acid is recommended for the pre-treatment of fossils in the acquisition of organic isotope data and careful consideration should always be given to the time period involved if the effects on the isotope geochemistry are to be negligible. For future studies of fossil ecosystems, specimens from friable siliciclastic deposits should be targeted, thus removing the need

for any chemical pre-treatment. Once fossils are extracted from any surrounding matrix, sample sizes of up to 72mg are required for the analysis of bulk N and C isotopes and for this study necessitated the use of entire fossil fish. This is a very destructive technique at present and as advances are made in mass spectrometry and the precision of equipment increases these analyses of Green River fish should be revisited. It is suggested from the results of experiments detailed in Chapter 6 that in future only scales from these fish should be analysed. Experiments of post-mortem isotopic variation in extant fish suggested that the non-porous hard parts such as scales were better at retaining N and C_{org} isotopic signatures rather than bones. However, the $\delta^{13}C_{org}$ isotopic signature of all tissues was found to undergo significant alteration during post-mortem decay and early diagenesis and this should be taken into account in future studies. It is suggested that $\delta^{15}N$ values are more robust when analysing fossil organisms and that non-porous tissues such as enamel, scales and chitin would be the most appropriate tissues for analysis. Encouragingly, temperature, salinity and oxygenation conditions did not appear to have a direct impact on the magnitude or the direction of alteration in bulk isotopic signatures, suggesting that fossil organisms from a variety of settings could be analysed in future, regardless of their preservational environment. Many of these findings were taken into account when selecting the Mata Amarilla Formation for study and the data presented in Chapter 8 appeared to successfully replicate the trophic levels that would be expected in such an ecosystem. A low C:N ratio of samples is thought to reflect isotopic endogeneity and could be used as a proxy of relative robustness within a data set. This is proposed here as a method for identifying the degree of biodegradation and diagenesis and therefore reliability of the bulk N and C isotope values. It follows that with lower C:N ratios the alteration of N and C isotopic signatures is less likely, and conversely higher C:N ratios indicate results that should be treated with caution as the isotopic signatures may be unreliable. Any future study that takes all of these findings into account should have an increased prospect of producing a robust data set.

9.1.4 Thesis results in context

As highlighted in Chapter 1, two studies regarding trophic level in fossil organisms have been reported in the literature subsequent to the inception of this PhD project (Schweizer

et al. 2006 and 2007). Both of these studies focussed on lagerstätten from Tertiary lacustrine ecosystems and reported viable $\delta^{15}N$ and $\delta^{13}C$ values used to reconstruct trophic structure. It is useful to reassess the robustness of their findings in the light of the insights gained into potential methodological problems by the research herein. From the Oligocene Enspel lagerstätte, Germany, one species each of fossil fish and tadpole were studied from the bituminous shales in which soft tissues are preserved by bacterial biofilms, along with diatoms, plants, chitinous insects and coprolites and teeth of higher organisms (Schweizer *et al.* 2006). Critically, as the host sediment is not carbonate, no pre-treatment of their samples was necessary, apart from a crocodilian tooth which was ground and treated with 10% HCl to remove biogenic carbonate. The results presented in Chapter 4 of this thesis suggest treatment with HCl is too harsh for bioapatites and is likely to have altered the $\delta^{15}N$ and $\delta^{13}C_{org}$ signature recovered from this tooth. This would account for the erroneously low values reported. The remainder of the Enspel stable isotope data is reported to be consistent with the ecology of the taxa as inferred from other criteria although the primary focus of the study was organisms and plants at the base of the food chain. Whether the results are equally robust at higher trophic levels remains to be investigated. Absolute values of $\delta^{15}N$ for mixtures of fish soft tissue and bone were similar to those reported from the smaller Green River clupeomorphs from the ash plate discussed in Chapter 5, although the percentages of N present were an order of magnitude higher. C:N values were 22±6, much lower than those obtained from the fish of Fossil Lake, similar to the lowest values obtained from the Mata Amarilla Formation presented in Chapter 8.

The Eocene Messel lagerstätte in Germany comprises fossiliferous oil shales deposited below the anoxic benthic layer of a large maar lake (Schweizer *et al.* 2007). In this study Schweizer *et al.* (2007) also sampled fossil insects, as well as three different species of fish exhibiting preservation of the soft tissue outlines by bacterial biofilms. It is unclear precisely what was sampled of the fish, but it appears that the biofilms analysed (thought to represent soft tissues) were retrieved from different areas of each fossil carcass beneath the scales. Percentage N values reported from the three species of fossil fish were much higher than the Green River fossil fish studied herein, by up to two orders of magnitude.

$\delta^{15}N$ values from Lake Messel fish (~8‰) were slightly higher than those reported from Green River ash plate (4-6‰), with C:N values between 9.5 and 33.7. Interestingly, the highest C:N value reported for a Lake Messel fish is from the hard preserved tissues. The hard tissues from a bowfin, reported to be bones and scales, gave significantly lighter $\delta^{15}N$ signatures when compared with the bacterial biofilms preserving soft tissues of the same species. Average soft tissue values (n = 4) were found to be 5.4‰ more enriched in terms of $\delta^{15}N$ signature than the average value given for hard tissues (n = 25). Following the results of Chapter 6 in this thesis, these data for hard parts from Lake Messel may be unreliable as they include bones, as may the data from rib bones sampled from a snake in the same study. Schweizer *et al.* (2007) stated that direct comparisons could not be made between the isotope data from the fish hard parts and the biofilms, although comparisons were made between fish biofilm data and data from many plants and insects. It is suggested here that the discrepancy between the fish bone and scale $\delta^{15}N$ values and those of the biofilms could indicate that the signature reported as soft tissue may actually be an original bacterial signature, perhaps as a result of the bacterial overgrowth fractionating the soft tissues due to metabolic processes. If the N isotope values were from a secondary process of bacterial ingestion of the original tissues, any difference in isotopic signal between species should still be reflected and assumptions of trophic level from the data would therefore still be valid. Isotopic data from rare terrestrial vertebrates are also reported from Lake Messel by Schweizer *et al* (2007) which appear to have been obtained from a variety of biomineralized tissues and biofilms, with just one data point produced for each animal. This serves to highlight the difficulty of producing a rigorous data set from a census assemblage of co-existing taxa. Where taxa are rare, particularly major predators, sampling is not always possible. In the Green River Formation such rare vertebrates are of high commercial value and even small samples from whole specimens are unattainable. If access to a partial specimen can be gained, then this limits the area and type of tissue available for analysis. As discussed in Chapter 6, some tissues are thought to preserve stable isotopic values with higher fidelity than others, and comparison between partial specimens is then confounded. Overall, the preserved biofilms and organic material from Lake Enspel and Lake Messel appear to retain $\delta^{15}N$ and $\delta^{13}C_{org}$ isotopic signatures which reflect the original trophic structure of each lacustrine community with greater

success than those of the hard biomineralized tissues from Fossil Lake. The percentages of N and C preserved within the organic material described by Schweizer *et al.* (2006 and 2007) are also much higher than those found in either the Green River or Mata Amarilla fauna reported here. Preserved biofilms may retain isotopic signatures with higher fidelity than the fossilized hard tissues discussed within this thesis, however whether they entirely reflect the endogenous original signature of the fossils cannot be assumed. Whether the isotopic signatures from these Tertiary sites in Germany are original could be confirmed using organic geochemical protocol similar to that used here, in Chapter 7.

9.2 Suggestions for further work

9.2.1 Constraining isotopic shift using compound specific isotope analyses

Nitrogen isotopic distributions are widely acknowledged to be robust measures of trophic position in many modern aquatic ecosystems. $\delta^{15}N$ analysis can help to identify the main structural features in complex modern food webs, providing a time-integrated biochemical record reflecting the average consumption of prey by consumers. Although many studies of trophodynamics have been carried out using extant organisms since the discovery of $\delta^{15}N$ isotopic enrichment of organisms compared with their food source (DeNiro & Epstein 1981; Minagawa & Wada 1984; Peterson & Fry 1987), some of the original estimates of the extent of dietary isotopic shift between species have been questioned. Previous authors have assumed a dietary isotopic shift or trophic enrichment factor (TEF) of +3.4‰ per trophic level (e.g. DeNiro & Epstein 1981; Peterson & Fry 1987; Pinnegar *et al.* 2002) although Peterson & Fry (1987) reported wide variations around this average. Subsequently other substantial differences have been reported in TEF, particularly between species feeding on different diets. McCutchan *et al.* (2003) report that trophic shift was lower for consumers raised on invertebrate diets (+1.4‰) than for consumers raised on high-protein diets (+3.3‰) and was intermediate for consumers raised on plant and algal diets (+2.2‰). Other investigators have suggested that TEF may be unreliable for a single species and may even be negligible depending on prey (e.g. Jenkins *et al.* 2001; Oelbermann & Scheu 2002; Vanderklift & Ponsard 2003; Spence & Rosenheim 2005). Ratios of N isotopes can change between diet and consumer due to basal nutrient input, prey quality, C:N ratio of diet, ontogeny, taxonomic class of consumer and the

differential digestion or fractionation during assimilation and metabolic processes (Oelbermann & Scheu 2002; McCutchan *et al.* 2003; Vanderklift & Ponsard 2003; Trueman *et al.* 2005). Additionally, within a single consumer different classes of compounds (e.g. lipids) may differ considerably in their stable isotope ratio from other compounds (Jenkins *et al.* 2001). Collectively, the substantial variations reported in TEF not only between different species but also within tissues from the same individual highlight the need for further work to constrain the processes that lead to the enrichment of isotopes in extant food webs. Due to this isotopic heterogeneity many ecologists are increasingly utilising compound specific trophic level estimates using the $\delta^{15}N$ signature from individual amino acids. While essential amino acids show no TEF, non-essential amino acids of consumers show large differences of up to 7‰ above their food source (McClelland & Montoya 2002). This methodology is thought to eliminate some of the inter- and intra- species heterogeneity inherent in bulk isotopic signatures. Using gut content analyses as an independent proxy for trophic level, isotopic data from non-essential amino acids from the same animals yield the trophic level estimates predicted (Popp *et al.* 2007). It remains to be determined whether amino acids can be extracted from fossil material in any systematic fashion; compound specific isotope data from this source could however, eliminate many of the equivocal interpretations that have confounded the interpretation of the bulk isotopic information derived in the course of this study. It is recommended that any use of individual amino acids in an investigation of organisms from geological or, more plausibly, archaeological contexts should be undertaken only after an analysis of potential post-mortem change in extant organisms similar to that carried out in Chapter 6. The possibility that diagenetic alteration of any signal has occurred should not be underestimated.

9.2.2 Selection of a fossil ecosystem for future study

The N and C_{org} isotopic signatures derived from fossil organisms remain a plausible method for investigating fossil food webs, however careful consideration when selecting sites for future study is essential. The fossil fish of the Green River Formation, southwest Wyoming were chosen as the main experimental fauna for this research and a sampling strategy was devised prior to commencing the field campaign to target specific groups of

organisms. The principal fieldwork objective was to collect as many diverse fossil species as possible from assumed different trophic levels from one bedding plane, plus at least one more similar bedding plane for comparison; however this was not fully realised. Only one such bedding plane containing just six different fossil fish species with no taxa from lower trophic levels was obtained for this research. Organisms of the same species but at different stages of ontogeny were also targeted for sampling to see whether change of diet with age was preserved in their isotopic signatures. In the field mass mortality beds were found to be monospecific, with little difference in ontogenetic stage for any of the species present. Despite the wealth of literature regarding this well-studied ecosystem, the field sampling strategies constructed in advance proved unrealistic and had to be altered in the field. This highlights the need for careful site selection for future studies of the isotopic signature and trophic level of fossils in order to obtain a comprehensive fossil ecosystem. Following the recommendations in Section 9.1.3, fossils with hard parts such as enamel, scales and chitin are preferable for isotopic analysis, as are those interred in a friable, siliciclastic setting. Collectively the fossils retrieved from the Mata Amarilla Formation, although meeting many of these recommendations, were from too similar a trophic level to unequivocally prove that the bulk stable isotope technique can work in a fossil ecosystem of geological age. Taking these experiences into account a set of criteria can be identified that future sites should meet. A clearly hierarchical ecosystem with many trophic levels including different primary producers, crustacea, fish and major reptilian predators should be sought for a future study. Different ontogenetic stages, ideally coeval examples thereof, are required to address whether there are dietary shifts with ontogeny in fossil organisms; this could be instrumental in proving that this technique is viable in a different setting. Assuming the preservation of relevant biomolecules, compound specific stable isotope analyses supplementing, or instead of, bulk isotope data may offer greater insight into the preservation of these dietary signals.

9.2.3 Proxies for diagenetic alteration of fossil fluorapatite

As a proxy for diagenetic change the method of using C:N ratios can only be used as a first approximation at this point in time, showing relative reliability within a data set. Further work to produce a suite of results for a similar extant aquatic community would

provide the framework on which to take this idea further by producing absolute values for different genera and their skeletal tissues. Another possible method for assessing the degree of diagenetic change in fossil organisms would be to investigate the rare earth element (REE) content and oxygen isotopes from phosphatic remains. The analysis of the suite of REE elements present combined with phosphatic and biogenic carbonate $\delta^{18}O$ values can provide an insight into whether these signals are endogenous to the organism, or are partially or completely diagenetic due to groundwater exchange and late stage diagenesis involving recrystallisation of the apatite in the presence of aqueous fluids (e.g. Lécuyer *et al.* 2003). Potentially, if information regarding the physiology and thermal regime of the vertebrates analysed is likely to have survived diagenetic exchange, the likelihood of diagenetic alteration of $\delta^{15}N$ and $\delta^{13}C_{org}$ signatures may also be reduced. If $\delta^{18}O$ data are found to be robust then it would also be useful for gathering more information regarding changing temperature in lacustrine environments such as Fossil Lake. Whole rock carbonate $\delta^{18}O$ data presented in Chapter 5 showed strong covariance with $\delta^{13}C_{carbonate}$, suggesting a closed-lake system thus eliminating the possibility of palaeotemperature reconstructions. $\delta^{18}O$ data from fossil bones and teeth can offer a means of providing palaeotemperature estimates (e.g. Koch *et al.* 1995; Fricke *et al.* 1998; Showers *et al.* 2002) and this may be useful in other similar settings. Where possible, multiple-taxon comparisons using data from coexisting homeothermic and heterothermic animals also has an advantage in that it does not assume modern day mean annual temperature ^{18}O gradients for the past (e.g. Matson & Fox 2008).

9.2.4 Further work regarding the palaeoenvironment of Fossil Lake

Whole rock samples were collected from the Green River Formation for geochemical analyses using various well established methodologies. These results have improved our understanding of the geology and chemostratigraphy of Fossil Lake and complement the trophic level data collected for this study. In particular, the strong covariance of the $\delta^{13}C$ and $\delta^{18}O$ data produced suggests that the carbonate precipitated in a closed-lake system where the water had a long residence time (Talbot 1990). The succession analysed was of insufficient length to infer the presence of large-scale variations such as Milankovitch cycles or to identify small-scale annual to decadal variations. This is the first time that

$\delta^{13}C$ and $\delta^{18}O$ data have been reported from the carbonates of Fossil Lake and it appears that a future isotopic study of the carbonate phases at high resolution throughout the entire succession could proffer robust detailed information regarding hydrological changes in the basin. The collection of $\delta^{13}C$ and $\delta^{18}O$ data coupled with precise stratigraphic measurements offers a potential method to test the role that astronomical cycles played in driving such changes. Although characterisation of the organic matter within the fish from Fossil Lake presented in Chapter 7 did not clarify the chemical origin of the ancient isotopic signatures, lipids from both sediment and fossil samples did provide information on the original assemblage of micro-organisms present in Fossil Lake during the late Early Eocene. The absence of 2-methylhopanoids in all FAMEs profiles and the lack of archaeol in all polar fraction profiles imply the complete absence of cyanobacteria and Archaea respectively, at time of deposition. However, the presence of dinosterane in the apolar fractions indicates an abundance of dinoflagellates and thus presents a possible mechanism for the mass mortality horizons in Fossil Lake. Although a combination of factors are probable, dinoflagellate blooms are suggested here to have been a major cause of fish mass mortality events. This hypothesis can be tested by carrying out further lipid analysis on other fish-bearing horizons and, most importantly, on sedimentary units that do not contain fish fossils, referred to locally by quarry workers as the 'Dead Zone'. The confirmation that other fish horizons contain dinosteroids, but samples devoid of fossil fish also lack dinoflagellate biomarkers would be strong support for the hypothesis. Further CHN analyses may also verify the presence of algal blooms at time of deposition in Fossil Lake; higher TOC values would be expected due to the increased volume of planktonic biomass. In Lake Enspel it has been suggested that periodic ash falls may have enhanced nutrient supply to the lake resulting in algal blooms (Schwark *et al.* 1995). Inputs of terrestrial iron-rich dust have long been thought to influence primary productivity in the neritic zone of the oceans, instigating large phytoplankton blooms (Martin 1991). Whether Fe from volcanic sources would be bioavailable is unclear. In Fossil Lake the regular volcanic ash deposits may have instigated toxic dinoflagellate blooms, leading to the observed mass mortality horizons of fish and other organisms. However, the mass mortality events in Fossil Lake do not appear to correlate with ash

deposition, as would be expected if plankton blooms were influenced by ash fall. Further research could be carried out to clarify this matter.

9.2.5 Suggestions for future biomarker analyses of Fossil Lake fish

Further work is required to irrefutably characterise the nature of the degraded organic matter present in the fish of Eocene Fossil Lake. Fourier transform infrared (FTIR) spectroscopy could offer a way to confirm the presence or absence of preserved collagen (see Salamon *et al.* 2005); equally matrix-assisted laser desorption/ionization–mass spectrometry (MALDI–MS) is emerging as a new tool for collagen identification (see Buckley *et al.* 2008b). Immunological response could also be investigated, to see whether the antigens consistent with fossil collagen exist within the fish (e.g. Schweitzer *et al.* 2002), as could the microstructure of any remaining collagen by transmission electron microscopy (TEM) (e.g. Schweitzer *et al.* 2007b). Continued analyses and interpretation of lipid preservation using techniques such as py-GC-MS and GC-IRMS may also serve to elucidate this problem. Compound specific isotope measurements could be employed to clarify the contributions of different molecules to the bulk isotopic signatures produced herein. Pyrolysis-gas chromatography-mass spectrometry (py-GC-MS) could further characterise the original composition and structure of the ancient macromolecules preserved in the specimens (see Yang *et al.* 2005) and is favoured as an integral aspect of any future work. The techniques used in Chapter 7 for the extraction of lipids are bulk techniques requiring approximately 10g of sample, necessitating use of the large *Phareodus* fossil endoskeletons discussed previously. Using these techniques for other fossil sites and for compound specific isotope studies would continue to restrict investigations to larger specimens (in practice probably predators) due to the sample sizes required for lipid extraction prior to amino acid analysis. If future compound specific analyses were to be carried out then alternative techniques should be explored. Usefully, py-GC-MS uses only minimal amounts (0.5-2mg) of lipid-extracted residue and extant fish could also be analysed for comparison. As discussed in Chapter 6, scales from the fossil fish may provide a more reliable source of original organic matter than the bone and py-GC-MS provides a tool for their analysis. The organic geochemistry aspect of this project was the least explored; further study of this complex series of ancient organic molecules and their diagenetic reactions is a challenging and exciting prospect.

References

Agassiz, J. L. R. (1832). Untersuchungen über die fossile Fische der Lias-Formation. *Neues Jahrbuch für Mineralogie, Geologie und Paläontologie* **3** 130-149.

Agassiz, J. L. R. (1843). *Recherches sur les poisons fossils*. Imprimérie de Petitpierre, Neuchâtel, Switzerland 1420pp.

Aldridge, R. J. (1990). *Extraction of Microfossils*. **In:** Briggs, D. E. G. and Crowther, P. R. (Eds.). Palaeobiology - A synthesis. Blackwell Scientific, Oxford, UK. 583pp.

Ambrose, P., Bartels, W. S., Gunnell, G. F. and Williams, E.M. (1997). Stratigraphy and vertebrate paleontology of the Wasatch Formation, Fossil Butte National Monument, Wyoming. *Journal of Vertebrate Paleontology* **17**(3) 29.

Ambrose, S. H. and Norr, L. (1993). *Experimental evidence for the relationship of carbon isotope ratios of whole diet and dietary protein to those of bone collagen and carbonate*. **In:** Lambert, J. B. and Grupe, G. (Eds.). Prehistoric Human Bone: Archaeology at the Molecular Level. Springer-Verlag, Berlin, Germany 1–37pp.

Ameghino, F. (1898). Sinopsis geológico-paleontológica de la Argentina. **In:** Secundo Censo Nacional de la República Argentina: *Territorio* **1** 115-228.

Adanson, M. (1763). *Familles de Plantes* **2**. Vincent, Paris, France. 640pp.

Arambourg, C. and Bertin, L. (1958). On the fossil fishes found by Mr. Gardner in the Province of Ceará, in the North of Brazil. *Edinburgh New Philosophical Journal* **30** 82–84.

Arrington, D. A. and Winemiller, K. O. (2002). Preservation effects on stable isotope analysis of fish muscle. *Transactions of the American Fisheries Society* **131**(2) 337-342.

Asara, J. M., Schweitzer, M. H., Freimark, L. M., Phillips, M. and Cantley, L. C. (2007). Protein sequences from Mastadon and *Tyrannosaurus Rex* revealed by mass spectrometry. *Science* **316** 280-285.

Ascaso, C., Wierzchos, J., Speranza, M., Gutiérrez, J. C., González, A. M., de los Ríos, A. and Alonso, J. (2005). Fossil protists and fungi in amber and rock substrates. *Micropaleontology* **51**(1) 59-72.

Avci, R., Schweitzer, M. H., Boyd, R. D., Wittmeyer, J. L., Terán Arce, F. and Calvo, J. O. (2005). Preservation of bone collagen from the Late Cretaceous period studied by immunological techniques and atomic force microscopy. *Langmuir* **21**(8) 3584-3590.

Bada, J. L., Wang, X. S. and Hamilton, H. (1999). Preservation of key biomolecules in the fossil record: current knowledge and future challenges. *Philosophical Transactions of the Royal Society of London. Series B: Biological Sciences* **354**(1379) Molecular Information and Prehistory 77-87.

Balasse, M., Bocherens, H. and Mariotti, A. (1999). Intra-bone variability of collagen and apatite isotopic composition used as evidence of a change of diet. *Journal of Archaeological Science* **26** 593–598.

Balogh, B., Wilson, D. M. and Burlingame, A. L. (1971). Carbon-13 NMR study of the stereochemistry of steranes from oil shale of the Green River formation (Eocene). *Nature* **233**(5317) 261-263.

Balter, V., Saliège, J-F., Bocherens, H. and Person, A. (2002). Evidence of physico-chemical and isotopic modifications in archaeological bones during controlled acid etching. *Archaeometry* **44**(3) 329-336.

Balzer, A., Gleixner, G., Grupe, G., Schmidt, H-L., Schramm, S. and Turban-Just, S. (1997). *In vitro* decomposition of bone collagen by soil bacteria: the implications for stable isotope analysis in archaeometry. *Archaeometry* **39**(2) 415-429.

Barker, S., Greaves, M. and Elderfield, H. (2003). A study of cleaning procedures used for foraminiferal Mg/Ca paleothermometry. *Geochemistry Geophysics Geosystems* **4**(9) 1525-2027.

Barrick, R. E. and Showers, W. J. (1994). Thermophysiology of *Tyrannosaurus rex*: evidence from oxygen isotopes. *Science* **265** 222-224.

Barthel, K. W., Swinburne, N. H. M. and Conway Morris, S. (1990). *Solnhofen: A study in Mesozoic palaeontology.* Cambridge University Press, Cambridge, UK. 236pp.

Bauld, J. (1981). Occurrence of benthic microbial mats in saline lakes. *Hydrobiologia* **81** 87-111.

Beltrán, M., Fernández-Borrás, J., Médale, F., Pérez-Sánchez, J., Kaushik, S. and Blasco, J. (2009). Natural abundance of ^{15}N and ^{13}C in fish tissues and the use of stable isotopes as dietary protein tracers in rainbow trout and gilthead sea bream. *Aquaculture Nutrition* **15** 9-18.

Benton, R. C., Buchheim, H. P. and Grande, L. (1994). *Paleontology, sedimentology and paleoenvironments of Eocene Fossil Lake: Field trip guide.* **In:** Benton, R. C. and Elder, A. (Eds.). Proceedings of the third conference on fossil resources in the National Park Service. *Natural Resources Report NPS/NRFOBU/NRR-94/14* 87-98.

Berg, L. S. (1940). Classification of fishes both recent and fossil. *Trudy Zoologicheskogo Instituta, Akademia Nauk S.S.S.R., Leningrad* **5** 346–517.

Berg, L. S. (1958). *System der rezenten und fossilen Fischartigen und Fische.* Deutsche Verlag Wissenschaft, Berlin, Germany 310pp.

Berman-Frank, I., Zohary, T., Erez, J. and Dubinsky, Z. (1994). CO_2 availability, carbonic anhydrase, and the annual dinoflagellate bloom in Lake Kinneret. *Limnology and Oceanography* **39**(8) 1822-1834.

Beynon, R. J. & Easterby, J. S. (1996). Buffer solutions, the basics. IRL Press at Oxford University Press, Oxford, UK. 84pp.

Billon-Bruyat, J., Lécuyer, C., Martineau, F. and Mazin, J. (2005). Oxygen isotope compositions of Late Jurassic vertebrate remains from lithographic limestones of western Europe: implications for the ecology of fish, turtles, and crocodilians. *Palaeogeography, Palaeoclimatology, Palaeoecology* **216**(3-4) 359-375.

Biaggi, R. E. and Buchheim, H. P. (1999). Paleoecology and paleoenvironments during the initial stages of Eocene Fossil Lake, SW Wyoming. *National Park Service Paleontological Research* **4** 54-65.

Biaggi, R. E., Buchheim, H. P. and Cushman, R. A. (2000). Deposition of a laminated, fossil rich facies in a nearshore oxic paleoenvironment, Eocene Lake Gosiute, Wyoming. *Geological Society of America Abstracts with Programs* **32**(7).

Blake, R. E., O'Neil, J. R. and Garcia, G. A. (1997). Oxygen isotope systematics of biologically mediated reactions of phosphate: I. Microbial degradation of organophosphorus compounds. *Geochimica et Cosmochimica Acta* **61**(20) 4411-4422.

Bocherens, H., Fizet, M., Mariotti, A., Lange-Badre, B., Vandersmeech, B., Borel, J. P. and Bellon, G. (1991). Isotopic biogeochemistry ^{13}C, ^{15}N of fossil vertebrate collagen: application to the study of a past food web including Neanderthal man. *Journal of Human Evolution* **20** 481-492.

Bohacs, K. M., Carroll, A. R., Pietras, J., Rhodes, M. and Smith, M. (2002). Evolution of the great lakes system of the Green River Formation: tectonically & topographically conditioned records of climate change. *Geological Society of America Abstracts with Programs* **34**(6).

Bonsall, C., Lennon, R., McSweeney, K., Stewart. C., Harkness, D., Boronean, V., Bartosiewicz, L., Payton, R. and Chapman, J. (1997). Mesolithic and Early Neolithic in the Iron Gates: a palaeodietary perspective. *Journal of European Archaeology* **5**(1) 50-92.

Bosley, K. L. and Wainright, S. C. (1999). Effects of preservatives and acidification on the stale isotope ratio (^{15}N:^{14}N, ^{13}C:^{12}C) of two species of marine animals. *Canadian Journal of Fisheries and Aquatic Sciences* **56**(11) 2181-2185.

Bradley, W. H. (1929). *Varves and Climate of the Green River Epoch.* **In:** US Geological Survey Professional Paper **158** 87-110.

Bradley, W. H. (1948). Limnology and the Eocene Lakes of the Rocky Mountain region. *Geological Society of America Bulletin* **59**(7) 635-648.

Bradley, W. H. and Eugster, H. P. (1969). Geochemistry and paleolimnology of the trona deposits and associated authigenic minerals of the Green River Formation of Wyoming. *Geological Survey Professional Paper* **496B** 1-71.

Briggs, D. E. G. (1995). Experimental taphonomy. *Palaios* **10**(6) 539-550.

Briggs, D. E. G. (1999). Molecular taphonomy of animal and plant cuticles: selective preservation and diagenesis. *Philosophical Transactions of the Royal Society of London. Series B: Biological Sciences* **354**(1379) 7-17.

Briggs, D. E. G. (2003). The role of decay and mineralization in the preservation of soft-bodied fossils. *Annual Review of Earth and Planetary Sciences* **31** 275-301.

Briggs, D. E. G., Evershed, R. P. and Lockheart, M. J. (2000). The biomolecuar paleontology of continental fossils. *Paleobiology* **26**(4) 169-193.

Briggs, D. E. G. and Kear, A. J. (1993). Fossilization of soft tissue in the laboratory. *Science* **259** 1439-1442.

Briggs, D. E. G. and Kear, A. J. (1994). Decay and mineralization of shrimps. *Palaios* **9**(5) 431-456.

Britton, D. R. and Buchheim, H. P. (2002). A taphonomic assessment of the stratified lake model. *Geological Society of America Abstracts with Programs* **34**(6).

Brocks, J. J., Buick, R., Summons, R. E, and Logan, G. A. (2003). A reconstruction of Archean biological diversity based on molecular fossils from the 2.78 to 2.45 billion-year-old Mount Bruce Supergroup, Hamersley Basin, Western Australia. *Geochimica et Cosmochimica Acta* **67**(22) 4321-4335.

Brocks, J. J., Logan, G. A., Buick, R. and Summons, R. E. (1999). Archean molecular fossils and the early rise of eukaryotes. *Science* **285** 1033-1036.

Buchheim, H. P. (1994a). Paleoenvironments, Lithofacies and Varves of the Fossil Butte Member of the Eocene Green River Formation, Southwestern Wyoming. *Contributions to Geology, University of Wyoming* **30**(1) 3-14.

Buchheim, H. P. (1994b). Eocene Fossil Lake, Green River Formation, Wyoming: A history of fluctuating salinity, **in:** Sedimentology and Geochemistry of Modern and Ancient Saline Lakes, *SEPM Special Publication* **50** 239-247.

Buchheim, H. P. (1998). A walk through time at Fossil Butte: historical geology of the Green River Formation at Fossil Butte National Monument. *National Park Service Technical Report* NPS/NRGRD/GRDTR-98/01 73-80.

Buchheim, H. P., Biaggi, R. E. and Cushman, R. A. (2004). Evolution of Fossil Lake, Wyoming during deposition of the Eocene Green River Formation. *Geological Society of* America *Abstracts with Programs* **36**(5) 35.

Buchheim, H. P. and Eugster, H. P. (1998). Eocene Fossil Lake: The Green River Formation of Fossil Basin, southwestern Wyoming, **In:** Pitman, J. K. and Carroll, A.R. (Eds.), Modern and ancient lake systems; new problems and perspectives. *Utah Geological Association Publication* **26** 191–208.

Buchheim, H. P., Loewen, M. A., Cushman, R. A. and Biaggi, R. E. (2002). Stratigraphic revision of the Green River Formation in fossil basin, Wyoming: three distinct phases of Fossil Lake. *Geological Society of America Abstracts with Programs* **34**(6).

Buchheim, H. P. and Surdam, R. C. (1977). Fossil catfish and the depositional environment of the Green River Formation, Wyoming. *Geology* **5**(4) 196 - 198.

Buckley, M., Collins, M. and Thomas-Oates, J. (2008b). A method of isolating the collagen (I) ∗2 chain carboxytelopeptide for species identification in bone fragments. *Analytical Biochemistry* **374**(2) 325-334.

Buckley, M., Walker, A., Ho, S. Y. W., Yang, Y., Smith, C., Ashton, P., Oates, J. T., Cappellini, E., Koon, H., Penkman, K., Elsworth, B., Ashford, D., Solazzo, C., Andrews, P., Strahler, J.,

Shapiro, B., Ostrom, P., Gandhi, H., Miller, W., Raney, B., Zylber, M. I., Gilbert, M. T. P., Prigodich, R. V., Ryan, M., Rijsdijk, K. F., Janoo, A. and Collins, M. J. (2008a). Comment on "Protein Sequences from Mastodon and Tyrannosaurus rex Revealed by Mass Spectrometry". *Science* **319** 33c.

Bull, I. D., Van Bergen, P. F., Poulton, P. R. and Evershed, R. P. (1998). Organic geochemical studies of soils from the Rothamsted Classical Experiments-II, Soils from the Hoosfield Spring Barley Experiment treated with different quantities of manure. *Organic Geochemistry* **28**(1-2) 11-26.

Bunn, S. E., Loneragan, N. R. and Kempster, M. A. (1995). Effects of acid washing on stable isotope ratios of C and N in panaeid shrimp and seagrass: Implications for food-web studies using multiple stable isotopes. *Limnology and Oceanography* **40**(3) 622-625.

Butterfield, N. J., Balthasar, U. and Wilson, L. A. (2007). Fossil diagenesis in the Burgess Shale. *Palaeontology* **50**(3) 537-543.

Buscalioni, A. D., Fregenal, M. A., Bravo, A., Poyato-Ariza, F. J., Sanchíz, B., Báez, A. M., Cambra Moo, O., Martín Closas, C., Evans, S. E. and Marugán Lobón, J. (2008). The vertebrate assemblage of Buenache de la Sierra (Upper Barremian of Serrania de Cuenca, Spain) with insights into its taphonomy and palaeoecology. *Cretaceous Research* **29**(4) 687-710.

Cabana, G. and Rasmussen, J. B. (1994). Modelling food chain structure and contaminant bioaccumulation using stable nitrogen isotopes. *Nature* **372** 255-257.

Carabel, S., Godínez-Domínguez, E., Verísimo, P., Fernández, L. and Freire, J. (2006). An assessment of sample processing methods for stable isotope analyses of marine food webs. *Journal of Experimental Marine Biology and Ecology* **336** 254–261.

Carpenter, S. R. (1996). Microcosm experiments have limited relevance for community and ecosystem ecology. *Ecology* **77**(3) 677-680.

Carroll, A. R., Chetel, L. M. and Smith, M. E. (2006). Feast to famine: Sediment supply control on Laramide basin fill. *Geology* **34**(3) 197-200.

Carroll, A. R., Smith, M. E., Pietras, J. T., Rhodes, M. K. and Singer, B. (2002). Accumulation rates in ancient lakes: relationship to lake type evolution of the Green River Formation, Wyoming. *Geological Society of America Abstracts with Programs* **34**(6).

Chandler, M. R. (2006). The provenance of Eocene tuff beds in the Fossil Butte Member of the Green River Formation, Wyoming: Relation to the Absaroka and Challis volcanic fields. Unpublished M.S. thesis. Brigham Young University, Provo, Utah, USA. 89pp.

Chase, C. G., Gregory-Wodzicki, K. M., Parrish, J. T. and DeCelles, P. G. (1998). *Topographic history of the Western Cordillera of North America and controls on climate.* **In:** Crowley, T. J. and Burke, K. (Eds.). Tectonic Boundary Conditions for Climate Reconstruction. Oxford University Press, New York, USA. 285pp.

Cherel, Y. and Hobson, K. A. (2005). Stable isotopes, beaks and predators: a new tool to study the trophic ecology of cephalopods, including giant and colossal squids. *Proceedings of the Royal Society B: Biological Sciences* **272** 1601-1607.

Child, A. M. (1995). Towards an Understanding of the Microbial Decomposition of Archaeological Bone in the Burial Environment. *Journal of Archaeological Science* **22**(2) 165-174.

Church, M. and Buchheim, H. P. (2002). Varves and varve-derived climate cycles? Evidence from Eocene Fossil Lake, Green River Formation. *Geological Society of America Abstracts with Programs* **34**(6) 555.

Cione, A. L., Gouiric, S., Goin, F. and Poiré, D. G. (2007). *Atlantoceratodus*, a new genus of lungfish from the upper Cretaceous of South America and Africa. *Revista Museo La Plata, Paleontología* **10** (62) 1-12.

Close, B., Banister, K., Baumans, V., Bernoth, E-M., Bromage, N., Bunyan, J., Erhardt, W., Flecknell, P., Gregory, N., Hackbarth, H., Morton, D. and Warwick, C. (1997). Recommendations for euthanasia of experimental animals: part 2. European Commission Working Party Report, *Laboratory Animals* **31** 1-32.

Collister, J. W., Summons, R. E., Lichtfouse, E. and Hayes, J. M. (1992). An isotopic biogeochemical study of the Green River oil shale. *Organic Geochemistry* **19**(1-3) 265-276.

Compagno, L. J. V. (1977). Phyletic relationships of living sharks and rays. *American Zoologist* **17** 303–322.

Connolly, R. M. (2003). Differences in trophodynamics of commercially important fish between artificial waterways and natural coastal wetlands. *Estuarine, Coastal and Shelf Science* **58**(4) 929-936.

Constenius, K. N. (1996). Late Paleogene extensional collapse of the Cordilleran foreland fold and thrust belt. *Geological Society of America Bulletin* **108** 20 – 39.

Cooper, J. E. and Evans, W. S. (1983). Ammonium-nitrogen in Green River Formation oil shale. *Science* **219**(4584) 492-493.

Cope, E. D. (1865). Third contribution to the herpetology of tropical America. *Proceedings of the Academy of Natural Sciences of Philadelphia* **1865** 185-198.

Cope, E. D. (1871). On the fishes of the Tertiary shales of Green River, Wyoming Territory. *U.S Geological and Geographical Survey of the Territories Annual Report* **4**.

Cope, E. D. (1877). A contribution to the knowledge of the ichthyological fauna of the Green River Shales. *Bulletin of the United States Geological and Geographical Survey of the Territories* **3**(4) 807-819.

Cope, E. D. (1878). Descriptions of fishes from the Cretaceous and Tertiary deposits west of the Mississippi River. *U.S Geological and Geographical Survey of the Territories Bulletin* **4**(1) 67-77.

Cope, E. D. (1883). A new chondrostean from the Eocene. *American Naturalist* **17** 1152-1153.

Cope, E. D. (1884). The vertebrata of the Tertiary Formations of the West. *U.S Geological and Geographical Survey of the Territories Report* **3**(1) 1-1009.

Cope, E. D. (1885). Eocene paddle-fish and Gonorhynchidae. *American Naturalist* **19** 1090-1091.

Cope, E. D. (1887). Zittel's manual of palaeontology. *American Naturalist* **21** 1014–1019.

Crowley, K. D., Cuchon, C. E. and Rhi, J. (1986). Climate Record in Varved Sediments of the Eocene Green River Formation. *Journal of Geophysical Research* **91**(D8) 8637-8647.

Crowson, R. A. and Showers, W. J (1991). Preparation of phosphate samples for oxygen isotope analysis. *Analytical Chemistry* **63** 2397-2400.

Cushman, R. A. J. (2002). Vegetational History and Age of the Green River Formation in Fossil Basin, Wyoming. *Geological Society of America Abstracts with Programs* **34**(6).

Cuvier, G. (1825). Recherches sur les Ossements fossiles, oú l'on rérablit les charactères de plusieurs animaux dont les revolutions du globe ont dètruit les espèces. Third Edition **5** (2). Dufour and D'Ocagne, Paris, France 547pp.

Davis, P. G. and Briggs, D. E. G. (1998) The impact of decay and disarticulation on the preservation of fossil birds. *Palaios* **13**(1) 3-13.

DeCelles, P. G. (2004). Late Jurassic to Eocene Evolution of the Cordilleran thrust neslt and foreland basin system, western USA. *American Journal of Science* **304** 105-168.

DeLucia, E. H., Casteel, C. L., Nabity, P. D. and O'Neill, B. F. (2008). Insects take a bigger bite out of plants in a warmer, higher carbon dioxide world. *Proceedings of the National Academy of Sciences* **105**(6) 1781-1782.

DeNiro, M. J. and Epstein, S. (1978). Infuence of diet on the distribution of carbon isotopes in animals. *Geochimica et Cosmochimica Acta* **42** 495-506.

DeNiro, M. J. and Epstein, S. (1981). Influence of diet on the distribution of nitrogen isotopes in animals. *Geochimica et Cosmochimica Acta* **45** 341-351.

DeNiro, M. J. and Weiner, S. (1988). Organic matter within crystalline aggregates of hydroxyapatite: A new substrate for stable isotopic and possibly other biogeochemical analyses of bone. *Geochimica et Cosmochimica Acta* **52**(10) 2415-2423.

Denys, C. (2002). Taphonomy and experimentation. *Archaeometry* **44**(3) 469-484.

Derenne, S., Knicker, H., Largeau, C. and Hatcher, P. (1998). *Timing and mechanisms of changes in nitrogen functionality during biomass fossilization.* **In:** Stankiewicz, B. A. and van Bergen, P. F. (Eds.). Nitrogen-containing macromolecules in the bio- and geosphere. American Chemical Society, Washington, DC, USA. 370pp.

Dodson, P. (1990). *Sauropod palaeoecology.* **In:** Weishampel, D. B., Dodson, P. and Osmolska, H. (Eds.). The Dinosauria. University of California Press, Berkeley, USA. 756pp.

Doemel, W. N. and Brock, T. D. (1976). Vertical distribution of sulfur species in benthic algal mats. *Limnology and Oceanography* **21**(2) 237-244.

Drucker, D. and Bocherens, H. (2004). Carbon and nitrogen stable isotopes as tracers of change in diet breadth during middle and upper Palaeolithic in Europe. *International Journal of Osteoarchaeology* **14** 162–177.

Dunne, J. A., Williams, R. J., Martinez, N. D., Wood, R. A. and Erwin, D. H. (2008). Compilation and network analyses of Cambrian food webs. *PLoS Biology* **6**(4) e102.

Edmonds, J. S., Steckis, R. A. Moran, M. J., Caputi, N. and Morita, M. (2005). Stock delineation of pink snapper and tailor from Western Australia by analysis of stable isotope and strontium/calcium ratios in otolith carbonate. *Journal of Fish Biology* **55**(2) 243-259.

Eglinton, G, Douglas, A. G., Maxwell, J. R., Ramsay, J. N. and Ställberg-Stenhagen, S. (1966). Occurrence of isoprenoid fatty acids in the Green River shale. *Science* **153**(3740) 1133-1135.

Eglinton, G. and Logan, G. A. (1991) Molecular Preservation. *Philosophical Transactions of the Royal Society of London. Series B: Biological Sciences* **333**(1268) Molecules Through Time: Fossil Molecules and Biochemical Systematics 315-328.

Elderfield, H., Vautravers, M. and Cooper, M. (2002). The relationship between shell size and Mg/Ca, Sr/Ca, $\delta^{18}O$, and $\delta^{13}C$ of species of planktonic foraminifera. *Geochemistry Geophysics Geosystems* **3**(8) 1-13.

Elsdon, T. S., Wells, B. K., Campana, S. E., Gillanders, B. M., Jones, C. M., Limburg, K. E., Secor, D. H., Thorrold, S. R. and Walther, B. D. (2008). Otolith chemistry to describe movements and life-history parameters of fishes: hypotheses, assumptions, limitations and inferences. *Oceanography and Marine Biology: An Annual Review* **46** 297-330.

Evershed, R. P., Dudd, S. N., Charters, S., Mottram, H., Stott, A. W., Raven, A., van Bergen, P. F. and Bland, H. A. (1999). Lipids as Carriers of Anthropogenic Signals from Prehistory. *Philosophical Transactions of the Royal Society of London. Series B: Biological Sciences* **354**(1379) 19-31.

Fahy, E., Subramaniam, S., Brown, H. A., Glass, C. K., Merrill, Jr., A. H., Murphy, R. C., Raetz, C. R. H., Russell, D. W., Seyama, Y., Shaw, W., Shimizu, T., Spener, F., van Meer, G., VanNieuwenhze, M. S., White, S. H., Witztum, J. L. and Dennis, E. A. (2005). A comprehensive classification system for lipids. *Journal of Lipid Research* **46**(5):839-862.

Fensome, R. A., Macrae, R. A., Moldowan, J. M., Taylor, F. J. R. and Williams, G. L. (1996). The early Mesozoic radiation of dinoflagellates. *Paleobiology* **22** 329-338.

Ferber, C. T. and Wells, N. A. (1995). Paleolimnology and taphonomy of some fish deposits in "Fossil" and "Uinta" Lakes of the Eocene Green River Formation, Utah and Wyoming. *Palaeogeography, Palaeoclimatology, Palaeoecology* **117** (3) 185-210.

Fernández-Jalvo, Y., Sánchez-Chillón, B., Andrews, P., Fernández-López, S. and Alcalá Martínez, L. (2002a). Morphological taphonomic transformations of fossil bones in continental environments, and repercussions on their chemical composition. *Archaeometry* **44**(3) 353-361.

Fernández-Jalvo, Y., Sánchez-Chillón, B. and Alcalá, L. (2002b). The fourth international meeting on bone diagenesis. *Archaeometry* **44**(3) 315-318.

Fischer, A., Olsen, J., Richards, M., Heinemeier, J., Sveinbjörnsdóttir, A. E. and Bennike, P. (2007). Coast-inland mobility and diet in the Danish Mesolithic and Neolithic: evidence from stable isotope values of humans and dogs. *Journal of Archaeological Science* **34** 2125-2150.

Fischer, A. G. and Roberts, L. T. (1991). Cyclicity in the Green River Formation (Lacustrine Eocene) of Wyoming. *Journal of Sedimentary Petrology.* **6**(7) 1146-1154.

Fischer, P., Rademacher, K. and Kils, U. (1991). *In situ* investigations on the respiration and behaviour of the eelpout *Zoarces viviparous* under short-term hypoxia. *Marine Ecology Progress Series* **88** 181-184.

Fleming, L. E., Backer, L. C. and Baden, D. G. (2005). Overview of Aerosolized Florida Red Tide Toxins: Exposures and Effects. *Environmental Health Perspectives* **113**(5) 618–620.

Fowler, M. E. and Cubas, Z. S. (2001). *Biology, Medicine, and Surgery of South American Wild Animals*. Blackwell Publishing, Boston, USA 536pp.

France, C. A. M., Zelanko, P. M., Kaufman, A. J. and Holtz, T. R. (2007). Carbon and nitrogen isotopic analysis of Pleistocene mammals from the Saltville Quarry (Virginia, USA): Implications for trophic relationships. *Palaeogeography, Palaeoclimatology, Palaeoecology* **249** 271–282.

France, R. (1995). Stable nitrogen isotopes in fish: literature synthesis on the influence of ecotonal coupling. *Estuarine, Coastal and Shelf Science* **41**(6) 737-742.

Franzese, J., Spalletti, L., Gómez Pérez, I. and Macdonald, D. (2003). Tectonic and paleoenvironmental evolution of Mesozoic sedimentary basins along the Andean foothills of Argentina (32°–54°S). *Journal of South American Earth Sciences* **16**(1) 81-90.

Fricke, H. C., Clyde, W. C. O'Neil, J. R. and Gingerich, P. D. (1998). Evidence for rapid climate change in North America during the latest Paleocene thermal maximum: oxygen isotope compositions of biogenic phosphate from the Bighorn Basin (Wyoming). *Earth and Planetary Science Letters* **160** 193-208.

Friedman, M., Tarduno, J. A. and Brinkman, D. B. (2003). Fossil fishes from the high Canadian Arctic: further palaeobiological evidence for extreme climatic warmth during the Late Cretaceous (Turonian–Coniacian). *Cretaceous Research* **24** 615–632.

Froehlich, D. J. and Breithaupt, B. H. (1998). Mammals from the Eocene epoch Fossil Butte Member of the Green River Formation, Fossil Basin, Wyoming. *Journal of Vertebrate Paleontology* **18**(3) 43–44.

Fry, B. (1988). Food web structure on Georges Bank from stable C, N, and S isotopic compositions. *Limnology and Oceanography* **33**(5) 1182-1190.

Georges, A. (1982). Diet of the Australian freshwater turtle *Emydura krefftii* (Chelonia: Chelidae), in an unproductive lentic environment. *Copeia* **1982**(2) 331-336.

Ghosh, P., Adkins, J., Affek, H., Balta, B., Guo, W. F., Schauble, E. A., Schrag, D. and Eiler, J. M. (2006). ^{13}C-^{18}O bonds in carbonate minerals: a new kind of paleothermometer. *Geochimica et Cosmochimica Acta* **70**(6) 1439-1456.

Ghosh, P., Eiler, J., Campana, S. E. and Feeney, R. F. (2007). Calibration of the carbonate 'clumped isotope' paleothermometer for otoliths. *Geochimica et Cosmochimica Acta* **71** 2736-2744.

Gillette, D. D. (1999). *Vertebrate paleontology in Utah.* Utah Geological Survey, Utah, USA 554pp.

Glyckman, L. S (1958). Rates of Evolution in laminoid sharks. *Doklady Akademii Nauk SSSR* **123** 568-571.

Goin, F. J., Poiré, D. G., De la Fuente, M. S., Cione, A. L., Novas, F. E., Bellosi, E. S., Ambrosio, A., Ferrer, O., Canessa, N. D., Carloni, A., Ferigolo, J., Ribeiro, A. M., Sales Viana, M. S., Reguero, M. A., Vucetich, M. G., Marenssi, S., de Lima Filho, M. F. and Agostinho, S. (2002). Paleontología y geología de los sedimentos del Cretácico superior aflorantes al sur del Río Shehuen (Mata Amarilla, Provincia De Santa Cruz, Argentina). *Actas del XV Congresso Geológico Argentin,. El Calafate.* **1** 603-608.

Golenberg, E. M. (1991). Amplification and Analysis of Miocene Plant Fossil DNA. *Philosophical Transactions of the Royal Society of London. Series B, Biological Sciences* **333**(1268) 419-427.

Grande, L. (1979). *Eohiodon falcatus*, a new species of hiodontid (Pisces) from the late Early Eocene Green River Formation of Wyoming. *Journal of Paleontology* **53**(1) 103-111.

Grande, L. (1984). Palaeontology of the Green River Formation, with a review of the fish fauna. Second edition: *The Geological Survey of Wyoming Bulletin* **63** 1-333.

Grande, L. (2001). *An updated review of the fish fauna from the Green River Formation, the world's most productive lagerstätten.* **In:** Eocene vertebrates: Unusual occurrences and rarely sampled habitats. Gunnell, G. F. (Ed.). Plenum, New York, USA. 452pp.

Grande, L. and Buchheim, H. P. (1994). Paleontological and Sedimentological Variation in Early Eocene Fossil Lake. *Contributions to Geology, University of Wyoming* **30**(1) 33-56.

Grande, L. and Grande, T. (2008). Redescription of the type species for the genus *Notogoneus* (Teleostei: Gonorynchidae) based on new, well-preserved material. *Journal of Paleontology* **82** 1-31.

Green, O.R. (2001). *A manual of practical laboratory and field techniques in palaeobiology.* Kluwer Academic Publishers, Dordrecht, The Netherlands. 538pp.

Greenwood, D. R. and Wing, S. L. (1995). Eocene continental climates and latitudinal temperature gradients. *Geology* **23** 1044-1048.

Grob, K. Jr., Grob, G. and Grob, K. (1978). Comprehensive, standardized quality test for glass capillary columns. *Journal of Chromatography* **156** 1-20.

Grob, K., Grob, G. and Grob, K. Jr. (1981). Testing capillary gas chromatographic columns. *Journal of Chromatography* **219** 13-20.

Guelinckx, J., Maes, J., De Brabadore, L., Dehairs, F. and Ollevier, F. (2006). Migration dynamics of clupeoids in the Schelde estuary: a stable isotope approach. *Estuarine, Coastal and Shelf Science* **66**(3-4) 612-623.

Gunter, G., Williams, R. H., Davis, C. C. and Smith, F. G. W. (1948). Catastrophic Mass Mortality of Marine Animals and Coincident Phytoplankton Bloom on the West Coast of Florida, November 1946 to August 1947. *Ecological Monographs* **18**(3) 310-324.

Gupta, N. S., Briggs, D. E. G., Collinson, M. E., Evershed, R. P., Michels, R. and Pancost, R. D. (2007). Molecular preservation of plant and insect cuticles from the Oligocene Enspel Formation, Germany: Evidence against derivation of aliphatic polymer from sediment. *Organic Geochemistry* **38**(3) 404-418.

Hagadorn, J. W. and Bottjer, D. J. (1997). Wrinkle structures: Microbially mediated sedimentary structures common in subtidal siliciclastic settings at the Proterozoic-Phanerozoic transition. *Geology* **25**(11) 1047-1050.

Hagadorn, J. W. and Bottjer, D. J. (1999). Restriction of a Late Neoproterozoic biotope: suspect-microbial structures and trace fossils at the Vendian-Cambrian transition. *Palaios* **14** 73-85.

Hammarlund, D., Bjorck, S., Buchardt, B., Israelson, C. and Thomsen, C. T. (2003). Rapid hydrological changes during the Holocene revealed by stable isotope records of lacustrine carbonates from Lake Igelsjon, southern Sweden. *Quaternary Science Reviews* **22** 353-370.

Hay, O. P. (1929). Second bibliography and catalogue of the fossil vertebrata of North America. *Carnegie Institution of Washington Publication* **2** 390.

Hayden, F. V. (1869). Preliminary field report of the U.S. Geological Survey of Colorado and New Mexico. *U.S Geological and Geographical Survey of the Territories Third Annual Report* 155pp.

Hecky, R. E. and Hesslein, R. H. (1995). Contributions of benthic algae to lake food webs as revealed by stable isotope analysis. *Journal of the North American Benthological Society* **14** 631-653.

Hedges, R. E. M. (2002). Bone diagenesis: an overview of processes. *Archaeometry* **44**(3) 319-328.

Hedges, R. E. M. and Reynard, L. M. (2007). Nitrogen isotopes and the trophic level of humans in archaeology. *Journal of Archaeological Science* **34** 1240-1251.

Heil, C. A., Glibert, P. M., Al-Sarawi, M. A., Faraj, M., Behbehani, M. and Husain, M. (2001). First record of a fish-killing *Gymnodinium* sp. bloom in Kuwait Bay, Arabian Sea: chronology and potential causes. *Marine Ecology Progress Series* **214** 15–23.

Herrgesell, P. L., Sibley, T. H. and Knight, A. W. (1976). Some Observations on Dinoflagellate Population Density During a Bloom in a California Reservoir. *Limnology and Oceanography* **21**(4) 619-624.

Hobson, K. A. (2008). Using endogenous and exogenous markers in bird conservation. *Bird Conservation International* **18** S174-S199.

Hobson, K. A., Fisk, A., Karnovsky, N., Holst, M., Gagnon, J. M. and Fortier, M. (2002). A stable isotope ($\delta^{13}C$, $\delta^{15}N$) model for the North Water food web: implications for evaluating trophodynamics and the flow of energy and contaminants. *Deep Sea Research Part II: Topical Studies in Oceanography* **49**(22-23)5131-5150.

Hobson, K. A. and Welch, H. E. (1992). Determination of trophic relationships within a high Arctic marine food web using $\delta^{13}C$ and $\delta^{15}N$ analysis. *Marine Ecology Progress Series* **84** 9-18.

Hof, C. H. J and Briggs, D. E. G. (1997). Decay and mineralization of mantis shrimps (Stromatopoda; Crustacae); a key to their fossil record. *Palaios* **12**(5) 420-438.

Horsfield, B., Curry, D. J., Bohacs, K., Littke, R., Rullkoetter, J., Schenk, H. J., Radke, M., Schaefer, R. G., Carroll, A. R., Isaksen, G. and Witte, E. G. (1995). Organic geochemistry of freshwater and alkaline lacustrine sediments in the Green River Formation of the Washakie Basin, Wyoming, U.S.A. *Advances in Organic Geochemistry* **22**(3) 415-440.

Huang, Y., Lockheart, M. J., Logan, G. A. and Eglinton, G. (1996). Isotope and molecular evidence for the diverse origins of carboxylic acids in leaf fossils and sediments from the Miocene Lake Clarkia deposit, Idaho, USA. *Organic Geochemistry* **24**(3) 289-299.

Huber, M. and Caballero, R. (2003). Eocene El Niño: Evidence for robust tropical dynamics in the "hothouse". *Science* **299** 877-881.

Huc, A. Y. (1988) Aspects of depositional processes of organic matter in sedimentary basins. *Organic Geochemistry* **13** 263-272.

Huene, F. von. (1932). Die fossile reptile-ordnung Saurischia, ihre entwicklung und geschichte. *Monographien zur Geologie und Paleontologie* **4**(1) 1-361.

Iacumin, P. Nikolaev, V. and Ramigni, M. (2000). C and N stable isotope measurements on Eurasian fossil mammals, 40 000 to 10 000 years BP: Herbivore physiologies and palaeoenvironmental reconstruction. *Palaeogeography, Palaeoclimatology, Palaeoecology* **163** 33–47.

Iglesias, A., Zamuner, A. B., Poiré, D. G. and Larriestra, F. (2007). Diversity, taphonomy and palaeoecology of an angiosperm flora from the Cretaceous (Cenomanian-Coniacian) in Southern Patagonia, Argentina. *Palaeontology* **50** 445-466.

Inger, R., Ruxton, G. D., Newton, J., Colhoun, K., Robinson, J. A., Jackson, A. L. and Bearhop, S. (2006). Temporal and intrapopulation variation in prey choice of wintering geese determined by stable isotope analysis. *Journal of Animal Ecology* **75** 1190-1200.

Jacob, U., Mintenbeck, K., Brey, T., Knust, R.and Beyer, K. (2005). Stable isotope food web studies: a case for standardized sample treatment. *Marine Ecology Progress Series* **287** 251-253.

Jardine, T. D., Gray, M. A., McWilliam, S. M. and Cunjak, R. A. (2005). Stable isotope variability in tissues of temperate stream fishes. *Transactions of the American Fisheries Society* **134** 1103-1110.

Jenkins, S. G., Partridge, S. T., Stephenson, T. R., Farley, S. D. and Robbins, C. T. (2001). Nitrogen and Carbon Isotope Fractionation between Mothers, Neonates, and Nursing Offspring. *Oecologia* **129**(3) 336-341.

Jennings, S. and Mackinson, S. (2003). Abundance-body mass relationships in size-structured food webs. *Ecology Letters* **6** 971-974.

Jennings, S., Pinnegar, J. K., Polunin, N. V. C., Warr, K. J. (2002). Linking size-based and trophic analyses of benthic community structure. *Marine Ecology Progress Series* **226** 77–85.

Jeppsson, L. and Anehus, R. (1995). A buffered formic-acid technique for conodont extraction. *Journal of Paleontology* **69**(4) 790-794.

Jeppsson, L., Anehus, R. and Fredholm, D. (1999). The optimal acetate buffered acetic acid technique for extracting phosphatic fossils. *Journal of Paleontology* **73**(5) 964-972.

Jeppsson, L., Fredholm, D. and Mattiasson, B. (1985). Acetic-acid and phosphatic fossils - a warning. *Journal of Paleontology* **59**(4) 952-956.

Jim, S., Ambrose, S. H. and Richard P. Evershed, R. P. (2004). Stable carbon isotopic evidence for differences in the dietary origin of bone cholesterol, collagen and apatite: implications for their use in palaeodietary reconstruction. *Geochimica et Cosmochimica Acta* **68**(1) 61-72.

John, U., Fensome, R. A. and. Medlin, L. K. (2003). The application of a molecular clock based on molecular sequences and the fossil record to explain biogeographic distributions within the *Alexandrium tamarense* "Species Complex" (Dinophyceae). *Molecular Biology and Evolution* **20**(7) 1015-1027.

Jones, A. M., O'Connell, T. C., Young, E. D., Scott, K., Buckingham, C. M., Iacumin, P. and Brasier, M. D. (2001). Biogeochemical data from well preserved 200 ka collagen and skeletal remains. *Earth and Planetary Science Letters* **193** 143-149.

Jordan, D. S. (1907). The fossil fishes of California; with supplementary notes on other species of extinct fishes. *Bulletin of the Department of Geology, University of California* **5** 95-145.

Kaehler, S. and Pakhomov, E. A. (2001). Effects of storage and preservation on the $\delta^{13}C$ and $\delta^{15}N$ signatures of selected marine organisms. *Marine Ecology Progress Series* **219** 299–304.

Kawamura, K., Tannenbaum, E., Huizinga, B. J. and Kaplan, I. R. (1986). Long-chain carboxylic acids in pyrolysates of Green River kerogen. *Organic Geochemistry* **10** 1059-1065.

Kaye, T. G., Gaugler, G. and Sawlowicz, Z. (2008). Dinosaurian Soft Tissues Interpreted as Bacterial Biofilms. *PLoS ONE* **3**(7) e2808.

Kear, B. P. (2007). First record of a Pachycormid fish (actinopterygii: pachycormiformes) from the Lower Cretaceous of Australia. *Journal of Vertebrate Paleontology* **27**(4) 1033–1038.

Kemp, A. (2002). Growth and hard tissue remodelling in the dentition of the Australian lungfish, *Neoceratodus forsteri* (Osteichthyes: Dipnoi). *Journal of Zoology* **257**(2) 219-235.

Kim, Y. and Kim, B. (2006). Application of a 2-dimensional water quality model (CE-QUAL-W2) to the turbidity interflow in a deep reservoir (Lake Soyang, Korea). *Lake and Reservoir Management* **22**(3):213-222.

Kline, T. C., Wilson, W. J. and Goering, J. J. Natural isotope indicators of fish migration at Prudhoe Bay, Alaska. *Canadian Journal of Fisheries and Aquatic Sciences* **55**(6) 1494-1502.

Kling, G. W., Fry, B. and O'Brien, W. J. (1992). Stable isotopes and planktonic trophic structure in arctic lakes. *Ecology* **73** 561-566.

Knight, D. H. (1994). Mountains and plains: The ecology of Wyoming landscapes. Yale University Press, New Haven, Connecticut, USA. 338pp.

Koch, P. L., Tuross, N. and Fogel, M. L. (1997). The effects of sample treatment and diagenesis on the isotopic integrity of carbonate in biogenic hydroxylapatite. *Journal of Archaeological Science* **24** 417–429.

Koch, P. L., Zachos, J. C. and Dettman, D. L. (1995). Stable isotope stratigraphy and paleoclimatology of the Paleogene Bighorn Basin (Wyoming, USA). *Palaeogeography, Palaeoclimatology, Palaeoecology* **115** 61-89.

Kolodny, Y., Luz, B. and Navon, O. (1983). Oxygen isotope variations in phosphate of biogenic apatites, I. Fish bone apatite - rechecking the rules of the game. *Earth and Planetary Science Letters* **64**(3) 398-404.

Kosiba, S. B., Tykot, R. H. and Carlsson, D. (2007). Stable isotopes as indicators of change in the food procurement and food preference of Viking Age and Early Christian populations on Gotland (Sweden). *Journal of Anthropological Archaeology* **26** 394–411.

Lamontagne, S., Geddes, M. C., Fernandes, M. and Krull, E. (2007). *Analysis of fish diet from the Murray Estuary using C, N, and S isotopes*. Water for a Healthy Country National Research Flagship, CSIRO, Australia. 25pp.

Lécuyer, C., Bogey, C., Garcia, J.-P., Grandjean, P., Barrat, J.-A., Floquet, M., Bardet, N. and Pereda-Superbiola, X. (2003). Stable isotope composition and rare earth element content of vertebrate remains from the Late Cretaceous of northern Spain (Lanõ): did the environmental record survive? *Palaeogeography, Palaeoclimatology, Palaeoecology* **193** 457-471.

Lee-Thorp, J. A. (2002). Two decades of progress towards understanding fossilization processes and isotopic signals in calcified tissue minerals. *Archaeometry* **44**(3) 435-446.

Lee-Thorp, J. A. and Sealy, J. (Eds.) (2008). Beyond documenting diagenesis: the fifth International Bone Diagenesis Workshop. *Palaeogeography, Palaeoclimatology, Palaeoecology* **266** 129-133.

Lehmann, M. F., Bernasconi, S. M., Barbieri, A. and McKenzie, J. A. (2002). Preservation of organic matter and alteration of its carbon and nitrogen isotope composition during simulated and in situ early sedimentary diagenesis. *Geochimica et Cosmochimica Acta* **66**(20) 3573-3584.

Leidy, J. (1856). Notice of some remains of fishes discovered by Dr. John E. Evans. *Proceedings of the Academy of Natural. Sciences of Philadelphia* **8** 256-257.

Leidy, J. (1865). Cretaceous reptiles of the United States. *Smithsonian Contributions to Knowledge* **14** 1–135.

Leidy, J. (1873) *Contributions to the extinct vertebrate fauna of the western territories.* **In:** Hayden, F. V., Report of the United States Geological Survey of the Territories: Volume 1 Fossil vertebrates. Department of the Interior, Government Printing Office, Washington, D .C. 358pp

Leopold, L. B. (2000). Temperature profiles and bathymetry of some high mountain lakes *Proceedings of the National Academy of Sciences* **97**(12) 6267-6270.

Li, H-C. and Ku, T-L. (1997). $\delta^{13}C$-$\delta^{18}O$ covariance as a paleohydrological indicator for closed-basin lakes. *Palaeogeography, Palaeoclimatology, Palaeoecology* **133** 69-80.

Lindholm, W. A. (1929). Revidiertes Verzeichnis der Gattungen der rezenten Schildkröten nebst Notizen zur Nomenklatur einiger Arten. *Zoologischer Anzeiger* **81** 275-272.

Lindsay, W. (1987). The acid technique in vertebrate palaeontology: a review. *Geological Curator* **4** 455-461.

Linnaeus, C. (1758) Systema Naturae, Ed. X. (Systema naturae per regna tria naturae, secundum classes, ordines, genera, species, cum characteribus, differentiis, synonymis, locis. Tomus I. Editio decima, reformata.) Holmiae. *Systema Naturae* **10** 1-824.

Liu, A. G., McIlroy, D., Antcliffe, J. B. and Brasier, M. D. (2008). Taphomorphs and taxonomy of the Ediacara Biota in Avalonia. Abstracts, *The Palaeontological Association 52nd Annual Meeting, University of Glasgow, UK* 27.

Lockheart, M. J., van Bergen, P. F and Evershed, R. P. (2000). Chemotaxonomic classification of fossil leaves from the Miocene Clarkia lake deposit, Idaho, USA based on *n*-alkyl lipid distributions and principal component analyses. *Organic Geochemistry* **31**(11) 1223-1246.

Loewen, M. A., Hynek, S. A. and Cushman, R. A. J (2003). False indicators of a climatic shift in the green river formation of fossil basin and the importance of recognizing stream capture in regional correlation of kerogen-rich lacustrine sediments. *Geological Society of America Abstracts with Programs* **35**(6).

Logan, G. A., Boon, J. J. and Eglinton, G. (1993). Structural Biopolymer Preservation in Miocene Leaf Fossils from the Clarkia Site, Northern Idaho. *Proceedings of the National Academy of Sciences of the United States of America* **90**(6) 2246-2250.

Longinelli, A. (1996). Pre-Quaternary isotope palaeoclimatological and palaeo-environmental studies: science or artefact? *Chemical Geology* **129**(1-2) 163-166.

Lowenstam, H.A. and Weiner, S. (1989). *On Biomineralization.* Oxford University Press, New York, USA 324 pp.

Macko, S. A., Engel, M. H., Andrusevich, V., Lubec, G., O'Connell, T. C. and Hedges, R. E. M. (1999). Documenting the diet in ancient human populations through stable isotope analysis of hair. *Philosophical Transactions of the Royal Society of London. Series B: Biological Sciences* **354**(1379) 65-76.

Maillard, L. C. (1917). General reaction between amino acids and sugars: the biological consequences. *Comptes Rendus Des Seances De La Societe De Biologie Et De Ses Filiales* **72** 599-601.

Manchester, S. R. and Kester, P. R. (2002). Paleobotanical investigation of the Green River lacustrine flora of Fossil Butte, Wyoming. *Geological Society of America Abstracts with Programs* **34**(6).

Marsh, O. C. (1877). New vertebrate fossils. *American Journal of Science (III)* **14** 249-256.

Marsh, O. C. (1878). Principal characters of American Jurassic dinosaurs. Part I. *American Journal of Science and Arts* **16** 411-416.

Martill, D. M. (1988). Preservation of fish in the Cretaceous Santana Formation of Brazil. *Palaeontology* **31**(1) 1-18.

Martill, D. M. (1991). *Bones as stones; the contribution of vertebrate remains to the lithological record.* **In:** Donovan, S. K. (Ed.). The process of fossilization. Belhaven Press, London, UK. 303pp.

Martill, D. M. and Harper, E. (1990). Critical point drying, a technique for palaeontologists. *Palaeontology* **35** 423-428.

Martin, J. H. (1991). Iron, Liebig's law, and the greenhouse. *Oceanography* **4**(2) 52-55.

Martin, R. E. (1999). *Taphonomy: a process approach*. Cambridge University Press, Cambridge, UK. 508pp.

Mason, N. W. H., Lanoiselée, C., Mouillot, D., Wilson, J. B. and Argillier, C. (2008). Does niche overlap control relative abundance in French lacustrine fish communities? A new method incorporating functional traits. *Journal of Animal Ecology* **77**(4) 661-669.

Masters, P. (1987). Preferential preservation of noncollagenous protein during bone diagenesis: Implications for chronometric and stable isotope measurements. *Geochimica et Cosmochimica Acta* **51**(12) 3209-3214.

Matson, S. D. and Fox, D. L. (2008). Can oxygen isotopes from turtle bone be used to reconstruct paleoclimates? *Palaios* **23** 24-34.

Mazumder, A., Taylor, W. D., McQueen, D. J. and Lean, D. R. S. (1990). Effects of fish and plankton on lake temperature and mixing depth. *Science* **247** 312-315.

McArthur, J. M., Hamilton, P. J., Greensmith, J. T., Boyce, A. J., Fallick, A. E., Birch, G., Walsh, J. N. , Benmore, R. A. and Coleman, M. L. (1987). Phosphorite geochemistry: Isotopic evidence for meteoric alteration of francolite on a local scale. *Chemical Geology: Isotope Geoscience section* **65**(3-4) 415-425.

McClelland, J. W. and Montoya, J. P. (2002). Trophic relationships and the nitrogen isotopic composition of amino acids in plankton. *Ecology* **83**(8) 2173-2180.

McCrae, C. and Potze, S. (2007). A fresh look at chemical fossil extraction. *Palaeontologia Africana* **42** 115-116.

McCutchan, J. H., Lewis, W. M., Kendall, C., McGrath, C. C. (2003). Variation in trophic shift for stable isotope ratios of carbon, nitrogen, and sulfur. *Oikos* **102**(2) 378-390.

McGrew, P. O. (1975). Taphonomy of Eocene fish from Fossil Basin, Wyoming. *Fieldiana: Geology* **33**(14) 257-270.

McGrew, P. O. and Casilliano, M. (1975). The geologic history of Fossil Butte National Monument and Fossil Basin. *National Park Service Occasional Paper* **3** 37pp.

McNamara, M. E. and Orr, P. J. (2008). Experimental degradation of vertebrates: taphonomy of keratinous tissues and implications for the fossil record. Abstracts, *The Palaeontological Association 52nd Annual Meeting, University of Glasgow, UK* 29.

McNamara, M. E., Orr, P. J., Kearns, S., Alcalà, L., Anadón, P. and Peñalver-Mollá, E (2006). High fidelity preservation of bone marrow in c. 10 million year old amphibians. *Geology* **34**(8) 641-644.

Mendes, S., Newton, J.,·Reid, R. J., Zuur, A. F. and Pierce, G. J. (2007). Stable carbon and nitrogen isotope ratio profiling of sperm whale teeth reveals ontogenetic movements and trophic ecology. *Oecologia* **151** 605–615.

Mercone, D., Thomson, J., Abu-Zied, R. H., Croudace, I. W. and Rohling, E. J. (2001). High-resolution geochemical and micropalaeontological profiling of the most recent eastern Mediterranean sapropel. *Marine Geology* **177**(1-2) 25-44.

Meyers, S. R. (2008). Resolving Milankovitchian controversies: the Triassic Latemar limestone and the Eocene Green River Formation. *Geology* **36** 319-322.

Michener, R. H. and Schell, D. M. (1994). *Stable isotope ratios as tracers in marine aquatic food webs.* **In:** Lajtha, K. and Michener, R. H. (Eds.). Stable isotopes in ecology and environmental science. Methods in Ecology Series, Blackwell Scientific Publications, Oxford, UK. 316pp.

Miki, S. (1941). On the change of flora in eastern Asia since Tertiary Period: I. The clay or lignite beds flora in Japan with special reference to the Pinus trifolia bed in central Hondo. *Japanese Journal of Botany* **11** 237–303.

Mill, A. C., Pinnegar, J. K. and Polunin, N. V. C. (2007). Explaining isotope trophic-step fractionation: why herbivorous fish are different. *Functional Ecology* **21**(6) 1137-1145.

Minami, M. and Nakamura, T. (2005). Carbon and nitrogen isotopic fractionation in bone collagen during chemical treatment. *Chemical Geology* **222** 65– 74.

Minagawa, M. and Wada, E. (1984). Stepwise enrichment of ^{15}N along food chains: further evidence and the relation between $\delta^{15}N$ and animal age. *Geochimica et Cosmochimica Acta* **48** 1135-1140.

Moldowan, J. M., Jacobsen, S. R., Dahl, J., Al-Hajji, A., Huizinga, B. J. and Fago, F. J. (2001). Molecular fossils demonstrate Precambrian origin of dinoflagellates, **in:** Zhuravlev, A. and Riding,

R. (Eds.). *Ecology of the Cambrian radiation.* Columbia University Press, New York, USA. 474–492pp.

Müller, J. and Henle, J. (1839). *Systematische Beschreibung der Plagiostomen.* Veit und Co., Berlin, Germany. 200pp.

Müller, J. (1844) Über den Bau und die Grenen der Ganoiden, und über das natürliche System der Fische. *Abhandlungen der Königlichen Akademie der Wissenschaften zu Berlin, Physikalisch-Mathematische Klasse* **1844** 117–216.

Murphy, S. M., McCormick, A. and Eglinton, G. (1967). Perhydro-beta-carotene in the Green River shale. *Science* **157**(3792) 1040-1042.

Murry, B. A., Farrell, J. M., Teece, M. A. and Smyntek, P. M. (2006). Effect of lipid extraction on the interpretation of fish community trophic relationships determined by stable carbon and nitrogen isotopes. *Canadian Journal of Fisheries and Aquatic Sciences* **63**(10) 2167-2172.

Niklas, K. J. and Brown Jr., R. M. (1981). Ultrastructural and palaeobiochemical correlations among fossil leaf tissues from the St. Maries River (Clarkia) area, Northern Idaho, USA. *American Journal of Botany* **68** 332–341.

Noffke, N., Beukes, N., Gutzmer, J. and Hazen R. (2006). Spatial and temporal distribution of microbially induced sedimentary structures: A case study from siliclastic storm deposits of the 2.9 Ga Witwatersrand Supergroup, South Africa. *Precambrian Research* **146** 35-44.

Norris, R. D., Corfield, R. M and Hayes-Baker, K. (2000). *Mountains and Eocene Climate.* **In:** Huber, B. T., MacLeod, K. G. and Wing, S. L. (Eds.). Warm Climates in Earth History. Cambridge University Press, Cambridge, UK. 462pp.

Oelbermann, K. and Scheu, S. (2002). Stable isotope enrichments (d15N and d13C) in a generalist predator (*Pardosa lugubris*, Araneae: Lycosidea): effects of prey quality. *Oecologia* **130**(3) 337-344.

O'Reilly, C. M., Alin, S. R., Plisnier, P-D., Cohen, A. S. and McKee, B. A. (2003). Climate change decreases aquatic ecosystem productivity of Lake Tanganyika, Africa. *Nature* **424** 766-768.

Oren, A. and Gurevich, P. (1995). Dynamics of a bloom of halophilic archaea in the Dead Sea. *Hydrobiologia* **315**(2) 149-158.

Organ, C. L., Schweitzer, M. H., Zheng, W., Freimark, L. M., Cantley, L. C. and Asara, J. M. (2008). Molecular Phylogenetics of Mastodon and *Tyrannosaurus rex. Science* **320** (5875) 499.

Oriel, S. S., and Tracey, J. I. J. (1970). Uppermost Cretaceous and Tertiary Stratigraphy of Fossil Basin, Southwestern Wyoming. *Geological Survey Professional Paper* **635** 1-53.

Ostrom, P. H., Zonneveld, J. P. and Robbins, L. L. (1994). Organic geochemistry of hard parts: assessment of variability and indigeneity. *Palaeogeography Palaeoclimatology Palaeoecology* **107** 201-212.

Otto, A., Simoneit, B. R. T. and Rember, W. C. (2004). Conifer and angiosperm biomarkers in clay sediments and fossil plants from the Miocene Clarkia Formation, Idaho, USA. *Organic Geochemistry* **36**(6) 907-922.

Pate, F. D. (1994). Bone chemistry and palaeodiet. *Journal of Archaeological Method and Theory* **1**(2) 161-209.

Pearce, J. A., Harris, N. B. W. and Tindle, A. G. (1984). Trace element discrimination diagrams for the tectonic interpretation of granitic rocks. *Journal of Petrology* **25** 956-983.

Pearson, P. N., Ditchfield, P. W., Singano, J., Harcourt-Brown, K. G., Nicholas, C. J., Olsson, R. K., Shackleton, N. J. and Hall, M. A. (2001). Warm tropical sea surface temperatures in the Late Cretaceous and Eocene epochs. *Nature* **413** 481–487.

Pearson, P. N., van Dongen, B. E., Nicholas, C. J., Pancost, R. D., Schouten, S., Singano, J. M. and Wade, B. S. (2007). Stable warm tropical climate through the Eocene Epoch. *Geology* **35**(3) 211-214.

Perea, D., Ubilla, M. and Pineiro, G. (1996). First fossil record (Late Miocene) of *Phrynops* (*P. geoffroanus* complex: Chelidae) from Uruguay: Biostratigraphical and palaeoenvironmental context. *Copeia* **1996**(2) 445-451.

Petchey, F. and Higham, T. (2000). Bone diagenesis and radiocarbon dating of fish bones at the Shag River Mouth Site, New Zealand. *Journal of Archaeological Science* **27** 135-150.

Peters, K. E., Walters, C. C. and Moldowan, J. M. (2005). *The Biomarker Guide: Biomarkers and isotopes in the environment and human history.* Second Edition, Volume 1. Cambridge University Press, Cambridge, UK. 471pp.

Peterson, B. J. and Fry, B. (1987). Stable isotopes in ecosystem studies. *Annual Review of Ecology and Systematics* **18** 293-320.

Pfretzschner, H-U. (2004). Fossilization of Haversian bone in aquatic environments. *Comptes Rendus Palevol* **3**(6-7) 605-616.

Pietras, J. T., Carroll, A. R. and Rhodes, M. K. (2003). Lake basin response to tectonic drainage diversion: Eocene Green River Formation, Wyoming. *Journal of Paleolimnology* **30**(2) 115-125.

Pietras, J. T., Carroll, A. R., Singer, B. S. and Smith, M. E. (2003). 10 k.y. depositional cyclicity in the early Eocene: stratigraphic and $^{40}Ar/^{39}Ar$ evidence from the lacustrine Green River Formation. *Geology* **31** 593-596.

Pingitore, N. E., Fretzdorff, S. B., Seitz, B. P., Estrada, L. Y., Borrego, P. M., Crawford, G. M. and Love, K. M. (1993). Dissolution kinetics of $CaCO_3$ in common laboratory solvents. *Journal of Sedimentary Petrology* **63**(4) 641-645.

Pinnegar, J. K., Jennings, S., O'Brien, C. M. and Polunin, N. V. C. (2002). Long-term changes in the trophic level of the Celtic Sea fish community and fish market price distribution. *Journal of Applied Ecology* **39**(3) 377-390.

Pinnegar, J. K. and Polunin, N. V. C. (1999). Differential fractionation of $\delta^{13}C$ and $\delta^{15}N$ among fish tissues: implications for the study of trophic interactions. *Functional Ecology* **13** 225-231.

Pinnegar, J. K. and Polunin, N. V. C. (2000). Contributions of stable-isotope data to elucidating food webs of Mediterranean rocky littoral fishes. *Oecologia* **122** 399-409.

Poiré, D. G., Goin, F., Iglesias, A., Canessa, N., Larriestra, C. N., Varela, A. N., Calvo Marcillese, L. and Larriestra, F. (2004b). Ambientes sedimentarios relacionados a las tafofloras de las formaciones Piedra Clavada y Mata Amarilla (Cretácico), Tres Lagos, Cuenca Austral, Argentina. *Resúmenes Décima Reunión Argentina de Sedimentología, San Luis* 140-141.

Poiré, D. G., Zamuner, A. B., Iglesias, A., Varela, A. N. and Larriestra, F. (2004a). Palaeoenvironmental conditions related with the taphoflora from the Piedra Clavada and Mata Amarilla formations (Cretaceous), Tres Lagos, Southern Patagonia, Argentina. Abstracts, *Seventh International Organization of Paaleobotany Conference, Bariloche* 88–89.

Popp, B. N., Graham, B. S., Olson, R. J., Hannides, C. C. S., Lott, M. J., Lopez-Ibarra, G. A., Galvan-Magana, F. and Fry, B. (2007). *Insight into the trophic ecology of yellowfin tuna, Thunnus albacares, from compound-specific nitrogen isotopes analysis of proteinaceous amino acids.* **In:** Dawson, T. and Siegwolf, R. (Eds.). Isotopes as tracers of ecological change. Elsevier Academic Press, Oxford, UK. pp 173-190.

Post, D. M. (2005). The long and short of food-chain length. *Trends in Ecology and Evolution* **117**(6) 269-277.

Potier, M., Marsac, F.; Cherel, Y., Lucas, V., Sabatie, R., Maury, O. and Menard, F. (2007). Forage fauna in the diet of three large pelagic fishes (lancetfish, swordfish and yellowfin tuna) in the western equatorial Indian Ocean. *Fisheries Research* **83**(1) 60-72.

Prothero, D. R. (2006). *After the dinosaurs: the age of mammals*. Indiana University Press, Indiana, USA. 362pp.

Radtke, R. L., Lenz, P., Showers, W. and Moksness, E. (1996). Environmental information stored in otoliths: insights from stable isotopes. *Marine Biology* **127**(1) 161-170.

Raff, E. C., Villinski, J. T., Turner, F. R., Donoghue, P. C. J. and Raff, R. A. (2006). Experimental taphonomy shows the feasibility of fossil embryos. *Proceedings of the National Academy of Sciences* **103**(15) 5846-5851.

Rafinesque, C. S. (1810). *Caratteri di alcuni nuovi generi e nuove specie di animali e piante della Sicilia con varie osservazioni sopra i medesimi*. San Filippo, Palermo, Italy 105pp.

Ramette, R. W., Culberson, C. H. and Bates, R. G. (1977). Acid-base properties of tris(hydroxymethyl)aminomethane (TRIS) buffers in seawater from 5 to 40°C. *Analytical Chemistry* **49** 867-870.

Rashby, S. E., Sessions, A. L., Summons, R. E. and Newman, D. K (2007). Biosynthesis of 2-methylbacteriohopanepolyols by an anoxygenic phototroph. *Proceedings of the National Academy of Sciences* **104**(38): 15099-15104.

Rau, G. H., Mearns, A. J., Young, D. R., Oson, R. J., Shafer, H. A. and Kaplan, I. R. (1983). Animal $^{13}C/^{12}C$ correlates with trophic level in pelagic food webs. *Ecology* **64** 1314-1318.

Regan, C. T. (1923). The skeleton of *Lepidosteus*, with remarks on the origin and evolution of the lower neopterygian fishes. *Proceedings of the Zoological Society* 445–461.

Reiche, I., Vignaud, C. and Menu, M. (2002). The crystallinity of ancient bone and dentine: new insights by transmission electron microscopy. *Archaeometry* **44**(3) 447-459.

Riccardi, A. C. and Rolleri, E. O. (1980). *Cordillera Patagónica Austal*. **In:** Leanza, A. F. (Ed.). Geología regional Argentina. Second Edition. Academia Nacional de Ciencias, Córdoba, Argentina. 1717pp.

Richards, M. P. and Hedges, R. E. M. (2003). Variations in bone collagen $\delta^{13}C$ and $\delta^{15}N$ values of fauna from Northwest Europe over the last 40,000 years. *Palaeogeography, Palaeoclimatology, Palaeoecology*. **193** 261–267.

Richards, M. P., Pettitt, P. B., Trinkaus, E., Smith, F. H., Paunović, M. and Karavanić, I. (2000). Neanderthal diet at Vindija and Neanderthal predation: The evidence from stable isotopes. *Proceedings of the National Academy of Sciences* **97**(13) 7663-7666.

Richter, G. and Baszio, S. (2006). First evidence of size-related change of diet ("switching") in a fossil fish. *Palaeogeography, Palaeoclimatology, Palaeoecology* **237** 270-279.

Ripepe, M., Roberts, L. T. and Fischer, A. G. (1991). Enso and Sunspot Cycles in Varved Eocene Oil Shales from Image Analysis. *Journal of Sedimentary Petrology* **61**(7) 1155-1163.

Rixon, A. E. (1976). *Fossil Animal Remains: their preparation and conservation*. The Athlone Press, University of London, UK. 304pp.

Robertson, C. R., Zeug, S. C. and Winemiller, K. O. (2008). Associations between hydrological connectivity and resource partitioning among sympatric gar species (Lepisosteidae) in a Texas river and associated oxbows. *Ecology of Freshwater Fish* **17** (1) 119-129.

Robinson, S., Nicholson, R. A., Pollard, A. M. and O'Connor, T. P. (2003) An evaluation of nitrogen porosimetry as a technique for predicting taphonomic durability in animal bone. *Journal of Archaeological Science* **30**(4) 391-403.

Roehler, H. W. (1992). Introduction to Greater Green River Basin geology, physiography, and history of investigations. *US Geological Survey Professional Paper* **1506-A** 1-12.

Rooker, J. R., Secor, D. H., Zdanowicz, V. S. and Itoh, T. (2001). Discrimination of northern bluefin tuna from nursery areas in the Pacific Ocean using otolith chemistry. *Marine Ecology Progress Series* **218** 275-282.

Ruiz-Cooley, R. I., Gendron, D., Anguiniga, S., Mesnick, S. and Carriquiry, J. D. (2004). Trophic relationships between sperm whales and jumbo squid using stable isotopes of C and N. *Marine Ecology Progress Series* **277** 275-283.

Sakano, H., Fujiwara, E., Nohara, S. and Ueda, H. (2005). Estimation of nitrogen stable isotope turnover rate of *Oncorhynchus nerka*. *Environmental Biology of Fishes* **72** 13-18.

Salamon, M., Tuross, N., Arensburg, B. and Weiner, S. (2005). Relatively well preserved DNA is present in the crystal aggregates of fossil bones. *Proceedings of the National Academy of Sciences* **102**(39) 13783-13788.

Sansom, R. S., Gabbott, S. E. and Purnell, M. A. (2008). Unlocking character preservation before chordate skeletonization: decay of the cephalochordate *Branchiostoma.* Abstracts, *The Palaeontological Association 52nd Annual Meeting, University of Glasgow, UK* 33.

Schäfer, W. (1972). *Ecology and palaeoecology of marine environments*. Oliver and Boyd, Edinburgh, UK. 568pp.

Schieber, J. (1999). Microbial Mats in Terrigenous Clastics: The Challenge of Identification in the Rock Record. *Palaios* **14**(1) Theme Issue: Unexplored Microbial Worlds 3- 12.

Schieber, J. (2007). *Benthic microbial mats as an oil shale component: Green River Formation (Eocene) of Wyoming and Utah.* **In:** Atlas of microbial mat features preserved within the clastic rock record. Schieber, J., Bose, P. K., Eriksson, P. G., Banerjee, S., Sarkar, A., Altermann, W. and Catuneau, O. (Eds.). Elsevier, Amsterdam, The Netherlands. 324pp.

Schoeninger, M., DeNiro, M. and Tauber, H. (1983). Stable nitrogen isotope ratios of bone collagen reflect marine and terrestrial components of prehistoric human diet. *Science* **220** 1381-1383.

Schultz, A. R. (1914). Geology and geography of a portion of Lincoln County, Wyoming. *U.S. Geological Survey Bulletin* **543** 1-141.

Schwark, L., Giessen, M., Spitthoff, B., Leythaeuser, D., Wuttke, M. (1995). *The Enspel Oil Shale deposit, FRG - Impact of catastrophic volcanic events on a fossil lake environment.* **In:** Grimalt J. O. (Ed.) Organic Geochemistry. pp123-125.

Schweitzer, M. H. (2007). Molecular paleobiology – what's possible (and what isn't). *American Paleontologist* **15**(1) 19-23.

Schweitzer, M. H. (2004). Molecular paleontology: some current advances and problems. *Annales de Paléontologie* **90**(2) 81-102.

Schweitzer, M. H., Hill, C. L., Asara, J. M., Lane, W. S. and Pincus, S. H. (2002). Identification of immunoreactive material in mammoth fossils, *Journal of Molecular Evolution* **55** 696–705.

Schweitzer, M. H., Suo, Z., Avci, R., Asara, J. M., Allen, M. A., Terán Arce, F. and Horner, J. R. (2007a). Analyses of soft tissue from *Tyrannosaurus rex* suggest the presence of protein. *Science* **316**(5822) 277–280.

Schweitzer, M. H., Wittmeyer, J. L. and Horner, J. R. (2007b). Soft tissue and cellular preservation in vertebrate skeletal elements from the Cretaceous to the present. *Proceedings of the Royal Society B: Biological Sciences* **274**(1607) 183–197.

Schweizer, M. K., Steele, A., Toporski, J. K. W. and Fogel, M. L. (2007). Stable isotopic evidence for fossil food webs in Eocene Lake Messel. *Paleobiology* **33**(4) 590-609.

Schweizer, M. K., Wooler, M. J., Toporski, J., Fogel, M. L. and Steele, A. (2006). Examination of an Oligocene lacustrine ecosystem using C and N stable isotopes. *Palaeogeography, Palaeoclimatology, Palaeoecology* **230** 335-351.

Seeley, H. G. (1888). On the classification of the fossil animals commonly named Dinosauria. *Proceedings of the Royal Society of London* **43** 165-171.

Seilacher, A., Reif, W. E. and Westphal, F. (1985). Sedimentological, ecological and temporal patterns of fossil Lagerstätten. *Philosophical Transactions of the Royal Society of London. Series B: Biological Sciences* **311** 5-23.

Selman, M. (2007). Eutrophication: an overview of status, trends, policies, and strategies. *Water Resources Institute Report*. 91pp.

Sewall, J. O. and Sloan, L. C. (2006). Come a little bit closer: A high-resolution climate study of the early Paleogene Laramide foreland. *Geology* **34**(2) 81-84.

Sharp, Z. D., Atudorei, V. and Furrer, H. (2000). The effect of diagenesis on oxygen isotope ratios of biogenic phosphates. *American Journal of Science* **300** 222-237.

Shemesh, A., Kolodny, Y. and Luz, B. (1983). Oxygen isotope variations in phosphate of biogenic apatites, II. Phosphorite rocks. *Earth and Planetary Science Letters* **64** 405-416.

Shimada, K. (2006). *Marine vertebrates from the Blue Hill Shale Member of the Carlile Shale (Upper Cretaceous: Middle Turonian) in Kansas.* **In:** Lucas, S. G. and Sullivan, R. M. (Eds.) Late Cretaceous vertebrates from the Western Interior. *New Mexico Museum of Natural History and Science Bulletin* **35**.

Showers, W. J., Barrick, R. and Genna, B. (2002). Isotopic analysis of dinosaur bones. *Analytical Chemistry* **74**(5) 143-150.

Sidow, A., Wilson, A. C. and Pääbo, S. (1991). Bacterial DNA in Clarkia fossils. *Philosophical Transactions of the Royal Society of London. Series B: Biological Sciences* **333**(1268) 429-432.

Silverman, S. R., Fugat, R. K. and Weiser, J. D. (1952). Quantitative determination. of calcite associated with. carbonate-bearing apatites. *American Mineralogist* **37** 211-222.

Sinninghe Damsté, J. S., Kohnen, M. E. L. and Horsfield, B. (1998). Origin of low-molecular weight alkylthiophenes in pyrolysates of sulphur-rich kerogens as revealed by microscale sealed vessel pyrolysis. *Organic Geochemistry* **29** 1891-1903.

Siqueira, A., Kolm, H. E., Pereira Brandini, F. (2006). Offshore distribution patterns of the cyanobacterium *Trichodesmium erythraeum* ehrenberg and associated phyto- and bacterioplankton in the southern Atlantic coast (Paraná, Brazil). *Brazilian Archives of Biology and Technology* **49**(2) 323-337.

Skinner, L. C., Shackleton, N. J. and Elderfield, H. (2003). Millennial-scale variability of deep-water temperature and $\delta 18O_{dw}$ indicating deep-water source variations in the northeast Atlantic, 0–34 cal. ka BP. *Geochemistry, Geophysics, Geosystems* **4**(12) 1-17.

Smale, M. J. (2005). The diet of the ragged-tooth shark *Carcharias taurus* Rafinesque 1810 in the Eastern Cape, South Africa. *African Journal of Marine Science* **27**(1) 331-336.

Smith, M. E., Carroll, A. R. and Singer, B. S. (2008). Synoptic reconstruction of a major ancient lake system: Eocene Green River Formation, western United States. *Geological Society of America Bulletin* **120**(1/2) 54-84.

Sotiropoulos, M. A., Tonn, W. M. and Wassenaar, L. I. (2004). Effects of lipid extraction on stable carbon and nitrogen isotope analyses of fish tissues: potential consequences for food web studies. *Ecology of Freshwater Fish* **13**(3) 155-160.

Spence, K. O. and Rosenheim, J. A. (2005). Isotopic enrichment in herbivorous insects: a comparative field-based study of variation. *Oecologia* **146**(1) 89-97.

Stankiewicz, B. A, Briggs, D. E. G., Evershed, R. P., Flannery, M. B. and Wuttke, M. (1997). Preservation of chitin in 25-million-year-old fossils. *Science* **276**(5318) 1541-1543.

Stanton-Thomas, K. J. and Carlson, S. J. (2004). Microscale $\delta^{18}O$ and $\delta^{13}C$ isotopic analysis of an ontogenetic series of the hadrosaurid dinosaur *Edmontosaurus*: implications for physiology and ecology. *Palaeogeography, Palaeoclimatology, Palaeoecology* **206** 257– 287.

Stathopoulou, E. (2008). Microbial activity in fossil skeletal remains from Greece and Cyprus. Abstracts, *3rd Meeting on Taphonomy and Fossilization, Universidad de Granada, Spain* 97-100.

Stephenson, J. and Scott, A. C. (1992). The geological history of insect-related plant damage. *Terra Nova* **4**(5) 542-552.

Surdam, R. C. and Stanley, K. O. (1979). Lacustrine sedimentation during the culminating phase of Eocene Lake Gosiute, Wyoming (Green River Formation). *Geological Society of America Bulletin* **90**(1) 93-110.

Sugden, M. A., Talbot, H. M. and Farrimond, P. (2005). Flash pyrolysis – a rapid method for screening bacterial species for the presence of bacteriohopanepolyols *Organic Geochemistry* **36**(6) 975-979.

Summons, R. E., Jahnke, L. L., Logan, G. A. & Hope, J. M. (1999). 2-Methylhopanoids as biomarkers for cyanobacterial oxygenic photosynthesis. *Nature* **398** 554-557.

Summons, R. E., Thomas, J., Maxwell, J. R. and Boreham, C. J. (1992). Secular and environmental constraints on the occurrence of dinosterane in sediments. *Geochimica et Cosmochimica Acta* **56**(6) 2437-2444.

Summons, R. E., Volkman, J. K. & Boreham, C. J. (1987) Dinosterane and other steroidal hydrocarbons of dinoflagellate origin in sediments and petroleum. *Geochimica et Cosmochimica Acta* **51** 3075-3082.

Sweeting, C. J., Barry, J., Barnes, C., Polunin, N. V. C. and Jennings, S. (2007). Effects of body size and environment on diet-tissue $\delta^{15}N$ fractionation in fishes. *Journal of Experimental Marine Biology and Ecology* **340**(1) 1-10.

Sweeting, C. J., Polunin, N. V. C. and Jennings, S. (2004). Tissue and fixative dependent shifts of $\delta^{13}C$ and $\delta^{15}N$ in preserved ecological material. *Rapid Communications in Mass Spectrometry* **18**(21) 2587-2592.

Sweeting, C. J., Polunin, N. V. C. and Jennings, S. (2006). Effects of chemical lipid extraction and arithmetic lipid correction on stable isotope ratios of fish tissues. *Rapid Communications in Mass Spectrometry* **20** 595-601.

Swift, M. J., Heal, O. W. and Anderson, J. M. (1979). *Decomposition in terrestrial ecosystems.* Blackwell Scientific Publications. Oxford, UK. 372pp.

Talbot, M. R. (1990). A review of the palaeohydrological interpretation of carbon and oxygen isotopic ratios in primary lacustrine carbonates. *Chemical Geology (Isotope Geoscience Section* **80** 261-279.

Trueman, C. N., Benton, M. J. and Palmer, M. R. (2003). Geochemical taphonomy of shallow marine vertebrate assemblages. *Palaeogeography, Palaeoclimatology, Palaeoecology* **197** 151-169.

Trueman, C. N., Chenery, C., Eberth, D. A. and Spiro, B. (2003). Diagenetic effects on the oxygen isotope composition of bones of dinosaurs and other vertebrates recovered from terrestrial and marine setting. *Journal of the Geological Society* **160** 895-901.

Trueman, C. N. and Martill, D. M. (2002). The long-term survival of bone: the role of bioerosion. *Archaeometry* **44**(3) 371-382.

Trueman, C. N., McGill, R. A. R. and Guyard, P. H. (2005). The effect of growth rate on tissue-diet isotopic spacing in rapidly growing animals. An experimental study with Atlantic salmon (*Salmo salar*). *Rapid Communications in Mass Spectrometry* **19** 3239-3247.

Turner-Walker, G. and Syversen, U. (2002). Quantifying histological changes in archaeological bones using BSE-SEM image analysis. *Archaeometry* **44**(3) 461-468.

Tütken, T., Vennemann, T. W. and Pfretzschner, H-U. (2008). Early diagenesis of bone and tooth apatite in fluvial and marine settings: constraints from combined oxygen isotope, nitrogen and REE analysis. *Palaeogeography, Palaeoclimatology, Palaeoecology* **266** 254-268.

Vanderklift, A. and Ponsard, S. (2003). Sources of variation in consumer-diet $\delta^{15}N$ enrichment: a meta-analysis Author. *Oecologia* **136**(2) 169-182.

Vander Zanden, M. J. and Rasmussen, J. B. (1999). Primary consumer $\delta^{13}C$ and $\delta\ ^{15}N$ and the trophic position of aquatic consumers. *Ecology* **80**(4) 1395-1404.

Veatch, A. C. (1907). Geography and geology of a portion of southwestern Wyoming with special reference to coal and oil. *U.S. Geological Survey Professional Paper* **56** 178pp.

Villar de Seoane, L. and Archangelsky, S. (2008). Taxonomy and biostratigraphy of Cretaceous megaspores from Patagonia, Argentina. *Cretaceous Research* **29**(2) 354-372.

Volkman, J. K. (1986). A review of sterol markers for marine and terrigenous organic matter. *Organic Geochemistry* **9** 83–99.

Walbaum, J. J. (1792). *Petri Artedi sueci genera piscium. In quibus systema totum ichthyologiae proponitur cum classibus, ordinibus, generum characteribus, specierum differentiis, observationibus plurimis. Redactis speciebus 242 ad genera 52.* **In:** Ichthyologiae pars III. A. F. Röse, Grypeswaldiae [Greifswald], Germany. 1-723pp.

Wang, N., Wu, Y. and Zhang, J. (2009). Comparison and unification of carbon stable isotope ratios in specific aquatic biota. *Communications in Nonlinear Science and Numerical Simulation* **14**(5) 2502-2506.

Wang, Y. and Cerling, T. E. (1994). A model of fossil tooth and bone diagenesis: implications for paleodiet reconstruction from stable isotopes. *Palaeogeography, Palaeoclimatology, Palaeoecology* **107** 281–289.

Westbroek, P., van der Meide, P. H., van der Wey-Kloppers, J. S., van der Sluis, R. J., de Leeuw, J. W. and de Jong, E. W. (1979). Fossil macromolecules from cephalopod shells: characterization, immunological response and diagenesis. *Paleobiology* **5**(2) 151-167.

Whitmore, J. H., Brand, L. and Buchheim, H. P. (2002). Implications of modern fish taphonomy for the preservation states and depositional environments of fossil fish, Fossil Butte Member, Green River Formation, southwestern Wyoming. *Geological Society of America Abstracts with Programs* **34**(6) 244.

Wierzchos, J., de Los Rios, A., and Ascaso, C. (2003). *Detecting life traces in extreme cold and dry conditions on earth: possible analogues of life on Mars.* **In:** Harris, R. A. and Ouwehand, L. (Eds). Proceedings of the Third European Workshop on Exo-Astrobiology, Madrid, Spain. 67-69.

Wilby, P. R., Briggs, D. E. G., Bernier, P and Gaillard, C. (1996). Role of microbial mats in the fossilization of soft tissues. *Geology* **24**(9) 787-790.

Wilde, P., Quinby-Hunt, M. S. and Berry, W. B. N. (1990). *Vertical advection from oxic or anoxic water from the main pycnocline as a cause of rapid extinction or rapid radiations.* **In:** Lecture Notes in Earth Sciences **30** Extinction Events in Earth History 85-98.

Wilf, P. (2000). Late Paleocene-early Eocene climate changes in southwestern Wyoming: paleobotanical analysis. *Geological Society of America Bulletin* **112**(2) 292-307.

Williams, B. (2006). Hydrobiological modelling: processes, numerical methods and applications. Lulu.com, Newcastle, NSW, Australia. 700 pp.

Wing, S. L. and Greenwood, D. R. (1993). Fossils and fossil climate: the case for equable continental interiors. *Philosophical Transactions of the Royal Society of London. Series B: Biological Sciences* **341** 243-252.

Woodward, A. S. (1890). Note on certain vertebrate remains from the Nagpur district with description of a fish skull. *Records of the Geological Survey of India* **23** 20–24.

Woodward, A. S. (1895). *Catalogue of the Fossil Fishes in the British Museum.* Part 3. British Museum of Natural History, London, UK 544pp.

Wright, L. E. and Schwarcz, H. P. (1999). Correspondence between stable carbon, oxygen and nitrogen isotopes in human tooth enamel and dentine: infant diets at Kaminaljuyú. *Journal of Archaeological Science* **26** 1159-1170.

Wüest, A., Piepke, G. and Halfman, J. D. (1996). *Combined effects of dissolved solids and temperature on the density stratification of Lake Malawi.* In: Johnson, T. C., Odada, E. O. and Whittaker, K. T. (Eds.). The Limnology, Climatology and Paleoclimatology of the East African Lakes. CRC Press, London, UK. 664pp.

Yang, H., Huang, Y., Leng, Q., LePage, B. A. and Williams, C. J. (2005). Biomolecular preservation of Tertiary *Metasequoia* fossil lagerstätten revealed by comparative pyrolysis analysis. *Review of Palaeobotany and Palynology* **134** 237-256.

Zachos, J. C., Stott, L. D. and Lohmann, K. C. (1994), Evolution of Early Cenozoic marine temperatures. *Paleoceanography* **9**(2) 353–387.

Zazzo, A., Balasse, M. and Patterson, W. P. (2006). The reconstruction of mammal individual history: refining high-resolution isotope record in bovine tooth dentine. *Journal of Archaeological Science* **33** 1177-1187.

Zazzo, A., Bocherens, H., Brunet, M., Beauvilain, A., Billiou, D., Mackaye, H. T., Vignaud, P. and Mariotti, A. (2000). Herbivore paleodiet and paleoenvironmental changes in Chad during the Pliocene using stable isotope ratios of tooth enamel carbonate. *Paleobiology* **26**(2) 294–309.

Zazzo, A., Lécuyer, C. and Mariotti, A. (2004). Experimentally-controlled carbon and oxygen isotope exchange between bioapatites and water under inorganic and microbially-mediated conditions. *Geochimica et Cosmochimica Acta* **68**(1) 1-12.

Zeebe, R. E. and Wolf-Gladrow, D. A. (2001) *CO_2 in Seawater: Equilibrium, Kinetics, Isotopes.* Elsevier Oceanography Series 65, Amsterdam, The Netherlands. 346pp.

Appendix 1

AP1 ***K. eocaena***

AP2 ***K. eocaena***

AP3 ***K. eocaena***

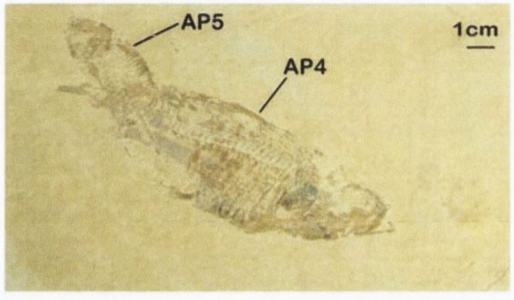

AP4 & AP5 ***K. Alta & K. eocaena***

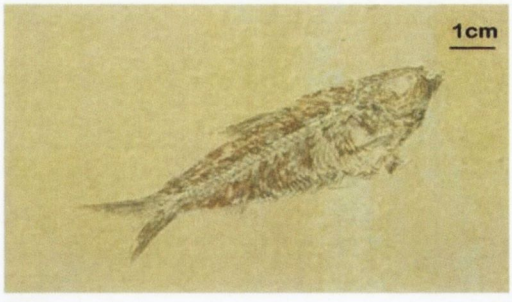

AP6 ***K. alta***

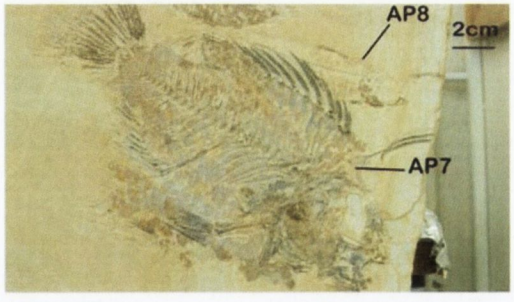

AP7 & AP8 ***P. Liops & K. eocaena***

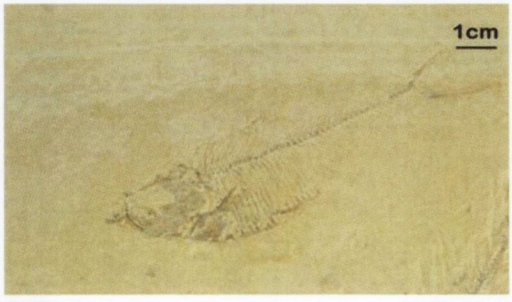

AP9 ***D. dentatus***

AP10 ***D. dentatus***

AP11 ***P. encaustus***

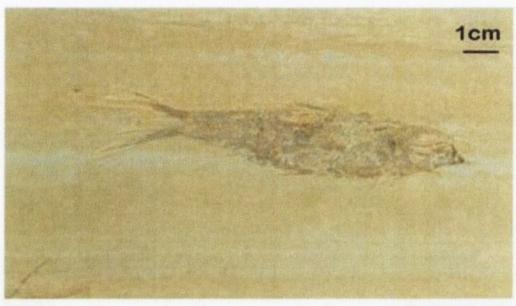

AP12 ***K. eocaena***

AP13 ***M. labracoides***

AP14 ***K. eocaena***

AP15 ***K. eocaena***

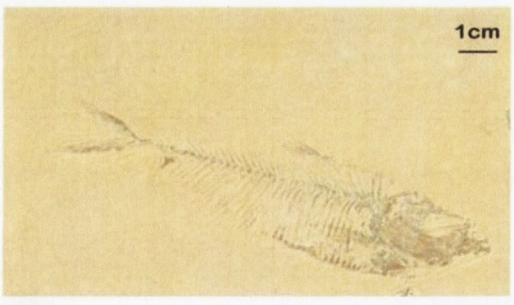

AP16 ***D. dentatus***

AP17 ***D. dentatus***

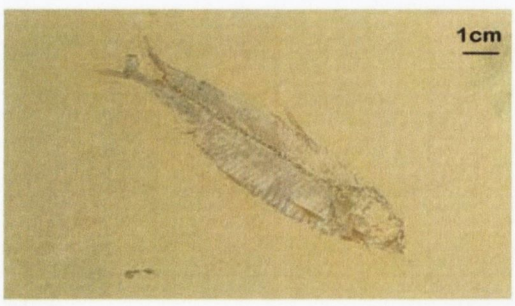

AP18 ***K. eocaena***

AP19 ***D. dentatus***

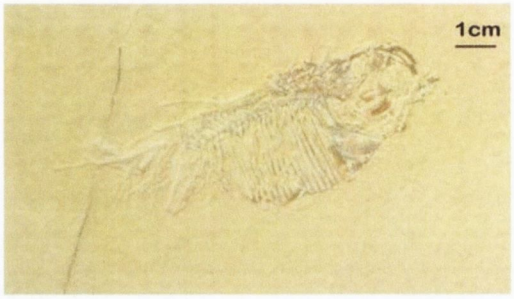

AP20 ***D. dentatus***

AP21 ***K. alta***

AP22 ***K. eocaena***

AP23 ***K. eocaena***

AP24 ***D. dentatus***

AP25 ***K. eocaena***

AP27 ***K. eocaena***

Appendix 1

RH100612 ***D. dentatus***

RH100614 ***D. dentatus***

RH110602 ***K. eocaena***

RH110603 ***K. eocaena***

RH130607 ***K. eocaena***

RH130609 ***D. dentatus***

RH130610c ***K. eocaena***

RH130610d ***K. eocaena***

RH130612 ***D. dentatus***

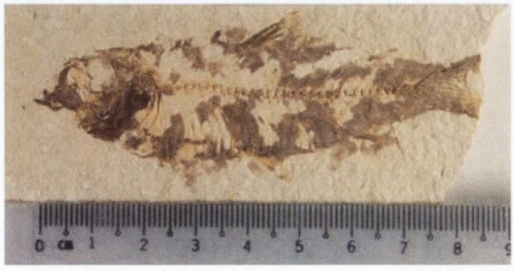

RH140602 ***K. eocaena***

RH150601 ***K. eocaena***

RH150602 ***K. eocaena***

RH150605 ***D. dentatus***

RH150606 ***K. eocaena***

RH150609 ***D. dentatus***

RH170601 ***K. eocaena***

RH170604 ***K. alta***

RH170605 ***K. eocaena***

RH170610 ***D. dentatus***

RH180601 ***K. eocaena***

RH180602 ***K. eocaena***

RH180603 ***D. dentatus***

RH180605 ***K. eocaena***

RH180606 ***D. dentatus***

RH180607 ***K. eocaena***

RH180608 ***K. eocaena***

RH180609 ***K. eocaena***

RH180610 ***K. eocaena***

RH180612 ***D. dentatus***

RH180613 ***D. dentatus***

RH180614 ***D. dentatus***

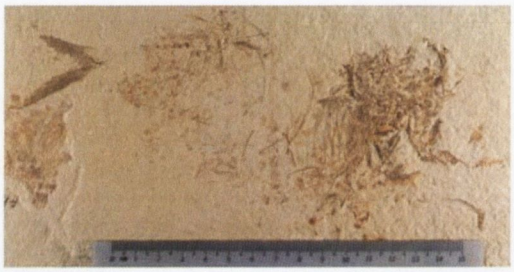

RH180615 ***D. dentatus***

RH190601 ***K. eocaena***

RH190604 ***D. dentatus***

RH190605 ***K. eocaena***

RH190611 ***K. eocaena***

RH190612 ***D. dentatus***

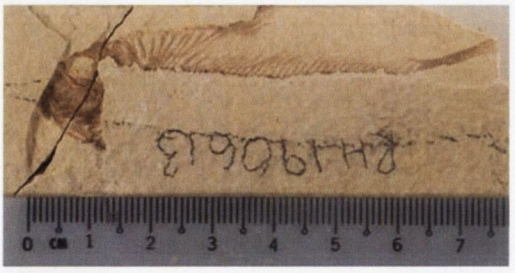

RH190613 ***D. dentatus***

RH190615a ***K. eocaena***

RH190616 ***K. eocaena***

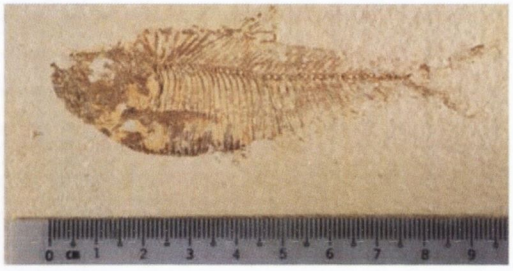

RH190618 ***D. dentatus***

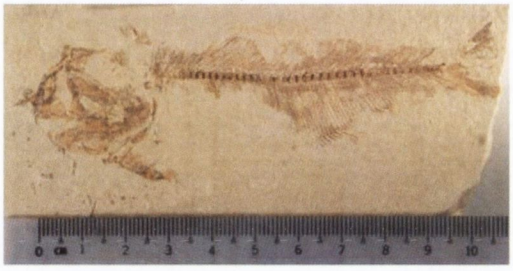

RH190619 ***D. dentatus***

RH190620a ***K. eocaena***

RH190622 ***K. eocaena***

RH190623 ***K. eocaena***

RH230602 ***D. dentatus***

RH230602b ***D. dentatus***

RH230603 ***D. dentatus***

RH230604 ***D. dentatus***

RH230605a ***K. eocaena***

RH230605b ***K. eocaena***

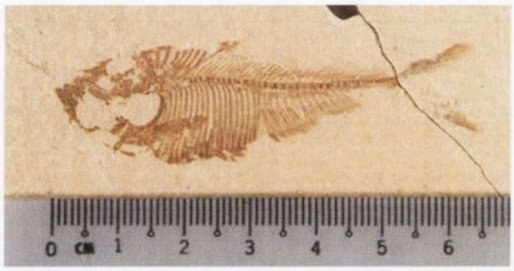

RH230605c ***D. dentatus***

RH230607 ***K. eocaena***

RH230608 ***K. alta***

RH230610 ***D. dentatus***

RH230613 ***K. eocaena***

RH230614 ***K. eocaena***

RH230615 ***P. encaustus***

RH230616 ***K. eocaena***

RH230619 ***K. alta***

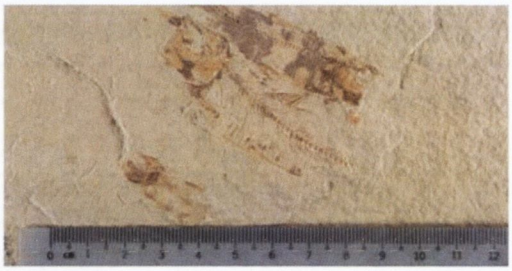

RH240601 ***K. eocaena***

RH240603 ***K. eocaena***

RH240604 ***K. eocaena***

RH240606 ***K. alta***

RH240607 ***K. alta***

RH240609 ***K. alta***

RH240610 ***D. dentatus***

RH240612 ***D. dentatus***

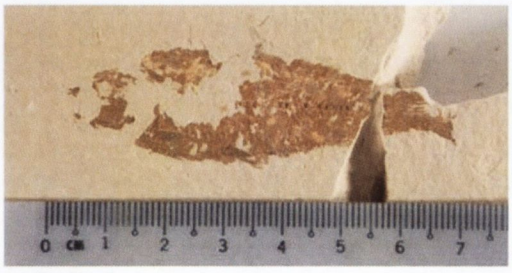

RH240613 ***K. eocaena***

RH240614a ***D. dentatus***

RH240615a ***D. dentatus***

RH240615b ***K. alta***

RH240615c ***K. alta***

RH240617 ***K. alta***

RH240620 ***D. dentatus***

RH240623 ***D. dentatus***

RH020701 ***K. Eocaena***

RH020703 ***K. eocaena***

RH020704 ***K. eocaena***

RH020706 ***K. eocaena***

RH020708 ***K. eocaena***

RH020708 ***D. dentatus***

RH020709 ***K. eocaena***

RH020710 ***K. Eocaena***

RH020711 ***K. eocaena***

RH020714 ***K. Eocaena***

RH020716 ***K. eocaena***

RH020717 ***K. eocaena***

RH020721 ***K. alta***

RH020723 ***K. eocaena***

Appendix 1

Appendix 2

4.4 Results of acid treatment effects on $\delta^{15}N$ and $\delta^{13}C$

Acid treatment	Time (hours)	pH at t_0	pH at $t_{½}$	pH at t_1	Weight (mg) at t_1	$\delta^{15}N$ (‰)	$\delta^{13}C_{org}$ (‰)	*n* =
A1	1.5	2.8	3.0	3.0	70.50	6.86	-22.37	3
A1	3	2.9	3.1	3.0	84.89	7.16	-22.97	4
A1	6	2.9	3.0	3.0	78.11	7.13	-22.50	9
A1	12	2.8	3.0	3.0	75.99	7.37	-23.22	4
A1	24	2.8	3.0	3.0	74.23	5.13	-23.25	3
A1	48	2.8	3.1	3.1	61.78	6.93	-24.59	2
A1	96	2.9	3.1	3.2	63.63	4.03	-22.95	2
A1	192	2.9	3.2	3.3	62.41	3.28	-23.82	3
A1	384	2.9	3.2	3.3	63.16	3.84	-23.74	3
A1	768	2.9	3.3	3.7	85.11	3.94	-22.93	6

Acid treatment	Time (hours)	pH at t_0	pH at $t_{½}$	pH at t_1	Weight (mg) at t_1	$\delta^{15}N$ (‰)	$\delta^{13}C_{org}$ (‰)	*n* =
A2	1.5	2.7	2.7	2.9	75.03	6.10	-21.55	4
A2	3	2.6	2.8	2.8	60.81	7.03	-23.55	3
A2	6	2.6	2.8	2.7	77.36	6.33	-23.66	6
A2	12	2.7	2.8	2.7	72.57	7.04	-23.02	4
A2	24	2.6	2.8	2.8	59.11	6.29	-23.81	3
A2	48	2.6	2.8	2.8	62.95	6.14	-23.43	4
A2	96	2.6	2.8	2.9	47.85	5.50	-24.67	2
A2	192	2.6	2.9	3.0	51.44	2.66	-25.03	3
A2	384	2.6	2.9	3.2	53.55	1.75	-22.90	4
A2	768	2.6	3.0	3.3	57.49	4.34	-23.24	4

Acid treatment	Time (hours)	pH at t_0	pH at $t_{½}$	pH at t_1	Weight (mg) at t_1	$\delta^{15}N$ (‰)	$\delta^{13}C_{org}$ (‰)	*n* =
A3	1.5	2.5	2.6	2.7	77.69	7.14	-21.33	4
A3	3	2.5	2.7	2.7	74.78	5.71	-23.01	4
A3	6	2.7	2.7	2.7	73.14	6.97	-23.47	13
A3	12	2.5	2.6	2.6	70.85	5.83	-23.79	3
A3	24	2.5	2.6	2.7	71.59	6.37	-23.63	5
A3	48	2.5	2.6	2.6	49.23	7.04	-25.17	4
A3	96	2.5	2.6	2.7	42.29	4.19	-24.48	3
A3	192	2.5	2.7	2.8	38.56	2.09	-25.19	3
A3	384	2.5	2.8	2.9	46.97	1.10	-24.95	3
A3	768	2.5	2.8	3.0	44.73	5.81	-25.06	3

Acid treatment	Time (hours)	pH at t_0	pH at $t_{½}$	pH at t_1	Weight (mg) at t_1	$\delta^{15}N$ (‰)	$\delta^{13}C_{org}$ (‰)	*n* =
F1	1.5	2.1	2.2	2.3	49.04	7.27	-24.51	3
F1	3	2.1	2.1	2.2	46.93	7.19	-24.16	4
F1	6	2.1	2.2	2.1	35.47	6.14	-25.86	3
F1	12	2.1	2.2	2.2	14.19	7.29	-27.32	4
F1	24	2.1	2.2	2.2	10.89	7.59	-27.80	2
F1	48	2.1	2.3	2.3	10.59	7.10	-28.14	2
F1	96	2.1	2.3	2.3	9.19	6.63	-28.36	1
F1	192	2.1	2.3	2.3	9.35	7.36	-28.07	2
F1	384	2.1	2.3	2.4	10.13	7.81	-28.55	1
F1	768	2.1	2.4	2.5	9.53	7.26	-27.56	2

Acid treatment	Time (hours)	pH at t_0	pH at $t_{½}$	pH at t_1	Weight (mg) at t_1	$\delta^{15}N$ (‰)	$\delta^{13}C_{org}$ (‰)	*n* =
FB3	1.5	3.0	3.0	3.0	73.32	6.14	-23.10	3
FB3	3	3.0	3.0	3.0	68.58	7.15	-22.66	6
FB3	6	3.0	3.0	3.0	66.40	6.24	-23.45	9
FB3	12	3.0	3.0	3.0	58.31	6.04	-23.70	3
FB3	24	3.0	3.0	3.0	51.04	7.52	-24.23	4
FB3	48	3.0	3.0	3.0	40.98	7.72	-24.71	2
FB3	96	3.0	3.0	3.1	28.47	6.94	-26.06	2
FB3	192	3.0	3.1	3.2	40.54	4.28	-24.85	1
FB3	384	3.0	3.1	3.3	37.66	5.04	-25.39	2
FB3	768	3.0	3.3	3.5	62.23	7.33	-24.92	5

Acid treatment	Time (hours)	pH at t_0	pH at $t_{½}$	pH at t_1	Weight (mg) at t_1	$\delta^{15}N$ (‰)	$\delta^{13}C_{org}$ (‰)	*n* =
FB4	1.5	3.7	3.7	3.7	89.14	6.93	-22.55	4
FB4	3	3.7	3.7	3.7	87.27	6.66	-22.51	2
FB4	6	3.7	3.8	3.7	85.48	7.50	-23.18	8
FB4	12	3.8	3.7	3.7	84.22	7.36	-22.72	3
FB4	24	3.8	3.7	3.8	81.50	8.08	-21.83	3
FB4	48	3.7	3.8	3.8	77.58	6.90	-22.85	5
FB4	96	3.7	3.8	3.8	70.22	7.13	-22.60	3
FB4	192	3.7	3.8	3.9	65.20	6.13	-24.84	1
FB4	384	3.7	3.8	3.9	76.61	6.58	-22.14	3
FB4	768	3.7	3.9	4.3	70.31	7.40	-21.78	3

5.4.1 Fractionation of $\delta^{15}N$ and $\delta^{13}C$ among fish tissues

AP7 ***P. liops***	**$\delta^{15}N$ (‰)**	**$\delta^{13}C_{org}$ (‰)**	**%C**	**%N**	**C:N ratio**
Scales	4.21	-10.76	0.78	0.02	34.01
Scales	3.86	-11.05	0.72	0.03	28.37
Scales	2.26	-11.44	0.78	0.03	25.40
Vertebrae	3.30	-11.38	0.67	0.01	45.02
Vertebrae	2.06	-10.14	0.60	0.01	46.49
Vertebrae	2.05	-10.40	0.83	0.02	43.71
Ribs	2.27	-10.54	0.91	0.02	49.06
Ribs	1.11	-11.69	1.00	0.02	49.05
Ribs	0.93	-10.72	0.99	0.02	45.12
Operculum	2.39	-8.91	0.97	0.01	64.82
Operculum		-9.29	0.93	0.01	62.81
Operculum	2.93	-8.22	1.08	0.02	67.67
Operculum	2.66	-8.23	1.07	0.02	67.21
Operculum	2.41	-8.26	1.09	0.02	70.06
Fins	5.73	-10.79	0.80	0.02	48.53
Fins	4.27	-10.16	0.80	0.01	55.87
Dorsal spines	2.91	-7.82	1.09	0.01	75.93
Dorsal spines	3.06	-7.82	1.08	0.01	74.81
Dorsal spines	2.82	-7.66	1.08	0.01	74.83
Pharyngeal teeth	0.63	-10.85	1.00	0.02	52.30

AP11 ***P. encaustus***	**$\delta^{15}N$ (‰)**	**$\delta^{13}C_{org}$ (‰)**	**%C**	**%N**	**C:N ratio**
Scales	3.33	-9.15	0.94	0.02	48.31
Scales	3.39	-9.36	0.86	0.02	43.08
Scales	3.28	-9.48	0.93	0.02	44.50
Scales	3.26	-9.97	1.01	0.03	40.43
Ribs	3.09	-11.29	0.91	0.02	45.09
Ribs	3.51	-9.77	1.10	0.02	49.19
Ribs	3.74	-9.68	1.10	0.02	47.04
Operculum	3.50	-8.31	0.97	0.02	62.60
Operculum	2.97	-8.40	0.98	0.02	62.81
Operculum	2.84	-8.25	0.98	0.02	63.97
Fins	3.93	-11.23	1.05	0.03	41.00

Modern trout *O. mykiss*	**$\delta^{15}N$ (‰)**	**$\delta^{13}C_{org}$ (‰)**	**%C**	**%N**	**C:N ratio**
Scales	21.20	8.03	2.64	11.96	-18.42
Scales	24.15	9.36	2.58	11.86	-18.12
Scales	23.87	8.98	2.66	12.17	-18.17
Scales	22.56	8.58	2.63	12.26	-18.10
Scales	23.09	8.96	2.58	12.06	-18.17
Scales	25.78	10.13	2.55	11.67	-18.04
Scales	22.46	8.75	2.57	12.04	-18.10
Vertebrae	21.03	3.25	6.47	10.92	-22.56
Vertebrae	13.51	3.34	4.05	11.29	-20.88
Vertebrae	25.03	3.49	7.17	10.47	-22.49
Ribs	15.19	4.58	3.32	10.62	-19.02
Ribs	14.13	4.38	3.23	10.66	-18.82
Ribs	16.79	5.05	3.32	10.82	-19.24
Operculum	15.06	5.09	2.96	10.97	-18.27
Operculum	19.11	6.33	3.02	11.17	-18.54
Operculum	17.74	5.79	3.06	11.07	-18.79
Pectoral fin	13.73	4.06	3.38	12.21	-19.34
Pectoral fin	12.56	3.89	3.23	12.10	-18.67
Pectoral fin	14.20	4.35	3.26	12.06	-19.07
Pelvic fin	14.17	4.75	2.99	12.63	-18.86
Pelvic fin	13.57	4.48	3.03	11.91	-18.54
Pelvic fin	15.71	5.05	3.11	11.80	-18.78
Anal fin	30.44	4.23	7.19	11.66	-20.14
Anal fin	15.58	4.06	3.84	12.08	-20.93
Anal fin	23.98	6.01	3.99	12.36	-21.05
Dorsal spines	25.40	8.06	3.15	13.13	-19.70
Dorsal spines	19.19	6.08	3.16	13.49	-19.64
Dorsal spines	18.94	5.84	3.24	11.69	-19.70
Pharyngeal teeth	23.52	6.13	3.83	11.70	-20.52
Pharyngeal teeth	39.65	3.90	10.17	11.16	-23.72
Pharyngeal teeth	24.69	5.90	4.19	11.72	-20.94
Caudal fin	23.65	8.41	2.81	12.03	-18.81
Caudal fin	25.01	8.72	2.87	12.28	-18.90
Caudal fin	26.67	9.39	2.84	12.10	-18.85
Muscle	13.16	4.36	3.02	12.23	-19.95
Muscle	16.25	5.02	3.24	11.56	-20.76
Muscle	14.51	4.76	3.05	11.64	-20.47

5.4.3 Analysis of $\delta^{15}N$ in fossil fish and $\delta^{13}C$ and $\delta^{18}O$ of micrite from ash plate

Fossil sample	Species	Standard length (mm)	Number of replicates (*n*=)	%N	Mean $\delta^{15}N$ (‰)	$\delta^{15}N$ SD
AP1	*K. eocaena*	66	2	0.02	5.59	0.25
AP2	*K. eocaena*	101	3	0.03	5.88	0.84
AP3	*K. eocaena*	54	2	0.03	6.45	0.77
AP4	*K. alta*	94	6	0.02	4.50	0.13
AP5	*K. eocaena*	61	3	0.03	6.98	0.13
AP6	*K. alta*	71	7	0.02	5.30	0.21
AP7	*P. liops*	158	3	0.02	4.22	0.49
AP8	*K. eocaena*	83	3	0.02	4.21	0.62
AP9	*D. dentatus*	77	2	0.02	5.35	0.66
AP10	*D. dentatus*	71	3	0.03	7.07	0.24
AP11	*P. encasutus*	220	5	0.02	4.18	0.06
AP12	*K. eocaena*	83	4	0.02	5.70	0.38
AP13	*M. labracoides*	171	11	0.02	4.27	0.44
AP14	*K. eocaena*	78	2	0.02	4.51	0.09
AP15	*K. eocaena*	74	3	0.02	5.30	0.39
AP16	*D. dentatus*	98	5	0.02	5.21	0.63
AP17	*D. dentatus*	70	3	0.03	7.36	0.34
AP18	*K. eocaena*	85	3	0.02	5.22	0.25
AP19	*D. dentatus*	96	2	0.03	6.13	0.17
AP20	*D. dentatus*	75	3	0.03	6.80	0.28
AP21	*K. alta*	68	1	0.04	6.91	0.00
AP22	*K. eocaena*	65	1	0.04	6.60	0.00
AP23	*K. eocaena*	83	2	0.03	5.12	0.14
AP24	*D. dentatus*	60	1	0.04	6.16	0.00
AP25	*K. eocaena*	80	3	0.02	6.01	0.35
AP27	*K. eocaena*	71	3	0.03	5.26	0.48

Micrite sample	$\delta^{13}C$ (‰)	$\delta^{18}O$ (‰)
AP1	2.96	-3.40
AP2	3.36	-3.00
AP3	3.12	-3.11
AP4	3.15	-3.10
AP5	2.86	-3.58
AP6	3.02	-3.26
AP7	3.14	-3.15
AP8	2.96	-3.30
AP9	3.08	-3.07
AP10	3.30	-2.97
AP11	3.36	-3.46
AP12	3.32	-2.82
AP13	3.43	-2.73
AP14	2.87	-3.49
AP15	3.04	-3.18
AP16	2.79	-3.45
AP17	3.01	-3.47
AP18	3.16	-3.35
AP19	3.11	-3.78
AP20	2.89	-3.42
AP21	3.17	-3.48
AP22	3.39	-2.90
AP23	2.96	-3.51
AP24	3.03	-3.35
AP25	3.00	-3.33
AP27	3.16	-2.96

Micrite replicates	$\delta^{13}C$ (‰)	$\delta^{13}C$ SD	$\delta^{18}O$ (‰)	$\delta^{18}O$ SD
AP5	2.86		-3.58	
	3.13		-3.36	
	3.13	0.13	-3.71	0.14
AP16	2.79			
	2.81		-3.79	
	3.19	0.18	-3.47	0.16
AP24	3.03		-3.35	
	3.04		-3.23	
	3.01	0.01	-3.49	0.10

5.4.4 Fossil fish $\delta^{15}N$ and micrite $\delta^{13}C$ and $\delta^{18}O$ from the RH F-2 stratigraphy

Height above Base (cm)	Fossil sample	Species	Standard length (mm)	%N	$\delta^{15}N$ fish (‰)	$\delta^{13}C$ sediment (‰)	$\delta^{18}O$ sediment (‰)
1.5	RH020721	*K. alta*	100	0.03	3.22	1.81	-5.02
2.5	RH020723	*K. eocaena*	75	0.04	1.52	1.74	-5.30
5.5	RH020717	*K. eocaena*	71	0.03	2.60	1.99	-4.51
15.6	RH020716	*K. eocaena*	90	0.06	0.96	1.66	-5.09
16.1	RH020714	*K. eocaena*	65	0.04	1.31	1.53	-5.34
19.0	RH020710	*K. eocaena*	70	0.02	2.28	1.78	-4.98
19.0	RH020711	*K. eocaena*	90	0.03	2.81	1.44	-5.54
20.0	RH020709	*K. eocaena*	47	0.03	-2.92	1.58	-5.16
21.7	RH240607	*K. alta*	79	0.03	2.63	2.06	-4.15
21.7	RH020704	*K. eocaena*	78	0.03	1.98	2.27	-4.01
21.8	RH020708	*K. eocaena*	87	0.03	3.30	2.09	-4.03
22.4	RH240609	*K. alta*	93	0.03	3.31	2.00	-4.16
24.1	RH240610	*D. dentatus*	55	0.03	2.29	1.50	-5.11
24.5	RH230619	*K. alta*	90	0.03	3.17	1.96	-4.19
24.7	RH020703	*K. eocaena*	50	0.04	1.26	1.63	-4.89
25.5	RH020708	*D. dentatus*	114	0.03	1.76	2.15	-4.16
25.6	RH020701	*K. eocaena*	77	0.04	2.77	2.16	-4.07
29.5	RH030728	*K. eocaena*	98	0.02	4.01	2.12	-4.21
30.0	RH020706	*K. eocaena*	93	0.03	1.59	1.85	-4.45
30.2	RH170604	*K. alta*	67	0.03	4.01	1.99	-4.39
31.3	RH030727	*K. eocaena*	81	0.02	3.40	1.51	-5.27
32.5	RH030726	*K. eocaena*	78	0.04	1.76	1.76	-4.76
33.4	RH030725A	*D. dentatus*	102	0.02	3.84	1.80	-4.59
33.7	RH020707	*K. alta*	65	0.03	-0.99	1.38	-5.81
33.7	RH230616	*K. eocaena*	71	0.02	2.13	1.39	-5.49
35.3	RH230614	*K. eocaena*	68	0.02	1.59	1.99	-4.32
35.8	RH030724b	*K. eocaena*	73	0.03	4.12	1.92	-4.52
36.4	RH240604	*K. eocaena*	95	0.03	3.55	2.02	-4.31
37.9	RH240603	*K. eocaena*	69	0.03	2.15	1.71	-4.94
40.9	RH030722A	*K. eocaena*	70	0.03	2.00	1.75	-4.82
44.5	RH030720	*K. alta*	84	0.03	3.83	1.97	-4.53
46.0	RH030718	*K. eocaena*	83	0.02	3.48	1.96	-4.41

Height above Base (cm)	Fossil sample	Species	Standard length (mm)	%N	$\delta^{15}N$ fish (‰)	$\delta^{13}C$ sediment (‰)	$\delta^{18}O$ sediment (‰)
46.4	RH030717	*K. eocaena*	81	0.03	3.23	2.03	-4.18
46.4	RH030716	*K. eocaena*	53	0.03	2.28	1.91	-4.53
52.5	RH230610	*D. dentatus*	82	0.04	2.56	1.96	-4.32
53.9	RH030721	*D. dentatus*	85	0.04	3.50	2.00	-4.31
54.5	RH230608	*K. alta*	70	0.02	2.09	1.99	-4.31
55.3	RH030712	*D. dentatus*	133	0.03	3.82	1.83	-4.85
55.6	RH230607	*K. eocaena*	60	0.11	1.50	2.02	-4.21
58.9	RH030708	*K. eocaena*	55	0.03	2.00	2.01	-4.20
63.6	RH030707	*K. eocaena*	61	0.05	5.94	2.11	-4.14
65.4	RH240615c	*K. alta*	82	0.04	0.15	1.99	-4.07
65.4	RH240615b	*K. alta*	72	0.03	2.10	2.00	-4.16
65.4	RH240615a	*D. dentatus*	54	0.03	1.68	1.68	-5.03
65.4	RH240615b	*K. alta*	72	0.06	-0.16	1.99	-4.07
67.3	RH030711	*D. dentatus*	111	0.02	2.93	2.15	-3.99
67.6	RH150606	*K. eocaena*	60	0.16	0.76	1.93	-4.23
68.0	RH030702	*K. alta*	95	0.02	3.36	2.22	-3.99
69.5	RH030701	*D. dentatus*	77	0.03	3.54	1.97	-4.16
70.4	RH240614a	*D. dentatus*	64	0.03	2.15	1.93	-4.30
70.6	RH030703	*K. alta*	80	0.03	2.95	2.11	-4.02
71.2	RH030710	*K. eocaena*	85	0.03	3.57	2.02	-4.13
71.8	RH030704	*K. eocaena*	68	0.03	2.51	2.03	-4.22
73.6	RH140602	*K. eocaena*	76	0.02	2.82	2.02	-4.08
78.9	RH030705	*K. eocaena*	65	0.15	1.52	2.03	-4.01
79.1	RH180605	*K. eocaena*	50	0.05	2.06	1.97	-4.32
79.1	RH180610	*K. eocaena*	90	0.03	3.13	2.08	-4.17
79.1	RH180609	*K. eocaena*	75	0.07	1.93	2.06	-4.11
80.1	RH150609	*D. dentatus*	77	0.04	3.50	1.96	-4.24
81.2	RH150610	*K. eocaena*	83	0.05	1.75	2.00	-4.08
86.7	RH180601	*K. eocaena*	70	0.04	2.96	2.05	-4.11
87.0	RH180602	*K. eocaena*	80	0.02	3.25	1.95	-4.39
93.5	RH170602a	*K. alta*	87	0.04	2.87	1.98	-3.84
105.0	RH150602	*K. eocaena*	60	0.02	1.14	2.12	-3.96
105.0	RH150603	*K. eocaena*	100	0.04	3.48	2.31	-3.78
105.0	RH150605	*D. dentatus*	110	0.03	4.13	2.31	-3.93
105.5	RH130610d	*K. eocaena*	70	0.03	4.30	2.28	-3.83
105.5	RH180612	*D. dentatus*	71	0.04	3.43	2.12	-4.43

Height above Base (cm)	Fossil sample	Species	Standard length (mm)	%N	$\delta^{15}N$ fish (‰)	$\delta^{13}C$ sediment (‰)	$\delta^{18}O$ sediment (‰)
105.5	RH130610c	*K. eocaena*	60	0.05	3.34	2.39	-3.49
105.5	RH170605	*K. eocaena*	86	0.03	5.19	2.54	-3.59
107.0	RH150601	*K. eocaena*	64	0.03	3.23	2.33	-3.91
111.8	RH180608	*K. eocaena*	50	0.02	2.35	2.30	-3.95
111.8	RH180608b	*K. eocaena*	50	0.02	2.35	1.99	-4.26
117.2	RH180607	*K. eocaena*	105	0.02	2.93	2.22	-3.99
122.0	RH180606	*D. dentatus*	82	0.03	2.12	2.14	-3.98
123.5	RH130607	*K. eocaena*	77	0.02	3.85	2.18	-3.76
136.4	RH190620a	*K. eocaena*	70	0.03	0.88	2.10	-4.16
146.1	RH180613	*D. dentatus*	130	0.03	3.77	1.83	-5.02
150.6	RH180614	*D. dentatus*	52	0.03	0.02	1.81	-5.08
154.0	RH100614	*D. dentatus*	77	0.03	3.39	2.15	-4.07
154.0	RH100612	*D. dentatus*	129	0.03	3.99	2.12	-4.21
160.0	RH190611	*K. eocaena*	45	0.04	1.24	2.15	-4.04
164.0	RH190615a	*K. eocaena*	44	0.04	0.69	2.17	-4.46
164.0	RH190616a	*K. eocaena*	60	0.08	2.18	2.09	-4.15
166.5	RH190605	*K. eocaena*	70	0.05	-0.78	1.89	-4.72
168.9	RH230604	*D. dentatus*	67	0.03	1.86	2.24	-4.05
170.5	RH180603	*D. dentatus*	50	0.03	1.26	1.99	-4.57
173.5	RH180615b	*D. dentatus*	100	0.03	3.38	1.69	-5.29
173.5	RH180615	*D. dentatus*	150	0.03	4.67	1.72	-5.20
181.0	RH190604	*D. dentatus*	130	0.03	2.55	2.22	-3.93
181.1	RH240617	*K. alta*	80	0.02	3.08	2.37	-3.84
188.0	RH170604	*K. alta*	69	0.02	1.68	1.98	-4.44
191.0	RH240623	*D. dentatus*	90	0.08	4.91	2.18	-4.00
192.8	RH240620	*D. dentatus*	81	0.04	1.18	2.17	-3.97
203.8	RH240601	*K. eocaena*	55	0.04	4.36	2.05	-4.19
206.5	RH170601	*K. eocaena*	85	0.03	3.85	2.08	-4.17
207.0	RH240606	*K. alta*	81	0.03	1.85	2.25	-4.18
207.5	RH240613	*K. eocaena*	53	0.04	2.90	2.60	-3.71
207.5	RH240612	*D. dentatus*	97	0.03	2.62	2.32	-3.97
208.0	RH190601	*K. eocaena*	70	0.09	-0.68	2.11	-4.28
212.5	RH230615	*P. encaustus*	62	0.03	2.32	2.13	-4.52
214.7	RH230613	*K. eocaena*	55	0.03	2.18	2.05	-4.63
220.2	RH130612	*D. dentatus*	85	0.03	3.89	2.22	-4.02
223.6	RH110603	*K. eocaena*	65	0.04	1.46	2.30	-4.06

Height above Base (cm)	Fossil sample	Species	Standard length (mm)	%N	$\delta^{15}N$ fish (‰)	$\delta^{13}C$ sediment (‰)	$\delta^{18}O$ sediment (‰)
225.2	RH140601	*D. dentatus*	93	0.06	2.51	2.21	-3.82
226.2	RH230603	*D. dentatus*	67	0.03	0.57	2.24	-4.18
226.8	RH230602b	*D. dentatus*	90	0.03	0.91	2.23	-4.19
226.8	RH230602	*D. dentatus*	85	0.04	2.47	2.11	-4.36
228.2	RH230605a	*K. eocaena*	46	0.03	2.06	2.28	-3.92
228.2	RH230605c	*D. dentatus*	53	0.04	2.77	2.28	-3.92
228.2	RH230605b	*K. eocaena*	54	0.03	2.16	2.28	-3.92
229.2	RH170610	*D. dentatus*	89	0.03	2.80	2.38	-3.90
230.2	RH190622	*K. eocaena*	48	0.03	2.61	2.11	-4.32
231.5	RH190623	*K. eocaena*	45	0.05	2.94	2.23	-4.25
234.6	RH110602	*K. eocaena*	62	0.04	1.91	2.38	-3.87
237.6	RH190618	*D. dentatus*	76	0.05	1.02	2.08	-4.44
239.5	RH190619	*D. dentatus*	100	0.03	4.06	2.41	-3.64
244.5	RH130609	*D. dentatus*	81	0.03	4.20	2.03	-4.38
247.6	RH190613	*D. dentatus*	65	0.03	2.09	2.16	-4.12
247.6	RH190612	*D. dentatus*	120	0.02	1.89	2.45	-3.82

Fish replicates	$\delta^{15}N$ (‰)	$\delta^{15}N$ SD
RH180615	4.56	
	4.93	
	4.99	
	5.20	
	4.67	
	4.40	0.27
RH240611	3.34	
	3.37	0.02
RH030710	3.53	
	3.57	
	3.53	
	4.26	
	3.28	0.33
RH190612	1.89	
	1.35	
	1.67	0.22

Micrite replicates	$\delta^{13}C$ (‰)	$\delta^{13}C$ SD	$\delta^{18}O$ (‰)	$\delta^{18}O$ SD
RH130607	2.18		-3.76	
	2.19		-3.78	
	2.20	0.01	-3.74	0.02
RH130610	3.39		-2.47	
	2.36		-3.62	
	2.38		-3.67	
	3.42		-2.49	
	2.39		-3.49	
	2.28		-3.83	
	3.08	0.48	-2.99	0.53
RH140601	2.20		-3.83	
	2.21		-3.82	
	2.24	0.02	-3.82	0.01
RH180612	2.12		-4.43	
	3.40	0.64	-2.66	0.88
RH180613	1.80		-5.05	
	1.83	0.02	-5.02	0.02
RH180614	1.77		-5.05	
	1.78		-5.09	
	1.81	0.02	-5.08	0.02
RH190612	2.45		-3.82	
	2.45		-3.82	
	2.07	0.18	-4.14	0.15
RH190625	2.08		-4.35	
	2.11		-4.36	
	2.12	0.02	-4.26	0.05
RH240608	2.45		-3.56	
	2.46	0.01	-3.80	0.12

5.4.5 Major, trace and rare earth elements from the RH F-2 stratigraphy

Height above base (cm)	Sample number	SiO_2 (%)	Al_2O_3 (%)	CaO (%)	Cr_2O_3 (%)	Fe_2O_3 (%)	K_2O (%)
1.5	RH020721	2.77	0.60	51.89	<0.001	0.19	0.31
5.5	RH020717	2.27	0.51	51.52	<0.001	0.10	0.22
7.5	RH020720	2.32	0.46	51.62	<0.001	0.20	0.24
15.6	RH020716	1.14	0.22	52.61	<0.001	0.10	0.12
20.0	RH020709	1.31	0.27	53.41	<0.001	0.07	0.15
24.7	RH020703	0.99	0.19	54.17	<0.001	0.05	0.11
30.0	RH020706	0.92	0.18	53.94	<0.001	0.08	0.10
33.7	RH020707	1.01	0.19	53.39	<0.001	0.08	0.10
35.3	RH230614	1.36	0.23	53.08	<0.001	0.09	0.13
40.9	RH030722	0.89	0.14	55.00	<0.001	0.10	0.09
46.0	RH030718	0.87	0.15	55.17	<0.001	0.09	0.10
55.6	RH230607	1.11	0.18	53.04	<0.001	0.06	0.12
61.8	RH240624	0.93	0.17	53.72	<0.001	0.06	0.10
65.4	RH240615	0.91	0.17	53.67	<0.001	0.06	0.10
70.4	RH240614	0.93	0.17	53.43	<0.001	0.07	0.10
73.6	RH140602	0.98	0.18	55.94	<0.001	0.06	0.09
80.1	RH150609	1.02	0.20	55.94	<0.001	0.15	0.14
86.2	RH180604	0.89	0.16	53.42	<0.001	0.05	0.11
93.5	RH170602a	1.09	0.18	55.90	<0.001	0.05	0.11
100.7	RH020724	1.33	0.25	55.17	<0.001	0.10	0.17
105.0	RH150603	1.47	0.26	55.88	<0.001	0.08	0.17
105.5	RH130605	33.86	6.97	28.35	0.005	2.32	4.37
105.5	RH130610b	16.87	3.18	40.18	0.002	1.50	2.14
111.8	RH180608	2.54	0.49	51.99	<0.001	0.19	0.37
117.2	RH180607	2.62	0.47	51.93	<0.001	0.13	0.34
122.0	RH180606	1.80	0.32	54.07	<0.001	0.09	0.20
123.5	RH130607	1.80	0.30	55.51	<0.001	0.08	0.20
135.4	RH180612	0.79	0.16	54.42	<0.001	0.14	0.14
146.1	RH180613	1.56	0.27	53.52	<0.001	0.08	0.18
150.6	RH180614	1.34	0.23	53.26	<0.001	0.09	0.16
155.0	RH100614	3.13	0.56	53.98	<0.001	0.17	0.35
160.0	RH190611	3.04	0.72	51.58	<0.001	0.15	0.62
164.0	RH190615	1.72	0.31	52.16	<0.001	0.18	0.23
170.5	RH180603	1.92	0.35	51.62	<0.001	0.13	0.24

173.5	RH180615	1.51	0.28	52.81	<0.001	0.10	0.19
181.0	RH190604	3.57	0.71	49.61	<0.001	0.18	0.50
188.0	RH170604	0.83	0.15	53.61	<0.001	0.08	0.11
191.0	RH240623	2.35	0.44	50.82	<0.001	0.17	0.30
202.8	RH170602b	1.93	0.34	52.91	<0.001	0.15	0.21
205.1	RH240611	1.79	0.32	51.79	<0.001	0.19	0.22
208.0	RH190601	2.89	0.56	51.65	<0.001	0.29	0.36
214.7	RH230613	1.43	0.28	52.21	<0.001	0.13	0.21
220.2	RH130612	1.61	0.33	54.76	<0.001	0.13	0.21
225.2	RH140601	1.97	0.39	53.03	<0.001	0.15	0.24
229.2	RH170610	2.98	0.52	47.73	<0.001	0.22	0.35
234.6	RH110602	3.14	0.57	49.64	<0.001	0.18	0.35
239.5	RH190619	2.28	0.42	49.11	<0.001	0.16	0.29
244.5	RH130609	1.57	0.28	55.26	<0.001	0.08	0.19
250.1	RH190610	0.88	0.15	53.00	<0.001	0.06	0.11

Height above base (cm)	**Sample number**	**MgO (%)**	**MnO (%)**	**Na_2O (%)**	**P_2O_5 (%)**	**TiO_2 (%)**	**LOI @ 1000°C**
1.5	RH020721	2.85	0.009	0.06	0.47	0.03	42.24
5.5	RH020717	3.42	0.012	0.08	0.13	0.02	43.01
7.5	RH020720	3.53	0.013	0.08	0.48	0.02	42.60
15.6	RH020716	1.23	0.011	0.03	0.20	0.01	43.08
20.0	RH020709	1.19	0.010	0.03	0.06	0.01	43.07
24.7	RH020703	0.58	0.010	0.04	0.68	<0.01	42.96
30.0	RH020706	0.87	0.009	0.02	0.09	<0.01	43.20
33.7	RH020707	1.30	0.011	0.12	0.11	<0.01	43.32
35.3	RH230614	1.52	0.009	0.09	0.12	0.01	43.07
40.9	RH030722	1.05	0.008	0.06	0.12	<0.01	43.06
46.0	RH030718	1.19	0.007	0.05	0.10	<0.01	43.05
55.6	RH230607	1.70	0.006	0.09	0.18	<0.01	43.21
61.8	RH240624	0.79	0.005	0.03	0.09	<0.01	43.07
65.4	RH240615	1.22	0.009	0.05	0.10	<0.01	43.27
70.4	RH240614	0.90	0.006	0.08	0.25	<0.01	42.94
73.6	RH140602	1.00	0.005	0.04	0.21	<0.01	43.13
80.1	RH150609	0.55	0.006	0.03	0.08	<0.01	43.11
86.2	RH180604	1.00	0.006	0.06	0.10	<0.01	43.07
93.5	RH170602a	0.89	0.005	0.06	0.18	<0.01	42.90
100.7	RH020724	0.52	0.004	0.06	0.31	<0.01	42.46

105.0	RH150603	0.94	0.005	0.07	0.24	<0.01	42.79
105.5	RH130605	0.55	0.010	0.17	1.18	0.36	20.91
105.5	RH130610b	3.11	0.008	0.16	0.76	0.20	33.98
111.8	RH180608	1.54	0.009	0.11	0.17	0.02	42.53
117.2	RH180607	1.53	0.009	0.11	0.32	0.02	42.26
122.0	RH180606	0.69	0.006	0.09	0.30	0.02	42.45
123.5	RH130607	0.92	0.006	0.07	0.11	0.01	42.55
135.4	RH180612	0.67	0.009	0.09	0.08	0.01	43.32
146.1	RH180613	1.44	0.005	0.10	0.31	0.02	42.77
150.6	RH180614	1.34	0.006	0.08	0.14	0.01	42.84
155.0	RH100614	0.70	0.006	0.06	0.18	0.03	41.88
160.0	RH190611	0.95	0.011	0.09	0.18	0.03	41.90
164.0	RH190615	1.78	0.006	0.09	0.12	0.03	42.90
170.5	RH180603	1.69	0.006	0.10	0.12	0.02	42.77
173.5	RH180615	1.84	0.006	0.11	0.29	0.01	42.81
181.0	RH190604	3.07	0.006	0.13	0.48	0.04	41.80
188.0	RH170604	0.95	0.005	0.06	0.12	<0.01	43.24
191.0	RH240623	2.39	0.006	0.10	0.15	0.02	42.76
202.8	RH170602b	2.36	0.005	0.08	0.22	0.02	42.87
205.1	RH240611	1.74	0.006	0.09	0.62	0.01	42.47
208.0	RH190601	1.17	0.006	0.09	0.26	0.03	42.11
214.7	RH230613	1.32	0.009	0.05	0.22	0.02	43.00
220.2	RH130612	1.79	0.006	0.09	0.11	0.01	42.79
225.2	RH140601	2.49	0.005	0.09	0.16	0.02	42.90
229.2	RH170610	4.38	0.009	0.15	0.26	0.03	42.69
234.6	RH110602	4.85	0.010	0.14	0.31	0.04	42.59
239.5	RH190619	3.80	0.011	0.14	0.53	0.03	42.74
244.5	RH130609	1.55	0.010	0.07	0.20	0.02	42.74
250.1	RH190610	1.13	0.010	0.10	0.34	0.01	43.09

Height above base (cm)	Sample number	Ba (ppm)	Ce (ppm)	Dy (ppm)	Er (ppm)	Eu (ppm)	Ga (ppm)
1.5	RH020721	104.7	7.5	0.6	0.3	0.2	0.6
5.5	RH020717	109.0	2.1	0.2	0.2	<0.1	<0.5
7.5	RH020720	117.3	6.7	0.5	0.3	0.2	1.2
15.6	RH020716	139.2	2.3	0.2	0.2	<0.1	0.9
20.0	RH020709	65.7	1.3	<0.1	<0.1	<0.1	<0.5
24.7	RH020703	78.1	5.1	0.5	0.3	0.1	<0.5

30.0	RH020706	36.2	1.1	0.1	0.1	<0.1	0.7
33.7	RH020707	52.6	1.2	0.1	0.1	<0.1	0.6
35.3	RH230614	66.9	1.1	<0.1	0.1	<0.1	<0.5
40.9	RH030722	77.6	1.0	0.1	<0.1	<0.1	<0.5
46.0	RH030718	62.0	1.0	0.2	<0.1	<0.1	<0.5
55.6	RH230607	66.1	1.2	0.1	0.1	<0.1	<0.5
61.8	RH240624	56.0	1.0	0.1	<0.1	<0.1	<0.5
65.4	RH240615	60.9	1.1	0.1	0.1	<0.1	<0.5
70.4	RH240614	61.1	1.6	0.2	0.1	<0.1	0.8
73.6	RH140602	67.8	1.4	0.1	0.2	<0.1	<0.5
80.1	RH150609	66.1	1.2	0.1	<0.1	<0.1	<0.5
86.2	RH180604	63.4	1.0	<0.1	0.1	<0.1	<0.5
93.5	RH170602a	61.9	1.4	0.1	0.1	<0.1	<0.5
100.7	RH020724	74.2	2.9	0.4	0.3	<0.1	0.6
105.0	RH150603	76.3	2.0	0.3	0.2	<0.1	0.7
105.5	RH130605	290.7	52.2	3.3	1.7	1.0	8.7
105.5	RH130610b	214.6	11.8	1.3	0.9	0.2	3.9
111.8	RH180608	79.7	2.1	0.2	0.2	<0.1	<0.5
117.2	RH180607	82.2	3.4	0.4	0.3	<0.1	0.7
122.0	RH180606	75.5	3.1	0.4	0.2	<0.1	0.8
123.5	RH130607	62.9	1.9	0.2	0.1	<0.1	<0.5
135.4	RH180612	62.4	2.9	0.2	0.1	<0.1	<0.5
146.1	RH180613	85.3	3.0	0.3	0.2	<0.1	<0.5
150.6	RH180614	83.0	1.9	0.2	0.1	<0.1	<0.5
155.0	RH100614	83.0	2.4	0.3	0.2	<0.1	0.8
160.0	RH190611	106.0	6.2	0.3	0.1	<0.1	0.5
164.0	RH190615	79.6	2.5	0.2	0.1	<0.1	<0.5
170.5	RH180603	74.8	1.8	0.2	0.1	<0.1	<0.5
173.5	RH180615	81.9	3.5	0.3	0.2	<0.1	<0.5
181.0	RH190604	120.2	4.7	0.5	0.4	<0.1	1.1
188.0	RH170604	78.9	1.1	0.2	<0.1	<0.1	<0.5
191.0	RH240623	92.2	1.6	0.2	0.2	<0.1	<0.5
202.8	RH170602b	91.3	2.2	0.2	0.2	<0.1	<0.5
205.1	RH240611	95.6	5.3	0.5	0.5	<0.1	0.6
208.0	RH190601	97.6	3.0	0.3	0.2	<0.1	0.7
214.7	RH230613	84.0	3.6	0.2	0.2	<0.1	<0.5
220.2	RH130612	84.7	1.8	0.2	0.1	<0.1	0.7
225.2	RH140601	95.2	1.9	0.2	0.2	<0.1	0.7
229.2	RH170610	97.7	2.5	0.4	0.3	<0.1	0.7
234.6	RH110602	107.1	3.5	0.6	0.4	<0.1	0.5
239.5	RH190619	121.4	4.7	1.0	0.5	0.1	1.0

244.5	RH130609	85.1	3.2	0.5	0.3	<0.1	0.6
250.1	RH190610	86.6	4.3	0.8	0.3	0.1	<0.5

Height above base (cm)	Sample number	Gd (ppm)	Hf (ppm)	Ho (ppm)	La (ppm)	Lu (ppm)	Nb (ppm)
1.5	RH020721	0.7	<1	<0.1	4.1	<0.1	1.3
5.5	RH020717	0.3	<1	<0.1	1.4	<0.1	2.0
7.5	RH020720	0.7	<1	0.1	4.0	<0.1	3.1
15.6	RH020716	0.3	<1	<0.1	1.3	<0.1	<0.5
20.0	RH020709	0.2	<1	<0.1	0.9	<0.1	<0.5
24.7	RH020703	0.5	<1	<0.1	2.9	<0.1	<0.5
30.0	RH020706	0.1	<1	<0.1	0.9	<0.1	<0.5
33.7	RH020707	<0.1	<1	<0.1	0.8	<0.1	<0.5
35.3	RH230614	0.1	<1	<0.1	0.7	<0.1	<0.5
40.9	RH030722	0.1	<1	<0.1	0.6	<0.1	<0.5
46.0	RH030718	0.1	<1	<0.1	0.7	<0.1	<0.5
55.6	RH230607	<0.1	<1	<0.1	0.7	<0.1	<0.5
61.8	RH240624	0.1	<1	<0.1	0.6	<0.1	<0.5
65.4	RH240615	<0.1	<1	<0.1	0.7	<0.1	<0.5
70.4	RH240614	0.1	<1	<0.1	0.9	<0.1	<0.5
73.6	RH140602	0.2	<1	<0.1	0.8	<0.1	1.8
80.1	RH150609	0.1	<1	<0.1	0.8	<0.1	<0.5
86.2	RH180604	0.1	<1	<0.1	0.6	<0.1	<0.5
93.5	RH170602a	0.1	<1	<0.1	0.8	<0.1	<0.5
100.7	RH020724	0.4	<1	<0.1	1.8	<0.1	0.5
105.0	RH150603	0.2	<1	<0.1	1.2	<0.1	0.6
105.5	RH130605	4.7	3	0.5	27.7	0.2	7.1
105.5	RH130610b	1.3	1	0.2	6.4	0.1	4.3
111.8	RH180608	0.2	<1	<0.1	1.2	<0.1	<0.5
117.2	RH180607	0.3	<1	<0.1	1.9	<0.1	<0.5
122.0	RH180606	0.4	<1	<0.1	1.7	<0.1	<0.5
123.5	RH130607	0.3	<1	<0.1	1.1	<0.1	0.5
135.4	RH180612	0.3	<1	<0.1	1.4	<0.1	<0.5
146.1	RH180613	0.3	<1	<0.1	1.7	<0.1	<0.5
150.6	RH180614	0.1	<1	<0.1	1.1	<0.1	<0.5
155.0	RH100614	0.3	<1	<0.1	1.4	<0.1	0.8
160.0	RH190611	0.3	<1	<0.1	4.0	<0.1	<0.5
164.0	RH190615	0.2	<1	<0.1	1.3	<0.1	<0.5

170.5	RH180603	0.2	<1	<0.1	1.0	<0.1	<0.5
173.5	RH180615	0.3	<1	<0.1	1.8	<0.1	<0.5
181.0	RH190604	0.4	<1	0.1	2.5	<0.1	0.7
188.0	RH170604	<0.1	<1	<0.1	0.7	<0.1	<0.5
191.0	RH240623	0.2	<1	<0.1	0.9	<0.1	<0.5
202.8	RH170602b	0.3	<1	<0.1	1.3	<0.1	<0.5
205.1	RH240611	0.4	<1	0.1	3.0	<0.1	<0.5
208.0	RH190601	0.3	<1	<0.1	1.7	<0.1	0.6
214.7	RH230613	0.2	<1	<0.1	2.2	<0.1	<0.5
220.2	RH130612	0.2	<1	<0.1	1.1	<0.1	<0.5
225.2	RH140601	0.2	<1	<0.1	1.2	<0.1	0.5
229.2	RH170610	0.3	<1	<0.1	1.4	<0.1	0.5
234.6	RH110602	0.4	<1	0.1	3.7	<0.1	0.8
239.5	RH190619	0.7	<1	0.2	2.5	<0.1	<0.5
244.5	RH130609	0.4	<1	<0.1	2.0	<0.1	0.6
250.1	RH190610	0.5	<1	0.1	2.3	<0.1	<0.5

Height above base (cm)	**Sample number**	**Nd (ppm)**	**Pr (ppm)**	**Rb (ppm)**	**Sc (ppm)**	**Sm (ppm)**	**Sn (ppm)**
1.5	RH020721	4.2	1.0	4.7	<1	0.8	<1
5.5	RH020717	1.1	0.3	3.6	<1	0.2	1
7.5	RH020720	3.7	0.9	4.3	<1	0.7	1
15.6	RH020716	1.1	0.3	1.8	<1	0.2	<1
20.0	RH020709	0.6	0.2	2.0	<1	0.1	<1
24.7	RH020703	2.9	0.7	1.6	<1	0.6	<1
30.0	RH020706	<0.5	0.1	1.4	<1	0.1	<1
33.7	RH020707	0.6	0.1	1.7	<1	<0.1	<1
35.3	RH230614	0.6	0.1	1.9	<1	0.1	<1
40.9	RH030722	0.5	0.1	1.2	1	<0.1	<1
46.0	RH030718	0.6	0.1	1.3	<1	0.1	<1
55.6	RH230607	0.6	0.2	1.2	<1	0.1	<1
61.8	RH240624	0.6	0.1	1.2	<1	<0.1	<1
65.4	RH240615	0.8	0.2	1.3	<1	0.1	1
70.4	RH240614	0.9	0.2	1.2	<1	0.1	<1
73.6	RH140602	0.8	0.2	1.3	<1	0.1	<1
80.1	RH150609	0.6	0.2	1.3	<1	0.1	<1
86.2	RH180604	<0.5	0.1	1.1	<1	0.1	<1
93.5	RH170602a	0.7	0.2	1.4	1	0.2	<1

100.7	RH020724	1.5	0.4	2.0	<1	0.3	<1
105.0	RH150603	1.0	0.3	1.8	<1	0.1	<1
105.5	RH130605	27.0	6.8	53.6	4	4.8	2
105.5	RH130610b	6.0	1.5	26.1	2	1.1	2
111.8	RH180608	1.0	0.3	3.3	<1	0.2	<1
117.2	RH180607	1.6	0.4	3.4	1	0.4	<1
122.0	RH180606	1.7	0.4	2.3	1	0.3	<1
123.5	RH130607	1.1	0.2	2.2	<1	0.2	<1
135.4	RH180612	1.4	0.4	0.9	1	0.3	<1
146.1	RH180613	1.8	0.4	2.1	<1	0.3	<1
150.6	RH180614	0.9	0.2	1.9	<1	0.2	<1
155.0	RH100614	1.2	0.3	4.5	1	0.2	<1
160.0	RH190611	2.4	0.7	4.3	<1	0.4	<1
164.0	RH190615	1.1	0.3	2.4	<1	0.2	<1
170.5	RH180603	0.9	0.2	2.7	<1	0.1	<1
173.5	RH180615	1.8	0.4	2.1	<1	0.3	<1
181.0	RH190604	2.1	0.6	5.5	<1	0.4	<1
188.0	RH170604	<0.5	0.1	1.1	<1	0.1	<1
191.0	RH240623	0.7	0.2	3.4	<1	0.2	3
202.8	RH170602b	1.1	0.3	2.8	<1	0.2	<1
205.1	RH240611	2.5	0.6	2.5	<1	0.4	<1
208.0	RH190601	1.7	0.4	4.1	<1	0.3	<1
214.7	RH230613	1.6	0.4	2.1	<1	0.4	<1
220.2	RH130612	1.0	0.2	2.5	<1	0.1	<1
225.2	RH140601	0.9	0.2	2.8	<1	0.2	<1
229.2	RH170610	1.3	0.3	4.2	1	0.2	<1
234.6	RH110602	1.7	0.4	4.8	<1	0.3	<1
239.5	RH190619	2.3	0.6	3.6	1	0.4	<1
244.5	RH130609	1.5	0.4	2.4	<1	0.3	<1
250.1	RH190610	2.3	0.6	1.2	1	0.4	<1

Height above base (cm)	**Sample number**	**Sr (ppm)**	**Ta (ppm)**	**Tb (ppm)**	**Th (ppm)**	**Tm (ppm)**	**U (ppm)**
1.5	RH020721	1392.7	0.1	0.1	1.4	<0.1	12.3
5.5	RH020717	1206.4	0.1	<0.1	1.2	<0.1	5.9
7.5	RH020720	1380.5	0.1	0.1	1.7	<0.1	11.6
15.6	RH020716	1123.8	<0.1	<0.1	<0.1	<0.1	5.8
20.0	RH020709	1079.7	<0.1	<0.1	<0.1	<0.1	3.2

24.7	RH020703	1201.5	<0.1	<0.1	1.3	<0.1	13.0
30.0	RH020706	1068.1	<0.1	<0.1	<0.1	<0.1	3.3
33.7	RH020707	1058.7	<0.1	<0.1	<0.1	<0.1	2.8
35.3	RH230614	1060.9	<0.1	<0.1	<0.1	<0.1	3.3
40.9	RH030722	1057.8	<0.1	<0.1	0.3	<0.1	2.7
46.0	RH030718	1110.7	<0.1	<0.1	0.4	<0.1	3.2
55.6	RH230607	1076.1	<0.1	<0.1	<0.1	<0.1	3.7
61.8	RH240624	1023.2	<0.1	<0.1	<0.1	<0.1	3.0
65.4	RH240615	1003.1	<0.1	<0.1	<0.1	<0.1	2.7
70.4	RH240614	1016.9	<0.1	<0.1	<0.1	<0.1	4.5
73.6	RH140602	1080.2	<0.1	<0.1	0.5	<0.1	4.4
80.1	RH150609	1008.6	<0.1	<0.1	<0.1	<0.1	2.3
86.2	RH180604	993.2	<0.1	<0.1	<0.1	<0.1	2.6
93.5	RH170602a	1031.3	<0.1	<0.1	0.1	<0.1	5.1
100.7	RH020724	1051.7	<0.1	<0.1	0.9	<0.1	6.5
105.0	RH150603	1031.3	<0.1	<0.1	0.3	<0.1	5.1
105.5	RH130605	768.6	0.7	0.6	6.7	0.2	29.4
105.5	RH130610b	1024.2	0.3	0.2	2.7	<0.1	22.1
111.8	RH180608	964.8	<0.1	<0.1	0.2	<0.1	3.7
117.2	RH180607	992.4	<0.1	<0.1	0.3	<0.1	5.7
122.0	RH180606	974.7	<0.1	<0.1	0.2	<0.1	5.3
123.5	RH130607	952.8	<0.1	<0.1	1.2	<0.1	3.5
135.4	RH180612	983.4	<0.1	<0.1	<0.1	<0.1	1.7
146.1	RH180613	1287.9	<0.1	<0.1	0.3	<0.1	4.4
150.6	RH180614	1299.1	<0.1	<0.1	0.2	<0.1	2.6
155.0	RH100614	1425.3	<0.1	<0.1	0.5	<0.1	3.1
160.0	RH190611	1095.5	<0.1	<0.1	0.2	<0.1	2.8
164.0	RH190615	1161.6	<0.1	<0.1	0.1	<0.1	2.3
170.5	RH180603	1145.4	<0.1	<0.1	0.1	<0.1	2.2
173.5	RH180615	1315.4	<0.1	<0.1	0.3	<0.1	4.3
181.0	RH190604	1406.0	<0.1	<0.1	0.7	<0.1	7.1
188.0	RH170604	1326.6	<0.1	<0.1	0.1	<0.1	2.3
191.0	RH240623	1355.1	<0.1	<0.1	<0.1	<0.1	3.1
202.8	RH170602b	1412.1	<0.1	<0.1	0.3	<0.1	3.4
205.1	RH240611	1488.4	<0.1	<0.1	0.4	<0.1	6.5
208.0	RH190601	1439.6	<0.1	<0.1	0.4	<0.1	3.9
214.7	RH230613	1467.0	<0.1	<0.1	0.1	<0.1	3.3
220.2	RH130612	1488.4	<0.1	<0.1	0.8	<0.1	2.4
225.2	RH140601	1427.3	<0.1	<0.1	0.6	<0.1	3.3
229.2	RH170610	1505.7	<0.1	<0.1	0.4	<0.1	4.3
234.6	RH110602	1440.6	<0.1	<0.1	0.7	<0.1	4.8

239.5	RH190619	1462.0	<0.1	0.1	0.6	<0.1	6.2
244.5	RH130609	1267.5	<0.1	<0.1	0.9	<0.1	3.4
250.1	RH190610	1184.0	<0.1	<0.1	0.5	<0.1	4.0

Height above base (cm)	Sample number	V (ppm)	W (ppm)	Y (ppm)	Yb (ppm)	Zr (ppm)
1.5	RH020721	39	1.8	3.6	0.3	5.5
5.5	RH020717	29	4.4	1.5	0.2	2.4
7.5	RH020720	28	6.9	3.7	0.2	3.6
15.6	RH020716	19	<0.5	1.5	0.2	<0.5
20.0	RH020709	14	<0.5	1.2	0.2	<0.5
24.7	RH020703	14	<0.5	3.5	0.3	8.2
30.0	RH020706	13	<0.5	1.0	0.1	<0.5
33.7	RH020707	14	<0.5	1.0	0.2	<0.5
35.3	RH230614	23	<0.5	1.0	0.1	2.4
40.9	RH030722	13	<0.5	0.9	0.1	3.9
46.0	RH030718	13	<0.5	1.0	0.1	2.1
55.6	RH230607	16	<0.5	1.2	<0.1	1.1
61.8	RH240624	13	<0.5	0.9	0.1	0.7
65.4	RH240615	17	<0.5	0.9	<0.1	1.5
70.4	RH240614	17	<0.5	1.4	0.1	2.0
73.6	RH140602	14	4.8	1.2	0.2	<0.5
80.1	RH150609	19	<0.5	0.7	0.1	1.2
86.2	RH180604	12	<0.5	1.1	<0.1	0.7
93.5	RH170602a	17	<0.5	1.3	0.2	1.9
100.7	RH020724	13	0.6	2.8	0.2	4.7
105.0	RH150603	8	1.0	1.8	0.2	1.8
105.5	RH130605	85	1.7	20.1	1.6	96.4
105.5	RH130610b	76	1.2	8.3	0.8	49.9
111.8	RH180608	16	<0.5	1.5	0.2	5.6
117.2	RH180607	11	<0.5	2.4	0.3	5.6
122.0	RH180606	11	<0.5	2.3	0.2	4.6
123.5	RH130607	12	<0.5	1.5	0.2	5.0
135.4	RH180612	8	<0.5	1.3	0.2	1.4
146.1	RH180613	11	<0.5	2.3	0.2	3.4
150.6	RH180614	9	<0.5	1.3	0.2	2.1
155.0	RH100614	21	<0.5	2.0	0.2	8.1
160.0	RH190611	13	<0.5	1.5	0.2	6.4

164.0	RH190615	22	<0.5	1.1	0.1	5.5
170.5	RH180603	20	<0.5	1.2	0.1	6.2
173.5	RH180615	20	<0.5	2.3	0.2	3.2
181.0	RH190604	24	0.7	4.0	0.3	10.1
188.0	RH170604	9	<0.5	1.0	0.1	1.5
191.0	RH240623	15	<0.5	1.5	0.1	5.4
202.8	RH170602b	16	<0.5	2.0	0.2	4.0
205.1	RH240611	14	<0.5	4.4	0.3	6.0
208.0	RH190601	15	<0.5	2.5	0.2	8.4
214.7	RH230613	7	<0.5	2.2	0.2	4.9
220.2	RH130612	13	<0.5	1.8	0.2	4.3
225.2	RH140601	20	<0.5	1.8	0.2	5.1
229.2	RH170610	22	<0.5	3.0	0.2	6.7
234.6	RH110602	45	<0.5	4.1	0.3	9.6
239.5	RH190619	20	<0.5	5.8	0.4	6.4
244.5	RH130609	24	<0.5	3.0	0.2	6.1
250.1	RH190610	11	<0.5	4.5	0.2	2.7

5.4.5 Correlation of major, trace and rare earth elements

	SiO_2	Al_2O_3	CaO	Cr_2O_3	Fe_2O_3	K_2O	MgO	MnO
SiO_2	1.00							
Al_2O_3	1.00	1.00						
CaO	-0.94	-0.94	1.00					
Cr_2O_3	0.97	0.97	-0.88	1.00				
Fe_2O_3	0.99	0.98	-0.93	0.94	1.00			
K_2O	1.00	1.00	-0.94	0.97	0.98	1.00		
MgO	0.04	0.03	-0.28	-0.10	0.05	0.02	1.00	
MnO	0.14	0.15	-0.26	0.12	0.12	0.14	0.34	1.00
Na_2O	0.54	0.53	-0.68	0.44	0.54	0.55	0.55	0.17
P_2O_5	0.76	0.76	-0.77	0.71	0.75	0.75	0.20	0.20
TiO_2	1.00	0.99	-0.96	0.97	0.99	1.00	-0.07	0.10
LOI	-1.00	-1.00	0.92	-0.98	-0.98	-0.99	0.04	-0.11
Ba	0.90	0.90	-0.92	0.82	0.90	0.90	0.29	0.25
Ce	0.95	0.96	-0.89	0.98	0.91	0.95	-0.04	0.20
Dy	0.93	0.93	-0.90	0.92	0.90	0.93	0.10	0.27
Er	0.94	0.94	-0.92	0.91	0.93	0.94	0.11	0.19
Eu	0.94	0.95	-0.91	0.99	0.88	0.94	-0.48	-0.20
Ga	0.99	0.99	-0.92	0.98	0.97	0.98	-0.02	0.15
Gd	0.95	0.96	-0.89	0.97	0.92	0.95	-0.01	0.24
Hf	0.92	0.93	-0.83	0.99	0.87	0.92	-0.14	0.13
Ho	0.96	0.97	-0.90	0.99	0.93	0.96	-0.04	0.15
La	0.95	0.96	-0.89	0.97	0.91	0.95	-0.01	0.23
Lu	0.95	0.96	-0.86	1.00	0.91	0.95	-0.12	0.12
Nb	0.91	0.91	-0.85	0.88	0.91	0.90	0.13	0.24
Nd	0.95	0.96	-0.88	0.98	0.91	0.95	-0.06	0.20
Pr	0.95	0.96	-0.88	0.98	0.91	0.95	-0.04	0.20
Pb	1.00	1.00	-0.94	0.97	0.99	1.00	0.05	0.15
Sc	0.93	0.93	-0.86	0.97	0.89	0.92	-0.09	0.18
Sm	0.95	0.96	-0.88	0.97	0.91	0.95	-0.05	0.22
Sn	0.46	0.45	-0.48	0.39	0.48	0.45	0.15	-0.01
Sr	-0.27	-0.27	0.10	-0.34	-0.26	-0.28	0.59	-0.02
Ta	0.99	0.99	-0.91	0.99	0.97	0.98	-0.03	0.15
Tb	0.94	0.95	-0.85	0.99	0.90	0.94	-0.12	0.13
Th	0.93	0.93	-0.84	0.92	0.90	0.92	0.08	0.22
Tm	0.00	0.00	0.00	0.00	0.00	0.00	0.00	0.00
U	0.87	0.86	-0.83	0.81	0.87	0.86	0.14	0.24
V	0.86	0.86	-0.86	0.77	0.88	0.85	0.36	0.24
W	0.12	0.13	-0.11	0.10	0.11	0.10	0.29	0.29
Y	0.93	0.93	-0.91	0.92	0.91	0.93	0.13	0.23
Yb	0.97	0.97	-0.93	0.94	0.95	0.97	0.09	0.21
Zr	0.99	0.99	-0.93	0.96	0.99	0.99	0.03	0.12

	MnO	Na_2O	P_2O_5	TiO_2	LOI	Ba	Ce	Dy
SiO_2								
Al_2O_3								
CaO								
Cr_2O_3								
Fe_2O_3								
K_2O								
MgO								
MnO	1.00							
Na_2O	0.17	1.00						
P_2O_5	0.20	0.53	1.00					
TiO_2	0.10	0.57	0.81	1.00				
LOI	-0.11	-0.50	-0.76	-0.99	1.00			
Ba	0.25	0.59	0.81	0.93	-0.88	1.00		
Ce	0.20	0.46	0.79	0.94	-0.97	0.85	1.00	
Dy	0.27	0.57	0.87	0.93	-0.93	0.88	0.96	1.00
Er	0.19	0.58	0.90	0.95	-0.94	0.91	0.94	0.98
Eu	-0.20	0.58	0.90	0.92	-0.96	0.88	1.00	0.97
Ga	0.15	0.49	0.77	0.99	-0.99	0.88	0.96	0.94
Gd	0.24	0.49	0.82	0.95	-0.96	0.87	0.99	0.98
Hf	0.13	0.39	0.66	0.91	-0.94	0.76	0.97	0.90
Ho	0.15	0.48	0.76	0.95	-0.97	0.84	0.97	0.95
La	0.23	0.47	0.80	0.94	-0.96	0.86	1.00	0.96
Lu	0.12	0.41	0.69	0.94	-0.97	0.79	0.98	0.91
Nb	0.24	0.42	0.74	0.92	-0.90	0.86	0.87	0.85
Nd	0.20	0.45	0.80	0.94	-0.96	0.85	1.00	0.96
Pr	0.20	0.46	0.79	0.94	-0.96	0.85	1.00	0.95
Pb	0.15	0.54	0.77	1.00	-1.00	0.90	0.95	0.93
Sc	0.18	0.48	0.70	0.92	-0.94	0.78	0.95	0.93
Sm	0.22	0.45	0.80	0.94	-0.96	0.85	1.00	0.95
Sn	-0.01	0.30	0.29	0.45	-0.43	0.44	0.35	0.34
Sr	-0.02	0.14	0.03	-0.43	0.31	-0.01	-0.24	-0.18
Ta	0.15	0.46	0.73	0.98	-0.99	0.87	0.96	0.92
Tb	0.13	0.41	0.68	0.93	-0.96	0.79	0.98	0.91
Th	0.22	0.44	0.81	0.93	-0.93	0.86	0.94	0.93
Tm	0.00	0.00	0.00	0.00	0.00	0.00	0.00	0.00
U	0.24	0.43	0.91	0.91	-0.86	0.86	0.85	0.88
V	0.24	0.55	0.71	0.87	-0.83	0.86	0.76	0.80
W	0.29	-0.03	0.20	0.11	-0.10	0.22	0.16	0.13
Y	0.23	0.58	0.89	0.93	-0.93	0.90	0.95	0.99
Yb	0.21	0.56	0.86	0.98	-0.97	0.91	0.95	0.97
Zr	0.12	0.55	0.79	1.00	-0.99	0.90	0.95	0.94

	Er	Eu	Ga	Gd	Hf	Ho	La	Lu
SiO_2								
Al_2O_3								
CaO								
Cr_2O_3								
Fe_2O_3								
K_2O								
MgO								
MnO								
Na_2O								
P_2O_5								
TiO_2								
LOI								
Ba								
Ce								
Dy								
Er	1.00							
Eu	0.95	1.00						
Ga	0.94	0.95	1.00					
Gd	0.96	1.00	0.97	1.00				
Hf	0.87	1.00	0.94	0.96	1.00			
Ho	0.94	0.97	0.98	0.98	0.97	1.00		
La	0.94	1.00	0.95	0.99	0.96	0.97	1.00	
Lu	0.89	1.00	0.96	0.97	1.00	0.98	0.97	1.00
Nb	0.87	0.86	0.92	0.89	0.82	0.87	0.87	0.85
Nd	0.93	1.00	0.96	0.99	0.97	0.97	1.00	0.98
Pr	0.94	1.00	0.96	0.99	0.97	0.97	1.00	0.98
Pb	0.95	0.94	0.99	0.96	0.92	0.96	0.95	0.95
Sc	0.89	0.98	0.94	0.95	0.96	0.96	0.95	0.97
Sm	0.94	1.00	0.96	0.99	0.97	0.97	0.99	0.97
Sn	0.37	0.62	0.42	0.36	0.33	0.38	0.34	0.36
Sr	-0.14	-0.82	-0.30	-0.25	-0.33	-0.29	-0.23	-0.34
Ta	0.93	0.96	0.99	0.96	0.95	0.97	0.95	0.97
Tb	0.88	1.00	0.96	0.97	1.00	0.98	0.97	1.00
Th	0.92	0.93	0.93	0.96	0.89	0.91	0.94	0.91
Tm	0.00	0.00	0.00	0.94	0.00	0.00	0.00	0.00
U	0.90	0.82	0.87	0.87	0.74	0.82	0.85	0.78
V	0.84	0.75	0.83	0.79	0.69	0.77	0.78	0.73
W	0.14	0.15	0.14	0.18	0.10	0.09	0.16	0.10
Y	0.99	0.92	0.94	0.97	0.89	0.95	0.95	0.90
Yb	0.98	0.93	0.96	0.97	0.90	0.96	0.96	0.92
Zr	0.95	0.93	0.98	0.95	0.91	0.96	0.94	0.94

	Nb	Nd	Pr	Rb	Sc	Sm	Sn	Sr
SiO_2								
Al_2O_3								
CaO								
Cr_2O_3								
Fe_2O_3								
K_2O								
MgO								
MnO								
Na_2O								
P_2O_5								
TiO_2								
LOI								
Ba								
Ce								
Dy								
Er								
Eu								
Ga								
Gd								
Hf								
Ho								
La								
Lu								
Nb	1.00							
Nd	0.88	1.00						
Pr	0.88	1.00	1.00					
Pb	0.92	0.95	0.95	1.00				
Sc	0.82	0.96	0.96	0.93	1.00			
Sm	0.88	1.00	1.00	0.95	0.95	1.00		
Sn	0.44	0.34	0.35	0.45	0.34	0.35	1.00	
Sr	-0.25	-0.26	-0.25	-0.26	-0.34	-0.27	-0.06	1.00
Ta	0.93	0.96	0.96	0.99	0.94	0.96	0.44	-0.34
Tb	0.85	0.98	0.98	0.94	0.97	0.97	0.35	-0.33
Th	0.93	0.94	0.94	0.94	0.87	0.95	0.36	-0.20
Tm	0.00	0.00	0.00	0.00	0.00	0.00	0.00	0.00
U	0.90	0.85	0.85	0.87	0.76	0.86	0.40	-0.19
V	0.86	0.76	0.77	0.87	0.70	0.77	0.43	-0.12
W	0.49	0.16	0.17	0.13	0.07	0.17	0.08	0.04
Y	0.86	0.95	0.95	0.94	0.91	0.95	0.36	-0.10
Yb	0.88	0.95	0.95	0.97	0.92	0.95	0.39	-0.18
Zr	0.90	0.94	0.94	0.99	0.92	0.94	0.45	-0.25

	Ta	Tb	Th	Tm	U	V	W	Y
SiO_2								
Al_2O_3								
CaO								
Cr_2O_3								
Fe_2O_3								
K_2O								
MgO								
MnO								
Na_2O								
P_2O_5								
TiO_2								
LOI								
Ba								
Ce								
Dy								
Er								
Eu								
Ga								
Gd								
Hf								
Ho								
La								
Lu								
Nb								
Nd								
Pr								
Pb								
Sc								
Sm								
Sn								
Sr								
Ta	1.00							
Tb	0.96	1.00						
Th	0.94	0.90	1.00					
Tm	0.00	0.00	0.00	1.00				
U	0.86	0.77	0.91	0.00	1.00			
V	0.83	0.72	0.83	0.00	0.85	1.00		
W	0.17	0.11	0.31	0.00	0.31	0.23	1.00	
Y	0.92	0.90	0.93	0.00	0.89	0.81	0.14	1.00
Yb	0.95	0.92	0.94	0.00	0.90	0.84	0.13	0.98
Zr	0.98	0.93	0.93	0.00	0.88	0.86	0.08	0.94

	Yb	Zr
SiO_2		
Al_2O_3		
CaO		
Cr_2O_3		
Fe_2O_3		
K_2O		
MgO		
MnO		
Na_2O		
P_2O_5		
TiO_2		
LOI		
Ba		
Ce		
Dy		
Er		
Eu		
Ga		
Gd		
Hf		
Ho		
La		
Lu		
Nb		
Nd		
Pr		
Pb		
Sc		
Sm		
Sn		
Sr		
Ta		
Tb		
Th		
Tm		
U		
V		
W		
Y		
Yb	1.00	
Zr	0.97	1.00

Appendix 2

6.3.3 Trinity College Bio Resources Ethics Committee approval

UNIVERSITY OF DUBLIN
BIO RESOURCES UNIT

Telephone: + 353 1 6081621 Direct Dial.
Fax: + 353 1 677 2400

TRINITY COLLEGE,
DUBLIN 2, IRELAND.

Peter Nowlan, M.V.B., MSc., Cert LAS., M.R.C.V.S.
Director, Bio Resources Unit
Lecturer (Biochemistry).
E-mail Address : pnowlan@tcd.ie

Re: Ethics Review Process of the following project

Approval by the Bio Resources Unit

Name: Joanne Hellawell Ref:- 150408B

Project title: Nitrogen and carbon isotopes in modern and fossil aquatic ecosystems

Address: Department of Geology, Museum Building Trinity College, Dublin 2

Contact number: 01-896-1363 or 0863129320 **E-mail:** hellawej@tcd.ie

Severity banding:

Species: Common goldfish (*Carassius auratus auratus* (Linnaeus, 1758)) **Numbers:** 150

Licensed procedures:

Euthanasia by carbon dioxide poisoning.

This is deemed to be the most humane method of euthanasia in these unusual circumstances and the only suitable procedure to ensure that rigorous scientific results are produced overall. Suffering will be minimal and euthanasia will only take a matter of minutes as the fish gradually slow down and lose consciousness.

To whom it may concern,
The Bio Resources Ethics Review Process has approved the above project
A copy of the process is attached

Signed: **Date:** 10-6-08

Chairman, Bio Resources Ethics Committee

6.5.1 & 6.5.2 N and C_{org} isotope data and C:N ratio data from fish samples

Sample (mean)	$\delta^{15}N$ scales (‰)	$\delta^{13}C_{org}$ scales (‰)	C:N ratio scales	$\delta^{15}N$ muscle (‰)	$\delta^{13}C_{org}$ muscle (‰)	C:N ratio muscle	$\delta^{15}N$ bone (‰)	$\delta^{13}C_{org}$ bone (‰)	C:N ratio bone
HSO1	3.09	-23.41	2.72	4.14	-26.20	3.22	3.57	-27.37	5.01
HSO2	2.96	-23.25	2.75	4.01	-25.97	3.40	3.44	-25.69	4.13
HSO3	2.96	-23.26	2.72	4.38	-25.86	3.66	3.77	-27.04	5.34
HSO4	2.93	-23.45	2.68	3.85	-26.27	3.46	3.41	-28.18	6.69
HSO5	2.59	-23.39	2.77	3.54	-26.52	3.77	3.39	-27.94	6.69
HSO6	3.34	-23.62	2.90	4.41	-26.88	4.51	3.66	-27.85	7.00
HSO7	3.44	-23.24	2.83	4.11	-28.02	6.19	3.60	-27.69	6.77
HSO8	3.12	-22.92	2.73				3.23	-28.62	9.45
HSO9							3.52	-27.85	10.04
HSO10	3.18	-22.13	3.11				2.99	-24.54	6.21

Sample (mean)	$\delta^{15}N$ scales (‰)	$\delta^{13}C_{org}$ scales (‰)	C:N ratio scales	$\delta^{15}N$ muscle (‰)	$\delta^{13}C_{org}$ muscle (‰)	C:N ratio muscle	$\delta^{15}N$ bone (‰)	$\delta^{13}C_{org}$ bone (‰)	C:N ratio bone
HSA1	3.02	-23.67	2.74	4.09	-26.03	3.39	3.59	-25.45	3.72
HSA2	3.05	-23.73	2.71	4.45	-26.41	3.50	3.84	-27.46	5.19
HSA3	3.06	-23.77	2.82	3.96	-26.58	4.15	3.42	-27.86	6.67
HSA4	2.79	-23.24	2.75	3.65	-26.62	4.10	3.46	-27.79	6.62
HSA5	2.98	-23.24	2.76	3.73	-28.27	5.59	3.44	-27.99	7.24
HSA6	3.23	-23.45	2.88	3.75	-27.49	5.90	3.07	-27.51	6.83
HSA7	3.25	-23.50	2.87	4.99	-28.63	7.92	3.39	-28.35	7.80
HSA8	3.32	-23.13	3.31				3.61	-27.79	7.95
HSA9	3.94	-24.00	3.67				3.94	-24.00	3.67
HSA10	3.30	-23.69	4.34				2.99	-27.63	8.54

Sample (mean)	$\delta^{15}N$ scales (‰)	$\delta^{13}C_{org}$ scales (‰)	C:N ratio scales	$\delta^{15}N$ muscle (‰)	$\delta^{13}C_{org}$ muscle (‰)	C:N ratio muscle	$\delta^{15}N$ bone (‰)	$\delta^{13}C_{org}$ bone (‰)	C:N ratio bone
HFO1	2.93	-23.41	2.81	3.62	-26.01	3.68	3.41	-26.82	5.07
HFO2	2.94	-23.51	2.74	4.02	-25.73	3.31	3.68	-26.38	4.40
HFO3	3.24	-23.26	2.79	4.18	-26.33	3.60	3.35	-28.09	6.61
HFO4	3.09	-23.68	2.84	4.25	-26.64	4.34	3.64	-27.36	5.62
HFO5	3.00	-23.70	2.97	4.66	-27.56	6.59	3.52	-27.29	6.43
HFO6	3.48	-23.61	2.89	4.36	-27.87	7.44	3.64	-26.10	5.03
HFO7	4.30	-23.53	2.90	7.14			3.24	-29.08	12.28
HFO8	3.22	-22.88	3.21				3.40	-24.98	5.58
HFO9	3.60	-23.46	3.08				3.74	-29.90	16.69
HFO10	4.63	-23.70	3.26				3.33	-27.65	8.30

Sample (mean)	$\delta^{15}N$ scales (‰)	$\delta^{13}C_{org}$ scales (‰)	C:N ratio scales	$\delta^{15}N$ muscle (‰)	$\delta^{13}C_{org}$ muscle (‰)	C:N ratio muscle	$\delta^{15}N$ bone (‰)	$\delta^{13}C_{org}$ bone (‰)	C:N ratio bone
HFU1	3.10	-23.69	2.80	3.91	-26.09	3.21	3.74	-27.06	4.71
HFU2	2.99	-23.41	2.64	3.83	-26.03	3.19	3.28	-28.14	6.66
HFU3	2.92	-23.41	2.81	3.84	-25.96	3.66	3.42	-27.02	5.17
HFU4	2.73	-23.53	2.67	4.42	-26.69	3.71	3.45	-27.58	6.44
HFU5	3.00	-24.03	2.86	4.71	-28.50	6.65	3.38	-27.90	5.99
HFU6	3.21	-23.60	2.83	4.38	-26.98	5.36	3.63	-29.23	10.30
HFU7	3.20	-23.65	2.97	5.11	-26.24	8.57	3.04	-28.34	8.96
HFU8	3.38	-23.63	3.14				3.60	-27.99	8.25
HFU9	3.16	-23.18	2.83				3.33	-26.78	6.34
HFU10	3.11	-24.85	3.68				2.76	-26.27	5.91

Sample (mean)	$\delta^{15}N$ scales (‰)	$\delta^{13}C_{org}$ scales (‰)	C:N ratio scales	$\delta^{15}N$ muscle (‰)	$\delta^{13}C_{org}$ muscle (‰)	C:N ratio muscle	$\delta^{15}N$ bone (‰)	$\delta^{13}C_{org}$ bone (‰)	C:N ratio bone
HFA1	3.17	-23.65	2.82	3.80	-25.72	3.23	3.43	-26.51	4.79
HFA2	2.99	-23.33	2.72	3.97	-26.05	3.23	3.52	-26.91	4.94
HFA3	2.80	-23.12	2.76	4.28	-26.05	3.63	3.49	-27.62	6.78
HFA4	2.90	-23.07	2.70	4.80	-26.45	4.10	3.43	-28.13	7.13
HFA5	2.92	-23.71	2.90	3.66	-26.92	5.25	3.02	-26.92	5.76
HFA6	3.30	-23.44	2.86	5.88	-28.42	9.16	3.50	-28.48	8.82
HFA7	3.34	-23.44	2.79	3.25	-25.93	5.36	3.65	-28.85	10.56
HFA8	2.90	-25.50	4.64				3.07	-27.77	8.99
HFA9	3.20	-27.12	3.75				4.38	-30.41	12.99
HFA10	3.38	-24.65	3.50				2.79	-27.47	7.56

Sample (mean)	$\delta^{15}N$ scales (‰)	$\delta^{13}C_{org}$ scales (‰)	C:N ratio scales	$\delta^{15}N$ muscle (‰)	$\delta^{13}C_{org}$ muscle (‰)	C:N ratio muscle	$\delta^{15}N$ bone (‰)	$\delta^{13}C_{org}$ bone (‰)	C:N ratio bone
HSU1	2.71	-23.66	2.92	3.98	-25.92	3.34	3.08	-27.99	6.99
HSU2	2.71	-23.64	2.74	3.72	-26.00	3.43	3.26	-26.80	4.87
HSU3	2.88	-23.08	2.91	4.31	-26.06	3.86	3.49	-25.95	5.09
HSU4	2.75	-23.38	2.69	3.73	-26.54	3.96	3.25	-25.92	4.70
HSU5	2.70	-23.52	2.68	3.84	-27.40	4.62	3.36	-28.18	6.85
HSU6	3.28	-23.35	2.81	4.52	-26.81	4.51	3.60	-28.64	8.89
HSU7	3.62	-23.42	2.84	4.06	-28.67	11.12	3.46	-28.06	7.51
HSU8	3.77	-22.82	4.05				3.43	-27.33	9.19
HSU9	3.30	-24.12	3.92				3.52	-28.60	12.17
HSU10	3.84	-24.48	3.56				3.59	-25.01	4.40

Sample (mean)	$\delta^{15}N$ scales (‰)	$\delta^{13}C_{org}$ scales (‰)	C:N ratio scales	$\delta^{15}N$ muscle (‰)	$\delta^{13}C_{org}$ muscle (‰)	C:N ratio muscle	$\delta^{15}N$ bone (‰)	$\delta^{13}C_{org}$ bone (‰)	C:N ratio bone
CSO1	2.89	-23.41	2.70	3.97	-25.78	3.40	3.30	-26.25	4.31
CSO2	3.03	-23.50	2.68	4.09	-26.09	3.33	3.41	-27.06	5.01
CSO3	2.85	-23.33	2.71	3.79	-26.08	3.38	3.21	-26.59	4.88
CSO4	2.61	-23.64	2.78	3.60	-26.01	3.38	3.14	-25.68	3.95
CSO5	2.16	-23.23	2.64	3.43	-26.08	3.87	3.22	-26.16	4.79
CSO6	3.44	-23.79	2.98	4.40	-26.77	4.01	3.79	-27.68	6.01
CSO7	3.38	-23.23	2.86	3.54	-28.74	8.40	3.16	-28.87	10.94
CSO8	3.23	-23.10	2.82				3.26	-29.13	11.98
CSO9	3.19	-24.29	3.19				3.30	-27.24	6.78
CSO10	2.67	-23.76	2.94				2.90	-26.41	6.21

Sample (mean)	$\delta^{15}N$ scales (‰)	$\delta^{13}C_{org}$ scales (‰)	C:N ratio scales	$\delta^{15}N$ muscle (‰)	$\delta^{13}C_{org}$ muscle (‰)	C:N ratio muscle	$\delta^{15}N$ bone (‰)	$\delta^{13}C_{org}$ bone (‰)	C:N ratio bone
CFO1	3.03	-23.89	2.78	3.63	-26.21	3.35	3.28	-26.85	4.71
CFO2	3.10	-23.33	2.76	4.15	-25.72	3.13	3.68	-27.24	5.36
CFO3	3.04	-23.14	2.77	4.07	-26.01	3.40	3.39	-27.17	5.61
CFO4	2.84	-23.38	2.81	3.77	-26.01	3.36	3.18	-26.28	4.56
CFO5	2.53	-23.65	2.91	3.63	-26.01	3.48	2.84	-26.48	4.91
CFO6	3.44	-23.50	2.93	5.66	-27.43	5.56	4.25	-28.65	9.12
CFO7	3.47	-23.21	2.83	6.63	-29.22	14.20	3.90	-28.62	9.99
CFO8	3.47	-23.67	2.88				3.98	-29.49	10.41
CFO9	3.12	-23.33	2.91				3.86	-28.71	11.26
CFO10	3.17	-23.08	2.88				3.82	-28.64	9.91

Sample (mean)	$\delta^{15}N$ scales (‰)	$\delta^{13}C_{org}$ scales (‰)	C:N ratio scales	$\delta^{15}N$ muscle (‰)	$\delta^{13}C_{org}$ muscle (‰)	C:N ratio muscle	$\delta^{15}N$ bone (‰)	$\delta^{13}C_{org}$ bone (‰)	C:N ratio bone
CSA1	2.94	-23.13	2.82	4.10	-25.89	3.31	3.60	-27.45	5.76
CSA2	3.05	-23.19	2.69	4.19	-25.85	3.26	3.39	-27.16	4.88
CSA3	2.64	-23.20	2.72	3.64	-25.67	3.37	3.00	-26.96	5.65
CSA4	2.80	-23.32	2.68	3.82	-26.47	3.61	3.54	-27.08	5.29
CSA5	2.45	-23.47	2.75	3.26	-26.10	3.31	2.83	-27.07	5.43
CSA6	3.44	-23.57	2.85	4.54	-26.33	3.83	3.85	-27.57	6.37
CSA7	2.88	-22.64	2.83	3.73	-25.94	4.36	2.84	-25.25	4.98
CSA8	2.88	-22.88	2.76				3.32	-28.25	8.15
CSA9	2.87	-23.88	2.94				3.32	-28.08	7.81
CSA10	2.88	-22.89	3.02				3.10	-27.49	7.24

Sample (mean)	$\delta^{15}N$ scales (‰)	$\delta^{13}C_{org}$ scales (‰)	C:N ratio scales	$\delta^{15}N$ muscle (‰)	$\delta^{13}C_{org}$ muscle (‰)	C:N ratio muscle	$\delta^{15}N$ bone (‰)	$\delta^{13}C_{org}$ bone (‰)	C:N ratio bone
CFU1	3.31	-23.87	2.81	4.13	-25.96	3.54	3.77	-27.71	5.73
CFU2	2.73	-23.68	2.76	3.94	-25.93	3.28	3.57	-26.96	5.10
CFU3	3.46	-23.88	2.69	4.49	-26.43	3.32	3.85	-28.27	6.31
CFU4	2.61	-23.69	2.72	3.51	-26.25	3.32	2.90	-27.83	5.54
CFU5	2.17	-23.41	2.75	3.15	-26.09	3.78	2.96	-27.31	5.95
CFU6	3.07	-23.83	2.91	4.51	-26.22	3.72	3.83	-28.13	6.45
CFU7	3.13	-23.54	2.75	4.91	-26.41	3.87	4.11	-28.04	6.76
CFU8	3.27	-23.42	2.80				3.70	-28.99	9.35
CFU9	3.41	-25.88	3.95				3.59	-28.77	8.70
CFU10	3.24	-23.83	2.99				3.46	-29.37	12.61

Sample (mean)	$\delta^{15}N$ scales (‰)	$\delta^{13}C_{org}$ scales (‰)	C:N ratio scales	$\delta^{15}N$ muscle (‰)	$\delta^{13}C_{org}$ muscle (‰)	C:N ratio muscle	$\delta^{15}N$ bone (‰)	$\delta^{13}C_{org}$ bone (‰)	C:N ratio bone
CFA1	2.87	-23.74	2.77	3.79	-26.37	3.27	3.32	-27.17	4.90
CFA2	3.14	-23.61	2.78	4.30	-26.01	3.32	3.93	-27.19	5.17
CFA3	3.23	-23.75	2.77	4.28	-26.00	3.38	3.60	-27.48	5.52
CFA4	3.01	-23.31	2.83	4.05	-26.10	3.51	3.58	-25.77	4.06
CFA5	2.69	-23.99	2.83	3.69	-26.41	3.41	3.24	-27.64	5.61
CFA6	3.04	-23.58	2.92	4.62	-26.56	4.23	3.58	-27.99	6.91
CFA7	3.77	-23.74	2.87	4.83	-28.35	8.05	3.69	-28.32	7.89
CFA8	3.14	-23.11	2.88				3.49	-27.91	8.95
CFA9	3.39	-24.08	3.03				3.75	-28.21	7.95
CFA10	3.43	-23.64	3.00				3.77	-27.90	9.10

Sample (mean)	$\delta^{15}N$ scales (‰)	$\delta^{13}C_{org}$ scales (‰)	C:N ratio scales	$\delta^{15}N$ muscle (‰)	$\delta^{13}C_{org}$ muscle (‰)	C:N ratio muscle	$\delta^{15}N$ bone (‰)	$\delta^{13}C_{org}$ bone (‰)	C:N ratio bone
CSU1	3.06	-24.08	2.68	4.19	-26.74	3.46	3.57	-28.63	6.65
CSU2	3.02	-23.34	2.68	4.16	-25.96	3.43	3.51	-27.83	5.54
CSU3	2.74	-23.15	2.69	3.88	-25.89	3.46	3.47	-27.14	5.50
CSU4	2.81	-23.43	2.75	3.66	-26.56	3.34	3.34	-26.54	4.69
CSU5	2.27	-23.37	2.59	3.40	-26.23	3.24	2.86	-27.22	5.67
CSU6	3.60	-23.40	2.84	4.57	-26.38	3.80	3.93	-27.44	5.95
CSU7	3.52	-23.33	2.79	4.24	-27.73	5.73	3.47	-27.45	6.96
CSU8	2.79	-24.05	2.80				3.13	-27.14	6.84
CSU9	3.42	-24.49	3.13				3.69	-28.53	8.07
CSU10	3.39	-22.44	3.02				3.47	-25.37	4.93

Replicate samples	$\delta^{15}N$ scales (‰)	$\delta^{13}C_{org}$ scales (‰)	C:N ratio scales	$\delta^{15}N$ muscle (‰)	$\delta^{13}C_{org}$ muscle (‰)	C:N ratio muscle	$\delta^{15}N$ bone (‰)	$\delta^{13}C_{org}$ bone (‰)	C:N ratio bone
HSO2R1	3.10	-23.34	2.76	4.30	-26.10	3.40	3.51	-27.2	5.8
HSO2R2	2.95	-23.85	2.66	4.35	-26.17	3.37	3.79	-27.0	4.8
HSA10R1	5.78	-23.21	2.64				3.68	-29.9	14.3
HSA10R2	3.27	-23.49	2.90				3.70	-29.4	11.0
HFO4R1	3.41	-23.28	2.76	4.36	-26.57	4.32	3.74	-28.1	7.5
HFO4R2	3.17	-23.04	2.72	4.46	-25.92	3.71	3.70	-25.7	4.8
HFO4R3	3.16	-23.52	2.80	5.85	-28.44	6.54	4.06	-29.2	9.0
HFU6R1	3.45	-23.78	3.09	4.59	-27.64	7.41	3.38	-27.7	8.6
HFU6R2	3.22	-23.18	2.88	5.62	-27.93	9.40	3.48	-28.0	8.0
HFU6R3	3.74	-24.24	3.16				3.66	-27.3	6.9
HFA10R1	3.35	-23.24	3.31				2.91	-28.5	10.6
HFA10R2	3.13	-23.66	2.92				2.85	-26.7	5.7
HSU8R1	2.01	-13.22	5.01				3.59	-28.4	9.6
HSU8R2	3.39	-23.90	3.21				3.69	-27.2	7.2
CSO3R1	3.25	-23.70	2.74	4.20	-25.91	3.41	3.65	-25.4	3.8
CSO3R2	2.94	-23.19	2.65	4.23	-25.92	3.40	3.58	-27.6	6.1
CSO3R3	2.75	-23.51	2.79	4.29	-26.24	3.36	3.56	-25.7	4.1
CSA9R1	3.08	-25.12	3.48				3.31	-28.2	7.1
CSA9R2	3.38	-30.09	35.63				3.03	-28.1	8.8
CSA9R3	3.06	-24.62	3.38				3.49	-29.0	10.8
CFO1R1	3.13	-24.06	2.86	4.24	-25.90	3.27	3.76	-26.8	4.4
CFO1R2	3.17	-23.73	2.75	3.85	-25.70	3.17	3.34	-27.4	6.2
CFU7R1	3.39	-23.60	2.86	4.69	-26.59	4.10	4.02	-27.4	6.3
CFU7R2	3.59	-23.59	2.82	5.81	-27.73	6.79	3.91	-26.9	5.7
CFA9R1	2.97	-24.06	3.06				3.41	-28.2	8.0
CFA9R2	3.42	-23.81	2.99				3.61	-29.2	13.0

Repeat sub-samples	Mean $\delta^{15}N$ scales (‰)	$\delta^{15}N$ SD scales	$\delta^{15}N$ %RSD scales	Mean $\delta^{13}C_{org}$ scales (‰)	$\delta^{13}C_{org}$ SD scales	$\delta^{13}C_{org}$ %RSD scales	Mean C:N ratio scales	C:N ratio SD scales	C:N Ratio %RSD scales
HSO2	2.82	0.20	7.05	-22.83	0.60	2.61	2.78	0.0	1.7
HSA10	3.30	0.12		-23.69	0.83		4.34	0.8	
HFO4	3.11	0.06	1.84	-23.68	0.13	0.53	2.88	0.1	2.0
HFU6	3.23	0.03	0.92	-23.59	0.03	0.14	2.77	0.1	2.9
HFA10	3.38	0.11		-24.65	0.30		3.50	0.0	
CSO3	2.80	0.09	3.32	-23.35	0.03	0.13	2.74	0.0	1.7
CFO1	2.95	0.12	3.95	-23.48	0.58	2.48	2.82	0.0	1.6
CSA9	2.87	0.04		-23.88	0.12		2.94	0.0	
CFU7	3.12	0.01	0.39	-23.50	0.06	0.24	2.70	0.1	2.5
CFA9	3.39	0.04		-24.08	0.41		3.03	0.2	

Replicate samples	Mean $\delta^{15}N$ scales (‰)	$\delta^{15}N$ SD scales	$\delta^{15}N$ %RSD scales	Mean $\delta^{13}C_{org}$ scales (‰)	$\delta^{13}C_{org}$ SD scales	$\delta^{13}C_{org}$ %RSD scales	Mean C:N ratio scales	C:N ratio SD scales	C:N Ratio %RSD scales
HSO2R	3.01	0.07	2.30	-23.48	0.27	1.13	2.73	0.0	1.7
HSA10R	3.35	0.07	2.22	-35.61	0.56	1.57	4.95	0.7	15.1
HFO4R	3.21	0.12	3.80	-23.38	0.24	1.03	2.78	0.0	1.6
HFU6R	3.40	0.22	6.32	-23.70	0.38	1.59	2.99	0.1	4.7
HFA10R	3.28	0.10	2.97	-23.71	0.56	2.37	3.17	0.2	7.7
HSU8R	2.70	0.69	25.66	-24.12	5.60	23.20	6.14	0.7	12.0
CSO3R	2.94	0.19	6.34	-23.43	0.19	0.82	2.72	0.0	1.8
CFO1R	3.11	0.06	1.85	-23.90	0.13	0.55	2.80	0.0	1.6
CSA9R	3.10	0.18	5.81	-25.93	2.44	9.42	3.36	0.3	7.7
CFU7R	3.37	0.19	5.65	-23.58	0.03	0.11	2.81	0.0	1.6
CFA9R	3.26	0.21	6.31	-23.99	0.12	0.51	3.03	0.0	0.9

Repeat sub-samples	Mean $\delta^{15}N$ muscle (‰)	$\delta^{15}N$ SD muscle	$\delta^{15}N$ %RSD muscle	Mean $\delta^{13}C_{org}$ muscle (‰)	$\delta^{13}C_{org}$ SD muscle	$\delta^{13}C_{org}$ %RSD muscle	Mean C:N ratio muscle	C:N ratio SD muscle	C:N Ratio %RSD muscle
HSO2	3.93	0.11	2.84	-25.55	0.61	2.40	3.48	0.1	3.4
HFO4	4.57	0.52	11.47	-26.60	0.24	0.89	4.39	0.1	1.9
HFU6	4.46	0.26	5.92	-27.58	1.05	3.79	6.05	1.2	19.6
CSO3	3.77	0.02	0.58	-26.03	0.07	0.28	3.42	0.1	1.6
CFO1	3.52	0.15	4.34	-25.82	0.55	2.15	3.46	0.2	4.7
CFU7	4.84	0.17	3.61	-26.39	0.04	0.15	3.79	0.1	3.0

Replicate samples	Mean $\delta^{15}N$ muscle (‰)	$\delta^{15}N$ SD muscle	$\delta^{15}N$ %RSD muscle	Mean $\delta^{13}C_{org}$ muscle (‰)	$\delta^{13}C_{org}$ SD muscle	$\delta^{13}C_{org}$ %RSD muscle	Mean C:N ratio muscle	C:N ratio SD muscle	C:N Ratio %RSD muscle
HSO2R	4.22	0.15	3.60	-26.08	0.08	0.32	3.39	0.0	0.4
HFO4R	4.73	0.65	13.79	-26.89	0.94	3.49	4.73	1.1	22.8
HFU6R	4.86	0.54	11.17	-27.52	0.40	1.46	7.39	1.6	22.3
CSO3R	4.13	0.20	4.76	-26.04	0.13	0.51	3.39	0.0	0.5
CFO1R	3.91	0.25	6.43	-25.94	0.21	0.81	3.26	0.1	2.2
CFU7R	5.14	0.48	9.43	-26.91	0.58	2.17	4.92	1.3	27.0

Repeat sub-samples	Mean $\delta^{15}N$ bone (‰)	$\delta^{15}N$ SD bone	$\delta^{15}N$ %RSD bone	Mean $\delta^{13}C_{org}$ bone (‰)	$\delta^{13}C_{org}$ SD bone	$\delta^{13}C_{org}$ %RSD bone	Mean C:N ratio bone	C:N ratio SD bone	C:N Ratio %RSD bone
HSO2	3.35	0.14	4.28	-25.21	0.68	2.69	4.16	0.1	1.3
HSA10	2.99	0.04	1.26	-27.63	1.00	3.63	8.54	2.5	29.0
HFO4	3.66	0.05	1.32	-27.31	0.10	0.35	5.67	0.1	1.3
HFU6	3.63	0.04	1.20	-19.35	0.21		6.02	1.3	
HFA10	2.79	0.17		-27.47	0.23		7.56	0.4	
HSU8	3.43	0.03	0.94	-27.31	0.36	1.33	8.80	0.8	9.4
CSO3	3.11	0.15	4.66	-26.50	0.13	0.50	4.81	0.1	2.2
CFO1	3.17	0.16	5.06	-26.31	0.77	2.94	4.63	0.1	2.8
CSA9	3.32	0.05		-28.08	0.32		7.81	0.5	
CFU7	3.95	0.23	5.86	-28.11	0.17	0.61	6.80	0.2	3.7
CFA9	3.75	0.05		-28.21	0.18		7.95	0.2	

Replicate samples	Mean $\delta^{15}N$ bone (‰)	$\delta^{15}N$ SD bone	$\delta^{15}N$ %RSD bone	Mean $\delta^{13}C_{org}$ bone (‰)	$\delta^{13}C_{org}$ SD bone	$\delta^{13}C_{org}$ %RSD bone	Mean C:N ratio bone	C:N ratio SD bone	C:N Ratio %RSD bone
HSO2R	3.58	0.15	4.24	-26.62	0.67	2.51	4.89	0.7	13.9
HSA10R	3.44	0.36	10.36	-29.01	0.96	3.30	11.29	2.4	21.0
HFO4R	3.79	0.16	4.35	-27.58	1.27	4.60	6.74	1.7	24.6
HFU6R	3.52	0.10	2.98	-28.07	0.72	2.57	8.46	1.2	14.3
HFA10R	3.03	0.32	10.56	-27.46	0.65	2.36	7.72	1.8	23.5
HSU8R	3.57	0.11	3.01	-27.63	0.51	1.85	8.68	1.0	11.9
CSO3R	3.50	0.17	4.84	-26.32	0.86	3.26	4.71	0.9	18.7
CFO1R	3.46	0.22	6.23	-27.01	0.29	1.06	5.10	0.8	15.7
CSA9R	3.29	0.17	5.07	-28.34	0.39	1.38	8.62	1.4	16.1
CFU7R	4.01	0.08	2.03	-27.44	0.46	1.68	6.26	0.4	6.6
CFA9R	3.59	0.14	3.88	-28.53	0.45	1.59	9.65	2.4	24.6

6.5.3 C and O isotope data from sediments samples

Sample	$\delta^{13}C$ sediment (‰)	$\delta^{18}O$ sediment (‰)
HSO1	1.96	-4.47
HSO2	1.90	-4.61
HSO3	2.04	-4.45
HSO4	2.18	-4.13
HSO5	2.05	-4.59
HSO6	1.88	-4.73
HSO7	1.82	-4.84
HSO8	1.92	-4.72
HSO9	1.86	-4.72
HSO10	1.95	-4.83

Sample	$\delta^{13}C$ sediment (‰)	$\delta^{18}O$ sediment (‰)
HFO1	1.93	-4.53
HFO2	2.01	-4.54
HFO3	2.01	-4.45
HFO4	1.85	-4.60
HFO5	2.02	-4.49
HFO6	2.09	-4.33
HFO7	1.88	-4.65
HFO8	2.02	-4.45
HFO9	1.94	-4.49
HFO10	2.04	-4.83

Sample	$\delta^{13}C$ sediment (‰)	$\delta^{18}O$ sediment (‰)
HSA1	2.00	-4.41
HSA4	1.86	-4.65
HSA7	2.03	-4.30
HSA10	1.84	-4.66

Sample	$\delta^{13}C$ sediment (‰)	$\delta^{18}O$ sediment (‰)
HFU1	1.91	-4.20
HFU4	2.03	-4.23
HFU7	2.01	-4.22
HFU10	2.06	-4.26

Sample	$\delta^{13}C$ sediment (‰)	$\delta^{18}O$ sediment (‰)
HFA1	2.03	-4.25
HFA4	2.07	-4.28
HFA7	2.14	-4.20
HFA10	2.09	-4.27

Sample	$\delta^{13}C$ sediment (‰)	$\delta^{18}O$ sediment (‰)
HSU1	1.96	-4.36
HSU4	2.06	-4.25
HSU7	1.98	-4.54
HSU10	2.02	-4.27

Sample	$\delta^{13}C$ sediment (‰)	$\delta^{18}O$ sediment (‰)
CSO1	2.05	-4.49
CSO4	2.04	-4.26
CSO7	1.97	-4.29
CSO10	1.95	-4.40

Sample	$\delta^{13}C$ sediment (‰)	$\delta^{18}O$ sediment (‰)
CSA1	1.96	-4.43
CSA4	1.87	-4.70
CSA7	2.02	-4.33
CSA10	1.98	-4.38

Sample	$\delta^{13}C$ sediment (‰)	$\delta^{18}O$ sediment (‰)
CFO1	2.09	-4.24
CFO4	1.91	-4.50
CFO7	2.20	-4.07
CFO10	2.09	-4.26

Sample	$\delta^{13}C$ sediment (‰)	$\delta^{18}O$ sediment (‰)
CFU1	2.09	-4.21
CFU4	2.11	-4.18
CFU7	2.02	-4.41
CFU10	2.10	-4.18

Sample	$\delta^{13}C$ sediment (‰)	$\delta^{18}O$ sediment (‰)
CFA1	1.98	-4.50
CFA4	1.95	-4.49
CFA7	1.98	-4.35
CFA10	1.90	-4.45

Sample	$\delta^{13}C$ sediment (‰)	$\delta^{18}O$ sediment (‰)
CSU1	1.98	-4.51
CSU4	1.87	-4.68
CSU7	2.19	-4.24
CSU10	1.94	-4.36

6.5.4 Temperature, pH, nitrate and ammonia data from water samples

Sample	T°C	pH	NO_3^- mg/L	NH_3 mg/L
HSO1	14.0	7.6	3.10	2.94
HSO2	10.5	7.3	0.00	0.00
HSO3	19.2	7.0	21.26	38.81
HSO4	19.7	7.3	47.40	137.40
HSO5	19.3	7.8	49.17	226.56
HSO6	12.5	7.5	39.87	763.59
HSO7	20.2	7.1	6.20	367.11
HSO8	21.3	7.7	7.09	358.72
HSO9	21.2	7.4	8.86	320.96
HSO10	21.1	8.0	0.00	608.36

Sample	T°C	pH	NO_3^- mg/L	NH_3 mg/L
CSO1	13.9	7.3	0.00	0.00
CSO2	15.4	7.7	4.43	2.73
CSO3	12.7	7.2	3.10	20.45
CSO4	14.6	7.2	5.76	40.91
CSO5	14.2	7.5	26.14	77.09
CSO6	15.7	8.2	17.72	232.33
CSO7	12.6	8.0	8.86	455.22
CSO8	13.8	7.3	13.29	476.20
CSO9	12.6	8.0	0.00	404.87
CSO10	14.5	7.6	0.00	876.87

Sample	T°C	pH	NO_3^- mg/L	NH_3 mg/L
HSA1	20.0	6.8	3.99	3.25
HSA2	12.9	6.5	18.61	9.96
HSA3	19.3	6.4	13.29	220.27
HSA4	19.6	6.2	62.02	246.49
HSA5	18.5	6.7	35.44	323.06
HSA6	12.6	6.5	51.39	232.33
HSA7	20.5	6.6	105.88	474.10
HSA8	21.4	6.9	2.22	276.91
HSA9	21.3	6.3	8.86	553.81
HSA10	21.1	7.8	2.22	396.48

Sample	T°C	pH	NO_3^- mg/L	NH_3 mg/L
CFO1	14.2	8.1	3.54	0.52
CFO2	14.5	7.9	0.00	0.52
CFO3	13.6	7.6	1.77	16.78
CFO4	15.1	7.2	12.85	39.33
CFO5	15.4	7.9	21.26	114.85
CFO6	16.5	8.7	88.60	242.82
CFO7	12.3	8.6	26.58	602.06
CFO8	14.5	8.6	17.72	270.61
CFO9	13.1	8.9	0.89	320.96
CFO10	13.4	8.9	1.33	184.60

Sample	T°C	pH	NO_3^- mg/L	NH_3 mg/L
HFO1	20.2	8.0	6.20	8.92
HFO2	14.0	7.3	2.22	35.66
HFO3	19.0	7.7	60.25	162.05
HFO4	17.6	8.5	25.69	17.83
HFO5	19.6	8.6	53.16	199.29
HFO6	13.6	8.5	13.29	162.58
HFO7	20.4	8.6	28.35	43.00
HFO8	21.4	8.7	0.00	51.92
HFO9	21.1	9.0	0.00	148.94
HFO10	21.1	8.7	0.00	0.00

Sample	T°C	pH	NO_3^- mg/L	NH_3 mg/L
CSA1	12.0	7.1	3.10	2.10
CSA2	13.4	6.9	0.44	0.31
CSA3	13.8	6.9	0.00	14.68
CSA4	13.9	6.3	3.99	55.07
CSA5	13.2	6.6	15.51	26.75
CSA6	13.3	6.4	4.87	58.21
CSA7	10.7	6.5	18.16	117.48
CSA8	15.3	5.9	165.68	207.68
CSA9	9.8	6.5	42.53	272.71
CSA10	10.5	6.6	47.84	272.71

Sample	T°C	pH	NO_3^- mg/L	NH_3 mg/L
HFU1	20.2	7.6	0.89	3.36
HFU2	13.2	6.7	0.44	11.43
HFU3	19.1	7.0	4.87	61.88
HFU4	17.3	6.3	21.71	121.15
HFU5	19.6	7.2	36.33	404.87
HFU6	16.5	6.5	31.45	738.42
HFU7	20.4	7.0	0.00	211.88
HFU8	21.5	7.0	3.10	320.96
HFU9	21.3	8.3	0.00	677.58
HFU10	21.0	8.9	9.30	792.96

Sample	T°C	pH	NO_3^- mg/L	NH_3 mg/L
CFU1	13.4	7.7	4.43	0.10
CFU2	13.5	7.5	3.99	0.52
CFU3	12.3	7.4	0.00	9.96
CFU4	13.0	6.8	0.00	39.33
CFU5	12.6	6.7	2.22	20.45
CFU6	12.7	7.0	21.71	81.29
CFU7	9.7	6.7	65.56	528.64
CFU8	13.9	6.6	11.96	832.82
CFU9	11.4	6.8	11.52	341.94
CFU10	11.5	6.8	2.66	537.03

Sample	T°C	pH	NO_3^- mg/L	NH_3 mg/L
HFA1	16.5	7.6	0.89	2.10
HFA2	15.4	6.8	7.53	29.37
HFA3	18.8	6.8	0.00	61.36
HFA4	19.1	6.5	46.07	236.52
HFA5	19.4	6.7	0.00	176.21
HFA6	13.4	6.5	51.39	725.83
HFA7	20.4	6.5	13.29	939.80
HFA8	21.3	6.6	11.96	388.09
HFA9	21.4	7.6	9.30	409.07
HFA10	21.0	8.4	1.33	509.76

Sample	T°C	pH	NO_3^- mg/L	NH_3 mg/L
CFA1	11.8	8.0	3.99	0.73
CFA2	12.8	7.5	3.10	1.68
CFA3	13.9	7.1	0.00	2.62
CFA4	14.2	7.1	0.00	31.99
CFA5	13.6	7.0	11.52	119.05
CFA6	13.0	6.6	23.04	206.63
CFA7	11.0	6.9	11.08	193.00
CFA8	14.5	6.8	17.72	383.89
CFA9	11.4	6.6	3.99	50.35
CFA10	12.1	6.7	5.76	318.86

Sample	T°C	pH	NO_3^- mg/L	NH_3 mg/L
HSU1	20.2	6.9	6.65	1.36
HSU2	12.5	6.4	12.85	5.35
HSU3	19.2	6.6	5.32	44.05
HSU4	19.2	6.3	5.76	111.18
HSU5	19.1	6.3	36.77	213.45
HSU6	12.5	6.2	130.24	172.54
HSU7	20.4	6.3	19.94	446.83
HSU8	21.1	6.6	0.00	155.24
HSU9	21.6	6.5	2.66	520.25
HSU10	21.5	6.7	0.00	272.71

Sample	T°C	pH	NO_3^- mg/L	NH_3 mg/L
CSU1	13.4	6.5	0.00	0.31
CSU2	13.7	6.6	0.44	4.41
CSU3	12.0	6.9	1.33	2.36
CSU4	13.9	6.1	12.40	28.84
CSU5	11.8	6.6	12.85	45.63
CSU6	12.3	6.1	93.47	109.08
CSU7	9.9	6.4	0.00	218.17
CSU8	14.7	6.4	72.65	164.15
CSU9	11.3	6.5	6.20	201.39
CSU10	12.3	6.8	8.42	287.40

7.5.3 Apolar fraction profiles

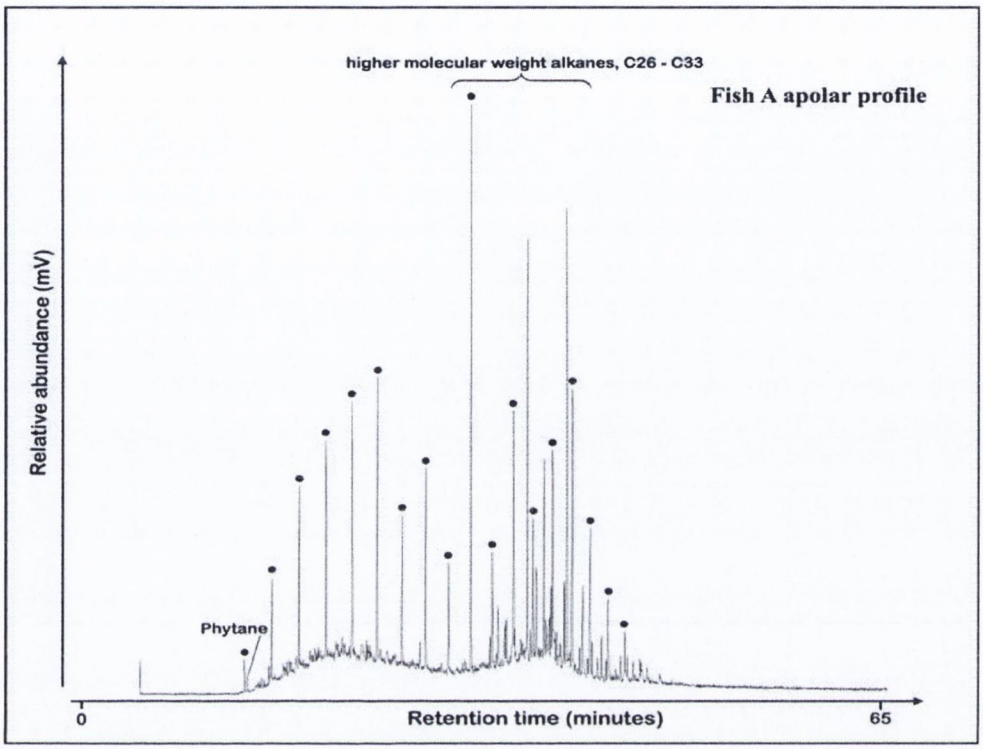

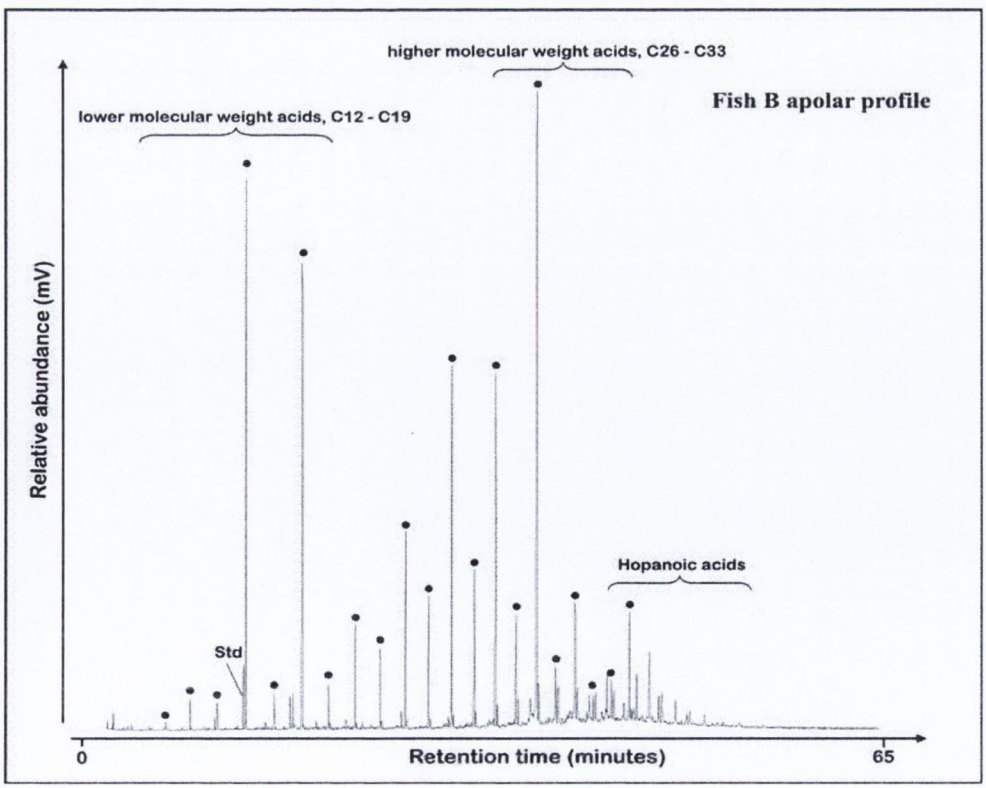

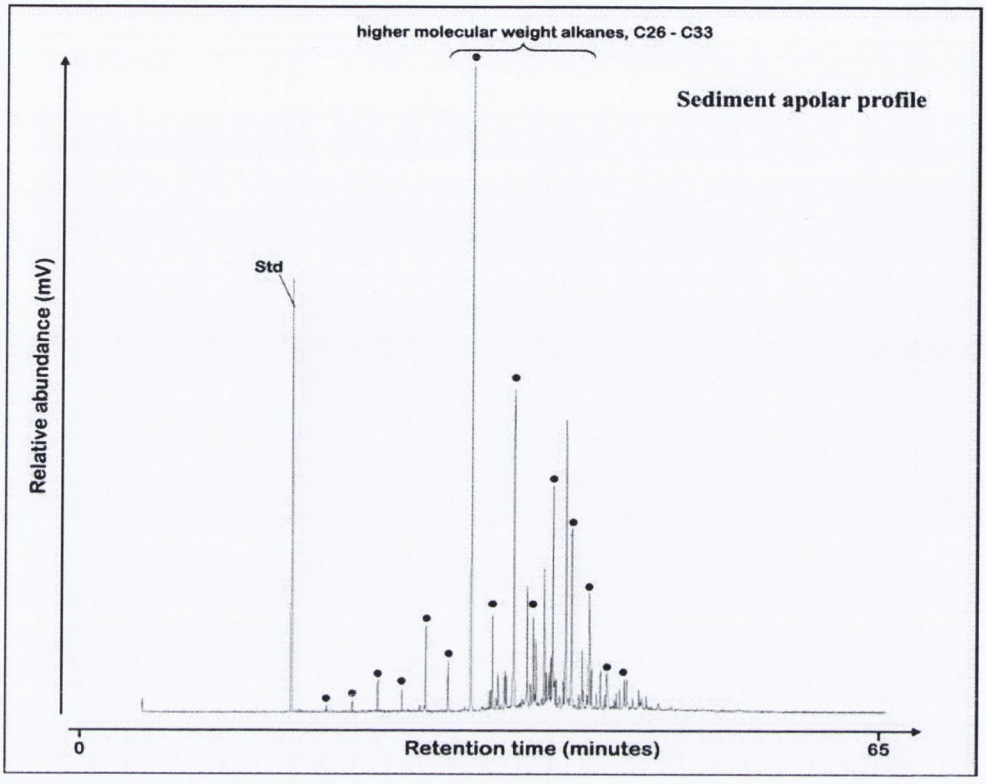
higher molecular weight alkanes, C26 - C33
Sediment apolar profile
Std
Relative abundance (mV)
0
Retention time (minutes)
65

7.5.4 Polar fraction profiles

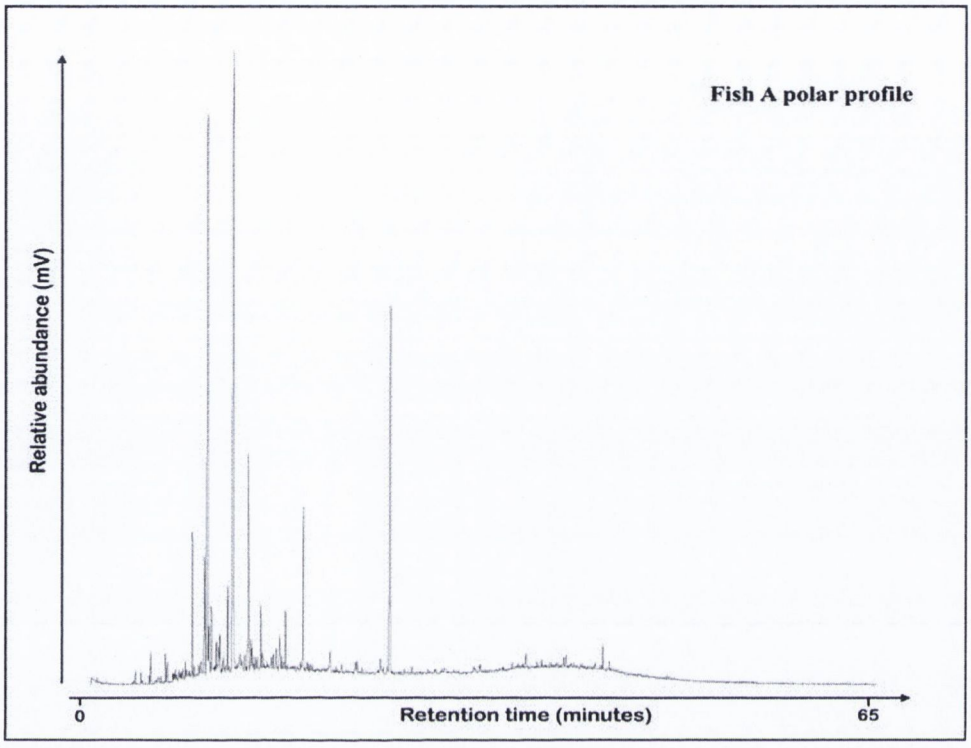

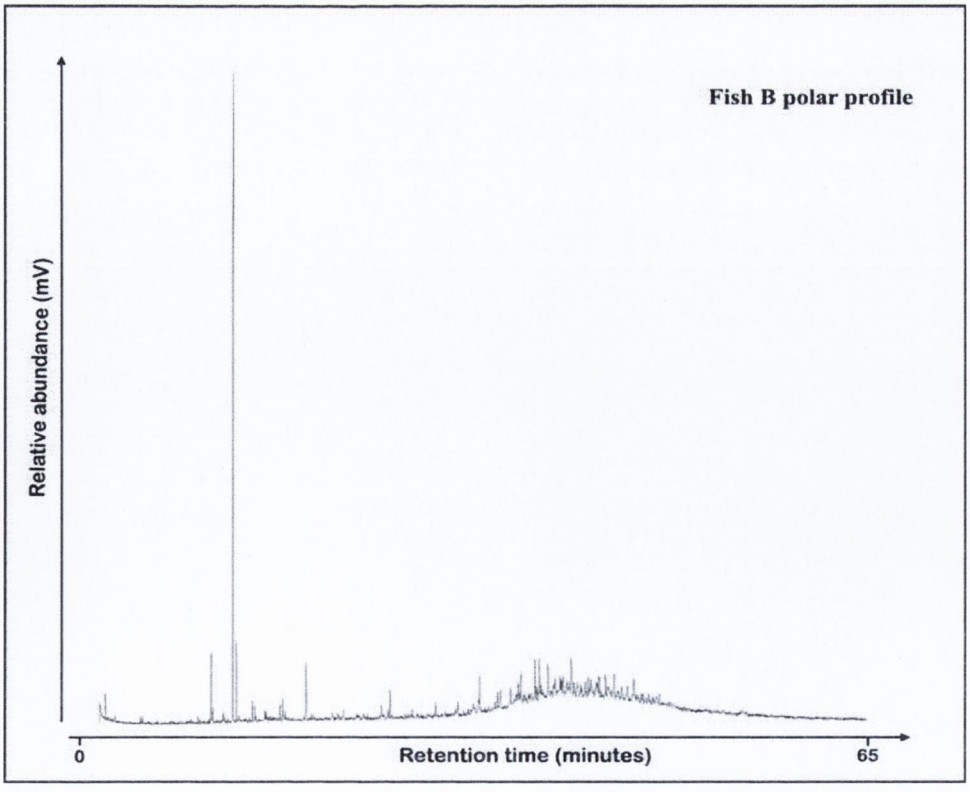

7.5.6 Amino acid data

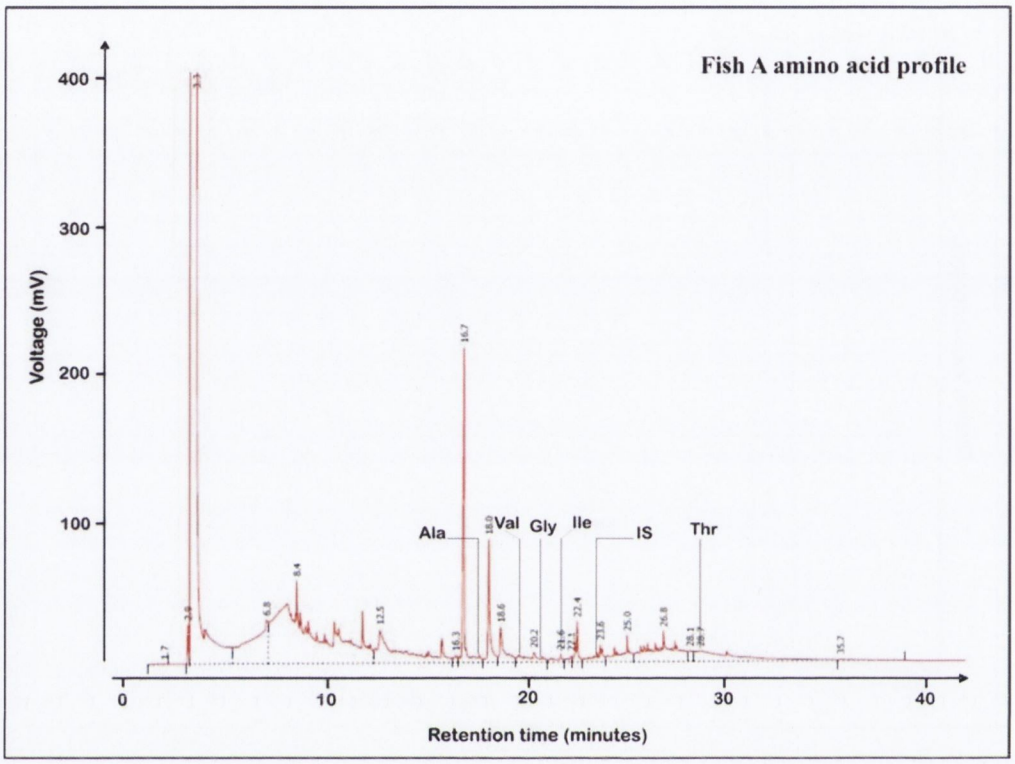

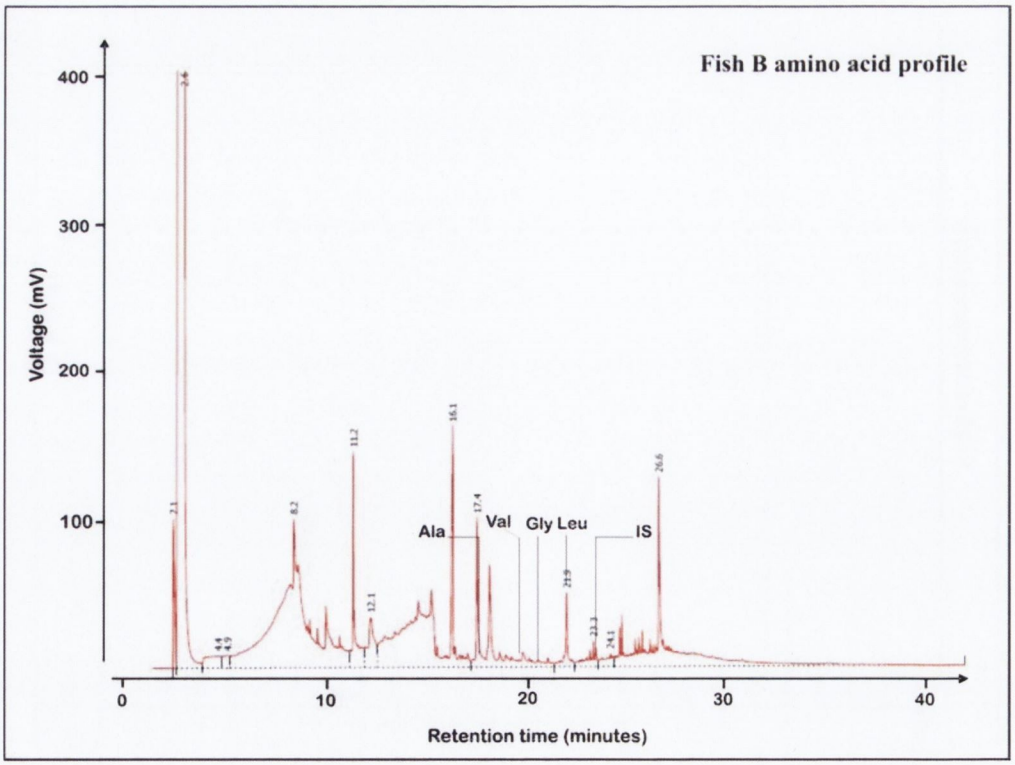

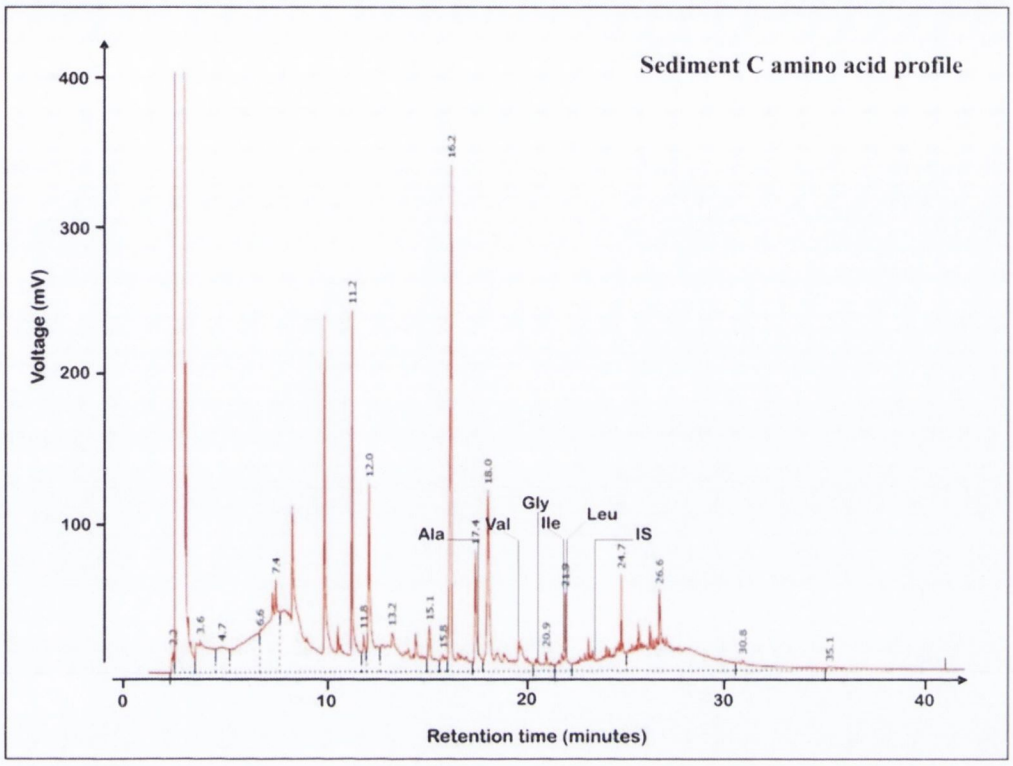
Sediment C amino acid profile
Voltage (mV)
400
300
200
100
0
10
20
30
40
Retention time (minutes)
Ala
Val
Gly
Ile
Leu
IS

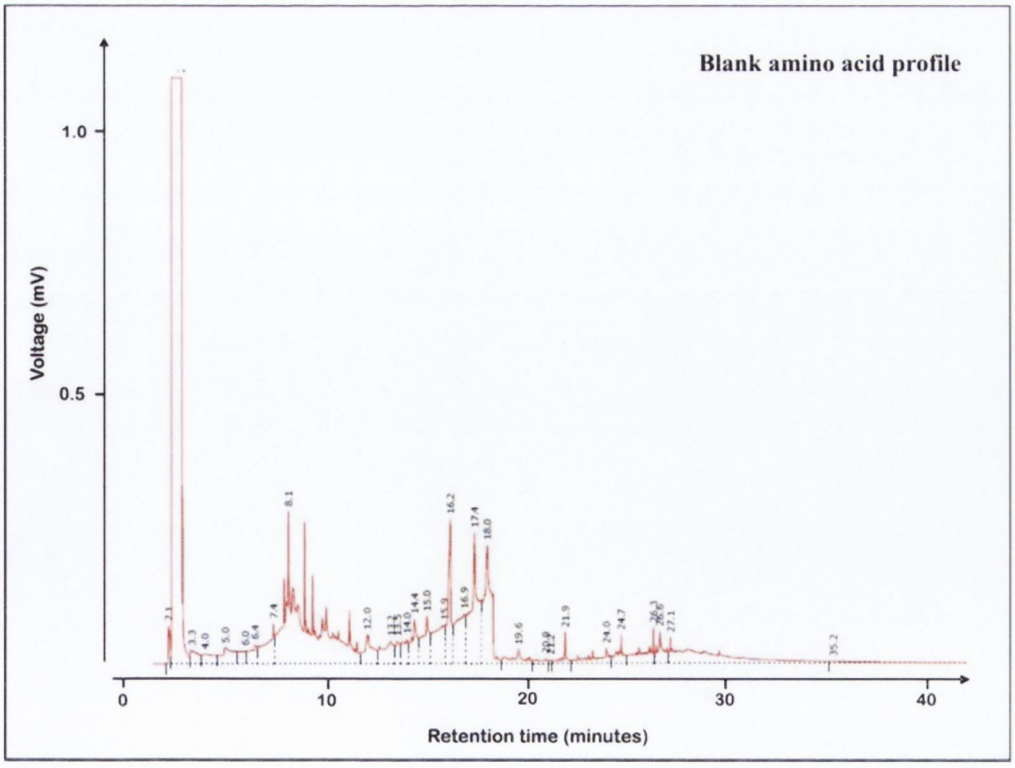
Blank amino acid profile
Voltage (mV)
1.0
0.5
0
10
20
30
40
Retention time (minutes)

Appendix 2

8.61 to 8.6.4 Results of N and C isotope analyses

Fossil sample	Species	Number of replicates (*n*=)	Mean $\delta^{15}N$ (‰)	$\delta^{15}N$ SD	Mean $\delta^{13}C$ (‰)	$\delta^{13}C$ SD
AI1	*A. iheringi*	7	4.43	0.35	-14.18	0.31
AI2	*A. iheringi*	4	4.03	0.24	-15.46	0.26
DB1A	Sauropoda indet.	3	1.25	0.57	-16.87	0.03
DB1B	Sauropoda indet.	3	0.07	0.35	-17.91	0.31
DB2A	Sauropoda indet.	3	3.48	0.31	-16.63	0.11
DB2B	Sauropoda indet.	3	2.34	0.48	-15.08	0.09
LS1	cf. Lepisosteidae indet.	3	3.99	0.04	-17.52	0.06
SP1	*Lepidotes* indet.	3	4.21	0.18	-18.65	0.22
ST1A	cf. *C. appendiculata*	4	9.10	0.87	-8.50	1.15
ST1B	cf. *C. appendiculata*	4	6.95	0.85	-7.27	0.10
ST1C	cf. *C. appendiculata*	2	8.85	0.02	-7.29	0.00
ST2A	cf. *C. appendiculata*	1	7.29		-10.35	
ST2B	cf. *C. appendiculata*	3	5.81	0.10	-8.15	0.11
ST2C	cf. *C. appendiculata*	4	3.42	0.96	-7.03	0.18
ST3	*Carcharias* indet.	2	7.99	0.36	-7.49	0.11
ST4	*Carcharias* indet.	2	5.08	0.12	-4.46	0.05
TP1A	Chelidae indet.	3	4.85	0.04	-12.83	0.17
TP1B	Chelidae indet.	6	4.73	0.15	-17.13	1.27
TP2A	Chelidae indet.	3	4.24	0.33	-12.32	0.39
TP2B	Chelidae indet.	3	4.66	0.05	-16.55	0.02
TP3A	Chelidae indet.	2	6.12	0.12	-13.17	0.05
TP3B	Chelidae indet.	3	6.31	0.72	-8.58	0.51
TP4A	Chelidae indet.	1	5.34		-11.22	
TP4B	Chelidae indet.	1	6.23		-11.69	
TP5A	Chelidae indet.	1	5.31		-13.14	
TP5B	Chelidae indet.	1	5.57		-13.80	
PT1A	*Protosphyraena* indet.	2	8.20	0.41	-6.83	0.19
PT1B	*Protosphyraena* indet.	2	8.96	0.05	-5.03	0.06

8.6.5 C:N ratios of all samples

Fossil sample	Species	Number of replicates (*n*=)	%C	%N	C:N ratio
AI1	*A. iheringi*	7	1.53	0.04	37.01
AI2	*A. iheringi*	4	1.74	0.05	33.18
DB1A	Sauropoda indet.	3	1.38	0.03	46.64
DB1B	Sauropoda indet.	3	0.66	0.03	21.92
DB2A	Sauropoda indet.	3	1.26	0.03	44.88
DB2B	Sauropoda indet.	3	0.95	0.03	35.87
LS1	cf. Lepisosteidae indet.	3	2.31	0.11	20.57
SP1	*Lepidotes* indet.	3	2.34	0.09	25.26
ST1A	cf. *C. appendiculata*	4	1.05	0.05	23.11
ST1B	cf. *C. appendiculata*	4	1.36	0.01	97.96
ST1C	cf. *C. appendiculata*	2	1.52	0.03	56.24
ST2A	cf. *C. appendiculata*	1	1.06	0.04	25.90
ST2B	cf. *C. appendiculata*	3	1.52	0.02	71.91
ST2C	cf. *C. appendiculata*	4	1.51	0.02	60.95
ST3	*Carcharias* indet.	2	1.05	0.01	86.54
ST4	*Carcharias* indet.	2	1.19	0.01	91.59
TP1A	Chelidae indet.	3	1.76	0.04	39.27
TP1B	Chelidae indet.	6	2.36	0.17	13.72
TP2A	Chelidae indet.	3	1.91	0.06	32.79
TP2B	Chelidae indet.	3	2.30	0.18	12.56
TP3A	Chelidae indet.	2	1.57	0.05	32.77
TP3B	Chelidae indet.	3	1.39	0.02	68.51
TP4A	Chelidae indet.	1	1.56	0.01	138.33
TP4B	Chelidae indet.	1	1.78	0.02	97.78
TP5A	Chelidae indet.	1	1.36	0.02	68.88
TP5B	Chelidae indet.	1	1.49	0.02	64.46
PT1A	*Protosphyraena* indet.	2	1.68	0.03	59.97
PT1B	*Protosphyraena* indet.	2	1.31	0.01	110.32